ISSN 1007-9327 (print)
ISSN 2219-2840 (online)

World Journal of *Gastroenterology*

World J Gastroenterol 2020 March 21; 26(11): 1107-1230

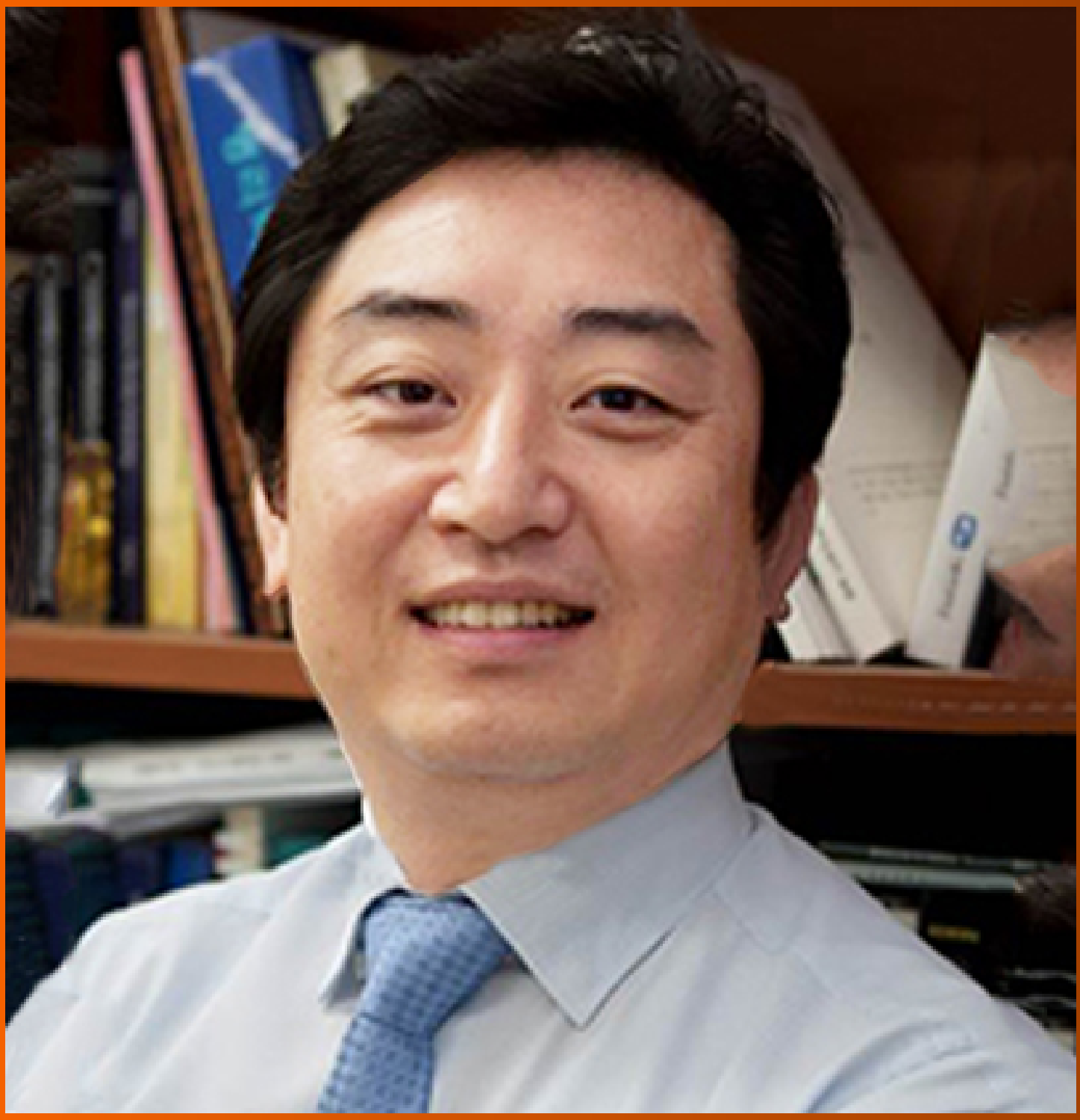

Published by Baishideng Publishing Group Inc

World Journal of Gastroenterology

Contents

Weekly Volume 26 Number 11 March 21, 2020

Observational Study

Contents

World Journal of Gastroenterology

Volume 26 Number 11 March 21, 2020

ABOUT COVER

Associate Editor of *World Journal of Gastroenterology*, Suk Woo Nam, PhD, Professor, Department of Pathology, The Catholic Univesity of Korea, College of Medicine, Seoul 137-701, South Korea

AIMS AND SCOPE

The primary aim of *World Journal of Gastroenterology* (*WJG*, *World J Gastroenterol*) is to provide scholars and readers from various fields of gastroenterology and hepatology with a platform to publish high-quality basic and clinical research articles and communicate their research findings online.

WJG mainly publishes articles reporting research results and findings obtained in the field of gastroenterology and hepatology and covering a wide range of topics including gastroenterology, hepatology, gastrointestinal endoscopy, gastrointestinal surgery, gastrointestinal oncology, and pediatric gastroenterology.

INDEXING/ABSTRACTING

The *WJG* is now indexed in Current Contents®/Clinical Medicine, Science Citation Index Expanded (also known as SciSearch®), Journal Citation Reports®, Index Medicus, MEDLINE, PubMed, PubMed Central, and Scopus. The 2019 edition of Journal Citation Report® cites the 2018 impact factor for *WJG* as 3.411 (5-year impact factor: 3.579), ranking *WJG* as 35th among 84 journals in gastroenterology and hepatology (quartile in category Q2). CiteScore (2018): 3.43.

RESPONSIBLE EDITORS FOR THIS ISSUE

Responsible Electronic Editor: *Yu-Jie Ma*

Proofing Production Department Director: *Xiang Li*

NAME OF JOURNAL
World Journal of Gastroenterology

ISSN
ISSN 1007-9327 (print) ISSN 2219-2840 (online)

LAUNCH DATE
October 1, 1995

FREQUENCY
Weekly

EDITORS-IN-CHIEF
Subrata Ghosh, Andrzej S Tarnawski

EDITORIAL BOARD MEMBERS
http://www.wjgnet.com/1007-9327/editorialboard.htm

EDITORIAL OFFICE
Ze-Mao Gong, Director

PUBLICATION DATE
March 21, 2020

INSTRUCTIONS TO AUTHORS
https://www.wjgnet.com/bpg/gerinfo/204

GUIDELINES FOR ETHICS DOCUMENTS
https://www.wjgnet.com/bpg/GerInfo/287

GUIDELINES FOR NON-NATIVE SPEAKERS OF ENGLISH
https://www.wjgnet.com/bpg/gerinfo/240

PUBLICATION MISCONDUCT
https://www.wjgnet.com/bpg/gerinfo/208

ARTICLE PROCESSING CHARGE
https://www.wjgnet.com/bpg/gerinfo/242

STEPS FOR SUBMITTING MANUSCRIPTS
https://www.wjgnet.com/bpg/GerInfo/239

ONLINE SUBMISSION
https://www.f6publishing.com

World Journal of Gastroenterology

Submit a Manuscript: https://www.f6publishing.com

World J Gastroenterol 2020 March 21; 26(11): 1107-1112

DOI: 10.3748/wjg.v26.i11.1107

ISSN 1007-9327 (print) ISSN 2219-2840 (online)

OPINION REVIEW

Current status of endoscopic sleeve gastroplasty: An opinion review

Jiunn-Wei Wang, Chih-Yen Chen

ORCID number: Jiunn-Wei Wang (0000-0003-2534-438X); Chih-Yen Chen (0000-0003-0937-0596).

Author contributions: Chen CY conceived and designed the study; Wang JW reviewed the literature and wrote the manuscript; Chen CY and Wang JW made critical revisions and approved the final version of the manuscript.

Conflict-of-interest statement: Jiunn-Wei Wang and Chih-Yen Chen have no potential conflicts of interest to declare.

Manuscript source: Invited manuscript

Received: November 12, 2019
Peer-review started: November 12, 2019
First decision: February 24, 2020
Revised: February 27, 2020
Accepted: March 9, 2020
Article in press: March 9, 2020
Published online: March 21, 2020

P-Reviewer: Fogli L
S-Editor: Wang YQ
L-Editor: A

Jiunn-Wei Wang, Division of Gastroenterology, Department of Internal medicine, Kaohsiung Medical University Hospital, Kaohsiung 80756, Taiwan

Jiunn-Wei Wang, Department of Medicine, College of Medicine, Kaohsiung Medical University, Kaohsiung 80756, Taiwan

Jiunn-Wei Wang, Graduate Institute of Clinical Medicine, College of Medicine, Kaohsiung Medical University, Kaohsiung 80756, Taiwan

Chih-Yen Chen, Division of Gastroenterology and Hepatology, Department of Medicine, Taipei Veterans General Hospital, Taipei 11217, Taiwan

Chih-Yen Chen, Endoscopy Center for Diagnosis and Treatment, Taipei Veterans General Hospital, Taipei 11217, Taiwan

Chih-Yen Chen, Faculty of Medicine and Institute of Emergency and Critical Medicine, National Yang-Ming University School of Medicine, Taipei 11217, Taiwan

Chih-Yen Chen, Institutional Review Board, Taipei Veterans General Hospital, Taipei 11217, Taiwan

Chih-Yen Chen, Chinese Taipei Society for the Study of Obesity, Taipei 11031, Taiwan

Corresponding author: Chih-Yen Chen, AGAF, MD, PhD, Professor, Division of Gastroenterology and Hepatology, Department of Medicine, Taipei Veterans General Hospital, 201, Section 2, Shih-Pai Road, Taipei 11217, Taiwan. chency@vghtpe.gov.tw

Abstract

Bariatric surgeries have been demonstrated to be safe and effective treatment options for morbid obesity patients, but operative risks and high health care costs limit their clinical application. Endoscopic bariatric therapies are emerging as valuable alternatives for patients with doubts about bariatric surgery or ineligible for it. Endoscopic sleeve gastroplasty (ESG), a relatively novel technique of endoscopic bariatric therapies, has gained standing in the past few years. The safety, feasibility, repeatability, and potential for reversibility of ESG have been proven by multicenter studies. Compared to other weight loss strategies, current evidence demonstrates that ESG offers satisfactory efficacy in weight loss. Even though it is inferior to laparoscopic sleeve gastrectomy, it has lower risks of adverse events than surgical interventions and intragastric balloon within one-year follow-up. Furthermore, ESG may be the ideal weight control strategy for patients who have poor adherence to behavioral interventions. Even so, trends in decreased weight loss effect over time, post-procedure weight regain, post-procedure gut hormone alteration, and possible effects of race and ethnicity on ESG still remain undetermined due to very limited reports and very short follow-

E-Editor: Ma YJ

ups. Further clinical trials are required to validate and answer these questions.

Key words: Obesity; Endoscopic bariatric therapy; Endoscopic sleeve gastroplasty; Laparoscopic sleeve gastrectomy; Intragastric balloon; Behavioral weight loss intervention

Core tip: Endoscopic sleeve gastroplasty offers satisfactory efficacy in weight loss, even though it is inferior to laparoscopic sleeve gastrectomy and has lower risks of adverse events than surgical interventions and intragastric balloon within one-year follow-up. Furthermore, it may be the ideal weight control strategy for patients who have poor adherence to behavioral interventions.

Citation: Wang JW, Chen CY. Current status of endoscopic sleeve gastroplasty: An opinion review. *World J Gastroenterol* 2020; 26(11): 1107-1112
URL: https://www.wjgnet.com/1007-9327/full/v26/i11/1107.htm
DOI: https://dx.doi.org/10.3748/wjg.v26.i11.1107

INTRODUCTION

Growing prevalence of obesity has become a current worldwide public health epidemic in adults, children, and adolescents. The increasing trend in obesity is also of concern owing to the high comorbidity and mortality in obesity patients and the expanding economic burden for society[1,2]. Bariatric surgeries have been demonstrated to be safe and effective treatment options for morbid obesity patients, but low patient acceptance due to fear of operative risks and high health care costs limit its clinical application[3]. In this situation, endoscopic bariatric therapies (EBTs), with their characteristics of minimally invasive nature, reversibility, and high applicability, are emerging as valuable alternatives for patients with doubts about bariatric surgery or ineligible for it[4]. Endoscopic sleeve gastroplasty (ESG), a relatively novel technique of EBTs, was first published by the Mayo Clinic in the USA in 2013 and has gained standing in the past few years[5]. ESG is an incisionless transoral endoscopic procedure that uses a full-thickness endoscopic suturing system to reduce stomach volume into a tubular gastric cavity[6]. The safety, feasibility, repeatability, and potential for reversibility of ESG have been shown by several multicenter studies[7,8]. Furthermore, there are many studies making a direct comparison between ESG and other weight loss strategies[9-12], which are separately discussed in the following sections.

ESG *VS* LAPAROSCOPIC SLEEVE GASTRECTOMY

Laparoscopic sleeve gastrectomy (LSG) is the most popular restrictive bariatric surgical procedure because of its high efficiency in weight loss, reduction in obesity-related morbidities, and simple surgical technique[13]. Novikov *et al*[9] conducted an unmatched cohort study to compare the outcomes of ESG with surgical interventions. The study showed that LSG achieved greater body mass index (BMI) decrease and percent total body weight loss (%TBWL) than ESG at 12-mo follow-up (29.28% *vs* 17.57%, $P < 0.001$). Furthermore, and there were no significant differences ($P = 0.21$) in %TBWL between the two procedures in the subgroup of patients with BMI < 40 kg/m^2 after multivariable adjustment. Significantly lower post-procedure length of stay (0.34 d ± 0.73 d *vs* 3.09 d ± 1.47 d, $P < 0.01$) and adverse event rate (2.20% *vs* 9.17%, $P < 0.05$) were both observed in ESG compared with those in LSG. The other case-match study by Fayad *et al*[10] enrolled 54 ESG and 83 LSG patients. ESG initially presented more %TBWL and BMI decrease than LSG at 30 d (9.8% *vs* 6.6%, $P < 0.001$; 9.4% *vs* 6.7%, $P < 0.001$, respectively), but reverse outcomes in both %TBWL and BMI decrease for ESG and LSG (17.1% *vs* 23.6%, $P < 0.001$; 17.2% *vs* 23.7%, $P < 0.001$, respectively) were shown at 6-mo follow-up. Moreover, a significantly lower rate of adverse events was observed in ESG than in LSG (5.2 *vs* 16.9%, $P < 0.05$), especially in new onset gastroesophageal reflux disease (1.9% *vs* 14.5%, $P < 0.05$). Both comparison

studies both demonstrated the superior weight loss effects of LSG and increased safety of ESG at 6-mo and 12-mo follow-up. In addition, the recent case-match retrospective study evaluated 6-mo quality of life after operation between 23 pairs of ESG and LSG patients with questionnaire[14]. ESG cohort reported significantly better results in gastrointestinal symptoms subdomain than LSG cohort (P = 0.001). No ESG patients but 7 LSG patients developed postoperative gastroesophageal reflux disease and required daily proton-pump inhibitors use (P = 0.004). Nevertheless, the current results are limited due to the retrospective nature of the studies and short-term follow-up, and they should be validated in future randomized controlled trials with longer follow-up.

ESG *VS* INTRAGASTRIC BALLOON INSERTION

EBTs have several promising applications in metabolic obesity disease, and one of them is intragastric balloon (IGB), whose efficacy in body weight loss and safety were demonstrated by a systematic review and meta-analysis[15]. IGB was introduced 30 years ago and underwent several upgraded product developments but, so far, weight regain remains the major limitation because of necessary removal of the balloon at 6 mo[16]. Likewise, ESG, a new emerging EBT, presented satisfactory effects against obesity disease. One recent retrospective study reported by Fayad and his colleague compared the two EBTs (ESG and IGB)[11]. All 58 ESG and 47 IGB patients achieved meaningful body weight loss. The ESG group showed significant higher mean %TBWL than the IGB group over 12 mo post-procedure (at 12-mo follow-up, 21.3% *vs* 13.9%, P = 0.005, respectively). Notably, a decreasing trend in %TBWL was seen in the ESG group and decreasing %TBWL presented after 6 mo for the IGB group, which can be explained by balloon removal at 6 mo. There was a significantly lower rate of adverse events in the ESG group than in the IGB group (5.2% *vs* 17.0%, P = 0.048, respectively). Up to 17% of IGB patients had adverse events requiring balloon removal, and these events completely subsided after balloon removal. In contrast, ESG-associated adverse events are more likely to require medical treatment. This study provided evidence that ESG may be a more appropriate EBT than IGB in clinical practice even with limitation of selection bias.

ESG *VS* BEHAVIORAL INTERVENTIONS

The United States Department of Health and Human Services has proposed lifestyle interventions, such as dietary therapy and physical activity, as first-line treatment for weight loss and maintenance since 1998[17]. One systemic review and meta-analysis revealed that behavioral interventions bring about small but significant benefits for weight loss and maintenance[18]. Certain obese patients prefer these non-surgical interventions over invasive therapies. Cheskin *et al*[12] conducted a case-matched study of 105 patients who underwent ESG and 281 patients who underwent high-intensity diet and lifestyle therapy (HIDLT) to compare weight loss between the two groups. The ESG group had a significantly greater mean %TBWL than the HIDLT group throughout the 12-mo follow-up (20.6% *vs* 14.3%, respectively). It is worth noting that ESG had no superiority in weight loss over 6 mo post-procedure compared with HIDLT in BMI > 40 kg/m^2 patients. In addition, a low proportion of patients (4.8%) experienced moderate-to-severe adverse events in the ESG group, and no subjects suffered from any adverse event in the HIDLT group. Consequently, ESG is likely a valuable alternative for patients who do not comply with HIDLT.

CONCLUSION

Current evidence, summarized in Table 1, indicates that ESG offers satisfactory efficacy in weight loss even if inferior to LSG, and has lower risks of adverse events compared to surgical interventions and IGB within one-year follow-up. Moreover, ESG may be the ideal weight control strategy for patients who have poor adherence to behavioral interventions. Even so, the reasons for the trends in decreased weight loss effect with time and post-procedure weight regain in ESG still remain undetermined. As gut hormones[19,20], cytokines[21], adipokines[22], hepatokines[23], and bile acids[24] play important roles in promoting weight loss, ameliorating type 2 diabetes mellitus and improving fatty liver disease, basic mechanistic insights into EBT, including ESG, are required. Since the Y-Y paradox exists between Caucasians and Asians[25], direct extrapolation of the results obtained from Western countries may not be proper in

Eastern countries. Thus, analyses of the possible effects of race, ethnicity, and comorbidities on weight loss outcomes in each cohort become more and more imperative. With very limited reports and very short follow-ups, this novel endoscopic technique for obesity treatment, ESG, will require more large-scale randomized controlled trials in order to validate its clinical efficacy and safety in long-term follow-up.

Table 1 Summary of comparison studies for weight control strategies

Ref.	Type of study	Comparison	Subject numbers	Length of follow-up (mo)	Weight loss efficacy (%TBWL)	Adverse event rate
Novikov *et al*[9] 2018	Retrospective cohort study, case-unmatched	ESG *vs* LSG *vs* LABG	91 ESG/120 LSG/67 LAGB	12	LSG (29.28%) > ESG (17.57%) > LAGB (13.30%), $P < 0.001$	LSG (9.17%) > LAGB (8.96%) > ESG (2.20%), $P < 0.05$
Fayad *et al*[10] 2019	Retrospective cohort study, case-matched	ESG *vs* LSG	54 ESG/83 LSG	6	LSG (23.6%) > ESG (17.1%), $P < 0.001$	LSG (16.9%) > ESG (5.2%), $P < 0.05$
Fiorillo *et al*[14] 2020	Retrospective cohort study, case-matched	ESG *vs* LSG	23 ESG/23 LSG	6	LSG (18.8%) > ESG (13.4%), $P = 0.03$	GERD symptoms LSG (30.7%) > ESG (0%), $P = 0.004$
Fayad *et al*[11] 2019	Retrospective cohort study, case-matched	ESG *vs* IGB	58 ESG/47 IGB	12	ESG (21.3%) > IGB (13.9%), $P = 0.005$	IGB (17.0%) > ESG (5.2%), $P = 0.048$
Cheskin *et al*[12] 2019	Retrospective cohort study, case-unmatched	ESG *vs* HIDLT	105 ESG/281 HIDLT	12	ESG (20.6%) > HIDLT (14.3%), $P < 0.001$	ESG (4.8%) > HIDLT (0.0%)

ESG: Endoscopic sleeve gastroplasty; GERD: Gastroesophageal reflux disease; HIDLT: High-intensity diet and lifestyle therapy; IGB: Intragastric balloon; LAGB: Laparoscopic adjustable gastric banding; LSG: Laparoscopic sleeve gastrectomy; %TBWL: Percent total body weight loss.

REFERENCES

1 **Flegal KM**, Kit BK, Orpana H, Graubard BI. Association of all-cause mortality with overweight and obesity using standard body mass index categories: a systematic review and meta-analysis. *JAMA* 2013; **309**: 71-82 [PMID: 23280227 DOI: 10.1001/jama.2012.113905]

2 **Wu WC**, Lee WJ, Yeh C, Chen SC, Chen CY. Impacts of Different Modes of Bariatric Surgery on Plasma Levels of Hepassocin in Patients with Diabetes Mellitus. *Reports* 2019; **2**: 24 [DOI: 10.3390/reports2040024]

3 **Welbourn R**, Pournaras DJ, Dixon J, Higa K, Kinsman R, Ottosson J, Ramos A, van Wagensveld B, Walton P, Weiner R, Zundel N. Bariatric Surgery Worldwide: Baseline Demographic Description and One-Year Outcomes from the Second IFSO Global Registry Report 2013-2015. *Obes Surg* 2018; **28**: 313-322 [PMID: 28822052 DOI: 10.1007/s11695-017-2845-9]

4 **Hill C**, Khashab MA, Kalloo AN, Kumbhari V. Endoluminal weight loss and metabolic therapies: current and future techniques. *Ann N Y Acad Sci* 2018; **1411**: 36-52 [PMID: 28884820 DOI: 10.1111/nyas.13441]

5 **Abu Dayyeh BK**, Rajan E, Gostout CJ. Endoscopic sleeve gastroplasty: a potential endoscopic alternative to surgical sleeve gastrectomy for treatment of obesity. *Gastrointest Endosc* 2013; **78**: 530-535 [PMID: 23711556 DOI: 10.1016/j.gie.2013.04.197]

6 **Lopez-Nava G**, Galvão MP, da Bautista-Castaño I, Jimenez A, De Grado T, Fernandez-Corbelle JP. Endoscopic sleeve gastroplasty for the treatment of obesity. *Endoscopy* 2015; **47**: 449-452 [PMID: 25380508 DOI: 10.1055/s-0034-1390766]

7 **Lopez-Nava G**, Sharaiha RZ, Vargas EJ, Bazerbachi F, Manoel GN, Bautista-Castaño I, Acosta A, Topazian MD, Mundi MS, Kumta N, Kahaleh M, Herr AM, Shukla A, Aronne L, Gostout CJ, Abu Dayyeh BK. Endoscopic Sleeve Gastroplasty for Obesity: a Multicenter Study of 248 Patients with 24 Months Follow-Up. *Obes Surg* 2017; **27**: 2649-2655 [PMID: 28451929 DOI: 10.1007/s11695-017-2693-7]

8 **Sartoretto A**, Sui Z, Hill C, Dunlap M, Rivera AR, Khashab MA, Kalloo AN, Fayad L, Cheskin LJ, Marinos G, Wilson E, Kumbhari V. Endoscopic Sleeve Gastroplasty (ESG) Is a Reproducible and Effective Endoscopic Bariatric Therapy Suitable for Widespread Clinical Adoption: a Large, International Multicenter Study. *Obes Surg* 2018; **28**: 1812-1821 [PMID: 29450845 DOI: 10.1007/s11695-018-3135-x]

9 **Novikov AA**, Afaneh C, Saumoy M, Parra V, Shukla A, Dakin GF, Pomp A, Dawod E, Shah S, Aronne LJ, Sharaiha RZ. Endoscopic Sleeve Gastroplasty, Laparoscopic Sleeve Gastrectomy, and Laparoscopic Band for Weight Loss: How Do They Compare? *J Gastrointest Surg* 2018; **22**: 267-273 [PMID: 29110192 DOI: 10.1007/s11605-017-3615-7]

10 **Fayad L**, Adam A, Schweitzer M, Cheskin LJ, Ajayi T, Dunlap M, Badurdeen DS, Hill C, Paranji N, Lalezari S, Kalloo AN, Khashab MA, Kumbhari V. Endoscopic sleeve gastroplasty versus laparoscopic sleeve gastrectomy: a case-matched study. *Gastrointest Endosc* 2019; **89**: 782-788 [PMID: 30148991 DOI: 10.1016/j.gie.2018.08.030]

11 **Fayad L**, Cheskin LJ, Adam A, Badurdeen DS, Hill C, Agnihotri A, Dunlap M, Simsek C, Khashab MA, Kalloo AN, Kumbhari V. Endoscopic sleeve gastroplasty versus intragastric balloon insertion: efficacy, durability, and safety. *Endoscopy* 2019; **51**: 532-539 [PMID: 30841009 DOI: 10.1055/a-0852-3441]

12 **Cheskin LJ**, Hill C, Adam A, Fayad L, Dunlap M, Badurdeen D, Koller K, Bunyard L, Frutchey R, Al-Grain H, Kahan S, Hedjoudje A, Khashab MA, Kalloo AN, Kumbhari V. Endoscopic sleeve gastroplasty versus high-intensity diet and lifestyle therapy: a case-matched study. *Gastrointest Endosc* 2020; **91**: 342-349.e1 [PMID: 31568769 DOI: 10.1016/j.gie.2019.09.029]

13 **Benaiges D**, Más-Lorenzo A, Goday A, Ramon JM, Chillarón JJ, Pedro-Botet J, Flores-Le Roux JA. Laparoscopic sleeve gastrectomy: More than a restrictive bariatric surgery procedure? *World J Gastroenterol* 2015; **21**: 11804-11814 [PMID: 26557004 DOI: 10.3748/wjg.v21.i41.11804]

14 **Fiorillo C**, Quero G, Vix M, Guerriero L, Pizzicannella M, Lapergola A, D'Urso A, Swanstrom L, Mutter D, Dallemagne B, Perretta S. 6-Month Gastrointestinal Quality of Life (QoL) Results after Endoscopic Sleeve Gastroplasty and Laparoscopic Sleeve Gastrectomy: A Propensity Score Analysis. *Obes Surg* 2020 [PMID: 31965488 DOI: 10.1007/s11695-020-04419-1]

15 **ASGE Bariatric Endoscopy Task Force and ASGE Technology Committee**, Abu Dayyeh BK, Kumar

N, Edmundowicz SA, Jonnalagadda S, Larsen M, Sullivan S, Thompson CC, Banerjee S. ASGE Bariatric Endoscopy Task Force systematic review and meta-analysis assessing the ASGE PIVI thresholds for adopting endoscopic bariatric therapies. *Gastrointest Endosc* 2015; **82**: 425-438.e5 [PMID: 26232362 DOI: 10.1016/j.gie.2015.03.1964]

16 **Genco A**, López-Nava G, Wahlen C, Maselli R, Cipriano M, Sanchez MM, Jacobs C, Lorenzo M. Multi-centre European experience with intragastric balloon in overweight populations: 13 years of experience. *Obes Surg* 2013; **23**: 515-521 [PMID: 23224509 DOI: 10.1007/s11695-012-0829-3]

17 Clinical Guidelines on the Identification, Evaluation, and Treatment of Overweight and Obesity in Adults--The Evidence Report. National Institutes of Health. *Obes Res* 1998; **6** Suppl 2: 51S-209S [PMID: 9813653]

18 **Dombrowski SU**, Knittle K, Avenell A, Araújo-Soares V, Sniehotta FF. Long term maintenance of weight loss with non-surgical interventions in obese adults: systematic review and meta-analyses of randomised controlled trials. *BMJ* 2014; **348**: g2646 [PMID: 25134100 DOI: 10.1136/bmj.g2646]

19 **Lee WJ**, Chen CY, Chong K, Lee YC, Chen SC, Lee SD. Changes in postprandial gut hormones after metabolic surgery: a comparison of gastric bypass and sleeve gastrectomy. *Surg Obes Relat Dis* 2011; **7**: 683-690 [PMID: 21996600 DOI: 10.1016/j.soard.2011.07.009]

20 **Lee WJ**, Chen CY, Ser KH, Chong K, Chen SC, Lee PC, Liao YD, Lee SD. Differential influences of gastric bypass and sleeve gastrectomy on plasma nesfatin-1 and obestatin levels in patients with type 2 diabetes mellitus. *Curr Pharm Des* 2013; **19**: 5830-5835 [PMID: 23768444 DOI: 10.2174/13816128113198880010]

21 **Chen CY**, Lee WJ, Asakawa A, Fujitsuka N, Chong K, Chen SC, Lee SD, Inui A. Insulin secretion and interleukin-1β dependent mechanisms in human diabetes remission after metabolic surgery. *Curr Med Chem* 2013; **20**: 2374-2388 [PMID: 23531221 DOI: 10.2174/09298673113201800008]

22 **Chen YC**, Inui A, Chang ES, Chen SC, Lee WJ, Chen CY. Comparison of gut hormones and adipokines stimulated by glucagon test among patients with type II diabetes mellitus after metabolic surgery. *Neuropeptides* 2016; **55**: 39-45 [PMID: 26621498 DOI: 10.1016/j.npep.2015.11.002]

23 **Huang HH**, Yeh C, Chen JC, Lee TH, Chen SC, Lee WJ, Chen CY. Does bariatric surgery influence plasma levels of fetuin-A and leukocyte cell-derived chemotaxin-2 in patients with type 2 diabetes mellitus? *PeerJ* 2018; **6**: e4884 [PMID: 29910974 DOI: 10.7717/peerj.4884]

24 **Huang HH**, Lee WJ, Chen SC, Chen TF, Lee SD, Chen CY. Bile Acid and Fibroblast Growth Factor 19 Regulation in Obese Diabetics, and Non-Alcoholic Fatty Liver Disease after Sleeve Gastrectomy. *J Clin Med* 2019; 8: E815 [PMID: 31181641 DOI: 10.3390/jcm8060815]

25 **Chen CY**, Tsai CY. From endocrine to rheumatism: do gut hormones play roles in rheumatoid arthritis? *Rheumatology (Oxford)* 2014; **53**: 205-212 [PMID: 23882111 DOI: 10.1093/rheumatology/ket255]

World Journal of Gastroenterology

Submit a Manuscript: https://www.f6publishing.com

World J Gastroenterol 2020 March 21; 26(11): 1113-1127

DOI: 10.3748/wjg.v26.i11.1113

ISSN 1007-9327 (print) ISSN 2219-2840 (online)

REVIEW

Circulating microRNAs as non-invasive biomarkers for hepatitis B virus liver fibrosis

Diana Gabriela Iacob, Adelina Rosca, Simona Maria Ruta

ORCID number: Diana Gabriela Iacob (0000-0003-2256-458X); Adelina Rosca (0000-0002-8003-2816); Simona Maria Ruta (0000-0002-2492-6073).

Author contributions: All authors contributed equally to this paper with conception and design of the study, literature review and analysis, drafting and critical revision and editing, and approval of the final version.

Supported by Ministerul Cercetarii si Inovarii, Programul 1, subprogramul 1.2. Performanta institutionala, No. PFE_23/2018.

Conflict-of-interest statement: Authors declare no conflict of interest.

Manuscript source: Invited manuscript

Received: December 20, 2019
Peer-review started: December 20, 2019
First decision: January 12, 2020

Diana Gabriela Iacob, Infectious Diseases Department, "Carol Davila" University of Medicine and Pharmacy, Bucharest 050474, Romania

Diana Gabriela Iacob, Bucharest Emergency University Hospital, Bucharest 050098, Romania

Adelina Rosca, Simona Maria Ruta, Virology Department, Carol Davila University of Medicine and Pharmacy, Bucharest 050474, Romania

Adelina Rosca, Simona Maria Ruta, Viral Emerging Diseases Department, Ștefan S. Nicolau Institute of Virology, Bucharest 030304, Romania

Corresponding author: Simona Maria Ruta, MD, PhD, Professor, Senior Researcher, Virology Chair, Virology Department, Carol Davila University of Medicine and Pharmacy, Eroii Sanitari 8, Bucharest 050474, Romania. simona.ruta@umfcd.ro

Abstract

Viruses can alter the expression of host microRNAs (miRNA s) and modulate the immune response during a persistent infection. The dysregulation of host miRNA s by hepatitis B virus (HBV) contributes to the proinflammatory and profibrotic changes within the liver. Multiple studies have documented the differential regulation of intracellular and circulating miRNA s during different stages of HBV infection. Circulating miRNA s found in plasma and/or extracellular vesicles can integrate data on viral-host interactions and on the associated liver injury. Hence, the detection of circulating miRNA s in chronic HBV hepatitis could offer a promising alternative to liver biopsy, as their expression is associated with HBV replication, the progression of liver fibrosis, and the outcome of antiviral treatment. The current review explores the available data on miRNA involvement in HBV pathogenesis with an emphasis on their potential use as biomarkers for liver fibrosis.

Key words: Hepatitis B virus; MicroRNA; Noncoding RNA; Liver fibrosis; Viral hepatitis; Non-invasive biomarkers; Extracellular vesicles; Hepatitis management

Core tip: The current review analyses the available data on the role of microRNAs (miRNA s) in the development and progression of liver fibrosis by focusing on their potential use as diagnostic and prognostic biomarkers for hepatitis B virus-infected patients. Cellular and circulating miRNA s (in plasma or extracellular vesicles) offer a unique glimpse into the virus-host relationship and the pathogenesis of chronic hepatitis

Revised: March 4, 2020
Accepted: March 9, 2020
Article in press: March 9, 2020
Published online: March 21, 2020

P-Reviewer: Esmat SM, Komatsu H, Rezaee-Zavareh MS, Said ZNA
S-Editor: Tang JZ
L-Editor: A
E-Editor: Zhang YL

B virus infection. The differential regulation of intracellular and circulating miRNA s during the natural and on treatment evolution of chronic hepatitis B is discussed.

Citation: Iacob DG, Rosca A, Ruta SM. Circulating microRNAs as non-invasive biomarkers for hepatitis B virus liver fibrosis. *World J Gastroenterol* 2020; 26(11): 1113-1127
URL: https://www.wjgnet.com/1007-9327/full/v26/i11/1113.htm
DOI: https://dx.doi.org/10.3748/wjg.v26.i11.1113

INTRODUCTION

MicroRNAs (miRNA s) are short noncoding RNAs involved in the epigenetic regulation of multiple intracellular and extracellular signalling pathways and in the posttranscriptional regulation of genes across numerous eukaryotic organisms[1-3]. Cellular miRNA s can modulate viral replication and the immune antiviral response[4,5]. Viruses can encode their own miRNA s[6] and can alter the cellular miRNome to create a favourable environment for viral replication or latency. Due to these complex roles, miRNA s have been increasingly evaluated as biomarkers for the diagnosis, prognosis and treatment of viral infections[7,8] as well as for distinct pathologies, including liver fibrosis.

Chronic hepatitis B virus (HBV) infection affects over 257 million people[9] and it is one of the most common causes of liver fibrosis. Liver fibrogenesis is a dynamic process, characterized by an excessive accumulation of extracellular matrix proteins in response to an ongoing liver inflammatory response, with gradual distortion of hepatic architecture and progression to liver cirrhosis[10]. Extracellular matrix is mainly synthesized by hepatic stellate cells (HSCs), which are activated following liver injury, together with proinflammatory cytokines and chemokines. Once activated, HSCs maintain this phenotype through autocrine or paracrine signalling loops[11]. Still, liver fibrosis is a reversible wound-healing process. Experimental studies have shown that an early detection and timely removal of the inciting factor can lead to a complete remission of the fibrotic changes, while interventions performed in later stages are less effective against the already formed architectural changes[12]. Furthermore, given the potential progression of liver fibrosis to hepatocellular carcinoma (HCC), an antifibrotic treatment would ideally need to be started early and would be precisely targeted against the molecular processes occurring at that stage.

Regarding HBV-associated fibrosis, between 8%-20% of untreated patients can progress to liver cirrhosis within 5 years depending on viral characteristics (HBV genotype, viral load, HBV mutations) and host-related factors (age, gender, other comorbidities or coinfections)[13]. Antiviral treatment, with either pegylated interferon-α or nucleoside analogues, halts or attenuates the development of fibrosis[14-18] and the initiation of treatment in the early stages of liver fibrosis is associated with a significant improvement of the histologic scores[17]. However, current treatment options do not ensure a complete cure of the HBV infection (with the elimination of viral reservoirs from hepatocytes) and a persistent activation of fibrotic signalling pathways is possible even in patients with undetectable HBV serum viral loads after treatment[19-21]. Hence, biomarkers which offer additional information on the viral-host interaction could potentially foreshadow new therapeutic agents.

Liver biopsy is currently the gold standard for a complete assessment of liver fibrosis, inflammation, and intrahepatic HBV replication. This technique is nevertheless limited by multiple risks and potential misclassifications, due to examiner variability and sampling[22]. Hence, a series of alternative non-invasive biomarkers have been proposed, including imaging data (elastographic techniques such as transient elastography, acoustic radiation force impulse imaging, two-dimensional shear wave elastography and magnetic resonance elastography), biochemical scores (APRI, Fib-4, Fibrotest), HBV RNA, and HBV core antigen[23-25] or even direct markers (molecules released in the serum following liver fibrogenesis of fibrolysis such as hyalyuronic acid, type IV collagen, matrix metalloproteases or tissue inhibitory metalloprotease-1)[26]. Non-invasive scores are more accessible, which explains why the World Health Organization recommends the use of Fib-4 and APRI for the assessment of liver fibrosis in HBV patients living in low-income countries[27]. Nevertheless, the diagnostic performance of these biomarkers in chronic HBV infection is moderate. Non-invasive methods are less reliable for the prediction of a specific stage of liver fibrosis, yet these can differentiate between an early and an

advanced stage of liver fibrosis or even cirrhosis (*e.g.*, F0-F1, ≥ F2 or ≥ F4)[26]. Therefore, combined scores with circulating and cellular miRNA s could represent an appealing alternative for the diagnosis and monitoring of viral-induced liver fibrosis[28] offering supplementary data on the viral-host interactions and the fibrotic signalling cascades in both the liver and blood.

The current review analyses the available data on the role of miRNA s in chronic hepatitis B, with an emphasis on their role in liver fibrogenesis and on their potential use as non-invasive biomarkers in the diagnosis, evolution, and treatment of HBV induced-liver fibrosis.

miRNA BIOGENSIS AND INTERFERENCE WITH HBV

Genes encoding for miRNA s are transcribed by the RNA polymerase II/III into primary RNA transcripts (pri-miRNA), further processed in the nucleus by the Drosha ribonuclease to a hairpin loop structure of ~ 60 nucleotides (the pre-miRNA transcript). Pre-miRNA s are further exported to the cytoplasm, where the Dicer enzyme cleaves the hairpin loop and leads to the mature double-stranded miRNA .

One strand of the mature miRNA is degraded, while the other one (less stable at the 5′ end) becomes the guide strand and is recruited into an RNA-induced silencing complex together with Argonaute proteins, TAR RNA-binding proteins, and other proteins and binds to the 3′ untranslated region of the target mRNAs[29]. Noncanonical interactions can also occur through "seed-like" motifs at the 5′ untranslated region or coding regions[30,31]. This intricate binding mechanism does not imply a perfect complementarity one miRNA can regulate one or more mRNAs, and multiple miRNA s can bind to the same mRNA. The concentrations of intracellular miRNA s are extremely variable, depending on the cellular context (cell cycle, metabolism, or differentiation) and concurrent pathologies. This variability could be exploited during viral-host interactions to influence viral tropism and hijack the host transcriptional machinery or to enable the host control on viral infections[32].

HBV modulates miRNA biogenesis by decreasing the expression of Drosha ribonuclease[33]. Novellino *et al*[34] showed that serum hepatitis B surface antigen (HBsAg) particles transport both Ago2 proteins and a series of miRNA s (miR-27a, miR-30b, miR-122, miR-126, miR-145, miR-106b, and miR-223) and identified a different miRNA profile in HBsAg particles and plasma[34]. Ago2 interacts with hepatitis B core antigen and HBsAg in various subcellular compartments of infected cells, indicating a potential role of HBV on miRNA packaging into extracellular vesicles (EVs)[35]. The function of extracellular miRNA s is not well elucidated, yet data on miRNA s found in EVs (like apoptotic bodies, microvesicles, or exosomes[36,37]) suggest multiple roles in paracrine signalling[38], epigenetic regulation of the recipient cell and regulation of the cellular inflammatory response, through the activation of toll-like receptor signalling pathways[39,40]. Incidentally, the first discovered HBV-encoded miRNA , HBV-miR-3[41] modulates the release of HBV virions and is also incorporated into exosomes and HBV core particles but not into HBsAg subviral particles. It would be interesting to explore if this differential packaging is the result of a viral-host competition and sequestration of host/viral miRNA s into a certain particle and further exploit these findings for diagnostic or therapeutic purposes.

miRNA S AS KEY REGULATORS OF LIVER FIBROSIS

Host-encoded miRNA s

Intracellular miRNA : There is a significant amount of data documenting the role of cellular miRNA s in liver fibrosis but no consensus on their exact regulatory functions. Various miRNA s are being proposed as either profibrotic or antifibrotic (Figure 1). This classification is theoretical, based on predicted signalling pathways and reports from various studies[42-44]. Overall, miRNA s modulate numerous steps during the development of liver fibrosis, including: HSC activation, proliferation, migration, and apoptosis[45-49]; transcription of profibrogenic factors and signalling pathways (such as Col1a1, transforming growth factor beta (TGFβ)-RII[46,47], SPRY2, HNF4a[48], matrix metalloproteinases[49,50], MeCP2[51], retinoid X receptor alpha[52]); modulation of the immune response and intrahepatic recruitment of inflammatory cells, indirectly contributing to the release of profibrotic cytokines such as tumor necrosis factor alpha, Interleukin-6, and Interleukin-1β, regulation of interferon gamma signalling and of the inflammasome pathway[57-60], regulatory activity on the metabolism of lipids, drugs, and alcohol[50,57,58,61]; and the regulation of angiogenesis[63].

The complete characterization of intracellular miRNA s is nevertheless difficult

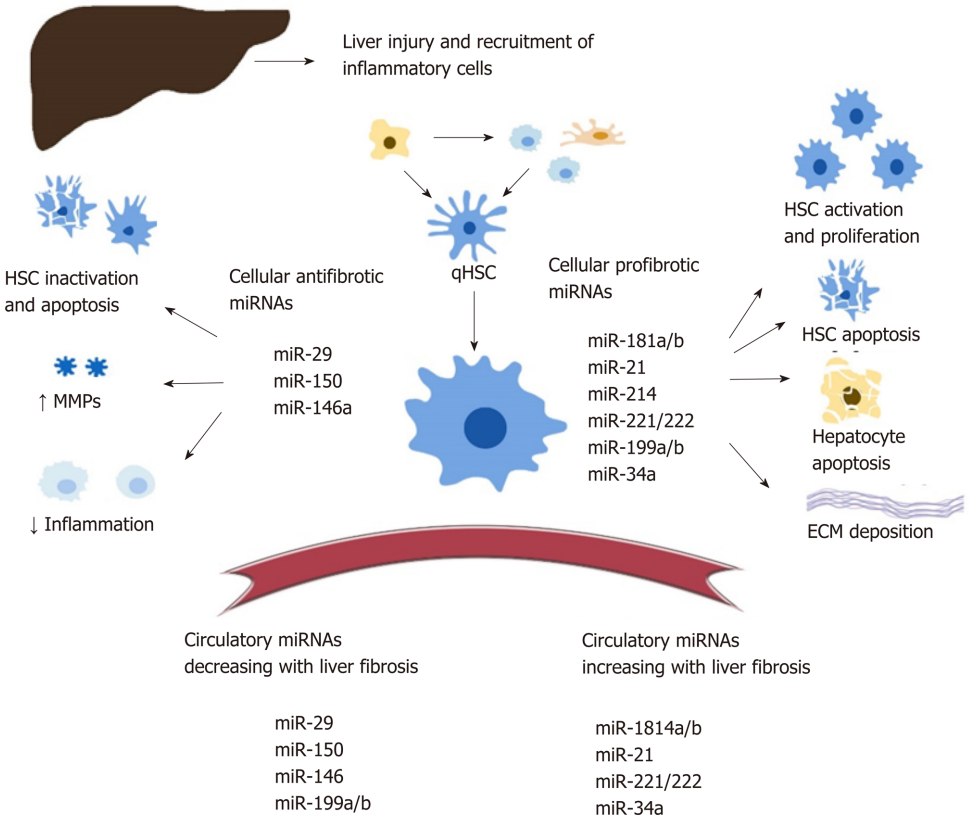

Figure 1 Profibrotic and antifibrotic intrahepatic and circulating microRNAs. MMP: Matrix metalloproteases, qHSC: Quiescent hepatic stellate cell, aHSC: Activated hepatic stellate cell; MiR: MicroRNA.

given that one miRNA can modulate multiple signalling pathways in various tissues. For example, miR-34 mediates both HSC activation through peroxisome proliferator-activated receptor gamma signalling[64] and hepatocyte apoptosis through the miR-34/sirtuin-1/p53 cascade[65]. On the other hand, miR-34a-5p can also display an antifibrotic role within HSC, as its overexpression was correlated with the downregulation of the TGFβ/Smad3 pathway[66].

Both miR-181b and miR-21 favour HSC activation through the inhibition of phosphatase and tensin homolog and activation of the phosphatidylinositol 3-kinase/Akt pathway[67,68]. MiR-29b, a significant antifibrotic cellular miRNA , induces HCS apoptosis, regulates the HSC phenotype, and decreases extracellular matrix synthesis through multiple signalling pathways (TGF-β / Smad, lipopolysaccharide / NF-kB, and oestradiol)[69-72]. HSC activation is also downregulated by multiple antifibrotic miRNA s, including miR-146 through the suppression of TGF-β / Smad[73], and miR-150 through c-myB and Sp1 signalling pathways[74,75].

Circulating miRNA s

Circulating miRNA s found in the plasma or serum have been extensively studied in the pathogenesis of liver disease due to various aetiologies, including viral hepatitis, nonalcoholic steatohepatitis and alcoholic liver disease, drug-associated liver injury, and HCC[62,76-79].

Circulating miRNA s correlate with the presence and progression of liver fibrosis and necroinflammation and can be used to predict the survival of patients with cirrhosis or HCC[80-82]. The link between circulating and cellular miRNA s is still under investigation. In this respect, Table 1 provides a correlation between the regulation of various miRNA s found in the serum and liver of patients with HBV infection.

miRNA S IN EVS

EVs are secreted in multiple body fluids and ensure the transport of various proteins, lipids or RNAs including miRNA s. Intrahepatic miRNA s are packaged into EVs and released from injured hepatocytes to further mediate the survival/proliferation or

Table 1 Circulating and intrahepatic microRNA regulation and target processes involved in liver fibrogenesis in hepatitis B virus infection

MicroRNA	Plasma level	Liver tissue	Mediated processes involved in liver fibrosis	Ref.
miR-34a	↑	↑	Cell-cycle regulator (cell differentiation, proliferation, metabolism, apoptosis); HSC activation	Guo *et al*[45]; Singh *et al*[42]
miR-221 miR-222	↑	↑	Collagen synthesis; HSC proliferation; Liver fibrosis; Oncogenesis	Singh *et al*[42]
miR 27a/b	↑	↑	HSC activation, differentiation and proliferation	Zhang *et al*[131]
miR 181a/b	↑	↑	Cell cycle regulator; HSC activation and proliferation	Yu *et al*[132]
miR 199a/b	↓	↑	HSC activation	Murakami *et al*[91]
miR-223	↓; ↓ EVs	↑	Inflammatory response	Akamatsu *et al*[133]; Bao *et al*[43]; Ye *et al*[59]; Wang *et al*[106]
miR-125 (-125a-5p/ -125b)	↑	↑	HSC activation, proliferation	Zheng *et al*[134]; You *et al*[49]
miR 21-5p	↑in total plasma; ↓ in EVs	↑	Collagen synthesis; Oncogenesis	Bao *et al*[43]; Wei *et al*[68]; Wang *et al*[135]

↑ means upregulation. ↓ means downregulation. EVs: Extracellular vesicles; HSC: Hepatic stellate cell; miR: MicroRNA.

infection in neighbouring cells[83-85]. Additionally, miRNA s associated to EVs have been shown to play various roles in cell-to-cell communication between parenchymatous and non-parenchymatous cells (such as HSCs, liver sinusoidal endothelial cells, Kupffer cells, or cholangiocytes). Extracellular miRNA s have been shown to mediate both profibrotic and antifibrotic signalling cascades. For example, hepatitis C virus-infected hepatocytes release EVs containing miR-192 or miR-19a that induce profibrotic TGFβ signalling pathways and activate HSCs[86,87]. Quiescent HSCs release EVs containing miR-214 and miR-199a-5p in order to downregulate fibrogenic pathways in neighbouring activated HSCs and hepatocytes[88,89]. The antifibrotic potential of these EVs is particularly intriguing given that both miR-214 and miR-199a-5p/3p have been known for their profibrotic action[48,90,91].

Compared to the miRNA s found in the total plasma, EVs can display different miRNA concentrations and even discordant miRNA subsets[92]. Lambrecht *et al*[93] showed that the same miRNA species can be upregulated in the serum and downregulated in the EVs and suggested that the miRNA signature from circulating EVs reflects the profile found in the vesicles released by activated HSCs *in vitro*. These discrepancies can also indicate either a higher stability of miRNA s packaged into EVs against plasma ribonucleases, different intercellular signalling mechanisms[94,95] or could be attributed to the distinct methodology used for miRNA detection and quantification.

HBV-encoded miRNA s

Current data on circulating miRNA s in HBV cirrhosis are limited to host-miRNA s. The only confirmed HBV-encoded miRNA , HBV-miR-3 is released in the circulation packed in HBV virions and EVs[41]. Given that HBV-miR-3 downregulates the synthesis of HBV virions, it is probable that this miRNA plays a role in the establishment of chronic HBV infection. Hence, the incorporation of HBV-miR-3 into a miRNA diagnostic score could help indicate the contribution of intrahepatic HBV replication to the development of liver inflammation and fibrosis. However, no data are currently available on the role of HBV-miR-3 in HBV-associated liver fibrosis/cirrhosis.

miRNA S DETECTION AND QUANTIFICATION

The assessment of miRNA profiles involves the extraction of total RNA and quality control analysis of this purified fraction, followed by their quantification using either reverse-transcription PCR, microarrays, or even next-generation RNA sequencing.

Compared to other non-invasive biomarkers, circulating miRNA s are better able to withstand a low pH, extreme temperatures, ribonucleases, and multiple freeze-thaw cycles[96]. Still, the interpretation of miRNA concentration requires a careful consideration of the methodology, as it depends on the timing of the sample collection, the isolation protocol[97] (*e.g*., plasma *vs* serum; miRNA s in exosomes *vs* free miRNA s in plasma or serum) and on the normalization method[98]. Currently, there are various approaches for normalization, including the use of exogenous spike-ins (such as cel-miR-39 from *Caenorhabditis elegans*), geometrical mean of the quantification cycle for the analysed miRNA s, and the use of one or more endogenous miRNA s, small RNAs, or even miRNA /small RNA constructs as reference points[99,100].

CIRCULATING miRNA S AS POTENTIAL BIOMARKERS OF LIVER FIBROSIS

One of the most important challenges for the use of circulating miRNA s in the clinical setting resides in their lack of specificity for a distinct tissue[101]. With few exceptions, such as miR-122, which accounts for an estimated 70% of all miRNA s in the liver[102], other miRNA s are less specific for the liver. Moreover, the significance of circulating miRNA s in chronic liver diseases is complicated by the simultaneous development of the necroinflammatory process and scarring as well as by the potential viral-host interactions. For example serum/plasma miR-122 appears to increase with the progression of the liver necro-inflammatory activity in patients with chronic hepatitis, including those with established liver fibrosis[103], yet it also varies with HBV replication within the liver. Hence, when looking at miRNA expression, a critical interpretation in the clinical context is required.

The circulating miRNA s associated with liver fibrosis differ between studies, and there is still no consensus on their uses as biomarkers of choice for the diagnosis, staging, or prognosis of liver fibrosis.

miRNA s for detection of liver fibrosis

The individual expression of miRNA s in plasma/serum can reach a moderate accuracy for the detection of liver fibrosis. Such an example is miR-29, an antifibrotic miRNA that exhibits an area under the curve between 0.619 to 0.838 in various studies[43,47,69]. The use of multiple miRNA s or the combination of noncoding RNAs and of other laboratory markers have significantly increased their diagnostic and prognostic accuracy[79,104-106]. Individual miRNA s and composite scores for liver fibrosis in HBV-infected patients are shown in Table 2 and Table 3. In a meta-analysis by Guo *et al*[79], the authors identified a panel of eight circulating miRNA s that could serve as diagnostic markers for liver cirrhosis, irrespective of the viral or nonviral aetiology, displaying an area under the curve of 0.93 (95% confidence interval: 0.91–0.95). Similarly, Murakami *et al*[91] identified a miRNA score which differentiated between chronic hepatitis B and chronic hepatitis C, non-alcoholic steatohepatitis, and healthy controls with accuracy of 98.35%, 87.5%, or 89.29%, respectively.

Studies on HBV-infected patients have shown that serum/plasma miRNA signatures can assist in the differentiation from other viral or nonviral liver pathologies[93,105,107]. Recently, Shang *et al*[108] identified a profile of urinary miRNA s that could serve as diagnostic biomarkers for HBV infection and non-alcoholic steatohepatitis. Nevertheless, there is still insufficient data to recommend a miRNA panel for the specific diagnosis of HBV *vs* other pathologies. On the other hand, miRNA s have been associated with a specific HBV immune profile, with the evolution of ne-croinflammatory activity and with the development of chronic liver disease[42,109,110].

miRNA s for staging of liver fibrosis

miRNA s can distinguish between early and late fibrosis with a comparable or even higher sensibility and specificity than APRI or Fib-4[43,106,107]. Panels exclusively composed of miRNA s[106] or panels including both circulating miRNA s and biological markers (*e.g*., platelet count and alkaline phosphates) have been evaluated[39,103]. Wang *et al*[106] showed that a miRNA signature displays a significantly higher accuracy than individual miRNA s for the detection of moderate and advanced liver fibrosis (area under the curve of 0.90 for stages beyond F2, 0.88 for F3-F4, and 0.83 for F4).

Serum/plasma miRNA s precede the increase of liver transaminases in studies on acute liver injury[111,112]. Translating this result in patients with chronic hepatitis is nevertheless challenging, due to the persistent elevation of laboratory markers in chronic liver diseases. In HBV-associated liver fibrosis diagnosis, it is important to

Table 2 Circulating microRNAs in hepatitis B virus infection and their significance for the staging of liver fibrosis

Circulating microRNAs, plasma or serum	Significance for liver disease	Ref.
Upregulated microRNAs		
miR-185	↑ in advanced (F3-F4) *vs* early liver fibrosis (F1-F2); and ↑ in early liver fibrosis *vs* healthy volunteers; No increase with HBV plasma DNA	Li *et al*[136]
miR-2861, miR-345-3p, miR-3620, miR-3656, miR-371a-5p, miR-4646-5p, miR-4651, miR-4695, miR-4800-5p, miR-638	Individually ↑ in F1-F4 *vs* F0; Plasma expression differs between each stage of liver fibrosis	Zhang *et al*[137]
miR-1, mR-10b-5p, miR-20b-5p, miR-96b-5p, miR-133b, miR-455-ep, miR-671-5p	Increase in the serum in F3-F4 liver fibrosis	Singh *et al*[42]
miR-499-5p	Increases in the serum in F1-F2 stages	Singh *et al*[42]
miR-106b, miR-181b	Panel for the diagnosis of liver cirrhosis due both HBV and non-HBV associated infection	Chen *et al*[44]
Downregulated microRNAs		
miR-29	↓ in liver cirrhosis *vs* healthy controls	Xing *et al*[138]; Wang *et al*[106]
miR-223	↓ with the progression of liver fibrosis from F0-F2 to F3-F4	Bao *et al*[43]; Wang *et al*[106]
miR-21		
miR-143		
miR-374		
miR-486-3p, miR-497-5p	Individually ↓ in F1-F4 *vs* F0; Plasma expression differs between each stage of liver fibrosis	Zhang *et al*[137]
miR-1227-3p	↓ in the serum in F1-F2 stages	Singh *et al*[42]

↑ means upregulation. ↓ means downregulation. HBV: Hepatitis B virus; miR: MicroRNA.

distinguish between miRNA s that signal the presence of liver inflammation *vs* fibrosis, a challenge in practice because both can be present in the progression of chronic livery injury. Examples of circulating miRNA s that correlate with either liver necroinflammation and/or fibrosis are presented in Table 4. Still, circulating miRNA s could be used as prognostic markers for survival as well as for the developing risk of HCC in cirrhotic patients, including those with chronic hepatitis B[113,114].

miR-122 gradually decreases in the serum of patients with decompensated liver cirrhosis and its value is independently associated with the survival and MELD score[115], while miR-34 indicates the degree of portal hypertension in patients with liver cirrhosis[116]. miRNA scores also yield a satisfactory sensitivity and sensibility for the detection of HCC in patients with cirrhosis due to viral and non-viral aetiologies[117-120]. Various profibrotic miRNA s, such as miR-21 and miR-221/222, are also well-known oncogenic miRNA s and regulate tumoral signalling pathways. Circulating miR-21 is associated with the detection of HCC and with the presence of distant metastasis[49,77,121-123]. Similarly, serum miR-221 plays an important role in the growth and proliferation of tumoral cells[124] and appears to be regulated by HBx[125]. In this respect, Huang *et al*[117] devised a miRNA score that differentiated between HBV- or hepatitis C virus-associated HCC.

Circulating miRNA s as predictive biomarkers during HBV treatment

Plasma miRNA expression varies in response to antiviral treatment and could provide a promising tool for treatment selection. Van der Ree *et al*[126] found higher pretreatment levels of miR-301a-3p and miR-145-5p in patients with HBsAg loss, while Yang *et al*[127] devised a combination of miR-3960 and miR-126-3p that correlated with the clearance of HBsAg.

miRNA panels have also been studied in patients receiving either interferon or nucleoside analogues. Zhang *et al*[128] constructed a model of 11 miRNA s for the prediction of an early virological response to an interferon-based regimen, while Brunetto *et al*[129] defined a miR-B index (combining serum miR-122, miR-99, miR-192, miR-335, miR-126, miR-320) for the prediction of a sustained virological response. Li *et al*[130] used a miRNA panel composed of miR-22, miR-210, and alanine aminotransaminase to predict the early and sustained virological response but did not find any correlations with HBsAg or HBeAg clearance during a regimen with interferon-alpha.

Further studies on the serum miRNA dynamics during treatment could help establish the correlation between a specific pretreatment miRNA profile and the outcome of the treatment measured as both viral suppression and fibrosis regression.

Table 3 Overview of the major studies on the use of microRNAs in hepatitis B virus infected patients for the staging of liver fibrosis

Study group	Fibrosis staging/validation method	microRNA detection method/sample[1]	Data normalization	microRNA regulation depending on fibrosis staging			microRNA panel for liver fibrosis	Ref.
102 treatment naïve CHB	58 pts F0-F2; 44 pts F3-F4 / liver biopsy and laboratory data	RT-qPCR / serum samples	Spiked-in cel-miR-39	F3-F4 *vs* F0-F2	miR-122, -27b miR-222, -224	↑ ↓	miR-122, -222, PLT, ALP	Appourchaux *et al*[107], 2016
330 CHB, 165 HC	165 pts F0-F3; 165 pts F4 / clinical and laboratory data	RT-qPCR / serum samples	Exogenous control using cel-miR-67	CHB: F4 *vs* F0-F3 CHB F4 *vs* HC CHB *vs* HC	miR-18a-5p, -21-5p, -29c-3p, -122-5p, -106b-5p, 185-5p miR-1, -146a-5p miR-451a miR-21-5p, -27a-3p, -122-5p, -146a-5p	↓ ↑ ↓ ↑	Three panels: F4 *vs* other stages: miR-18a-5p, -21-5p -29c-3p, -122-5p, -106b-5p, 185-5p; F4 *vs* HC: miR-1, -146a-5p, -451a; CHB *vs* HC: miR-21-5p, -27a-3p -122-5p, -146a-5p	Jin *et al*[139], 2015
123 treatment naïve CHB	69 pts F0-F2 *vs* 54 staged F3-F4 / liver biopsy	RT-qPCR; Serum samples	Spiked-in cel-miR-39	F3-F4 *vs* F0-F2	miR-29a, -143, -223, -21, -374	↓	miR-29a, -143, -223, PLT	Bao *et al*[43], 2017
8 ASC, 8 AVH, 7 HC, 49 treatment naïve CHB	49 CHB patients: 16 pts F0, 19 pts F1-F2, 14 pts F3-F4 / liver biopsy, clinical and laboratory data	RT-qPCR and microarray analysis; Serum samples	U6 RNA control relative miRNA	F1-F2 F3-F4	miR-499-5p miR-1227-3p miR-34b-3p, -1224-3p, -1, -10b-5p, -20b-5p, -96b-5p, -133, -455-3p, -671-5p	↑ ↓ ↑	Analysis of miRNA networks and of individual miRNA s	Singh *et al*[42], 2018
19 CHB, 14 HC	19 CHB pts with F0-F2	RT-qPCR total plasma EVs/liver stiffness	Spiked-in cel-miR-39	Plasma (F0-F2) EVs (F0-F2)	miR-192, -200b miR-192, -200b, -92a, -150	↑ ↓	Expression pattern of each individual miRNA in EVs *vs* total plasma	Lambrecht *et al*[93], 2017
207 CHB, 47 non-HBV-LC, 7 non-CHB, 137 HC	207 CHB of which: 127 pts F4; 79 pts F0-F3 / liver biopsy	RT-qPCR / plasma samples	miR-1228 control with a log-2 scale transformation	CHB F4 and non-CHB F4; *vs* other groups; (panel for F4 diagnosis)	miR-106b miR-181b	↓ ↑	Panel composed of miR-106 and miR-181b	Chen *et al*[44], 2013
50 treatment naïve CHB	10 pts F0, 10 pts F1, 10 pts F2, 10 pts F3, 10 pts F4 / liver biopsy	Microarray analysis / plasma samples	Log standardization of miRNA s whose target gene expression levels > 2 folds and FDR < 0.05	F4 *vs* F0	miR-2861, -345-3p, -3620-3p, -3656, -371a-5p, -4646-5p, -4651, 4695-5p, -4800-5p, -638, miR-497-5p, -486-3p	↑ ↓	Detailed differential expression of individual miRNA s for each stage of liver fibrosis F0-F4	Zhang *et al*[137], 2015
92 CHB	11 pts F0, 16 pts F1, 12 pts F2, 13 pts F3, 40 pts F4 / liver biopsy and laboratory data	RT-qPCR; Plasma samples	Quanto, EC1, EC2 controls; relative miRNA expression was assessed using $2^{-\Delta\Delta Cq}$ calculation	≥ F2 ≥ F3 F4 *vs* F0	miR-122-5p miR-223, -29c-3p miR-122-5p miR-122-5p, -29c-3p, -146a-5p, -223	↑ ↓ ↑ -/↓	miR-122-5p, -21-5p, -146a-5p, -223, -29c-3p, -22-3p, -381-3p	Wang *et al*[106], 2018

[1]miRNA sample refers only to the samples collected from the serum/plasma in each of the mentioned studies. ↑ means upregulation. ↓ means downregulation. ALP: Alkaline phosphatase; ASC: Asymptomatic carriers; AVH: Acute viral hepatitis; CHB: Chronic hepatitis B; EVs: Extracellular vesicles; FDR: False discovery rate; HC: Healthy controls; LC: Liver cirrhosis; miR: MicroRNA; PLT: Platelet; Pts: Patients; RT-qPCR: Real time quantitative polymerase chain reaction.

Table 4 Circulating microRNAs in hepatitis B virus infection and their role in necroinflammation *vs* fibrosis

Circulating microRNA	microRNA regulation	Clinical significance in HBV infection	Ref.
miR-122	↑	Correlates with the necroinflammatory activity, HBsAg and HBV DNA; Also correlated with ≥ F2 stage of liver fibrosis	Waidmann *et al*[103], Ji *et al*[109], Wang *et al*[106]
miR-210	↑	Marker of necroinflammation; Varies with the severity of HBV hepatitis	Song *et al*[140]
miR-125 (-125a-5p/ -125b)	↑	Correlates with HBV intrahepatic replication and necroinflammatory activity	Li *et al*[141], Zheng *et al*[134]
miR-124	↑	Marker of HBV-associated necroinflammation	Wang *et al*[142]
miR-29	↓	Marker of liver fibrosis irrespective of aetiology	Xing *et al*[139]
miR-223	↓	Marker of liver fibrosis, decreases with the progression to cirrhosis	Bao *et al*[43]
miR-185	↑	Increases in advanced HBV fibrosis; Could play a therapeutic role in HBV gene suppression in tumoral cells	Li *et al*[136], Fan *et al*[143]

↑ means upregulation. ↓ means downregulation. HBsAg: Hepatitis B surface antigen; HBV: Hepatitis B virus; miR: MicroRNA.

CONCLUSION

Cellular and circulating miRNA s offer a unique glimpse into the intrahepatic development of liver fibrosis and intrahepatic viral replication. Diagnostic and prognostic panels that combine different serum miRNA s alone or with other biological parameters display a moderately high sensibility and sensitivity compared to validated non-invasive scores. Although current data remain heterogenous, there is growing proof that serum miRNA s correlate with virologic, immunologic, and fibrotic changes in liver and could become powerful biomarkers during HBV infection.

REFERENCES

1 **Lau NC**, Lim LP, Weinstein EG, Bartel DP. An abundant class of tiny RNAs with probable regulatory roles in Caenorhabditis elegans. *Science* 2001; **294**: 858-862 [PMID: 11679671 DOI: 10.1126/science.1065062]
2 **Lagos-Quintana M**, Rauhut R, Lendeckel W, Tuschl T. Identification of novel genes coding for small expressed RNAs. *Science* 2001; **294**: 853-858 [PMID: 11679670 DOI: 10.1126/science.1064921]
3 **Pasquinelli AE**, Reinhart BJ, Slack F, Martindale MQ, Kuroda MI, Maller B, Hayward DC, Ball EE, Degnan B, Müller P, Spring J, Srinivasan A, Fishman M, Finnerty J, Corbo J, Levine M, Leahy P, Davidson E, Ruvkun G. Conservation of the sequence and temporal expression of let-7 heterochronic regulatory RNA. *Nature* 2000; **408**: 86-89 [PMID: 11081512 DOI: 10.1038/35040556]
4 **Li C**, Hu J, Hao J, Zhao B, Wu B, Sun L, Peng S, Gao GF, Meng S. Competitive virus and host RNAs: the interplay of a hidden virus and host interaction. *Protein Cell* 2014; **5**: 348-356 [PMID: 24723323 DOI: 10.1007/s13238-014-0039-y]
5 **Bruscella P**, Bottini S, Baudesson C, Pawlotsky JM, Feray C, Trabucchi M. Viruses and miRNA s: More Friends than Foes. *Front Microbiol* 2017; **8**: 824 [PMID: 28555130 DOI: 10.3389/fmicb.2017.00824]
6 **Pfeffer S**, Zavolan M, Grässer FA, Chien M, Russo JJ, Ju J, John B, Enright AJ, Marks D, Sander C, Tuschl T. Identification of virus-encoded microRNAs. *Science* 2004; **304**: 734-736 [PMID: 15118162 DOI: 10.1126/science.1096781]
7 **Auvinen E**. Diagnostic and Prognostic Value of MicroRNA in Viral Diseases. *Mol Diagn Ther* 2017; **21**: 45-57 [PMID: 27682074 DOI: 10.1007/s40291-016-0236-x]
8 **Rosca A**, Anton G, Botezatu A, Temereanca A, Ene L, Achim C, Ruta S. miR-29a associates with viro-immunological markers of HIV infection in treatment experienced patients. *J Med Virol* 2016; **88**: 2132-2137 [PMID: 27232693 DOI: 10.1002/jmv.24586]
9 **World Health Organization**. Global hepatitis report, 2017. World Health Organization. Apr 2017. Available from: https://apps.who.int/iris/handle/10665/255016. License: CC BY-NC-SA 3.0 IGO
10 **Baiocchini A**, Montaldo C, Conigliaro A, Grimaldi A, Correani V, Mura F, Ciccosanti F, Rotiroti N, Brenna A, Montalbano M, D'Offizi G, Capobianchi MR, Alessandro R, Piacentini M, Schininà ME, Maras B, Del Nonno F, Tripodi M, Mancone C. Extracellular Matrix Molecular Remodeling in Human Liver Fibrosis Evolution. *PLoS One* 2016; **11**: e0151736 [PMID: 26998606 DOI: 10.1371/journal.pone.0151736]
11 **Hernandez-Gea V**, Friedman SL. Pathogenesis of liver fibrosis. *Annu Rev Pathol* 2011; **6**: 425-456 [PMID: 21073339 DOI: 10.1146/annurev-pathol-011110-130246]
12 **Pellicoro A**, Ramachandran P, Iredale JP, Fallowfield JA. Liver fibrosis and repair: immune regulation of

wound healing in a solid organ. *Nat Rev Immunol* 2014; **14**: 181-194 [PMID: 24566915 DOI: 10.1038/nri3623]
13 **European Association for the Study of the Liver**. EASL clinical practice guidelines: Management of chronic hepatitis B virus infection. *J Hepatol* 2012; **57**: 167-185 [PMID: 22436845 DOI: 10.1016/j.jhep.2012.02.010]
14 **Dienstag JL**, Goldin RD, Heathcote EJ, Hann HW, Woessner M, Stephenson SL, Gardner S, Gray DF, Schiff ER. Histological outcome during long-term lamivudine therapy. *Gastroenterology* 2003; **124**: 105-117 [PMID: 12512035 DOI: 10.1053/gast.2003.50013]
15 **Hadziyannis SJ**, Tassopoulos NC, Heathcote EJ, Chang TT, Kitis G, Rizzetto M, Marcellin P, Lim SG, Goodman Z, Ma J, Brosgart CL, Borroto-Esoda K, Arterburn S, Chuck SL; Adefovir Dipivoxil 438 Study Group. Long-term therapy with adefovir dipivoxil for HBeAg-negative chronic hepatitis B for up to 5 years. *Gastroenterology* 2006; **131**: 1743-1751 [PMID: 17087951 DOI: 10.1053/j.gastro.2006.09.020]
16 **Chang TT**, Lai CL, Kew Yoon S, Lee SS, Coelho HS, Carrilho FJ, Poordad F, Halota W, Horsmans Y, Tsai N, Zhang H, Tenney DJ, Tamez R, Iloeje U. Entecavir treatment for up to 5 years in patients with hepatitis B e antigen-positive chronic hepatitis B. *Hepatology* 2010; **51**: 422-430 [PMID: 20049753 DOI: 10.1002/hep.23327]
17 **Marcellin P**, Gane E, Buti M, Afdhal N, Sievert W, Jacobson IM, Washington MK, Germanidis G, Flaherty JF, Aguilar Schall R, Bornstein JD, Kitrinos KM, Subramanian GM, McHutchison JG, Heathcote EJ. Regression of cirrhosis during treatment with tenofovir disoproxil fumarate for chronic hepatitis B: a 5-year open-label follow-up study. *Lancet* 2013; **381**: 468-475 [PMID: 23234725 DOI: 10.1016/S0140-6736(12)61425-1]
18 **Boyd A**, Bottero J, Miailhes P, Lascoux-Combe C, Rougier H, Girard PM, Serfaty L, Lacombe K. Liver fibrosis regression and progression during controlled hepatitis B virus infection among HIV-HBV patients treated with tenofovir disoproxil fumarate in France: a prospective cohort study. *J Int AIDS Soc* 2017; **20**: 21426 [PMID: 28362068 DOI: 10.7448/IAS.20.1.21426]
19 **Nassal M**. HBV cccDNA: viral persistence reservoir and key obstacle for a cure of chronic hepatitis B. *Gut* 2015; **64**: 1972-1984 [PMID: 26048673 DOI: 10.1136/gutjnl-2015-309809]
20 **Mu D**, Yuan FC, Chen Y, Jiang XY, Yan L, Jiang LY, Gong JP, Zhang DZ, Ren H, Liao Y. Baseline value of intrahepatic HBV DNA over cccDNA predicts patient's response to interferon therapy. *Sci Rep* 2017; **7**: 5937 [PMID: 28725013 DOI: 10.1038/s41598-017-05242-y]
21 **Zhang X**, Lu W, Zheng Y, Wang W, Bai L, Chen L, Feng Y, Zhang Z, Yuan Z. In situ analysis of intrahepatic virological events in chronic hepatitis B virus infection. *J Clin Invest* 2016; **126**: 1079-1092 [PMID: 26901811 DOI: 10.1172/JCI83339]
22 **Bravo AA**, Sheth SG, Chopra S. Liver biopsy. *N Engl J Med* 2001; **344**: 495-500 [PMID: 11172192 DOI: 10.1056/NEJM200102153440706]
23 **Wang J**, Shen T, Huang X, Kumar GR, Chen X, Zeng Z, Zhang R, Chen R, Li T, Zhang T, Yuan Q, Li PC, Huang Q, Colonno R, Jia J, Hou J, McCrae MA, Gao Z, Ren H, Xia N, Zhuang H, Lu F. Serum hepatitis B virus RNA is encapsidated pregenome RNA that may be associated with persistence of viral infection and rebound. *J Hepatol* 2016; **65**: 700-710 [PMID: 27245431 DOI: 10.1016/j.jhep.2016.05.029]
24 **Giersch K**, Allweiss L, Volz T, Dandri M, Lütgehetmann M. Serum HBV pgRNA as a clinical marker for cccDNA activity. *J Hepatol* 2017; **66**: 460-462 [PMID: 27826059 DOI: 10.1016/j.jhep.2016.09.028]
25 **Chen EQ**, Feng S, Wang ML, Liang LB, Zhou LY, Du LY, Yan LB, Tao CM, Tang H. Serum hepatitis B core-related antigen is a satisfactory surrogate marker of intrahepatic covalently closed circular DNA in chronic hepatitis B. *Sci Rep* 2017; **7**: 173 [PMID: 28282964 DOI: 10.1038/s41598-017-00111-0]
26 **Castera L**. Noninvasive methods to assess liver disease in patients with hepatitis B or C. *Gastroenterology* 2012; **142**: 1293-1302.e4 [PMID: 22537436 DOI: 10.1053/j.gastro.2012.02.017]
27 **World Health Organization**. Guideline on when to start antiretroviral therapy and on pre-exposure prophylaxis for HIV. World Health Organization. 2015. Available from: https://apps.who.int/iris/handle/10665/186275
28 **Lambrecht J**, Verhulst S, Mannaerts I, Reynaert H, van Grunsven LA. Prospects in non-invasive assessment of liver fibrosis: Liquid biopsy as the future gold standard? *Biochim Biophys Acta Mol Basis Dis* 2018; **1864**: 1024-1036 [PMID: 29329986 DOI: 10.1016/j.bbadis.2018.01.009]
29 **O'Brien J**, Hayder H, Zayed Y, Peng C. Overview of MicroRNA Biogenesis, Mechanisms of Actions, and Circulation. *Front Endocrinol (Lausanne)* 2018; **9**: 402 [PMID: 30123182 DOI: 10.3389/fendo.2018.00402]
30 **Broughton JP**, Lovci MT, Huang JL, Yeo GW, Pasquinelli AE. Pairing beyond the Seed Supports MicroRNA Targeting Specificity. *Mol Cell* 2016; **64**: 320-333 [PMID: 27720646 DOI: 10.1016/j.molcel.2016.09.004]
31 **Helwak A**, Kudla G, Dudnakova T, Tollervey D. Mapping the human miRNA interactome by CLASH reveals frequent noncanonical binding. *Cell* 2013; **153**: 654-665 [PMID: 23622248 DOI: 10.1016/j.cell.2013.03.043]
32 **Skalsky RL**, Cullen BR. Viruses, microRNAs, and host interactions. *Annu Rev Microbiol* 2010; **64**: 123-141 [PMID: 20477536 DOI: 10.1146/annurev.micro.112408.134243]
33 **Ren M**, Qin D, Li K, Qu J, Wang L, Wang Z, Huang A, Tang H. Correlation between hepatitis B virus protein and microRNA processor Drosha in cells expressing HBV. *Antiviral Res* 2012; **94**: 225-231 [PMID: 22554933 DOI: 10.1016/j.antiviral.2012.04.004]
34 **Novellino L**, Rossi RL, Bonino F, Cavallone D, Abrignani S, Pagani M, Brunetto MR. Circulating hepatitis B surface antigen particles carry hepatocellular microRNAs. *PLoS One* 2012; **7**: e31952 [PMID: 22470417 DOI: 10.1371/journal.pone.0031952]
35 **Hayes CN**, Akamatsu S, Tsuge M, Miki D, Akiyama R, Abe H, Ochi H, Hiraga N, Imamura M, Takahashi S, Aikata H, Kawaoka T, Kawakami Y, Ohishi W, Chayama K. Hepatitis B virus-specific miRNA s and Argonaute2 play a role in the viral life cycle. *PLoS One* 2012; **7**: e47490 [PMID: 23091627 DOI: 10.1371/journal.pone.0047490]
36 **Arroyo JD**, Chevillet JR, Kroh EM, Ruf IK, Pritchard CC, Gibson DF, Mitchell PS, Bennett CF, Pogosova-Agadjanyan EL, Stirewalt DL, Tait JF, Tewari M. Argonaute2 complexes carry a population of circulating microRNAs independent of vesicles in human plasma. *Proc Natl Acad Sci USA* 2011; **108**: 5003-5008 [PMID: 21383194 DOI: 10.1073/pnas.1019055108]
37 **Turchinovich A**, Samatov TR, Tonevitsky AG, Burwinkel B. Circulating miRNA s: cell-cell communication function? *Front Genet* 2013; **4**: 119 [PMID: 23825476 DOI: 10.3389/fgene.2013.00119]
38 **Kosaka N**, Iguchi H, Yoshioka Y, Takeshita F, Matsuki Y, Ochiya T. Secretory mechanisms and intercellular transfer of microRNAs in living cells. *J Biol Chem* 2010; **285**: 17442-17452 [PMID:

20353945 DOI: 10.1074/jbc.M110.107821]
39 **Fabbri M**, Paone A, Calore F, Galli R, Gaudio E, Santhanam R, Lovat F, Fadda P, Mao C, Nuovo GJ, Zanesi N, Crawford M, Ozer GH, Wernicke D, Alder H, Caligiuri MA, Nana-Sinkam P, Perrotti D, Croce CM. MicroRNAs bind to Toll-like receptors to induce prometastatic inflammatory response. *Proc Natl Acad Sci USA* 2012; **109**: E2110-E2116 [PMID: 22753494 DOI: 10.1073/pnas.1209414109]
40 **Lehmann SM**, Krüger C, Park B, Derkow K, Rosenberger K, Baumgart J, Trimbuch T, Eom G, Hinz M, Kaul D, Habbel P, Kälin R, Franzoni E, Rybak A, Nguyen D, Veh R, Ninnemann O, Peters O, Nitsch R, Heppner FL, Golenbock D, Schott E, Ploegh HL, Wulczyn FG, Lehnardt S. An unconventional role for miRNA : let-7 activates Toll-like receptor 7 and causes neurodegeneration. *Nat Neurosci* 2012; **15**: 827-835 [PMID: 22610069 DOI: 10.1038/nn.3113]
41 **Yang X**, Li H, Sun H, Fan H, Hu Y, Liu M, Li X, Tang H. Hepatitis B Virus-Encoded MicroRNA Controls Viral Replication. *J Virol* 2017; **91**: pii: e01919-16 [PMID: 28148795 DOI: 10.1128/jvi.01919-16]
42 **Singh AK**, Rooge SB, Varshney A, Vasudevan M, Bhardwaj A, Venugopal SK, Trehanpati N, Kumar M, Geffers R, Kumar V, Sarin SK. Global microRNA expression profiling in the liver biopsies of hepatitis B virus-infected patients suggests specific microRNA signatures for viral persistence and hepatocellular injury. *Hepatology* 2018; **67**: 1695-1709 [PMID: 29194684 DOI: 10.1002/hep.29690]
43 **Bao S**, Zheng J, Li N, Huang C, Chen M, Cheng Q, Yu K, Chen S, Zhu M, Shi G. Serum MicroRNA Levels as a Noninvasive Diagnostic Biomarker for the Early Diagnosis of Hepatitis B Virus-Related Liver Fibrosis. *Gut Liver* 2017; **11**: 860-869 [PMID: 28750488 DOI: 10.5009/gnl16560]
44 **Chen YJ**, Zhu JM, Wu H, Fan J, Zhou J, Hu J, Yu Q, Liu TT, Yang L, Wu CL, Guo XL, Huang XW, Shen XZ. Circulating microRNAs as a Fingerprint for Liver Cirrhosis. *PLoS One* 2013; **8**: e66577 [PMID: 23805240 DOI: 10.1371/journal.pone.0066577]
45 **Guo CJ**, Pan Q, Cheng T, Jiang B, Chen GY, Li DG. Changes in microRNAs associated with hepatic stellate cell activation status identify signaling pathways. *FEBS J* 2009; **276**: 5163-5176 [PMID: 19674103 DOI: 10.1111/j.1742-4658.2009.07213.x]
46 **Coll M**, El Taghdouini A, Perea L, Mannaerts I, Vila-Casadesús M, Blaya D, Rodrigo-Torres D, Affò S, Morales-Ibanez O, Graupera I, Lozano JJ, Najimi M, Sokal E, Lambrecht J, Ginès P, van Grunsven LA, Sancho-Bru P. Integrative miRNA and Gene Expression Profiling Analysis of Human Quiescent Hepatic Stellate Cells. *Sci Rep* 2015; **5**: 11549 [PMID: 26096707 DOI: 10.1038/srep11549]
47 **Wang J**, Chu ES, Chen HY, Man K, Go MY, Huang XR, Lan HY, Sung JJ, Yu J. microRNA-29b prevents liver fibrosis by attenuating hepatic stellate cell activation and inducing apoptosis through targeting PI3K/AKT pathway. *Oncotarget* 2015; **6**: 7325-7338 [PMID: 25356754 DOI: 10.18632/oncotarget.2621]
48 **Ma L**, Yang X, Wei R, Ye T, Zhou JK, Wen M, Men R, Li P, Dong B, Liu L, Fu X, Xu H, Aqeilan RI, Wei YQ, Yang L, Peng Y. MicroRNA-214 promotes hepatic stellate cell activation and liver fibrosis by suppressing Sufu expression. *Cell Death Dis* 2018; **9**: 718 [PMID: 29915227 DOI: 10.1038/s41419-018-0752-1]
49 **You K**, Li SY, Gong J, Fang JH, Zhang C, Zhang M, Yuan Y, Yang J, Zhuang SM. MicroRNA-125b Promotes Hepatic Stellate Cell Activation and Liver Fibrosis by Activating RhoA Signaling. *Mol Ther Nucleic Acids* 2018; **12**: 57-66 [PMID: 30195793 DOI: 10.1016/j.omtn.2018.04.016]
50 **Gupta P**, Sata TN, Yadav AK, Mishra A, Vats N, Hossain MM, Sanal MG, Venugopal SK. TGF-β induces liver fibrosis via miRNA -181a-mediated down regulation of augmenter of liver regeneration in hepatic stellate cells. *PLoS One* 2019; **14**: e0214534 [PMID: 31166951 DOI: 10.1371/journal.pone.0214534]
51 **Zhang Y**, Ghazwani M, Li J, Sun M, Stolz DB, He F, Fan J, Xie W, Li S. MiR-29b inhibits collagen maturation in hepatic stellate cells through down-regulating the expression of HSP47 and lysyl oxidase. *Biochem Biophys Res Commun* 2014; **446**: 940-944 [PMID: 24650661 DOI: 10.1016/j.bbrc.2014.03.037]
52 **Zhao J**, Tang N, Wu K, Dai W, Ye C, Shi J, Zhang J, Ning B, Zeng X, Lin Y. MiR-21 simultaneously regulates ERK1 signaling in HSC activation and hepatocyte EMT in hepatic fibrosis. *PLoS One* 2014; **9**: e108005 [PMID: 25303175 DOI: 10.1371/journal.pone.0108005]
53 **Iizuka M**, Ogawa T, Enomoto M, Motoyama H, Yoshizato K, Ikeda K, Kawada N. Induction of microRNA-214-5p in human and rodent liver fibrosis. *Fibrogenesis Tissue Repair* 2012; **5**: 12 [PMID: 22849305 DOI: 10.1186/1755-1536-5-12]
54 **Meng F**, Glaser SS, Francis H, Yang F, Han Y, Stokes A, Staloch D, McCarra J, Liu J, Venter J, Zhao H, Liu X, Francis T, Swendsen S, Liu CG, Tsukamoto H, Alpini G. Epigenetic regulation of miR-34a expression in alcoholic liver injury. *Am J Pathol* 2012; **181**: 804-817 [PMID: 22841474 DOI: 10.1016/j.ajpath.2012.06.010]
55 **Mann J**, Chu DC, Maxwell A, Oakley F, Zhu NL, Tsukamoto H, Mann DA. MeCP2 controls an epigenetic pathway that promotes myofibroblast transdifferentiation and fibrosis. *Gastroenterology* 2010; **138**: 705-714, 714.e1-714.e4 [PMID: 19843474 DOI: 10.1053/j.gastro.2009.10.002]
56 **Ji J**, Zhang J, Huang G, Qian J, Wang X, Mei S. Over-expressed microRNA-27a and 27b influence fat accumulation and cell proliferation during rat hepatic stellate cell activation. *FEBS Lett* 2009; **583**: 759-766 [PMID: 19185571 DOI: 10.1016/j.febslet.2009.01.034]
57 **Wang Y**, Zhu P, Qiu J, Wang J, Zhu H, Zhu Y, Zhang L, Zhu J, Liu X, Dong C. Identification and characterization of interferon signaling-related microRNAs in occult hepatitis B virus infection. *Clin Epigenetics* 2017; **9**: 101 [PMID: 28932321 DOI: 10.1186/s13148-017-0404-9]
58 **Ma F**, Xu S, Liu X, Zhang Q, Xu X, Liu M, Hua M, Li N, Yao H, Cao X. The microRNA miR-29 controls innate and adaptive immune responses to intracellular bacterial infection by targeting interferon-γ. *Nat Immunol* 2011; **12**: 861-869 [PMID: 21785411 DOI: 10.1038/ni.2073]
59 **Ye D**, Zhang T, Lou G, Liu Y. Role of miR-223 in the pathophysiology of liver diseases. *Exp Mol Med* 2018; **50**: 128 [PMID: 30258086 DOI: 10.1038/s12276-018-0153-7]
60 **Yang Z**, Peng Y, Yang S. MicroRNA-146a regulates the transformation from liver fibrosis to cirrhosis in patients with hepatitis B via interleukin-6. *Exp Ther Med* 2019; **17**: 4670-4676 [PMID: 31086599 DOI: 10.3892/etm.2019.7490]
61 **Li LM**, Wang D, Zen K. MicroRNAs in Drug-induced Liver Injury. *J Clin Transl Hepatol* 2014; **2**: 162-169 [PMID: 26357624 DOI: 10.14218/JCTH.2014.00015]
62 **Pirola CJ**, Fernández Gianotti T, Castaño GO, Mallardi P, San Martino J, Mora Gonzalez Lopez Ledesma M, Flichman D, Mirshahi F, Sanyal AJ, Sookoian S. Circulating microRNA signature in non-alcoholic fatty liver disease: from serum non-coding RNAs to liver histology and disease pathogenesis. *Gut* 2015; **64**: 800-812 [PMID: 24973316 DOI: 10.1136/gutjnl-2014-306996]

63 **Yang L**, Dong C, Yang J, Yang L, Chang N, Qi C, Li L. MicroRNA-26b-5p Inhibits Mouse Liver Fibrogenesis and Angiogenesis by Targeting PDGF Receptor-Beta. *Mol Ther Nucleic Acids* 2019; **16**: 206-217 [PMID: 30901579 DOI: 10.1016/j.omtn.2019.02.014]

64 **Li X**, Chen Y, Wu S, He J, Lou L, Ye W, Wang J. microRNA-34a and microRNA-34c promote the activation of human hepatic stellate cells by targeting peroxisome proliferator-activated receptor γ. *Mol Med Rep* 2015; **11**: 1017-1024 [PMID: 25370690 DOI: 10.3892/mmr.2014.2846]

65 **Tian XF**, Ji FJ, Zang HL, Cao H. Activation of the miR-34a/SIRT1/p53 Signaling Pathway Contributes to the Progress of Liver Fibrosis via Inducing Apoptosis in Hepatocytes but Not in HSCs. *PLoS One* 2016; **11**: e0158657 [PMID: 27387128 DOI: 10.1371/journal.pone.0158657]

66 **Feili X**, Wu S, Ye W, Tu J, Lou L. MicroRNA-34a-5p inhibits liver fibrosis by regulating TGF-β1/Smad3 pathway in hepatic stellate cells. *Cell Biol Int* 2018; **42**: 1370-1376 [PMID: 29957876 DOI: 10.1002/cbin.11022]

67 **Zheng J**, Wu C, Xu Z, Xia P, Dong P, Chen B, Yu F. Hepatic stellate cell is activated by microRNA-181b via PTEN/Akt pathway. *Mol Cell Biochem* 2015; **398**: 1-9 [PMID: 25148875 DOI: 10.1007/s11010-014-2199-8]

68 **Wei J**, Feng L, Li Z, Xu G, Fan X. MicroRNA-21 activates hepatic stellate cells via PTEN/Akt signaling. *Biomed Pharmacother* 2013; **67**: 387-392 [PMID: 23643356 DOI: 10.1016/j.biopha.2013.03.014]

69 **Roderburg C**, Urban GW, Bettermann K, Vucur M, Zimmermann H, Schmidt S, Janssen J, Koppe C, Knolle P, Castoldi M, Tacke F, Trautwein C, Luedde T. Micro-RNA profiling reveals a role for miR-29 in human and murine liver fibrosis. *Hepatology* 2011; **53**: 209-218 [PMID: 20890893 DOI: 10.1002/hep.23922]

70 **Zhang Y**, Wu L, Wang Y, Zhang M, Li L, Zhu D, Li X, Gu H, Zhang CY, Zen K. Protective role of estrogen-induced miRNA -29 expression in carbon tetrachloride-induced mouse liver injury. *J Biol Chem* 2012; **287**: 14851-14862 [PMID: 22393047 DOI: 10.1074/jbc.M111.314922]

71 **Jing F**, Geng Y, Xu XY, Xu HY, Shi JS, Xu ZH. MicroRNA29a Reverts the Activated Hepatic Stellate Cells in the Regression of Hepatic Fibrosis through Regulation of ATPase H Transporting V1 Subunit C1. *Int J Mol Sci* 2019; **20**: pii: E796 [PMID: 30781750 DOI: 10.3390/ijms20040796]

72 **Matsumoto Y**, Itami S, Kuroda M, Yoshizato K, Kawada N, Murakami Y. MiR-29a Assists in Preventing the Activation of Human Stellate Cells and Promotes Recovery From Liver Fibrosis in Mice. *Mol Ther* 2016; **24**: 1848-1859 [PMID: 27480597 DOI: 10.1038/mt.2016.127]

73 **Zou Y**, Cai Y, Lu D, Zhou Y, Yao Q, Zhang S. MicroRNA-146a-5p attenuates liver fibrosis by suppressing profibrogenic effects of TGFβ1 and lipopolysaccharide. *Cell Signal* 2017; **39**: 1-8 [PMID: 28739486 DOI: 10.1016/j.cellsig.2017.07.016]

74 **Zheng J**, Lin Z, Dong P, Lu Z, Gao S, Chen X, Wu C, Yu F. Activation of hepatic stellate cells is suppressed by microRNA-150. *Int J Mol Med* 2013; **32**: 17-24 [PMID: 23604143 DOI: 10.3892/ijmm.2013.1356]

75 **Venugopal SK**, Jiang J, Kim TH, Li Y, Wang SS, Torok NJ, Wu J, Zern MA. Liver fibrosis causes downregulation of miRNA -150 and miRNA -194 in hepatic stellate cells, and their overexpression causes decreased stellate cell activation. *Am J Physiol Gastrointest Liver Physiol* 2010; **298**: G101-G106 [PMID: 19892940 DOI: 10.1152/ajpgi.00220.2009]

76 **Ding W**, Xin J, Jiang L, Zhou Q, Wu T, Shi D, Lin B, Li L, Li J. Characterisation of peripheral blood mononuclear cell microRNA in hepatitis B-related acute-on-chronic liver failure. *Sci Rep* 2015; **5**: 13098 [PMID: 26267843 DOI: 10.1038/srep13098]

77 **Mirzaei HR**, Sahebkar A, Mohammadi M, Yari R, Salehi H, Jafari MH, Namdar A, Khabazian E, Jaafari MR, Mirzaei H. Circulating microRNAs in Hepatocellular Carcinoma: Potential Diagnostic and Prognostic Biomarkers. *Curr Pharm Des* 2016; **22**: 5257-5269 [PMID: 26935703 DOI: 10.2174/1381612822666160303110838]

78 **Torres JL**, Novo-Veleiro I, Manzanedo L, Alvela-Suárez L, Macías R, Laso FJ, Marcos M. Role of microRNAs in alcohol-induced liver disorders and non-alcoholic fatty liver disease. *World J Gastroenterol* 2018; **24**: 4104-4118 [PMID: 30271077 DOI: 10.3748/wjg.v24.i36.4104]

79 **Guo L**, Li W, Hu L, Zhou H, Zheng L, Yu L, Liang W. Diagnostic value of circulating microRNAs for liver cirrhosis: a meta-analysis. *Oncotarget* 2018; **9**: 5397-5405 [PMID: 29435187 DOI: 10.18632/oncotarget.23332]

80 **Zhang YC**, Xu Z, Zhang TF, Wang YL. Circulating microRNAs as diagnostic and prognostic tools for hepatocellular carcinoma. *World J Gastroenterol* 2015; **21**: 9853-9862 [PMID: 26379392 DOI: 10.3748/wjg.v21.i34.9853]

81 **Xu X**, Tao Y, Shan L, Chen R, Jiang H, Qian Z, Cai F, Ma L, Yu Y. The Role of MicroRNAs in Hepatocellular Carcinoma. *J Cancer* 2018; **9**: 3557-3569 [PMID: 30310513 DOI: 10.7150/jca.26350]

82 **Loosen SH**, Schueller F, Trautwein C, Roy S, Roderburg C. Role of circulating microRNAs in liver diseases. *World J Hepatol* 2017; **9**: 586-594 [PMID: 28515844 DOI: 10.4254/wjh.v9.i12.586]

83 **Nojima H**, Freeman CM, Schuster RM, Japtok L, Kleuser B, Edwards MJ, Gulbins E, Lentsch AB. Hepatocyte exosomes mediate liver repair and regeneration via sphingosine-1-phosphate. *J Hepatol* 2016; **64**: 60-68 [PMID: 26254847 DOI: 10.1016/j.jhep.2015.07.030]

84 **Bukong TN**, Momen-Heravi F, Kodys K, Bala S, Szabo G. Exosomes from hepatitis C infected patients transmit HCV infection and contain replication competent viral RNA in complex with Ago2-miR122-HSP90. *PLoS Pathog* 2014; **10**: e1004424 [PMID: 25275643 DOI: 10.1371/journal.ppat.1004424]

85 **Chen L**, Chen R, Kemper S, Brigstock DR. Pathways of production and delivery of hepatocyte exosomes. *J Cell Commun Signal* 2018; **12**: 343-357 [PMID: 29063370 DOI: 10.1007/s12079-017-0421-7]

86 **Devhare PB**, Sasaki R, Shrivastava S, Di Bisceglie AM, Ray R, Ray RB. Exosome-Mediated Intercellular Communication between Hepatitis C Virus-Infected Hepatocytes and Hepatic Stellate Cells. *J Virol* 2017; **91** [PMID: 28077652 DOI: 10.1128/jvi.02225-16]

87 **Kim JH**, Lee CH, Lee SW. Exosomal Transmission of MicroRNA from HCV Replicating Cells Stimulates Transdifferentiation in Hepatic Stellate Cells. *Mol Ther Nucleic Acids* 2019; **14**: 483-497 [PMID: 30753992 DOI: 10.1016/j.omtn.2019.01.006]

88 **Chen L**, Chen R, Kemper S, Charrier A, Brigstock DR. Suppression of fibrogenic signaling in hepatic stellate cells by Twist1-dependent microRNA-214 expression: Role of exosomes in horizontal transfer of Twist1. *Am J Physiol Gastrointest Liver Physiol* 2015; **309**: G491-G499 [PMID: 26229009 DOI: 10.1152/ajpgi.00140.2015]

89 **Chen L**, Chen R, Velazquez VM, Brigstock DR. Fibrogenic Signaling Is Suppressed in Hepatic Stellate Cells through Targeting of Connective Tissue Growth Factor (CCN2) by Cellular or Exosomal MicroRNA-199a-5p. *Am J Pathol* 2016; **186**: 2921-2933 [PMID: 27662798 DOI:

10.1016/j.ajpath.2016.07.011]
90 **Lino Cardenas CL**, Henaoui IS, Courcot E, Roderburg C, Cauffiez C, Aubert S, Copin MC, Wallaert B, Glowacki F, Dewaeles E, Milosevic J, Maurizio J, Tedrow J, Marcet B, Lo-Guidice JM, Kaminski N, Barbry P, Luedde T, Perrais M, Mari B, Pottier N. miR-199a-5p Is upregulated during fibrogenic response to tissue injury and mediates TGFbeta-induced lung fibroblast activation by targeting caveolin-1. *PLoS Genet* 2013; **9**: e1003291 [PMID: 23459460 DOI: 10.1371/journal.pgen.1003291]
91 **Murakami Y**, Toyoda H, Tanaka M, Kuroda M, Harada Y, Matsuda F, Tajima A, Kosaka N, Ochiya T, Shimotohno K. The progression of liver fibrosis is related with overexpression of the miR-199 and 200 families. *PLoS One* 2011; **6**: e16081 [PMID: 21283674 DOI: 10.1371/journal.pone.0016081]
92 **Chevillet JR**, Kang Q, Ruf IK, Briggs HA, Vojtech LN, Hughes SM, Cheng HH, Arroyo JD, Meredith EK, Gallichotte EN, Pogosova-Agadjanyan EL, Morrissey C, Stirewalt DL, Hladik F, Yu EY, Higano CS, Tewari M. Quantitative and stoichiometric analysis of the microRNA content of exosomes. *Proc Natl Acad Sci USA* 2014; **111**: 14888-14893 [PMID: 25267620 DOI: 10.1073/pnas.1408301111]
93 **Lambrecht J**, Jan Poortmans P, Verhulst S, Reynaert H, Mannaerts I, van Grunsven LA. Circulating ECV-Associated miRNA s as Potential Clinical Biomarkers in Early Stage HBV and HCV Induced Liver Fibrosis. *Front Pharmacol* 2017; **8**: 56 [PMID: 28232800 DOI: 10.3389/fphar.2017.00056]
94 **Yang J**, Li C, Zhang L, Wang X. Extracellular Vesicles as Carriers of Non-coding RNAs in Liver Diseases. *Front Pharmacol* 2018; **9**: 415 [PMID: 29740327 DOI: 10.3389/fphar.2018.00415]
95 **Szabo G**, Momen-Heravi F. Extracellular vesicles in liver disease and potential as biomarkers and therapeutic targets. *Nat Rev Gastroenterol Hepatol* 2017; **14**: 455-466 [PMID: 28634412 DOI: 10.1038/nrgastro.2017.71]
96 **Ishikawa H**, Yamada H, Taromaru N, Kondo K, Nagura A, Yamazaki M, Ando Y, Munetsuna E, Suzuki K, Ohashi K, Teradaira R. Stability of serum high-density lipoprotein-microRNAs for preanalytical conditions. *Ann Clin Biochem* 2017; **54**: 134-142 [PMID: 27166305 DOI: 10.1177/0004563216647086]
97 **Ramón-Núñez LA**, Martos L, Fernández-Pardo Á, Oto J, Medina P, España F, Navarro S. Comparison of protocols and RNA carriers for plasma miRNA isolation. Unraveling RNA carrier influence on miRNA isolation. *PLoS One* 2017; **12**: e0187005 [PMID: 29077772 DOI: 10.1371/journal.pone.0187005]
98 **Binderup HG**, Madsen JS, Heegaard NHH, Houlind K, Andersen RF, Brasen CL. Quantification of microRNA levels in plasma - Impact of preanalytical and analytical conditions. *PLoS One* 2018; **13**: e0201069 [PMID: 30024941 DOI: 10.1371/journal.pone.0201069]
99 **Faraldi M**, Gomarasca M, Sansoni V, Perego S, Banfi G, Lombardi G. Normalization strategies differently affect circulating miRNA profile associated with the training status. *Sci Rep* 2019; **9**: 1584 [PMID: 30733582 DOI: 10.1038/s41598-019-38505-x]
100 **Schwarzenbach H**, da Silva AM, Calin G, Pantel K. Data Normalization Strategies for MicroRNA Quantification. *Clin Chem* 2015; **61**: 1333-1342 [PMID: 26408530 DOI: 10.1373/clinchem.2015.239459]
101 **Ludwig N**, Leidinger P, Becker K, Backes C, Fehlmann T, Pallasch C, Rheinheimer S, Meder B, Stähler C, Meese E, Keller A. Distribution of miRNA expression across human tissues. *Nucleic Acids Res* 2016; **44**: 3865-3877 [PMID: 26921406 DOI: 10.1093/nar/gkw116]
102 **Chang J**, Nicolas E, Marks D, Sander C, Lerro A, Buendia MA, Xu C, Mason WS, Moloshok T, Bort R, Zaret KS, Taylor JM. miR-122, a mammalian liver-specific microRNA, is processed from hcr mRNA and may downregulate the high affinity cationic amino acid transporter CAT-1. *RNA Biol* 2004; **1**: 106-113 [PMID: 17179747 DOI: 10.4161/rna.1.2.1066]
103 **Waidmann O**, Bihrer V, Pleli T, Farnik H, Berger A, Zeuzem S, Kronenberger B, Piiper A. Serum microRNA-122 levels in different groups of patients with chronic hepatitis B virus infection. *J Viral Hepat* 2012; **19**: e58-e65 [PMID: 22239527 DOI: 10.1111/j.1365-2893.2011.01536.x]
104 **Murakami Y**, Toyoda H, Tanahashi T, Tanaka J, Kumada T, Yoshioka Y, Kosaka N, Ochiya T, Taguchi YH. Comprehensive miRNA expression analysis in peripheral blood can diagnose liver disease. *PLoS One* 2012; **7**: e48366 [PMID: 23152743 DOI: 10.1371/journal.pone.0048366]
105 **Yamaura Y**, Tatsumi N, Takagi S, Tokumitsu S, Fukami T, Tajiri K, Minemura M, Yokoi T, Nakajima M. Serum microRNA profiles in patients with chronic hepatitis B, chronic hepatitis C, primary biliary cirrhosis, autoimmune hepatitis, nonalcoholic steatohepatitis, or drug-induced liver injury. *Clin Biochem* 2017; **50**: 1034-1039 [PMID: 28823616 DOI: 10.1016/j.clinbiochem.2017.08.010]
106 **Wang TZ**, Lin DD, Jin BX, Sun XY, Li N. Plasma microRNA: A novel non-invasive biomarker for HBV-associated liver fibrosis staging. *Exp Ther Med* 2019; **17**: 1919-1929 [PMID: 30783469 DOI: 10.3892/etm.2018.7117]
107 **Appourchaux K**, Dokmak S, Resche-Rigon M, Treton X, Lapalus M, Gattolliat CH, Porchet E, Martinot-Peignoux M, Boyer N, Vidaud M, Bedossa P, Marcellin P, Bièche I, Estrabaud E, Asselah T. MicroRNA-based diagnostic tools for advanced fibrosis and cirrhosis in patients with chronic hepatitis B and C. *Sci Rep* 2016; **6**: 34935 [PMID: 27731343 DOI: 10.1038/srep34935]
108 **Shang JW**, Yan XL, Zhang H, Su SB. Expression and significance of urinary microRNA in patients with chronic hepatitis B. *Medicine (Baltimore)* 2019; **98**: e17143 [PMID: 31517857 DOI: 10.1097/MD.0000000000017143]
109 **Ji F**, Yang B, Peng X, Ding H, You H, Tien P. Circulating microRNAs in hepatitis B virus-infected patients. *J Viral Hepat* 2011; **18**: e242-e251 [PMID: 21692939 DOI: 10.1111/j.1365-2893.2011.01443.x]
110 **Xing T**, Xu H, Yu W, Wang B, Zhang J. Expression profile and clinical significance of miRNA s at different stages of chronic hepatitis B virus infection. *Int J Clin Exp Med* 2015; **8**: 5611-5620 [PMID: 26131144]
111 **Antoine DJ**, Dear JW, Lewis PS, Platt V, Coyle J, Masson M, Thanacoody RH, Gray AJ, Webb DJ, Moggs JG, Bateman DN, Goldring CE, Park BK. Mechanistic biomarkers provide early and sensitive detection of acetaminophen-induced acute liver injury at first presentation to hospital. *Hepatology* 2013; **58**: 777-787 [PMID: 23390034 DOI: 10.1002/hep.26294]
112 **Park HK**, Jo W, Choi HJ, Jang S, Ryu JE, Lee HJ, Lee H, Kim H, Yu ES, Son WC. Time-course changes in the expression levels of miR-122, -155, and -21 as markers of liver cell damage, inflammation, and regeneration in acetaminophen-induced liver injury in rats. *J Vet Sci* 2016; **17**: 45–51 [PMID: 27051339 DOI: 10.4142/jvs.2016.17.1.45]
113 **Wen Y**, Han J, Chen J, Dong J, Xia Y, Liu J, Jiang Y, Dai J, Lu J, Jin G, Han J, Wei Q, Shen H, Sun B, Hu Z. Plasma miRNA s as early biomarkers for detecting hepatocellular carcinoma. *Int J Cancer* 2015; **137**: 1679-1690 [PMID: 25845839 DOI: 10.1002/ijc.29544]
114 **Jin Y**, Wong YS, Goh BKP, Chan CY, Cheow PC, Chow PKH, Lim TKH, Goh GBB, Krishnamoorthy TL, Kumar R, Ng TP, Chong SS, Tan HH, Chung AYF, Ooi LLPJ, Chang JPE, Tan CK, Lee CGL. Circulating microRNAs as Potential Diagnostic and Prognostic Biomarkers in Hepatocellular Carcinoma.

Sci Rep 2019; **9**: 10464 [PMID: 31320713 DOI: 10.1038/s41598-019-46872-8]
115 **Waidmann O**, Köberle V, Brunner F, Zeuzem S, Piiper A, Kronenberger B. Serum microRNA-122 predicts survival in patients with liver cirrhosis. *PLoS One* 2012; **7**: e45652 [PMID: 23029162 DOI: 10.1371/journal.pone.0045652]
116 **Jansen C**, Eischeid H, Goertzen J, Schierwagen R, Anadol E, Strassburg CP, Sauerbruch T, Odenthal M, Trebicka J. The role of miRNA -34a as a prognostic biomarker for cirrhotic patients with portal hypertension receiving TIPS. *PLoS One* 2014; **9**: e103779 [PMID: 25068403 DOI: 10.1371/journal.pone.0103779]
117 **Huang YH**, Liang KH, Chien RN, Hu TH, Lin KH, Hsu CW, Lin CL, Pan TL, Ke PY, Yeh CT. A Circulating MicroRNA Signature Capable of Assessing the Risk of Hepatocellular Carcinoma in Cirrhotic Patients. *Sci Rep* 2017; **7**: 523 [PMID: 28364124 DOI: 10.1038/s41598-017-00631-9]
118 **Giray BG**, Emekdas G, Tezcan S, Ulger M, Serin MS, Sezgin O, Altintas E, Tiftik EN. Profiles of serum microRNAs; miR-125b-5p and miR223-3p serve as novel biomarkers for HBV-positive hepatocellular carcinoma. *Mol Biol Rep* 2014; **41**: 4513-4519 [PMID: 24595450 DOI: 10.1007/s11033-014-3322-3]
119 **Li LM**, Hu ZB, Zhou ZX, Chen X, Liu FY, Zhang JF, Shen HB, Zhang CY, Zen K. Serum microRNA profiles serve as novel biomarkers for HBV infection and diagnosis of HBV-positive hepatocarcinoma. *Cancer Res* 2010; **70**: 9798-9807 [PMID: 21098710 DOI: 10.1158/0008-5472.CAN-10-1001]
120 **Xu J**, Wu C, Che X, Wang L, Yu D, Zhang T, Huang L, Li H, Tan W, Wang C, Lin D. Circulating microRNAs, miR-21, miR-122, and miR-223, in patients with hepatocellular carcinoma or chronic hepatitis. *Mol Carcinog* 2011; **50**: 136-142 [PMID: 21229610 DOI: 10.1002/mc.20712]
121 **Bandopadhyay M**, Banerjee A, Sarkar N, Panigrahi R, Datta S, Pal A, Singh SP, Biswas A, Chakrabarti S, Chakravarty R. Tumor suppressor micro RNA miR-145 and onco micro RNAs miR-21 and miR-222 expressions are differentially modulated by hepatitis B virus X protein in malignant hepatocytes. *BMC Cancer* 2014; **14**: 721 [PMID: 25260533 DOI: 10.1186/1471-2407-14-721]
122 **Guo X**, Lv X, Lv X, Ma Y, Chen L, Chen Y. Circulating miR-21 serves as a serum biomarker for hepatocellular carcinoma and correlated with distant metastasis. *Oncotarget* 2017; **8**: 44050-44058 [PMID: 28477010 DOI: 10.18632/oncotarget.17211]
123 **Tomimaru Y**, Eguchi H, Nagano H, Wada H, Kobayashi S, Marubashi S, Tanemura M, Tomokuni A, Takemasa I, Umeshita K, Kanto T, Doki Y, Mori M. Circulating microRNA-21 as a novel biomarker for hepatocellular carcinoma. *J Hepatol* 2012; **56**: 167-175 [PMID: 21749846 DOI: 10.1016/j.jhep.2011.04.026]
124 **Li J**, Wang Y, Yu W, Chen J, Luo J. Expression of serum miR-221 in human hepatocellular carcinoma and its prognostic significance. *Biochem Biophys Res Commun* 2011; **406**: 70-73 [PMID: 21295551 DOI: 10.1016/j.bbrc.2011.01.111]
125 **Chen JJ**, Tang YS, Huang SF, Ai JG, Wang HX, Zhang LP. HBx protein-induced upregulation of microRNA-221 promotes aberrant proliferation in HBVrelated hepatocellular carcinoma by targeting estrogen receptor-α. *Oncol Rep* 2015; **33**: 792-798 [PMID: 25483016 DOI: 10.3892/or.2014.3647]
126 **van der Ree MH**, Jansen L, Kruize Z, van Nuenen AC, van Dort KA, Takkenberg RB, Reesink HW, Kootstra NA. Plasma MicroRNA Levels Are Associated With Hepatitis B e Antigen Status and Treatment Response in Chronic Hepatitis B Patients. *J Infect Dis* 2017; **215**: 1421-1429 [PMID: 28368488 DOI: 10.1093/infdis/jix140]
127 **Yang Y**, Liu M, Deng Y, Guo Y, Zhang X, Xiang D, Jiang L, You Z, Wu Y, Li M, Mao Q. Pretreatment microRNA levels can predict HBsAg clearance in CHB patients treated with pegylated interferon α-2a. *Virol J* 2018; **15**: 73 [PMID: 29685146 DOI: 10.1186/s12985-018-0982-y]
128 **Zhang X**, Chen C, Wu M, Chen L, Zhang J, Zhang X, Zhang Z, Wu J, Wang J, Chen X, Huang T, Chen L, Yuan Z. Plasma microRNA profile as a predictor of early virological response to interferon treatment in chronic hepatitis B patients. *Antivir Ther* 2012; **17**: 1243-1253 [PMID: 22997154 DOI: 10.3851/IMP2401]
129 **Brunetto MR**, Cavallone D, Oliveri F, Moriconi F, Colombatto P, Coco B, Ciccorossi P, Rastelli C, Romagnoli V, Cherubini B, Teilum MW, Blondal T, Bonino F. A serum microRNA signature is associated with the immune control of chronic hepatitis B virus infection. *PLoS One* 2014; **9**: e110782 [PMID: 25350115 DOI: 10.1371/journal.pone.0110782]
130 **Li J**, Zhang X, Chen L, Zhang Z, Zhang J, Wang W, Wu M, Shi B, Zhang X, Kozlowski M, Hu Y, Yuan Z. Circulating miR-210 and miR-22 combined with ALT predict the virological response to interferon-alpha therapy of CHB patients. *Sci Rep* 2017; **7**: 15658 [PMID: 29142236 DOI: 10.1038/s41598-017-15594-0]
131 **Zhang H**, Yan XL, Guo XX, Shi MJ, Lu YY, Zhou QM, Chen QL, Hu YY, Xu LM, Huang S, Su SB. MiR-27a as a predictor for the activation of hepatic stellate cells and hepatitis B virus-induced liver cirrhosis. *Oncotarget* 2018; **9**: 1075-1090 [PMID: 29416678 DOI: 10.18632/oncotarget.23262]
132 **Yu F**, Zhou G, Li G, Chen B, Dong P, Zheng J. Serum miR-181b Is Correlated with Hepatitis B Virus Replication and Disease Progression in Chronic Hepatitis B Patients. *Dig Dis Sci* 2015; **60**: 2346-2352 [PMID: 25976622 DOI: 10.1007/s10620-015-3649-1]
133 **Akamatsu S**, Hayes CN, Tsuge M, Miki D, Akiyama R, Abe H, Ochi H, Hiraga N, Imamura M, Takahashi S, Aikata H, Kawaoka T, Kawakami Y, Ohishi W, Chayama K. Differences in serum microRNA profiles in hepatitis B and C virus infection. *J Infect* 2015; **70**: 273–287 [PMID: 25452043 DOI: 10.1016/j.jinf.2014.10.017]
134 **Zheng J**, Zhou Z, Xu Z, Li G, Dong P, Chen Z, Lin D, Chen B, Yu F. Serum microRNA-125a-5p, a useful biomarker in liver diseases, correlates with disease progression. *Mol Med Rep* 2015; **12**: 1584-1590 [PMID: 25815788 DOI: 10.3892/mmr.2015.3546]
135 **Wang W**, Liu R, Su Y, Li H, Xie W, Ning B. MicroRNA-21-5p mediates TGF-β-regulated fibrogenic activation of spinal fibroblasts and the formation of fibrotic scars after spinal cord injury. *Int J Biol Sci* 2018; **14**: 178-188 [PMID: 29483836 DOI: 10.7150/ijbs.24074]
136 **Li BB**, Li DL, Chen C, Liu BH, Xia CY, Wu HJ, Wu CQ, Ji GQ, Liu S, Ni W, Yao DK, Zeng ZY, Chen DG, Qin BD, Xin X, Yan GL, Dan Tang, Liu HM, He J, Yan H, Zhu WJ, Yu HY, Zhu L. Potentials of the elevated circulating miR-185 level as a biomarker for early diagnosis of HBV-related liver fibrosis. *Sci Rep* 2016; **6**: 34157 [PMID: 27677421 DOI: 10.1038/srep34157]
137 **Zhang Q**, Xu M, Qu Y, Li Z, Zhang Q, Cai X, Lu L. Analysis of the differential expression of circulating microRNAs during the progression of hepatic fibrosis in patients with chronic hepatitis B virus infection. *Mol Med Rep* 2015; **12**: 5647-5654 [PMID: 26299203 DOI: 10.3892/mmr.2015.4221]
138 **Xing TJ**, Jiang DF, Huang JX, Xu ZL. Expression and clinical significance of miR-122 and miR-29 in hepatitis B virus-related liver disease. *Genet Mol Res* 2014; **13**: 7912-7918 [PMID: 25299106 DOI: 10.4238/2014.September.29.4]

139 **Jin BX**, Zhang YH, Jin WJ, Sun XY, Qiao GF, Wei YY, Sun LB, Zhang WH, Li N. MicroRNA panels as disease biomarkers distinguishing hepatitis B virus infection caused hepatitis and liver cirrhosis. *Sci Rep* 2015; **5**: 15026 [PMID: 26456479 DOI: 10.1038/srep15026]

140 **Song G**, Jia H, Xu H, Liu W, Zhu H, Li S, Shi J, Li Z, He J, Chen Z. Studying the association of microRNA-210 level with chronic hepatitis B progression. *J Viral Hepat* 2014; **21**: 272-280 [PMID: 24597695 DOI: 10.1111/jvh.12138]

141 **Li F**, Zhou P, Deng W, Wang J, Mao R, Zhang Y, Li J, Yu J, Yang F, Huang Y, Lu M, Zhang J. Serum microRNA-125b correlates with hepatitis B viral replication and liver necroinflammation. *Clin Microbiol Infect* 2016; **22**: 384.e1-384.e10 [PMID: 26802212 DOI: 10.1016/j.cmi.2015.12.024]

142 **Wang JY**, Mao RC, Zhang YM, Zhang YJ, Liu HY, Qin YL, Lu MJ, Zhang JM. Serum microRNA-124 is a novel biomarker for liver necroinflammation in patients with chronic hepatitis B virus infection. *J Viral Hepat* 2015; **22**: 128-136 [PMID: 25131617 DOI: 10.1111/jvh.12284]

143 **Fan HX**, Feng YJ, Zhao XP, He YZ, Tang H. MiR-185-5p suppresses HBV gene expression by targeting ELK1 in hepatoma carcinoma cells. *Life Sci* 2018; **213**: 9-17 [PMID: 30308183 DOI: 10.1016/j.lfs.2018.10.016]

World Journal of Gastroenterology

Submit a Manuscript: https://www.f6publishing.com

World J Gastroenterol 2020 March 21; 26(11): 1128-1141

DOI: 10.3748/wjg.v26.i11.1128

ISSN 1007-9327 (print) ISSN 2219-2840 (online)

MINIREVIEWS

Similarities and differences in guidelines for the management of pancreatic cysts

Gandhi Lanke, Jeffrey H Lee

ORCID number: Gandhi Lanke (0000-0002-5577-2257); Jeffrey H Lee (0000-0001-6740-3670).

Author contributions: Lanke G composed and drafted the paper; Lee JH conceptualized, designed, revised,and edited the draft.

Conflict-of-interest statement: There is no conflict of interest associated with any of the senior author or other coauthors related to the manuscript.

Manuscript source: Invited Manuscript

Received: December 6, 2019
Peer-review started: December 6, 2019
First decision: January 16, 2020
Revised: February 21, 2020
Accepted: March 1, 2020
Article in press: March 1, 2020
Published online: March 21, 2020

P-Reviewer: Kovacevic B
S-Editor: Wang J

Gandhi Lanke, Jeffrey H Lee, Department of Gastroenterology, Hepatology, and Nutrition, University of Texas MD Anderson Cancer Center, Houston, TX 77030, United States

Corresponding author: Jeffrey H Lee, MD, MPH, FACG, FASGE, AGAF President, Texas Society of President, Texas Society of Gastroenterology and Endoscopy (TSGE) Professor and Director, Advanced Endoscopy Program and Training Department of Gastroenterology and Hepatology, MD Anderson Cancer Center, 1515 Holcombe Blvd, Houston, TX 77030, United States. jefflee@mdanderson.org

Abstract

Accurate diagnosis of Pancreatic cysts (PC) is key in the management. The knowledge of indications for surgery, the role of endoscopic ultrasound-guided fine needle aspiration, cyst fluid analysis, imaging, and surveillance of PC are all important in the diagnosis and management of PC. Currently, there are many guidelines for the management of PC. The optimal use of these guidelines with a patient-centered approach helps diagnose early cancer and prevent the spread of cancer.

Key words: Pancreatic cysts; Serous cystadenoma; Main pancreatic duct; Intraductal papillary mucinous neoplasm; Endoscopic ultrasound-guided fine needle aspiration; Carcinoembryonic antigen

Core tip: The differentiation of mucinous and non-mucinous cysts is key in the effective management of pancreatic cysts. Thorough understanding of the absolute indications for surgery, the role of endoscopic ultrasound-guided fine needle aspiration, cyst fluid analysis, imaging, and the guidelines for surveillance are important in the diagnosis and treatment of pancreatic cysts. Patient-centered approach with a multidisciplinary team involving the surgeon, radiologist, pathologist, oncologist, and advanced endoscopist improves the management of pancreatic cysts.

Citation: Lanke G, Lee JH. Similarities and differences in guidelines for the management of pancreatic cysts. *World J Gastroenterol* 2020; 26(11): 1128-1141
URL: https://www.wjgnet.com/1007-9327/full/v26/i11/1128.htm
DOI: https://dx.doi.org/10.3748/wjg.v26.i11.1128

L-Editor: A
E-Editor: Ma YJ

INTRODUCTION

Pancreatic cysts (PC) are diagnosed more frequently with the widespread use of cross-sectional imaging, and most of them are found incidentally. The prevalence of PC varies with age and race and they are found approximately 3%-14% on routine computed tomography (CT) and Magnetic resonance imaging (MRI) for unrelated reasons[1,2]. They can be benign or neoplastic. Accurate determination of cyst categorization is key in the management. With the introduction of endoscopic ultrasound (EUS) and fine-needle aspiration (FNA), the accuracy of pancreatic cyst classification is improved. This review article focuses on the management of PC using different guidelines.

PANCREATIC CYST CLASSIFICATION

The pathological classification of PC (Table 1) includes inflammatory fluid collections (IFCs), non-neoplastic PC, and pancreatic cystic neoplasms (PCNs). PC can also be associated with an underlying disorder such as Von Hippel-Lindau or polycystic kidney disease[3,4]. IFCs are usually as a result of a complication of acute pancreatitis. IFCs are categorized according to the revised Atlanta classification into acute peripancreatic fluid collections, pseudocysts, acute necrotic collections, and walled-off pancreatic necrosis[5].

Non-neoplastic or benign PC include true cysts, retention cysts, mucinous non-neoplastic cysts, and lymphoepithelial cysts. They are typically seen after surgical resection of a pancreatic lesion that is suspected to be a pancreatic cystic neoplasm (PCN) preoperatively. According to World Health Organization histological classification, PCNs are classified into serous cystic tumors, mucinous cystic neoplasms (MCNs), intraductal papillary mucinous neoplasms (IPMNs) and solid pseudopapillary neoplasms (SPN).

HOW TO APPROACH PC

Serous cystic tumors are usually serous cystadenomas commonly seen in women over the age of 60 years and can arise anywhere in the pancreas[6]. Serous cystadenomas are classified into microcystic (composed of multiple small cystic spaces) and oligocystic (composed of fewer larger cystic spaces)[7,8]. Most of them are benign and malignant potential is low[9]. Serous cystadenomas are often found incidentally on imaging. Sometimes it is difficult to distinguish serous cystic neoplasms from mucinous neoplasms on imaging. EUS finding of honeycomb appearance with central calcification can be diagnostic (Figure 1)[10]. EUS-FNA with low carcinoembryonic antigen (CEA) in cyst fluid can help distinguish mucinous and serous cystic tumors[11]. Histologically, the cysts are lined by cuboidal epithelial cells with clear cytoplasm filled with glycogen[12].

The risk of malignant transformation to cystadenocarcinoma is approximately 0.2-3%[12,13]. Surgery should be reserved for symptomatic (jaundice, extrinsic organ compression) patients and when in doubt close follow up with multidisciplinary team approach is advocated[14,15]. Size > 4 cm alone should not be an indication for surgery, although some authors advocate it[16,17]. There is no consensus on guidelines for follow up in terms of imaging. Many authors recommend yearly CT/MRI although currently, it is uncertain about how long the patient needs follow up. Overall, conservative management is recommended for serous cystic tumors and the algorithm for management of serous cystic tumors is shown in Figure 2.

MCNs are found commonly in women over the age of 40 years and can occur in the body or tail of the pancreas (Figure 3)[8]. They secrete mucin, demonstrate ovarian like stroma, exhibit cellular atypia and do not communicate with the main pancreatic duct[8]. MCNs have the risk of malignant potential. MCNs are classified according to the grade of dysplasia into low, intermediate, high grade, or invasive carcinoma[18]. The prevalence of invasive carcinoma in MCNs is approximately 12% and most patients are young at presentation, which would require long term surveillance[19]. The current treatment recommendation for MCNs is surgical resection[20]. Also, MCNs do not require surveillance after surgical resection unless there is invasive cancer[21]. Some authors do not recommend surgery for MCNs < 3 cm without mural nodules or elevated tumor markers[22]. The algorithm for the management of MCNs is shown in Figure 2.

SPNs predominantly affect young females and are generally located in the tail of the pancreas (Figure 4A)[23]. They appear as solid and cystic components with areas of

Table 1 Pathological classification of most common pancreatic cysts

Inflammatory fluid collections
Acute peripancreatic fluid collections
Pseudocysts
Acute necrotic collections
Walled-off pancreatic necrosis
Non-neoplastic
True cysts
Mucinous non-neoplastic cysts
Lymphoepithelial cysts
Pancreatic cystic neoplasms
Serous cystic neoplasms
Mucinous cystic neoplasm
Intrapapillary mucinous neoplasm
Solid papillary neoplasm

hemorrhage, calcification, and a rim of the fibrous capsule[24]. They have malignant potential. Surgery is the treatment of choice and R_0 resection is curative[25]. The algorithm for the management of SPNs is shown in Figure 2.

IPMNs are mucin-producing papillary neoplasms of the pancreatic duct that exhibit variable cellular atypia with dilation of the pancreatic ducts and are more common over the age of 60 years[26]. Based on the involvement of the pancreatic duct, they are classified into branch duct, main duct (MD-IPMN), or mixed type of IPMN (Figure 4B-D) respectively[27]. IPMNs have malignant potential and according to the grade of dysplasia they are classified into mild dysplasia, moderate dysplasia, high-grade dysplasia, or invasive carcinoma[27].

SIMILARITIES AND DIFFERENCES OF VARIOUS GUIDELINES IN THE MANAGEMENT OF PC: WHICH PC CAN BE OBSERVED AND HOW LONG DO THEY NEED SURVEILLANCE?

European guidelines[28]

MCNs size < 4 cm without symptoms or mural nodules can undergo surveillance every 6 mo during the 1st year using EUS/MRI or both[21,29]. They can be followed annually if no interval change in cyst size. Lifelong surveillance is advocated if they are fit for surgery. IPMNs cyst size < 4 cm or low-grade dysplasia can be followed with serum CA 19-9 level, EUS/MRI or both every 6 mo during the 1st year. Followed by every year if no interval change in cyst size until no longer fit for surgery[28]. After surgical resection of high-grade dysplasia or MD-IPMN, EUS/MRI is recommended every 6 mo for the 1st two years and yearly follow-up afterward. Low-grade dysplasia or remnant IPMN after surgical resection should be followed in the same manner as non-resected IPMN. Lifelong follow up after surgical resection is recommended if the patient is fit and willing to undergo surgery.

American College of Gastroenterology guidelines[30]

The surveillance of IPMN/MCN is based on cyst size. Cyst size < 1 cm, MRI every 2 years for 4 years is recommended and lengthen the interval if cyst size is stable. Cyst size 1-2 cm, MRI every year for 3 years, followed by every 2 years for 4 years and lengthen the interval if cyst size is stable. Cyst size 2-3 cm, MRI/EUS every 6-12 mo for 3 years, followed by every year for 4 years and lengthen the interval once stable in size. Cyst size > 3 cm, MRI alternating with EUS every 6 mo for 3 years, followed by MRI alternating with EUS every year for 4 years and lengthen the interval once stable in size. Consider EUS-FNA if any increase in cyst size during follow up.

The risk of recurrence of IPMN after surgery varies based on the degree of dysplasia. EUS/MRI every 6 mo after surgical resection of IPMN-HGD is recommended. With low to intermediate grade dysplasia in the absence of PC in the remnant pancreas after surgical resection, MRI every 2 years is recommended. However, if IPMN or PC are present in the remnant pancreas after surgical resection, surveillance should be according to cyst size. Stop surveillance after surgical resection

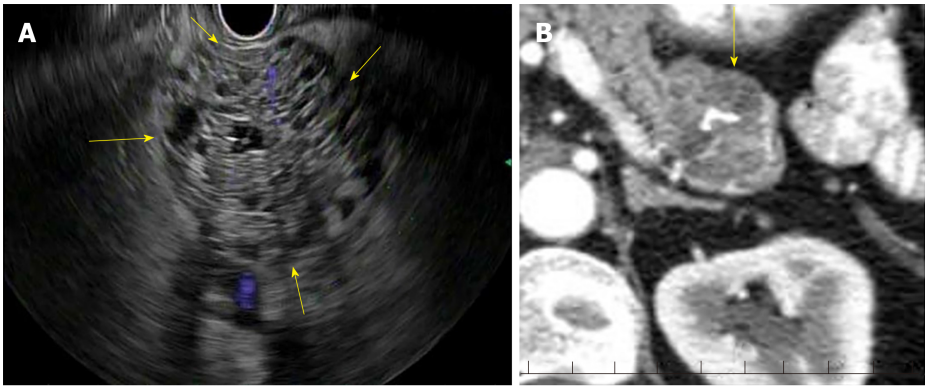

Figure 1 Endoscopic ultrasound (Honeycomb appearance). A: Endoscopic ultrasound: Serous cystadenoma; B: Computed tomography: Serous Cystadenoma. Computed tomography: Portal venous phase showing calcification.

of MCN if no invasive cancer is present or no longer a surgical candidate.

American Gastroenterological Association guidelines[31]

In asymptomatic pancreatic neoplastic cysts < 3 cm without a solid component or PD dilation, MRI is recommended in 1 year and every 2 years for 5 years. American Gastroenterology Association (AGA) recommends stopping surveillance when no longer fit for surgery or no change in cyst characteristics after 5 years of follow up.

Revised IAP 2017 Fukuoka guidelines[32]

In revised IAP 2017 guidelines, for cyst size 1-2 cm, CT/MRI every 6 mo for a year, followed by every year for 2 years and lengthen the interval if stable. For cyst size 2-3 cm, EUS in 3-6 mo for 1 year. Increase the interval to 1 year with EUS/MRI as appropriate. For cyst size > 3 cm, close surveillance alternating MRI with EUS every 3-6 mo. In surgically resected IPMN, surveillance is recommended with cross-sectional imaging twice a year for patients with a family history of pancreatic ductal adenocarcinoma, surgical margin positive for HGD, and non-intestinal sub-type of IPMN. For all others, every 6-12 mo of cross-sectional imaging is recommended.

American College of Radiology guidelines[33]

ACR guidelines are for the management of PC found incidentally on CT/MRI. These guidelines are based on the age of the patient and the size of the cyst. Cyst size < 1.5 cm and age < 65 years, CT/MRI every year for 5 years, followed by every 2 years for 4 years. Stop surveillance if stable over 9 years. Cyst size < 1.5 cm and age 65-79 years, CT/MRI every 2 years for a total of 10 years. Stop surveillance if the cyst is stable for 10 years. If there is interval change and cyst size < 1.5 cm, consider CT/MRI every year or EUS-FNA. If EUS-FNA shows a mucinous cyst or indeterminate cyst, CT/MRI every 6 mo for 2 years, followed by every year for 2 years and every 2 years for 6 years. Stop surveillance if the cyst is stable after 10 years.

Cyst size 1.5-1.9 cm with MPD communication, CT/MRI every year for 5 years, followed by every 2 years for 4 years. Stop surveillance if cyst size stable for over 9 years. Cyst size 2-2.5 cm with MPD communication, CT/MRI every 6 mo for 2 years, followed by every year for 2 years and subsequently every 2 years for 6 years. Stop surveillance if cyst size is stable for 10 years. If there is interval change and cyst size ≤ 2.5 cm, CT/MRI every 6 mo for 2 years, followed by every year for 2 years and subsequently every 2 years. If cyst size > 2.5 cm, consider EUS-FNA. If EUS-FNA shows a mucinous cyst or indeterminate cyst, CT/MRI every 6 mo for 2 years, followed by every year for 2 years and every 2 years for 6 years.

Cyst size 1.5-2.5 cm without MPD communication or cannot be determined, CT or MRI every 6 mo for 2 years, followed by every year for 2 years and subsequently every 2 years for 6 years. Stop surveillance if cyst size is stable after 10 years. If there is interval change and cyst size ≤ 2.5 cm, consider CT/MRI every 6 mo for 1 year, followed by every year for 5 years and subsequently every 2 years. If cyst size is > 2.5 cm, consider EUS-FNA.

Cyst size > 2.5 cm and low risk by imaging, consider CT/MRI every 6 mo for 2 years. If stable after 2 years, CT/MRI every year for 2 years and subsequently every 2 years for 6 years. Stop surveillance if stable in cyst size. Any interval changes in cyst size, consider EUS-FNA. Age ≥ 80 years with cyst size ≤ 2.5 cm, CT/MRI every 2 years for 4 years. Stop surveillance if the cyst is stable in size. If there is interval change and cyst size ≤ 2.5 cm, consider CT/MRI every year. Stop surveillance if cyst size stable or

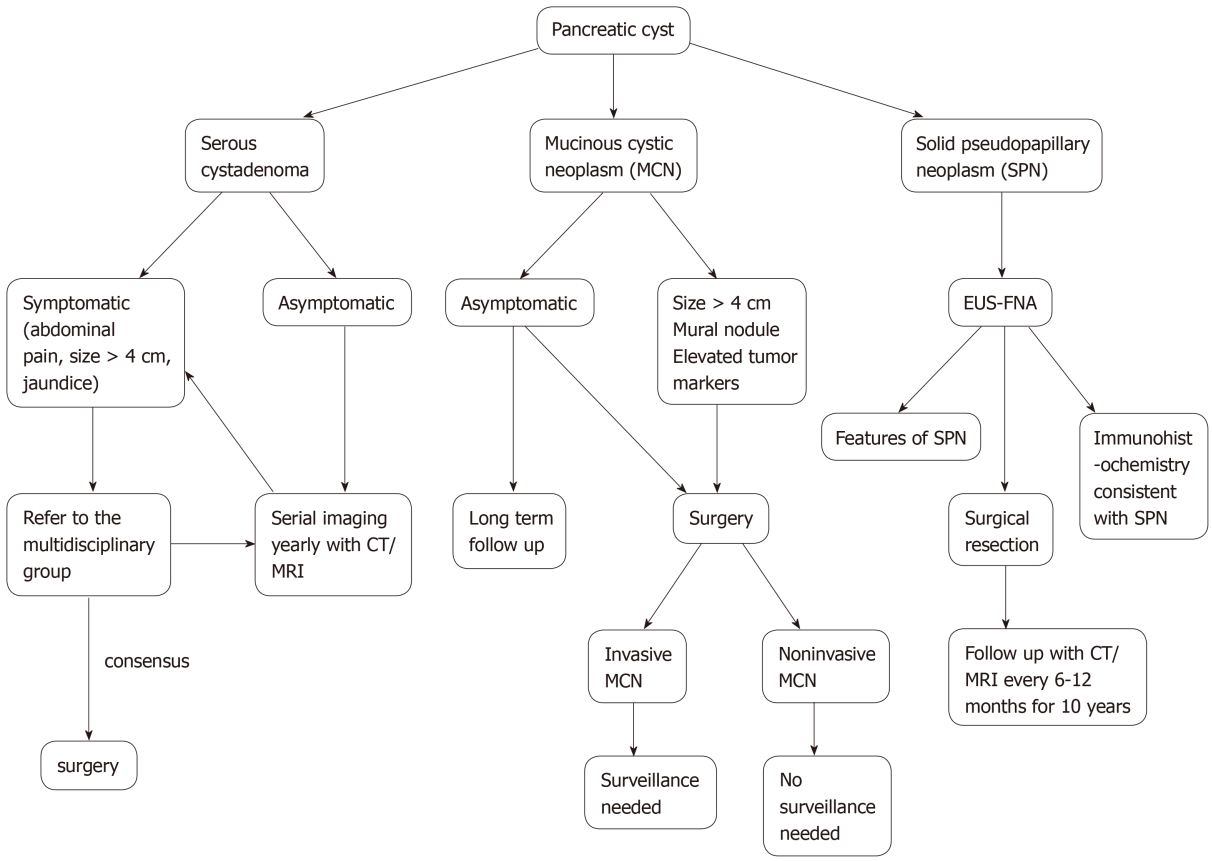

Figure 2 Algorithm for the management of pancreatic cysts. MCN: Mucinous cystic neoplasm; SPN: Solid pseudopapillary neoplasm; EUS-FNA: Endoscopic Ultrasound-Fine Needle aspiration; CT: Computed tomography; MRI: Magnetic resonance imaging.

not a surgical candidate. If there is interval change and cyst size > 2.5 cm, consider EUS-FNA. Age ≥ 80 years with cyst size > 2.5 cm and low risk by imaging, consider CT/MRI every 2 years for 4 years. Stop surveillance if cyst size is stable. If there is interval change in cyst size, consider EUS-FNA.

Surveillance of PC using different guidelines is illustrated in Table 2. Overall, there is no consensus on the surveillance of PC without high-risk stigmata or worrisome features. European guidelines recommend surveillance of MCN/IPMN cysts < 4 cm with EUS/MRI. American College of Gastroenterology (ACG) guidelines recommend surveillance of IPMN/MCN based on cyst size (< 1 cm, 1-2 cm, 2-3 cm, > 3 cm) with MRI and after surgical resection, follow up is recommended based on the degree of dysplasia. AGA recommends follow up with MRI if cyst size < 3 cm without solid component or MPD dilation. Lifelong surveillance is recommended if they are fit for surgery. Revised IAP or Fukuoka guidelines are based on cyst size (< 1 cm, 1-2 cm, 2-3 cm, and > 3 cm) but with increased surveillance using CT/MRI and EUS as needed. ACR guidelines are proposed for the management of asymptomatic incidental PC found on imaging and they are based on cyst size, age, low risk on imaging, and MPD communication. They are classified into age < 65 years with cyst size < 1.5 cm, age 65-79 years with cyst size < 1.5 cm, cyst size 1.5-1.9 cm with MPD communication, cyst size 1.5-2.5 cm without MPD communication, low risk by imaging with cyst size > 2.5 cm, age ≥ 80 years with cyst size ≤ 2.5 cm and age ≥ 80 years with low risk by imaging and cyst size > 2.5 cm. Surveillance is recommended using CT/MRI and EUS-FNA as needed.

ROLE OF BLOOD AND CYSTIC MARKERS IN THE DIAGNOSIS OF PC

European guidelines[28]

Serum cancer antigen (CA 19-9) can be considered when there is a concern for the malignant transformation of IPMN[34,35]. Guanine nucleotide-binding protein (GNAS) and Kirsten rat sarcoma viral oncogene homolog (KRAS) mutations using next-

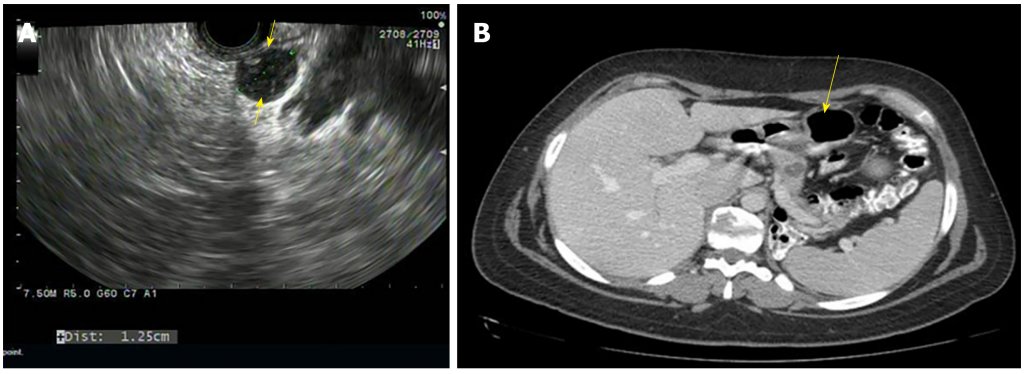

Figure 3 Endoscopic ultrasound - mucinous cystadenoma and computed tomography - mucinous cystadenoma. A: Endoscopic ultrasound-mucinous cystadenoma; B: Computed tomography-mucinous cystadenoma.

generation sequencing techniques can be used in identifying mucin-producing cysts when the diagnosis is not clear[36,37]. Cyst fluid carcinoembryonic antigen (CEA) > 192 ng/mL can help distinguish mucinous from non-mucinous cysts[38]. Cyst fluid amylase level can help identify pseudocysts but may not differentiate mucinous from non-mucinous cysts[11,39]. A combination of cytology, cyst fluid amylase, CEA and molecular markers can help differentiate mucinous from non-mucinous cysts.

ACG guidelines[30]

Cyst fluid cytology can assess for HGD-IPMN or cancer when imaging features are insufficient to warrant surgery. Cyst fluid CEA (> 192 ng/mL) can help differentiate IPMNs and MCNs from other cyst types[40]. Molecular markers like KRAS and GNAS mutations can help identify IPMNs or MCNs when the diagnosis is not clear[41,42]. Cyst fluid amylase level < 250 IU/L can help exclude the diagnosis of pseudocyst[11].

AGA guidelines[31]

Cyst fluid cytology is recommended for the evaluation of high-risk features on imaging and positive cytology increases the specificity for diagnosing malignancy. The role of cyst fluid molecular markers is not clear and further research is needed.

Revised IAP 2017 guidelines[32]

Cyst fluid CEA (> 192 ng/mL) can distinguish mucinous from non-mucinous but not benign from malignant cyst[38]. Cyst fluid cytology can be diagnostic but sometimes limited by scant cellularity[43,44]. Cyst fluid amylase can differentiate benign from malignant MCN and amylase levels are higher in pseudocysts than non-pseudocysts[45]. The role of molecular markers like KRAS and GNAS mutations is still evolving.

ACR guidelines[33]

Cyst fluid CEA > 192 ng/mL can help identify a mucinous cyst[46]. Cyst fluid amylase >250 IU/L suggests pseudocyst[11]. KRAS and GNAS molecular markers can help differentiate mucinous from non-mucinous cysts[47]. Cyst cytology can identify dysplastic cells. The role of cystic fluid analysis in the diagnosis of PC using different guidelines is illustrated in Table 3. Overall, cyst fluid analysis compliments imaging and can help differentiate mucinous from non-mucinous cysts. Cytology can aid in distinguishing HGD-IPMN and cancer. Cyst fluid CEA > 192 ng/mL can differentiate mucinous from non-mucinous cysts. Cyst fluid amylase > 250 IU/L can accurately diagnose pseudocysts. The use of molecular markers is still evolving, and it is promising for the future.

EUS-FNA INDICATIONS

European guidelines[28]

EUS-FNA can improve diagnostic accuracy with cyst fluid CEA, amylase, and cytology in differentiating mucinous *vs* non-mucinous cysts. Also, it distinguishes malignant *vs* benign cysts when CT or MRI is unclear. EUS-FNA should be performed only when results are expected to change clinical management.

ACG guidelines[30]

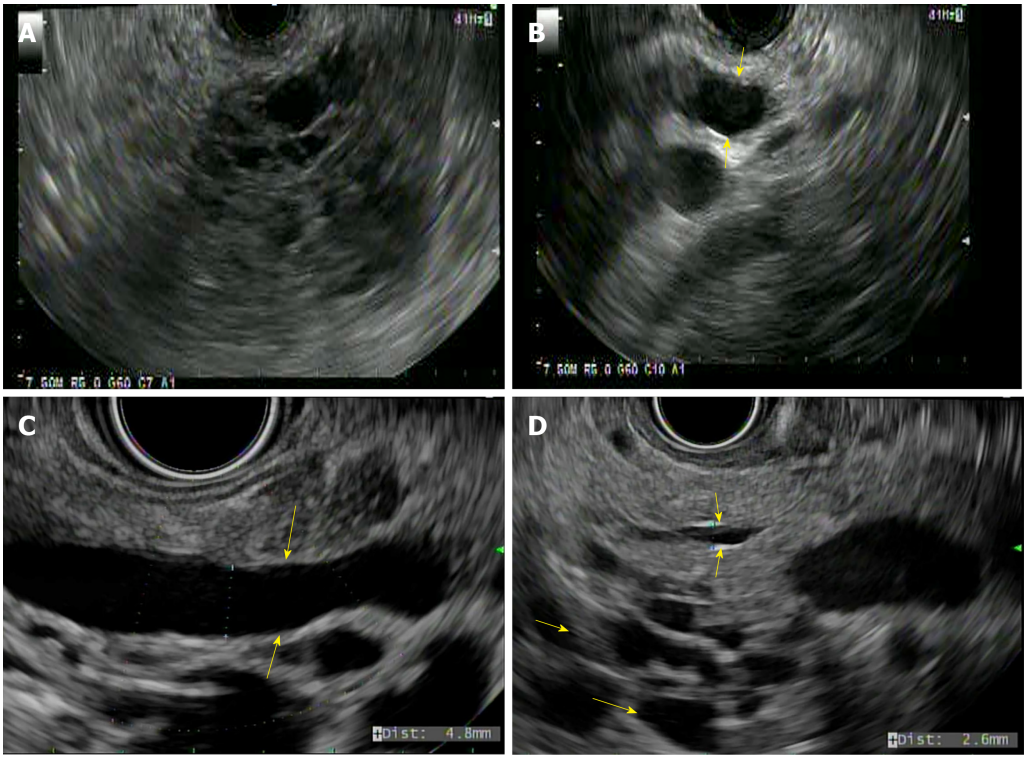

Figure 4 Endoscopic ultrasound. A: Solid pseudopapillary neoplasm, hypoechoic foci (solid areas) with anechoic cystic spaces; B: Main duct-intraductal papillary mucinous neoplasm; C: Mixed duct-intraductal papillary mucinous neoplasm; D: Branch duct-intraductal papillary mucinous neoplasm.

EUS-FNA is indicated in IPMNs/MCNs with jaundice or acute pancreatitis secondary to the cyst, new-onset or worsening diabetes and increase in cyst size > 3 mm/year during surveillance, significantly elevated serum CA 19-9, mural nodule, solid component within cyst or pancreatic parenchyma, dilation of MPD > 5 mm, focal dilation of PD concerning for MD-IPMN or obstructing lesion, and mucin-producing cyst size ≥ 3 cm; it is also indicated when the diagnosis of cysts is unclear; results will likely alter management; and when cyst fluid CEA can differentiate IPMNs and MCNs from other cyst types.

AGA guidelines[31]

EUS-FNA is indicated when a pancreatic cyst has at least 2 high-risk features such as cyst size ≥ 3 cm, dilated MPD, and solid component.

Revised IAP 2017 or Fukuoka guidelines[32]

EUS-FNA is recommended with pancreatitis, cyst size ≥ 3 cm, thickened/enhancing cyst wall, the main duct size 5-9 mm, non-enhancing mural nodule, an abrupt change in caliber of the pancreatic duct with distal pancreatic atrophy, lymphadenopathy, increased serum level of CA19-9, and cyst growth rate ≥ 5 mm/2 years.

ACR guidelines[33]

EUS-FNA is indicated for a mural nodule, wall thickening, dilation of MPD ≥ 7 mm, or extrahepatic biliary obstruction/jaundice. The indications of EUS-FNA for the diagnosis of PC using different guidelines are illustrated in Table 4. Overall, EUS-FNA is indicated when the results are likely to change the management. EUS-FNA is recommended for cyst ≥ 3 cm, mural nodule, thickened cyst wall, solid component in cyst, MPD > 5 mm, abrupt change in caliber of PD with distal pancreatic atrophy, lymphadenopathy, cyst growth ≥ 3-5 mm/year, acute pancreatitis, new-onset or worsening diabetes, jaundice and increased serum CA 19-9 level.

INDICATIONS FOR SURGERY

European guidelines[28]

Absolute indications for surgery include positive cytology for malignant/ HGD-IPMN, solid mass, jaundice (tumor-related), enhancing mural nodule ≥ 5 mm, and MPD ≥ 10 mm. Relative indications for surgery include cyst growth rate ≥ 5mm/year,

Table 2 Surveillance of pancreatic cysts

	Surveillance of pancreatic cysts
European guidelines[28]	Mucinous cystic neoplasm: Cyst size < 4 cm without symptoms or mural nodules should undergo surveillance every 6 mo for the 1st year using EUS/MRI or both[29]. Followed by annually, if no changes. Lifelong surveillance if they are fit for surgery
	Intraductal papillary mucinous neoplasm (IPMN): Every 6 mo for cysts less than 4cm or low-grade dysplasia for the 1st year with CA 19-9, EUS/MRI or both. Followed by yearly, until no longer fit for surgery
	After surgical resection, HGD or MD-IPMN should have imaging every 6 mo for the 1st 2 yr. Followed by yearly surveillance. Lifelong surveillance if they are fit for surgery
American College of Gastroenterology (ACG) guidelines[30]	Intraductal papillary mucinous neoplasm/Mucinous cystic neoplasm (IPMN/MCN): Cyst size < 1 cm: MRI every 2 yr × 4 yr. If stable in size, consider prolonging the time interval. Any increase in size, consider EUS-FNA in 6 mo and reevaluate
	Cyst size 1-2 cm: MRI every 1 yr × 3 yr. If stable, consider MRI every 2 yr × 4 yr. Once stable, consider prolonging the interval
	Cyst size 2-3 cm: MRI/EUS every 6-12 mo for 3 yr. If stable, MRI every 1-year × 4 yr. Once stable, consider prolonging the interval. Any increase in cyst size should be referred to the multidisciplinary group and consider EUS-FNA
	Cyst size > 3 cm: Referral to the multidisciplinary team. MRI alternating with EUS every 6 mo for 3 yr. Once stable in size, MRI alternating with EUS every year for 4 yr. Once stable in size, consider prolonging the interval
	Stop surveillance when a patient is no longer a surgical candidate or after surgical resection of MCN if no invasive cancer
	The risk of recurrence of IPMN after surgery varies based on the degree of dysplasia
	EUS/MRI every 6 mo after surgical resection of IPMN with HGD
	MRI every 2 yr after surgical resection of IPMN with low to intermediate grade dysplasia in the absence of pancreatic cysts in the remnant pancreas. However, if IPMN or pancreatic cysts are present in the remnant pancreas, then surveillance should be based on cyst size
American Gastroenterology Association (AGA) guidelines[31]	Cyst size < 3 cm without a solid component or PD dilation recommend MRI in 1 yr, followed by every 2 yr for 5 yr.
	Recommend stopping surveillance if no change in cyst characteristics after 5 yr or not a surgical candidate
Revised IAP 2017 or revised Fukuoka guidelines[32]	Branch duct-Intraductal papillary mucinous neoplasm (BD-IPMN): Cysts without high-risk stigmata should undergo CT/MRI every 3-6 mo to establish stability if prior imaging is not available. Subsequently, surveillance should be based on size stratification
	For cyst size < 1 cm, CT/MRI every 2 yr
	For cyst size 1-2 cm, CT/MRI every 6 mo for a year, followed by every year for 2 yr and prolong the interval if stable
	For cyst size 2-3 cm, EUS in 3-6 mo for 1 year. Increase the interval to 1 yr with EUS/MRI as appropriate. Consider surgery in young patients with a need for prolonged surveillance
	For cyst size > 3 cm, close surveillance alternating MRI with EUS every 3-6 mo. Strongly recommend surgery in young patients
	In surgically resected IPMN, surveillance is recommended with cross-sectional imaging twice a year for patients with a family history of pancreatic ductal adenocarcinoma, surgical margin positive for HGD and non-intestinal sub-type of IPMN. For all others, every 6-12 mo of cross-sectional imaging is recommended
American College of Radiology (ACR) guidelines[33]	Cyst size < 1.5 cm and age < 65 yr: CT/MRI every year for 5 yr, followed by every 2 yr for 4 yr. Stop surveillance if stable over 9 yr
	Cyst size < 1.5 cm and age 65-79 yr: CT/MRI every 2 yr for a total of 10 yr. Stop surveillance if the cyst is stable for 10 yr
	If there is interval change and cyst size < 1.5 cm, consider CT/MRI every year or EUS-FNA. EUS-FNA shows a mucinous cyst or indeterminate cyst, CT/MRI every 6 mo for 2 yr, followed by every year for 2 yr and every 2 yr for 6 yr. Stop surveillance if the cyst is stable after 10 yr
	Any further interval growth of cyst should be referred to surgery for further evaluation

	Cyst size 1.5-1.9 cm with MPD communication: CT/MRI every year for 5 yr, followed by every 2 yr for 4 yr. Stop surveillance if cyst size stable for over 9 yr
	Cyst size 2-2.5 cm with MPD communication: CT/MRI every 6 mo for 2 yr, followed by every year for 2 yr and subsequently every 2 yr for 6 yr. Stop surveillance if cyst size is stable for 10 yr
	If there is interval change and cyst size ≤ 2.5 cm, CT/MRI every 6 mo for 2 yr, followed by every year for 2 yr and subsequently every 2 yr. If cyst size > 2.5 cm, consider EUS-FNA
	If EUS-FNA shows a mucinous cyst or indeterminate cyst, CT/MRI every 6 mo for 2 yr, followed by every year for 2 yr and every 2 yr for 6 yr
	EUS-FNA is recommended for any mural nodule, wall thickening, dilation of MPD ≥ 7 mm or extrahepatic biliary obstruction/Jaundice irrespective of cyst size
	Cyst size 1.5-2.5 cm without MPD communication or cannot be determined: CT or MRI every 6 mo for 2 yr, followed by every year for 2 yr and subsequently every 2 yr for 6 yr. Stop surveillance if cyst size is stable after 10 yr
	If there is interval change and cyst size < 2.5 cm, consider CT/MRI every 6 mo for 1 year, followed by every year for 5 yr and subsequently every 2 yr. If cyst size is > 2.5 cm, consider EUS-FNA
	Cyst size >2.5 cm: If a cyst is a low risk by imaging, consider CT/MRI every 6 mo for 2 yr. If stable after 2 yr, CT/MRI every yr for 2 yr and subsequently every 2 yr for 6 yr. Stop surveillance if stable in cyst size
	Any interval changes in cyst size, consider EUS-FNA. Any high-risk stigmata like jaundice, enhancing mural nodule, wall thickening and MPD ≥ 10 mm refer to surgery for evaluation
	Age ≥ 80 yr with cyst size ≤ 2.5 cm: CT/MRI every 2 yr for 4 yr. Stop surveillance if cyst size is stable in size: If there is interval change and cyst size ≤ 2.5 cm, consider CT/MRI every year. Stop surveillance if the cyst stabilizes or not a surgical candidate; If there is interval change and cyst size > 2.5 cm, consider EUS-FNA
	Age ≥ 80 yer with cyst size ≥ 2.5 cm: If low risk by imaging, consider CT/MRI every 2 yr for 4 yr. Stop surveillance if cyst size is stable; If there is interval change in cyst size, consider EUS-FNA
	High risk (mural nodule, wall thickening, dilation of MPD ≥ 7 mm or extrahepatic biliary obstruction/Jaundice) features by imaging should be referred to EUS-FNA
	High-risk stigmata (jaundice, enhancing mural nodule, wall thickening, and MPD ≥ 10 mm) by EUS or imaging refer to surgery for evaluation

MCN: Mucinous cystic neoplasm; EUS-FNA: Endoscopic ultrasound-Fine needle aspiration; MRI: Magnetic resonance imaging; IPMN: Intraductal papillary mucinous neoplasm; HGD: High-grade dysplasia; MD-IPMN: Main duct-Intraductal papillary mucinous neoplasm; PD: Pancreatic duct; MPD: Main pancreatic duct.

increased levels of serum CA 19-9 (≥ 37 U/mL), MPD dilation 5-9.9 mm, cyst diameter ≥ 40 mm, new-onset diabetes mellitus, acute pancreatitis caused by the cyst, or enhancing mural nodule < 5 mm.

ACG guidelines[30]

Referral to multidisciplinary team is recommended for evaluation of surgery with jaundice or acute pancreatitis secondary to the cyst, significantly elevated serum CA 19-9 level, presence of a mural nodule or solid component within the cyst, MPD dilation > 5 mm, focal dilation of PD for MD-IPMN or an obstructing lesion, IPMNs or MCNs ≥ 3 cm and the presence of HGD-IPMN or pancreatic cancer on cytology.

AGA guidelines[31]

Surgery is recommended for cysts with both a solid component and a dilated PD and/ or concerning features on EUS-FNA positive for HGD/cancer.

Revised IAP 2017 guidelines[32]

Absolute indications for surgery include obstructive jaundice in a patient with a cystic lesion of the head of the pancreas, enhancing mural nodule > 5 mm and MPD ≥ 10 mm. Relative indications for surgery include cyst ≥ 3 cm, enhancing mural nodule < 5 mm, thickened cyst wall, MPD 5-9 mm, an abrupt change in caliber of PD with distal pancreatic atrophy, lymphadenopathy, increased serum level of CA 19-9 and cyst growth rate ≥ 5 mm/2 years.

ACR guidelines[33]

Table 3 Cyst fluid analysis

	Cyst fluid analysis
European guidelines[28]	Cyst fluid CEA with cytology, or KRAS/GNAS mutation analysis for differentiating IPMN or MCN from other pancreatic cysts
American College of Gastroenterology (ACG) guidelines[30]	Cyst fluid CEA to differentiate IPMNs and MCNs from other cyst types
	Cyst fluid cytology to assess for HGD or pancreatic cancer when imaging features are alone insufficient for surgery
	Molecular markers like KRAS or GNAS mutations can help identify IPMNs or MCNs when the diagnosis is not clear
American Gastroenterology Association (AGA) guidelines[31]	Cyst fluid cytology is recommended for the evaluation of high-risk features on imaging. The role of molecular markers is not clear and further research is needed
Revised IAP 2017 guidelines[32]	Cyst fluid CEA can distinguish mucinous from non-mucinous cysts. CEA level ≥ 192-200 ng/mL is 80% accurate for the diagnosis of mucinous cyst[38,45]
	Cyst fluid cytology can be diagnostic but sometimes limited by scant cellularity[43,44]
	Cyst fluid amylase can differentiate benign from malignant MCN and amylase levels are higher in pseudocysts than non-pseudocysts[45]. The role of molecular markers like KRAS and GNAS mutations is still evolving
American College of Radiology guidelines[33]	Cyst fluid CEA ≥ 192 ng/mL can help identify a mucinous cyst[46]
	Cyst fluid amylase > 250 IU/L suggests pseudocyst[11]
	KRAS and GNAS molecular markers can help differentiate mucinous from non-mucinous cysts[47]
	Cyst cytology can identify dysplastic cells

CEA: Carcinoembryonic antigen; IPMN: Intraductal papillary mucinous neoplasm; MCN: Mucinous cystic neoplasm; GNAS: Guanine nucleotide-binding protein; KRAS: Kirsten rat sarcoma viral oncogene homolog; HGD: High-grade dysplasia.

Absolute indications for surgery include obstructive jaundice with a cyst in the head of the pancreas, enhancing solid component within the cyst and MPD ≥ 10 mm in the absence of obstruction. Relative indications include cyst size ≥ 3 cm, thickened cyst wall, non-enhancing mural nodule, and MPD ≥ 7 mm. The indications of surgery for various PCNs using different guidelines are illustrated in Table 5. Overall, the absolute indications for surgery are consistent among all the guidelines and the cysts with relative indications for surgery can be closely followed with imaging and/EUS-FNA.

WHERE YOU GO "FIRST" MATTERS?

At MD Anderson cancer center, we get referrals from all over the country and abroad for evaluation of PC. By the time, patients come to us, they have already been seen two or three physicians with the recommendation for surgical resection. The majority of these patients do not need require resection but can be clinically followed with repeat imaging studies. Accurate characterization of the pancreatic cyst is the key in the management of PC. All patients with pancreatic cyst who are referred to MD Anderson cancer center get automatically enrolled in the pancreatic cyst database. There is a team of pancreatic surgeons, advanced endoscopists with expertise in EUS-FNA, oncologists, radiologists, and gastrointestinal pathologists who work closely with a concerted effort in accurately diagnosing and managing PC. Any high-risk features on imaging will be referred for EUS-FNA. If EUS-FNA shows HGD/cancer, the patients will be referred for surgical evaluation. Cyst fluid analysis can help distinguish mucinous from non-mucinous cysts. Surveillance is based on the type, size of the cyst, MPD dilation, and any high-risk features. We use both ACG and revised Fukuoka guidelines in the surveillance of PC.

CONCLUSION

With the increased incidence of asymptomatic PC on imaging, accurate diagnosis is the key in the management. A multidisciplinary team approach involving advanced endoscopist, pathologist, radiologist, and surgeon is paramount in the comprehensive

Table 4 Endoscopic ultrasound-fine needle aspiration indications

	Endoscopic ultrasound-Fine needle aspiration indications
European guidelines[28]	Differentiating mucinous *vs* non-mucinous
	Malignant *vs* benign
	CT or MRI unclear
	Only when results are expected to change clinical management
American College of Gastroenterology guidelines[30]	Jaundice
	Acute pancreatitis
	Significantly elevated serum CA 19-9
	Mural nodule
	A solid component within cyst or pancreatic parenchyma
	Dilation of MPD ≥ 5 mm
	Focal dilation of PD
	Cyst size > 3 cm
	When the diagnosis of cysts is unclear or results will likely alter management
	Cyst fluid CEA to differentiate IPMNs and MCNs from other cyst types
	New onset or worsening diabetes
	Increase in cyst size > 3 mm/yr
American Gastroenterology Association guidelines[31]	At least 2 high-risk features
	Cyst size ≥ 3 cm
	Dilated MPD
	Solid component
Revised IAP 2017 or revised Fukuoka guidelines[32]	Pancreatitis
	Cyst ≥ 3 cm
	Enhancing mural nodule < 5 mm
	Thickened/enhancing cyst wall
	Main duct size 5-9 mm
	An abrupt change in caliber of the pancreatic duct with distal pancreatic atrophy
	Lymphadenopathy
	Increased serum level of CA19-9
	Cyst growth rate ≥ 5 mm/2 yr
American College of Radiology guidelines[33]	Mural nodule
	Wall thickening
	Dilation of MPD ≥ 7 mm
	Extrahepatic biliary obstruction/Jaundice

EUS-FNA: Endoscopic ultrasound-Fine needle aspiration; MPD: Main pancreatic duct; PD: Pancreatic duct; MCN: Mucinous cystic neoplasm; CEA: Carcinoembryonic antigen; CT: Computed tomography; MRI: Magnetic resonance imaging; IAP: International association of pancreatology; IPMN: Intraductal papillary mucinous neoplasm.

management of PC. Surgical resection should be selectively offered considering absolute indications, high-risk features on imaging/EUS, and clinical setting of each patient. Surveillance using a cross-sectional imaging or EUS should be individualized based on the cyst type, size, involvement of the main duct, and/or presence of a mural nodule. Lastly, surgical resection should be performed at high volume centers to optimize the outcomes in morbidity and mortality.

Table 5 Indications of surgery for pancreatic cysts

	Absolute indications of surgery	Relative indications of surgery
European guidelines[28]	Intraductal papillary mucinous neoplasm: Cytology positive for malignancy/High-grade dysplasia; Solid mass; Jaundice; Mural nodule ≥ 5 mm; Main pancreatic duct dilation > 10 mm	Cyst growth rate > 5 mm/yr
	Mucinous cystic neoplasm: Size ≥ 4 cm	Serum CA 19-9 > 37 U/mL
	Symptomatic Mural nodule	MPD dilation 5-9 mm
		Cyst diameter ≥ 40 mm
		New-onset diabetes mellitus
		Acute pancreatitis related to IPMN
		Mural nodule < 5 mm
American College of Gastroenterology guidelines[30]	Intraductal papillary mucinous neoplasm or Mucinous cystic neoplasm:	N/A
	Referral to EUS-FNA/Multidisciplinary; team:	
	Jaundice	
	Acute pancreatitis	
	Significantly elevated CA 19-9	
	Mural nodule	
	A solid component in cyst/pancreatic parenchyma	
	MPD > 5 mm	
	Focal dilation of PD or MD-IPMN	
	HGD/Pancreatic cancer on cytology	
American Gastroenterology Association guidelines[31]	Pancreatic cysts:	N/A
	EUS-FNA cytology positive for -	
	HGD/cancer	
	Both solid component and dilated PD on MRI and EUS	
Revised IAP 2017 or revised Fukuoka guidelines[32]	Obstructive jaundice with pancreatic head cyst	Pancreatitis
	Enhancing mural nodule ≥ 5 mm	Enhancing mural nodule < 5 mm
	MPD ≥ 10 mm	Thickened/enhancing cyst wall
		Main duct size 5-9 mm
		An abrupt change in caliber of the pancreatic duct with distal pancreatic atrophy
		Lymphadenopathy
		Increase in serum level of CA 19-9
		Cyst growth rate ≥ 5 mm/2 yr
American College of Radiology guideline[33]	Obstructive jaundice with a cyst in the head of the pancreas	Cyst ≥ 3 cm
	Enhancing solid component within a cyst	Thickened/enhancing cyst wall
	MPD > 10 mm in the absence of obstruction	Non-enhancing mural nodule
		MPD ≥ 7 mm

IPMN: Intraductal papillary mucinous neoplasm; HGD: High-grade dysplasia; MPD Main pancreatic duct; PD: Pancreatic duct; EUS-FNA: Endoscopic ultrasound-Fine needle aspiration.

REFERENCES

1 **Laffan TA**, Horton KM, Klein AP, Berlanstein B, Siegelman SS, Kawamoto S, Johnson PT, Fishman EK, Hruban RH. Prevalence of unsuspected pancreatic cysts on MDCT. *AJR Am J Roentgenol* 2008; **191**: 802-807 [PMID: 18716113 DOI: 10.2214/AJR.07.3340]

2 **de Jong K**, Nio CY, Hermans JJ, Dijkgraaf MG, Gouma DJ, van Eijck CH, van Heel E, Klass G, Fockens P, Bruno MJ. High prevalence of pancreatic cysts detected by screening magnetic resonance imaging examinations. *Clin Gastroenterol Hepatol* 2010; **8**: 806-811 [PMID: 20621679 DOI: 10.1016/j.cgh.2010.05.017]

3 **Hammel PR**, Vilgrain V, Terris B, Penfornis A, Sauvanet A, Correas JM, Chauveau D, Balian A, Beigelman C, O'Toole D, Bernades P, Ruszniewski P, Richard S. Pancreatic involvement in von Hippel-Lindau disease. The Groupe Francophone d'Etude de la Maladie de von Hippel-Lindau. *Gastroenterology* 2000; **119**: 1087-1095 [PMID: 11040195 DOI: 10.1053/gast.2000.18143]

4 **Kim JA**, Blumenfeld JD, Chhabra S, Dutruel SP, Thimmappa ND, Bobb WO, Donahue S, Rennert HE,

Tan AY, Giambrone AE, Prince MR. Pancreatic Cysts in Autosomal Dominant Polycystic Kidney Disease: Prevalence and Association with PKD2 Gene Mutations. *Radiology* 2016; **280**: 762-770 [PMID: 27046073 DOI: 10.1148/radiol.2016151650]

5 **Banks PA**, Bollen TL, Dervenis C, Gooszen HG, Johnson CD, Sarr MG, Tsiotos GG, Vege SS; Acute Pancreatitis Classification Working Group. Classification of acute pancreatitis--2012: revision of the Atlanta classification and definitions by international consensus. *Gut* 2013; **62**: 102-111 [PMID: 23100216 DOI: 10.1136/gutjnl-2012-302779]

6 **Pyke CM**, van Heerden JA, Colby TV, Sarr MG, Weaver AL. The spectrum of serous cystadenoma of the pancreas. Clinical, pathologic, and surgical aspects. *Ann Surg* 1992; **215**: 132-139 [PMID: 1546898 DOI: 10.1097/00000658-199202000-00007]

7 **Lewandrowski K**, Warshaw A, Compton C. Macrocystic serous cystadenoma of the pancreas: a morphologic variant differing from microcystic adenoma. *Hum Pathol* 1992; **23**: 871-875 [PMID: 1644432 DOI: 10.1016/0046-8177(92)90397-l]

8 **Brugge WR**. Diagnosis and management of cystic lesions of the pancreas. *J Gastrointest Oncol* 2015; **6**: 375-388 [PMID: 26261724 DOI: 10.3978/j.issn.2078-6891.2015.057]

9 **Compagno J**, Oertel JE. Microcystic adenomas of the pancreas (glycogen-rich cystadenomas): a clinicopathologic study of 34 cases. *Am J Clin Pathol* 1978; **69**: 289-298 [PMID: 637043 DOI: 10.1093/ajcp/69.1.289]

10 **Kimura W**, Moriya T, Hirai I, Hanada K, Abe H, Yanagisawa A, Fukushima N, Ohike N, Shimizu M, Hatori T, Fujita N, Maguchi H, Shimizu Y, Yamao K, Sasaki T, Naito Y, Tanno S, Tobita K, Tanaka M. Multicenter study of serous cystic neoplasm of the Japan pancreas society. *Pancreas* 2012; **41**: 380-387 [PMID: 22415666 DOI: 10.1097/MPA.0b013e31822a27db]

11 **van der Waaij LA**, van Dullemen HM, Porte RJ. Cyst fluid analysis in the differential diagnosis of pancreatic cystic lesions: a pooled analysis. *Gastrointest Endosc* 2005; **62**: 383-389 [PMID: 16111956 DOI: 10.1016/s0016-5107(05)01581-6]

12 **Strobel O**, Z'graggen K, Schmitz-Winnenthal FH, Friess H, Kappeler A, Zimmermann A, Uhl W, Büchler MW. Risk of malignancy in serous cystic neoplasms of the pancreas. *Digestion* 2003; **68**: 24-33 [PMID: 12949436 DOI: 10.1159/000073222]

13 **Jais B**, Rebours V, Malleo G, Salvia R, Fontana M, Maggino L, Bassi C, Manfredi R, Moran R, Lennon AM, Zaheer A, Wolfgang C, Hruban R, Marchegiani G, Fernández Del Castillo C, Brugge W, Ha Y, Kim MH, Oh D, Hirai I, Kimura W, Jang JY, Kim SW, Jung W, Kang H, Song SY, Kang CM, Lee WJ, Crippa S, Falconi M, Gomatos I, Neoptolemos J, Milanetto AC, Sperti C, Ricci C, Casadei R, Bissolati M, Balzano G, Frigerio I, Girelli R, Delhaye M, Bernier B, Wang H, Jang KT, Song DH, Huggett MT, Oppong KW, Pererva L, Kopchak KV, Del Chiaro M, Segersvard R, Lee LS, Conwell D, Osvaldt A, Campos V, Aguero Garcete G, Napoleon B, Matsumoto I, Shinzeki M, Bolado F, Fernandez JM, Keane MG, Pereira SP, Acuna IA, Vaquero EC, Angiolini MR, Zerbi A, Tang J, Leong RW, Faccinetto A, Morana G, Petrone MC, Arcidiacono PG, Moon JH, Choi HJ, Gill RS, Pavey D, Ouaïssi M, Sastre B, Spandre M, De Angelis CG, Rios-Vives MA, Concepcion-Martin M, Ikeura T, Okazaki K, Frulloni L, Messina O, Lévy P. Serous cystic neoplasm of the pancreas: a multinational study of 2622 patients under the auspices of the International Association of Pancreatology and European Pancreatic Club (European Study Group on Cystic Tumors of the Pancreas). *Gut* 2016; **65**: 305-312 [PMID: 26045140 DOI: 10.1136/gutjnl-2015-309638]

14 **Galanis C**, Zamani A, Cameron JL, Campbell KA, Lillemoe KD, Caparrelli D, Chang D, Hruban RH, Yeo CJ. Resected serous cystic neoplasms of the pancreas: a review of 158 patients with recommendations for treatment. *J Gastrointest Surg* 2007; **11**: 820-826 [PMID: 17440789 DOI: 10.1007/s11605-007-0157-4]

15 **Le Borgne J**, de Calan L, Partensky C. Cystadenomas and cystadenocarcinomas of the pancreas: a multiinstitutional retrospective study of 398 cases. French Surgical Association. *Ann Surg* 1999; **230**: 152-161 [PMID: 10450728 DOI: 10.1097/00000658-199908000-00004]

16 **Malleo G**, Bassi C, Rossini R, Manfredi R, Butturini G, Massignani M, Paini M, Pederzoli P, Salvia R. Growth pattern of serous cystic neoplasms of the pancreas: observational study with long-term magnetic resonance surveillance and recommendations for treatment. *Gut* 2012; **61**: 746-751 [PMID: 21940725 DOI: 10.1136/gutjnl-2011-300297]

17 **Tseng JF**, Warshaw AL, Sahani DV, Lauwers GY, Rattner DW, Fernandez-del Castillo C. Serous cystadenoma of the pancreas: tumor growth rates and recommendations for treatment. *Ann Surg* 2005; **242**: 413-419; discussion 419-421 [PMID: 16135927 DOI: 10.1097/01.sla.0000179651.21193.2c]

18 **Sarr MG**, Carpenter HA, Prabhakar LP, Orchard TF, Hughes S, van Heerden JA, DiMagno EP. Clinical and pathologic correlation of 84 mucinous cystic neoplasms of the pancreas: can one reliably differentiate benign from malignant (or premalignant) neoplasms? *Ann Surg* 2000; **231**: 205-212 [PMID: 10674612 DOI: 10.1097/00000658-200002000-00009]

19 **Crippa S**, Salvia R, Warshaw AL, Domínguez I, Bassi C, Falconi M, Thayer SP, Zamboni G, Lauwers GY, Mino-Kenudson M, Capelli P, Pederzoli P, Castillo CF. Mucinous cystic neoplasm of the pancreas is not an aggressive entity: lessons from 163 resected patients. *Ann Surg* 2008; **247**: 571-579 [PMID: 18362619 DOI: 10.1097/SLA.0b013e31811f4449]

20 **Farrell JJ**. Pancreatic Cysts and Guidelines. *Dig Dis Sci* 2017; **62**: 1827-1839 [PMID: 28528374 DOI: 10.1007/s10620-017-4571-5]

21 **Tanaka M**, Fernández-del Castillo C, Adsay V, Chari S, Falconi M, Jang JY, Kimura W, Levy P, Pitman MB, Schmidt CM, Shimizu M, Wolfgang CL, Yamaguchi K, Yamao K; International Association of Pancreatology. International consensus guidelines 2012 for the management of IPMN and MCN of the pancreas. *Pancreatology* 2012; **12**: 183-197 [PMID: 22687371 DOI: 10.1016/j.pan.2012.04.004]

22 **Park JW**, Jang JY, Kang MJ, Kwon W, Chang YR, Kim SW. Mucinous cystic neoplasm of the pancreas: is surgical resection recommended for all surgically fit patients? *Pancreatology* 2014; **14**: 131-136 [PMID: 24650968 DOI: 10.1016/j.pan.2013.12.006]

23 **Lanke G**, Ali FS, Lee JH. Clinical update on the management of pseudopapillary tumor of pancreas. *World J Gastrointest Endosc* 2018; **10**: 145-155 [PMID: 30283597 DOI: 10.4253/wjge.v10.i9.145]

24 **Cai H**, Zhou M, Hu Y, He H, Chen J, Tian W, Deng Y. Solid-pseudopapillary neoplasms of the pancreas: clinical and pathological features of 33 cases. *Surg Today* 2013; **43**: 148-154 [PMID: 22825652 DOI: 10.1007/s00595-012-0260-3]

25 **Romics L**, Oláh A, Belágyi T, Hajdú N, Gyurus P, Ruszinkó V. Solid pseudopapillary neoplasm of the pancreas--proposed algorithms for diagnosis and surgical treatment. *Langenbecks Arch Surg* 2010; **395**: 747-755 [PMID: 20155425 DOI: 10.1007/s00423-010-0599-0]

26 **D'Angelica M**, Brennan MF, Suriawinata AA, Klimstra D, Conlon KC. Intraductal papillary mucinous

neoplasms of the pancreas: an analysis of clinicopathologic features and outcome. *Ann Surg* 2004; **239**: 400-408 [PMID: 15075659 DOI: 10.1097/01.sla.0000114132.47816.dd]
27 **Sohn TA**, Yeo CJ, Cameron JL, Hruban RH, Fukushima N, Campbell KA, Lillemoe KD. Intraductal papillary mucinous neoplasms of the pancreas: an updated experience. *Ann Surg* 2004; **239**: 788-97; discussion 797-9 [PMID: 15166958 DOI: 10.1097/01.sla.0000128306.90650.aa]
28 **European Study Group on Cystic Tumours of the Pancreas**. European evidence-based guidelines on pancreatic cystic neoplasms. *Gut* 2018; **67**: 789-804 [PMID: 29574408 DOI: 10.1136/gutjnl-2018-316027]
29 **Del Chiaro M**, Verbeke C, Salvia R, Klöppel G, Werner J, McKay C, Friess H, Manfredi R, Van Cutsem E, Löhr M, Segersvärd R; European Study Group on Cystic Tumours of the Pancreas. European experts consensus statement on cystic tumours of the pancreas. *Dig Liver Dis* 2013; **45**: 703-711 [PMID: 23415799 DOI: 10.1016/j.dld.2013.01.010]
30 **Elta GH**, Enestvedt BK, Sauer BG, Lennon AM. ACG Clinical Guideline: Diagnosis and Management of Pancreatic Cysts. *Am J Gastroenterol* 2018; **113**: 464-479 [PMID: 29485131 DOI: 10.1038/ajg.2018.14]
31 **Vege SS**, Ziring B, Jain R, Moayyedi P; Clinical Guidelines Committee; American Gastroenterology Association. American gastroenterological association institute guideline on the diagnosis and management of asymptomatic neoplastic pancreatic cysts. *Gastroenterology* 2015; **148**: 819-22; quize12-3 [PMID: 25805375 DOI: 10.1053/j.gastro.2015.01.015]
32 **Tanaka M**, Fernández-Del Castillo C, Kamisawa T, Jang JY, Levy P, Ohtsuka T, Salvia R, Shimizu Y, Tada M, Wolfgang CL. Revisions of international consensus Fukuoka guidelines for the management of IPMN of the pancreas. *Pancreatology* 2017; **17**: 738-753 [PMID: 28735806 DOI: 10.1016/j.pan.2017.07.007]
33 **Megibow AJ**, Baker ME, Morgan DE, Kamel IR, Sahani DV, Newman E, Brugge WR, Berland LL, Pandharipande PV. Management of Incidental Pancreatic Cysts: A White Paper of the ACR Incidental Findings Committee. *J Am Coll Radiol* 2017; **14**: 911-923 [PMID: 28533111 DOI: 10.1016/j.jacr.2017.03.010]
34 **Wang W**, Zhang L, Chen L, Wei J, Sun Q, Xie Q, Zhou X, Zhou D, Huang P, Yang Q, Xie H, Zhou L, Zheng S. Serum carcinoembryonic antigen and carbohydrate antigen 19-9 for prediction of malignancy and invasiveness in intraductal papillary mucinous neoplasms of the pancreas: A meta-analysis. *Biomed Rep* 2015; **3**: 43-50 [PMID: 25469245 DOI: 10.3892/br.2014.376]
35 **Kim JR**, Jang JY, Kang MJ, Park T, Lee SY, Jung W, Chang J, Shin Y, Han Y, Kim SW. Clinical implication of serum carcinoembryonic antigen and carbohydrate antigen 19-9 for the prediction of malignancy in intraductal papillary mucinous neoplasm of pancreas. *J Hepatobiliary Pancreat Sci* 2015; **22**: 699-707 [PMID: 26178866 DOI: 10.1002/jhbp.275]
36 **Singhi AD**, Nikiforova MN, Fasanella KE, McGrath KM, Pai RK, Ohori NP, Bartholow TL, Brand RE, Chennat JS, Lu X, Papachristou GI, Slivka A, Zeh HJ, Zureikat AH, Lee KK, Tsung A, Mantha GS, Khalid A. Preoperative GNAS and KRAS testing in the diagnosis of pancreatic mucinous cysts. *Clin Cancer Res* 2014; **20**: 4381-4389 [PMID: 24938521 DOI: 10.1158/1078-0432.CCR-14-0513]
37 **Springer S**, Wang Y, Dal Molin M, Masica DL, Jiao Y, Kinde I, Blackford A, Raman SP, Wolfgang CL, Tomita T, Niknafs N, Douville C, Ptak J, Dobbyn L, Allen PJ, Klimstra DS, Schattner MA, Schmidt CM, Yip-Schneider M, Cummings OW, Brand RE, Zeh HJ, Singhi AD, Scarpa A, Salvia R, Malleo G, Zamboni G, Falconi M, Jang JY, Kim SW, Kwon W, Hong SM, Song KB, Kim SC, Swan N, Murphy J, Geoghegan J, Brugge W, Fernandez-Del Castillo C, Mino-Kenudson M, Schulick R, Edil BH, Adsay V, Paulino J, van Hooft J, Yachida S, Nara S, Hiraoka N, Yamao K, Hijioka S, van der Merwe S, Goggins M, Canto MI, Ahuja N, Hirose K, Makary M, Weiss MJ, Cameron J, Pittman M, Eshleman JR, Diaz LA, Papadopoulos N, Kinzler KW, Karchin R, Hruban RH, Vogelstein B, Lennon AM. A combination of molecular markers and clinical features improve the classification of pancreatic cysts. *Gastroenterology* 2015; **149**: 1501-1510 [PMID: 26253305 DOI: 10.1053/j.gastro.2015.07.041]
38 **Cizginer S**, Turner BG, Bilge AR, Karaca C, Pitman MB, Brugge WR. Cyst fluid carcinoembryonic antigen is an accurate diagnostic marker of pancreatic mucinous cysts. *Pancreas* 2011; **40**: 1024-1028 [PMID: 21775920 DOI: 10.1097/MPA.0b013e31821bd62f]
39 **Al-Rashdan A**, Schmidt CM, Al-Haddad M, McHenry L, Leblanc JK, Sherman S, Dewitt J. Fluid analysis prior to surgical resection of suspected mucinous pancreatic cysts. A single centre experience. *J Gastrointest Oncol* 2011; **2**: 208-214 [PMID: 22811854 DOI: 10.3978/j.issn.2078-6891.2011.020]
40 **Thornton GD**, McPhail MJ, Nayagam S, Hewitt MJ, Vlavianos P, Monahan KJ. Endoscopic ultrasound guided fine needle aspiration for the diagnosis of pancreatic cystic neoplasms: a meta-analysis. *Pancreatology* 2013; **13**: 48-57 [PMID: 23395570 DOI: 10.1016/j.pan.2012.11.313]
41 **Rosenbaum MW**, Jones M, Dudley JC, Le LP, Iafrate AJ, Pitman MB. Next-generation sequencing adds value to the preoperative diagnosis of pancreatic cysts. *Cancer Cytopathol* 2017; **125**: 41-47 [PMID: 27647802 DOI: 10.1002/cncy.21775]
42 **Jones M**, Zheng Z, Wang J, Dudley J, Albanese E, Kadayifci A, Dias-Santagata D, Le L, Brugge WR, Fernandez-del Castillo C, Mino-Kenudson M, Iafrate AJ, Pitman MB. Impact of next-generation sequencing on the clinical diagnosis of pancreatic cysts. *Gastrointest Endosc* 2016; **83**: 140-148 [PMID: 26253016 DOI: 10.1016/j.gie.2015.06.047]
43 **Pitman MB**, Deshpande V. Endoscopic ultrasound-guided fine needle aspiration cytology of the pancreas: a morphological and multimodal approach to the diagnosis of solid and cystic mass lesions. *Cytopathology* 2007; **18**: 331-347 [PMID: 17559566 DOI: 10.1111/j.1365-2303.2007.00457.x]
44 **Pitman MB**, Genevay M, Yaeger K, Chebib I, Turner BG, Mino-Kenudson M, Brugge WR. High-grade atypical epithelial cells in pancreatic mucinous cysts are a more accurate predictor of malignancy than "positive" cytology. *Cancer Cytopathol* 2010; **118**: 434-440 [PMID: 20931638 DOI: 10.1002/cncy.20118]
45 **Park WG**, Mascarenhas R, Palaez-Luna M, Smyrk TC, O'Kane D, Clain JE, Levy MJ, Pearson RK, Petersen BT, Topazian MD, Vege SS, Chari ST. Diagnostic performance of cyst fluid carcinoembryonic antigen and amylase in histologically confirmed pancreatic cysts. *Pancreas* 2011; **40**: 42-45 [PMID: 20966811 DOI: 10.1097/MPA.0b013e3181f69f36]
46 **Rockacy M**, Khalid A. Update on pancreatic cyst fluid analysis. *Ann Gastroenterol* 2013; **26**: 122-127 [PMID: 24714589]
47 **Thiruvengadam N**, Park WG. Systematic Review of Pancreatic Cyst Fluid Biomarkers: The Path Forward. *Clin Transl Gastroenterol* 2015; **6**: e88 [PMID: 26065716 DOI: 10.1038/ctg.2015.17]

World Journal of Gastroenterology

Submit a Manuscript: https://www.f6publishing.com

World J Gastroenterol 2020 March 21; 26(11): 1142-1155

DOI: 10.3748/wjg.v26.i11.1142

ISSN 1007-9327 (print) ISSN 2219-2840 (online)

ORIGINAL ARTICLE

Basic Study

Effect of prolonged omeprazole administration on segmental intestinal Mg^{2+} absorption in male Sprague-Dawley rats

Nasisorn Suksridechacin, Punnisa Kulwong, Siriporn Chamniansawat, Narongrit Thongon

ORCID number: Nasisorn Suksridechacin (0000-0002-0236-6650); Punnisa Kulwong (0000-0002-1786-3545); Siriporn Chamniansawat (0000-0003-2609-6373); Narongrit Thongon (0000-0003-2475-9161).

Author contributions: Suksridechacin N performed experiments, analyzed the results, and edited the manuscript; Kulwong P performed experiments; Chamniansawat S performed experiments, analyzed the results, and wrote and edited the manuscript; Thongon N designed and performed experiments, analyzed and interpreted the results, and wrote and edited the manuscript.

Supported by Burapha University through National Research Council of Thailand, No. 15/2562.

Institutional review board statement: This study was reviewed and approved by Institutional Review Committee (ID# 23/2559).

Institutional animal care and use committee statement: This study was approved by the Ethics Committee on Animal Experiment of Burapha University, Thailand.

Conflict-of-interest statement: The authors declare no conflict of interest.

Data sharing statement: The data could be downloaded from the public databases, and no additional data are available.

ARRIVE guidelines statement: The

Nasisorn Suksridechacin, Punnisa Kulwong, Narongrit Thongon, Division of Physiology, Department of Biomedical Sciences, Faculty of Allied Health Sciences, Burapha University, Chonburi 20131, Thailand

Siriporn Chamniansawat, Division of Anatomy, Department of Biomedical Sciences, Faculty of Allied Health Sciences, Burapha University, Chonburi 20131, Thailand

Corresponding author: Narongrit Thongon, PhD, Associate Professor, Division of Physiology, Department of Biomedical Sciences, Faculty of Allied Health Sciences, Burapha University, No. 169 Long-Hard Bangsaen Road, Saensook, Muang, Chonburi 20131, Thailand. narongritt@buu.ac.th

Abstract

BACKGROUND

The exact mechanism of proton pump inhibitors (PPIs)-induced hypomagnesemia (PPIH) is largely unknown. Previous studies proposed that PPIH is a consequence of intestinal Mg^{2+} malabsorption. However, the mechanism of PPIs-suppressed intestinal Mg^{2+} absorption is under debate.

AIM

To investigate the effect of 12-wk and 24-wk omeprazole injection on the total, transcellular, and paracellular Mg^{2+} absorption in the duodenum, jejunum, ileum, and colon of male Sprague-Dawley rats.

METHODS

The rats received 20 mg/kg·d subcutaneous omeprazole injection for 12 or 24 wk. Plasma and urinary Mg^{2+}, Ca^{2+}, and PO_4^{3-} levels were measured. The plasma concentrations of 1α,25-dihydroxyvitamin D_3 (1α,25$(OH)_2D_3$), parathyroid hormone (PTH), fibroblast growth factor 23 (FGF-23), epidermal growth factor (EGF), and insulin were also observed. The duodenum, jejunum, ileum, and colon of each rat were mounted onto individual modified Using chamber setups to study the rates of total, transcellular, and paracellular Mg^{2+} absorption simultaneously. The expression of transient receptor potential melastatin 6 (TRPM6) and cyclin M4 (CNNM4) in the entire intestinal tract was also measured.

RESULTS

Single-dose omeprazole injection significantly increased the intraluminal pH of the stomach, duodenum, and jejunum. Omeprazole injection for 12 and 24 wk induced hypomagnesemia with reduced urinary Mg^{2+} excretion. The plasma Ca^{2+}

was normal but the urinary Ca^{2+} excretion was reduced in rats with PPIH. The plasma and urinary PO_4^{3-} levels increased in PPIH rats. The levels of $1\alpha,25(OH)_2D_3$ and FGF-23 increased, whereas that of plasma EGF decreased in the omeprazole-treated rats. The rates of the total, transcellular, and paracellular Mg^{2+} absorption was significantly lower in the duodenum, jejunum, ileum, and colon of the rats with PPIH than in those of the control rats. The percent suppression of Mg^{2+} absorption in the duodenum, jejunum, ileum, and colon of the rats with PPIH compared with the control rats was 81.86%, 70.59%, 69.45%, and 39.25%, respectively. Compared with the control rats, the rats with PPIH had significantly higher TRPM6 and CNNM4 expression levels throughout the intestinal tract.

CONCLUSION

Intestinal Mg^{2+} malabsorption was observed throughout the intestinal tract of rats with PPIH. PPIs mainly suppressed small intestinal Mg^{2+} absorption. Omeprazole exerted no effect on the intraluminal acidic pH in the colon. Thus, the lowest percent suppression of total Mg^{2+} absorption was found in the colon. The expression levels of TRPM6 and CNNM4 increased, indicating the presence of a compensatory response to Mg^{2+} malabsorption in rats with PPIH. Therefore, the small intestine is an appropriate segment that should be modulated to counteract PPIH.

Key words: Adverse effect; Colon; Mg^{2+} absorption; Proton pump inhibitors-induced hypomagnesemia; Small intestine

Core tip: Proton pump inhibitors (PPIs) induced hypomagnesemia (PPIH) has attracted attention in the past decade. Previous studies proposed that PPIH is a consequence of intestinal Mg^{2+} malabsorption. However, the effect of prolonged PPI administration on duodenal, jejunal, ileal, and colonic Mg^{2+} absorption is largely unknown. In this study, the rats received 20 mg/ kg·d subcutaneous omeprazole injection for 12 and 24 wk, which is comparable to 5 and 10 human years, respectively. Omeprazole injection induced hypomagnesemia with reduced urinary Mg^{2+} excretion. The rates of total, paracellular, and transcellular Mg^{2+} absorption reduced in the duodenum, jejunum, ilium, and colon were discovered in PPIH rats.

Citation: Suksridechacin N, Kulwong P, Chamniansawat S, Thongon N. Effect of prolonged omeprazole administration on segmental intestinal Mg^{2+} absorption in male Sprague-Dawley rats. *World J Gastroenterol* 2020; 26(11): 1142-1155
URL: https://www.wjgnet.com/1007-9327/full/v26/i11/1142.htm
DOI: https://dx.doi.org/10.3748/wjg.v26.i11.1142

INTRODUCTION

Mg^{2+} is an essential ion that mediates several physiological functions in the brain, lung, heart and vessel, pancreas and liver, muscle, and bone[1]. Mg^{2+} disturbance has been implicated in the pathophysiological mechanisms of several diseases in those organs; therefore, Mg^{2+} supplement is a potential therapeutic regime in many of these diseases[1]. Over 99% of total body Mg^{2+} is stored in the bone, muscle, and soft tissues[1,2]. The remaining 1% is found in the plasma, which is tightly regulated by intestinal absorption and renal excretion[1,2]. Intestinal epithelium absorbs Mg^{2+} through paracellular passive and transcellular active mechanisms[2]. Transcellular Mg^{2+} absorption requires the activities of luminal transient receptor potential melastatin 6 (TRPM6) and basolateral cyclin M4 (CNNM4), whereas paracellular absorption is regulated by tight junction-associated claudin proteins. However, the study of transepithelial Mg^{2+} transport is limited by the poor understanding on the mechanism of intestinal Mg^{2+} absorption[2]. Previous studies proposed that paracellular and transcellular Mg^{2+} absorption exclusively proceeds in the small and large intestines, respectively[1,3,4]. In addition, the expression of TRPM6 mRNA is

authors have read the ARRIVE guidelines, and the manuscript was prepared and revised according to the ARRIVE guidelines.

Manuscript source: Invited manuscript

Received: November 18, 2019
Peer-review started: November 18, 2019
First decision: January 19, 2020
Revised: February 6, 2020
Accepted: March 5, 2020
Article in press: March 5, 2020
Published online: March 21, 2020

P-Reviewer: de Talamoni NGT, Huang LY
S-Editor: Wang YQ
L-Editor: A
E-Editor: Ma YJ

barely detected in mouse duodenum[4]. Conversely, another report demonstrated paracellular and transcellular Mg^{2+} absorption in the duodenum[5]. Immunofluorescence imaging clearly showed the expression and localization of TRPM6 protein in the brush-border villi of the duodenum[6]. CNNM4 protein was also identified in small intestinal epithelium[7]. Therefore, the simultaneous study on the transcellular and paracellular Mg^{2+} absorption in the duodenum, jejunum, ileum, and colon will provide data on the mechanism of intestinal Mg^{2+} absorption.

Proton pump inhibitor (PPI)-induced hypomagnesemia (PPIH) has been reported since 2006[8-16]. Approximately 61% and 29% of patients with PPIH have PPIs prescription for at least 5 and 10 years, respectively[10]. However, PPIH was also diagnosed in patients who used PPIs for 2 months[17]. Clinical observations suggested that PPIH is a consequence of intestinal Mg^{2+} malabsorption[9,12,15], the mechanism of which is currently under debate. Previous studies proposed that PPIs suppress colonic Mg^{2+} absorption in normal and PPIH mice[4,13]. However, the effect of PPIs administration on colonic Mg^{2+} absorption had not been investigated[4,13]. Moreover, the stimulation of colonic Mg^{2+} absorption by using inulin fibers could not normalize plasma Mg^{2+} level in those PPIH mice[13]. A recent study has reported that omeprazole injection for 24 wk induces systemic Mg^{2+} deficiency and hypomagnesemia in male Sprague-Dawley rats[5]. The rate of transcellular and paracellular duodenal Mg^{2+} absorption is suppressed in rats with PPIH[5]. However, the effect of prolonged PPIs administration on jejunal, ileal, and colonic Mg^{2+} absorption in a PPIH model remains unknown.

The present study aimed to observe the paracellular and transcellular Mg^{2+} transport across the duodenum, jejunum, ileum, and colon in control and prolonged omeprazole-treated male Sprague-Dawley rats. The expression of TRPM6 and CNNM4 proteins in each intestinal segment was also studied. Plasma and urinary Mg^{2+}, Ca^{2+}, and PO_4^{3-} levels were measured. The plasma concentrations of hormones that modulate Mg^{2+} homeostasis, such as 1α,25-dihydroxyvitamin D_3 [1α,25$(OH)_2D_3$], parathyroid hormone (PTH), fibroblast growth factor 23 (FGF-23), epidermal growth factor (EGF), and insulin[3,18-21], were also determined. Given that 16.7 rat days are equivalent to 1 human year[22], the animals were treated with 20 mg/kg omeprazole daily for 12 and 24 wk which is comparable to 5 and 10 human years, respectively.

MATERIALS AND METHODS

Animals

This study was performed in strict compliance with the Animal for Scientific Purposes Act of Thailand and in accordance with Ethical Principles and Guidelines for the Use of Animals for Scientific Purposes, National Research Council of Thailand. All experimental procedures were approved by the Ethics Committee on Animal Experiment of Burapha University, Thailand. Male Sprague-Dawley rats (9 weeks old) were randomly divided into three experimental groups: control, 12-wk omeprazole, and 24-wk omeprazole treatments. The rats were acclimatized for 7 days and fed with standard pellet chow and reverse osmosis water given ad libitum. The health, body weight, and food intake were monitored and recorded daily.

The effect of single-dose subcutaneous omeprazole injection (20 mg/kg: Ocid® IV; Zydus Cadila, India) on intraluminal gastrointestinal pH was observed. The pellet chow was removed 4 h before and then retrieved 30 min after sham or omeprazole injection. At 2 and 24 h after administration, the stomach, duodenum, jejunum, ileum, cecum, and proximal colon were removed under thiopental anesthesia (70 mg/kg; Anesthal, Jagsonpal Pharmaceuticals Ltd., India). The intraluminal pH levels of the stomach, duodenum, jejunum, ileum, cecum, and proximal colon were measured by diagnostic test strips (MColorpHast™ pH-Indicator Strips, Merck-Millipore, German).

To study the effect of prolonging omeprazole injection, control and 24-wk-omeprazole-treated rats received subcutaneous sham or omeprazole (20 mg/kg) injection daily for 24 wk. The rats in the 12-wk-omeprazole-treated group received subcutaneous sham injected daily for 12 wk followed by subcutaneous omeprazole injection for 12 wk. At 24 h prior to the experimental endpoint, the rats were housed in a metabolic cage to collect food and water intake. Urinary and fecal output was also collected. The rats were anesthetized, blood was collected from the left ventricle, and the rats were subsequently sacrificed. The duodenum, jejunum, ileum, and colon were rapidly collected. The plasma concentrations of 1α,25$(OH)_2D_3$, PTH, FGF-23, EGF, and insulin were determined by Labhouse Chonburi Co. Ltd., Thailand. Plasma and urine Mg^{2+}, Ca^{2+}, and PO_4^{3-} concentrations were also measured.

Magnesium flux measurement

The total, paracellular, and transcellular Mg^{2+} flux was studied in accordance with the method described by Thongon *et al*[5]. In brief, the duodenum, jejunum, ileum, and colon from individual rats were dissected into two pieces, which then were rapidly mounted onto individually modified Ussing chamber setups. Intestinal samples were bathed and equilibrated for 10 min with physiological bathing solution containing (in mmol/mL) 118 NaCl, 4.7 KCl, 1.1 $MgCl_2$, 1.25 $CaCl_2$, 23 $NaHCO_3$, 12 D-glucose, 2.5 L-glutamine, and 2 D-mannitol (osmolality of 290-295 mmol/kg H_2O and pH of 7.4). The solution was maintained at 37 °C and continuously gassed with 5% CO_2 in 95% O_2. The first piece of each intestinal segment was subjected to study the rate of total Mg^{2+} transport. The apical solution of each Ussing chamber setup was substituted with a Mg^{2+}-containing bathing solution supplemented with (in mmol/L) 40 $MgCl_2$, 2.5 $CaCl_2$, 4.5 KCl, 12 D-glucose, 2.5 L-glutamine, 115 mannitol, and 10 HEPES (pH 7.4). Meanwhile, the basolateral solution was substituted with a Mg^{2+}-free bathing solution containing (in mmol/L) 1.25 $CaCl_2$, 4.5 KCl, 12 D-glucose, 2.5 L-glutamine, 250 D-mannitol, and 10 HEPES pH 7.4. To study the rate of paracellular Mg^{2+} transport, another piece of each intestinal segment was incubated with Mg^{2+} channel blocker Co(III)hexaammine (1 mmol/L; Sigma, St. Louis, MO, United States)[23] to inhibit transcellular Mg^{+} flux. The Mg^{2+}-containing and Mg^{2+}-free bathing solutions were also used to study paracellular Mg^{2+} transport. At 30, 60, and 120 min after solution replacements, a 100 μL solution was collected from the basolateral and apical sides. The Mg^{2+} concentration and Mg^{2+} flux rates were determined as previously described by Thongon and Krishnamra[24]. The rate of transcellular Mg^{2+} transport was calculated by subtracting the rate of total Mg^{2+} transport with the rate of paracellular Mg^{2+} transport from the same intestinal segment of the individual rats.

Western blot analysis

Western blot analysis was performed as previously described[5]. Epithelial cells of the duodenum, jejunum, ileum, and colon were collected and lysed in Piece® Ripa Buffer (Thermo Fisher Scientific Inc.) with 10% v/v protease inhibitor cocktail (Sigma). After being sonicated, centrifuged, and heated, 50 μg samples were loaded and separated on SDS-PAGE gel and then transferred to a polyvinylidene difluoride membrane. The membrane was blocked and probed with 1:1000 primary antibodies (Santa Cruz Biotechnology) raised against CNNM4 and TRPM6. The membranes were also reprobed with 1:5000 anti-β-actin monoclonal antibodies (Santa Cruz Biotechnology). Subsequently, the membrane was incubated with 1:10000 HRP-conjugated secondary antibodies (Santa Cruz Biotechnology), visualized by Thermo Scientific SuperSignal® West Pico Substrate (Thermo Fisher Scientific Inc.), and captured on CL-XPosure Film (Thermo Fisher Scientific Inc.). Densitometric analysis was performed using ImageJ for Mac Os X.

Statistical analysis

Results were expressed as mean ± SE. Two sets of data were compared using the unpaired Student's t-test. One-way ANOVA with Dunnett's post-test was used for comparison of multiple sets of data. All data were analyzed by GraphPad Prism for Mac Os (GraphPad Software Inc., San Diego, CA, United States).

RESULTS

Single-dose omeprazole injection increased gastrointestinal pH

Our previous study showed that 20 mg/kg oral gavage and subcutaneous omeprazole administration markedly suppress gastric acid secretion[5]. In the present study, the rats were subjected to prolonged omeprazole administration (24 wk). Therefore, subcutaneous administration that often causes minimal pain or discomfort was chosen. The injection site was changed to avoid the repeated damage or irritation of the rat tissue.

These experiments were performed to observe the effect of single-dose 20 mg/kg subcutaneous omeprazole injection on gastric acid secretion and gastrointestinal pH. Intraluminal pH of the stomach, duodenum, jejunum, ileum, cecum, and proximal colon were measured at 2 and 24 h after injection. In the vehicle-treated control group, the intraluminal pH levels of the stomach, duodenum, jejunum, ileum, cecum, and colon were 1.83 ± 0.31, 5.83 ± 0.30, 6.33 ± 0.21, 7.67 ± 0.42, 6.50 ± 0.22, and 6.67 ± 0.31, respectively. Omeprazole significantly increased gastric, duodenal, and jejunal pH at 24 h after injection (Figure 1). However, omeprazole did not affect the intraluminal acidic environment of the cecum and colon. These results indicated that 20 mg/kg omeprazole injection daily effectively suppressed the gastric acid secretion and

increased the intraluminal pH of the stomach, duodenum, and jejunum through 24 wk of treatment.

Metabolic characteristic of omeprazole-treated rats

As demonstrated in Figure 2A, all rats showed equal growth after the 24 wk of the experiment (Figure 2A). Food intake (Figure 2B) and fecal excretion (Figure 2D) of all experimental groups were equal. Water intake (Figure 2C) and urine excretion (Figure 2E) significantly increased in the omeprazole-treated groups.

Omeprazole-induced hypomagnesemia

The 12- and 24-wk-omeprazole-treated rats had significantly reduced plasma (Figure 3A) and urinary Mg^{2+} concentration (Figure 3D). The plasma concentrations of the 12- and 24-omeprazole-treated groups were 1.41 ± 0.08 mg/dL and 1.37 ± 0.14 mg/dL respectively, which were lower than the reference rage of plasma Mg^{2+} concentration (1.7-2.4 mg/dL). Therefore, omeprazole induced hypomagnesemia in our rat model. In addition, the urinary Mg^{2+} concentrations of the 12- and 24-omeprazole-treated groups were 1.26 ± 0.72 mg/dL and 1.48 ± 0.52 mg/dL, respectively, which were also lower than the normal reference of 1.7-3.0 mg/dL. While the plasma Ca^{2+} concentration (Figure 3B) did not change, the urinary Ca^{2+} concentrations of the 12- (1.63 ± 0.28 mg/dL) and 24-wk-omeprazole-treated (1.42 ± 0.23 mg/dL) groups were significantly lower than those of the control group (4.06 ± 0.87 mg/dL) (Figure 3E). The plasma (Figure 3C) and urinary phosphate concentrations (Figure 3F) of the 12- and 24-omeprazole-treated groups significantly increased in comparison to its corresponding control group.

Hormonal change in PPIH rats

In consideration that $1\alpha,25(OH)_2D_3$, PTH, FGF-23, EGF, and insulin modulate Mg^{2+} homeostasis[3,18-21], their plasma concentrations in the rats with PPIH were determined. The plasma $1\alpha,25(OH)_2D_3$ (Figure 4A) and FGF-23 (Figure 4C) concentrations of the 24-wk-omeprazole-treated rats significantly increased compared with those of the control group. The plasma PTH (Figure 4B) and insulin (Figure 4E) of all experimental groups showed no difference. The 12- and 24-wk-omeprazole-treated groups had significantly lower plasma EGF levels than the control rats (Figure 4D).

Segmental intestinal Mg^{2+} transport in PPIH rats

Previous research proposed that paracellular passive and transcellular active Mg^{2+} transport exclusively occur in the small and large intestines, respectively. In the present study, the total, paracellular, and transcellular Mg^{2+} transport rates of the vehicle-treated control group were 27.68 ± 1.36 nmol/h·cm^2, 23.04 ± 1.19 nmol/h·cm^2, and 4.65 ± 0.59 nmol/h·cm^2, respectively, in the duodenum (Figure 5A); 31.00 ± 1.19 nmol/h·cm^2, 23.73 ± 1.22 nmol/h·cm^2, and 7.27 ± 0.81 nmol/h·cm^2, respectively, in the jejunum (Figure 5B); 30.77 ± 0.94 nmol/h·cm^2, 22.23 ± 0.88 nmol/h·cm^2, and 8.53 ± 0.58 nmol/h·cm^2, respectively, in the ileum (Figure 5C); and 19.77 ± 0.99 nmol/h·cm^2, 9.83 ± 0.51 nmol/h·cm^2, and 9.93 ± 0.52 nmol/h·cm^2, respectively, in the colon (Figure 5D). In the 12-wk-omeprazole-treated rats, the total, paracellular, and transcellular Mg^{2+} transport rates were 8.55 ± 1.27 nmol/h·cm^2, 5.78 ± 1.03 nmol/h·cm^2, and 2.77 ± 0.53 nmol/h·cm^2, respectively, in the duodenum (Figure 5A); 12.36 ± 0.79 nmol/h·cm^2, 8.47 ± 0.57 nmol/h·cm^2, and 3.88 ± 0.42 nmol/h·cm^2, respectively, in the jejunum (Figure 5B); 12.39 ± 0.76 nmol/h·cm^2, 9.01 ± 0.45 nmol/h·cm^2, and 3.39 ± 0.44 nmol/h·cm^2, respectively, in the ileum (Figure 5C); and 15.41 ± 0.90 nmol/h·cm^2, 7.39 ± 0.33 nmol/h·cm^2, and 8.03 ± 0.67 nmol/h·cm^2, respectively, in the colon (Figure 5D). In the 24-wk-omeprazole-treated rats, the total, paracellular, and transcellular Mg^{2+} transport rates were 5.02 ± 0.51 nmol/h·cm^2, 3.59 ± 0.59 nmol/h·cm^2, and 1.43 ± 0.29 nmol/h·cm^2, respectively, in the duodenum (Figure 5A); 9.13 ± 0.75 nmol/h·cm^2, 6.48 ± 0.45 nmol/h·cm^2, and 2.65 ± 0.36 nmol/h·cm^2, respectively, in the jejunum (Figure 5B); 9.40 ± 0.40 nmol/h·cm^2, 7.43 ± 0.21 nmol/h·cm^2, and 1.97 ± 0.34 nmol/h·cm^2, respectively, in the ileum (Figure 5C); and 12.01 ± 0.56 nmol/h·cm^2, 6.29 ± 0.36 nmol/h·cm^2, and 5.71 ± 0.21 nmol/h·cm^2, respectively, in the colon (Figure 5D). In the small intestinal segment, Mg^{2+} was absorbed mainly through the paracellular route (Figure 5A-C and E). By contrast, the large intestine absorbed Mg^{2+} through the paracellular and transcellular routes in a comparable amount (Figure 5D). The rate of transcellular Mg^{2+} transport was the highest in the colon and the lowest in the duodenum (Figure 5F). In the 12- and 24-wk-omeprazole-treated rats, the total, paracellular, and transcellular Mg^{2+} transport rates were significantly lower in the duodenum, jejunum, ileum, and colon than in those of the corresponding vehicle-treated control rats (Figure 5A-D). These results suggest that prolonged omeprazole injection suppresses Mg^{2+} absorption throughout the intestinal tract.

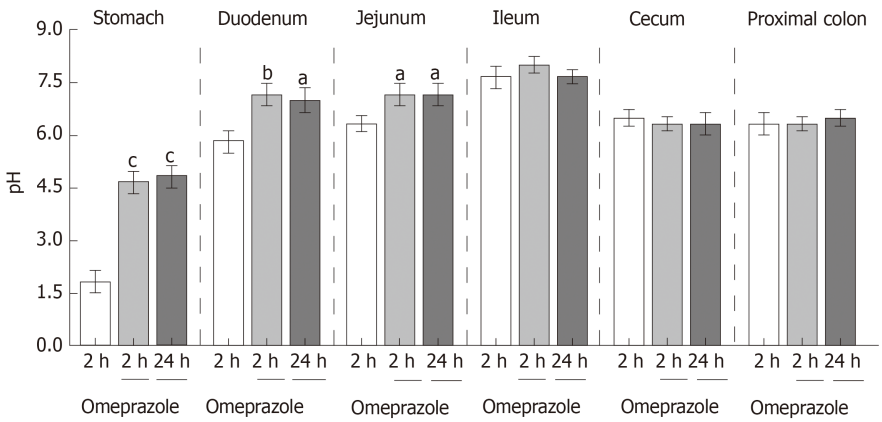

Figure 1 Effect of subcutaneous omeprazole injection on rat gastrointestinal pH. Intraluminal pH was measured by using test strips after 2 or 24 h after omeprazole administration. $^{a}P < 0.05$, $^{b}P < 0.01$, $^{c}P < 0.001$,*vs* the control group ($n = 6$).

Segmental intestinal TRPM6 and CNNM4 expression in PPIH rats

Regarding our recent results on Mg^{2+} transport throughout the intestinal tract, these series of experiment aimed to study the expression of TRPM6 and CNNM4 in the duodenum, jejunum, ileum, and colon. As demonstrated in Figure 6, TRPM6 protein was detected in the duodenum, jejunum, ileum, and colon of all experimental groups. The level of TRPM6 expression was the lowest in the duodenum and the highest in the colon of the control (Figure 6A), 12-wk- (Figure 6B), and 24-wk-omeprazole (Figure 6C)-treated rats. The 12- and 24-wk-omeprazole-treated groups had significantly higher TRPM6 expression in the duodenum, jejunum, ileum, and colon than the vehicle-treated control group (Figure 7). Similar to TRPM6, CNNM4 protein was detected throughout the intestinal tract (Figure 8). The expression of CNNM4 protein significantly increased in the duodenum, jejunum, ileum, and colon of the 12- and 24-wk-omeprazole-treated groups compared with those of the control group.

DISCUSSION

The present study showed paracellular and transcellular Mg^{2+} transport in the duodenum, jejunum, ileum, and colon. The rate of total Mg^{2+} transport was shown (in order of highest to lowest) in the jejunum, ileum, duodenum, and colon. Small intestinal epithelium absorbed Mg^{2+} mainly through the paracellular route. A comparable rate of paracellular and transcellular Mg^{2+} transport was shown in the colon.

The mechanism by which prolonged PPIs administration induce hypomagnesemia is currently unclear. In the present study, 12- and 24-wk omeprazole injection induced systemic Mg^{2+} depletion and hypomagnesemia. Similar to previous reports in PPIH patients[8,9,12-16], urinalysis of a recent PPIH rat model revealed reduced urinary Mg^{2+} excretion (less than 8.5 mg/dL), excluding urinary Mg^{2+} loss. The depletion of stored Mg^{2+} was also demonstrated in patients[9] and rats[5] with PPIH. Our results clearly showed that transcellular and paracellular Mg^{2+} transport mechanisms were markedly suppressed in the entire intestinal tract of rats with PPIH. Regarding the rate of total Mg^{2+} absorption, the length of intestinal segment, and diameter (Table 1)[25], the small intestine was the major intestinal segment for Mg^{2+} absorption. The percent suppression of total Mg^{2+} absorption in the duodenum, jejunum, ileum, and colon of the rats with PPIH rats was 81.86%, 70.59%, 69.45%, and 39.25% (Table 1), respectively. The percent suppression can be calculated using the following formula: 100 - [(total Mg^{2+} absorption of 24-wk-omeprazole group × 100) / total Mg^{2+} absorption of the control group]. Therefore, the small intestine is the major affected organs for the adverse effect of prolonged PPI administration. The stimulation of small intestinal Mg^{2+} absorption in PPIH is probably normalizing plasma Mg^{2+} level and requires further study. The present study demonstrated a higher expression level of TRPM6 protein in the colon compared with the small intestinal segment. The up-regulation of TRPM6 and CNNM4 expression in the rats with PPIH was also higher in the colon. The rate of transcellular Mg^{2+} absorption was the highest in the colon of the control and PPIH rats. However, the lowest percent suppression of total Mg^{2+} absorption was found in the colon of the rats with PPIH because single-dose

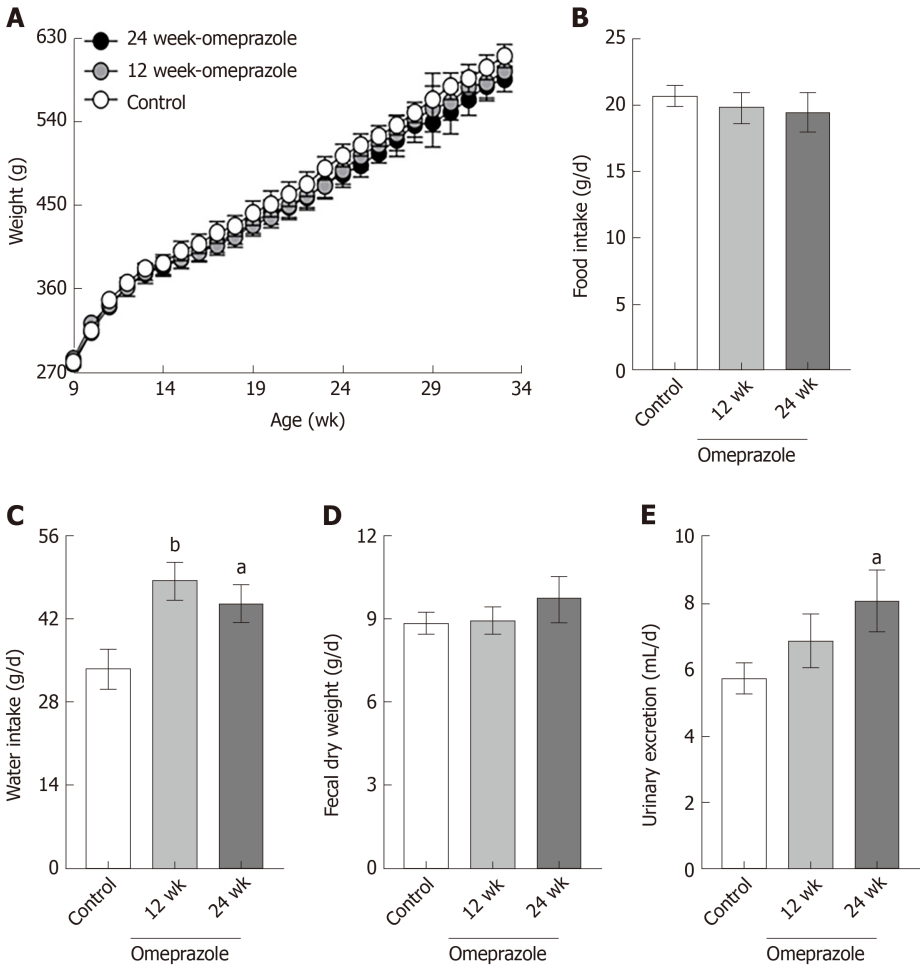

Figure 2 Metabolic characteristics. A: Body weight; B: Food intake; C: Water intake; D: Fecal dry weight; E: Urinary excretion of control, 12 wk-omeprazole-treated, and 24 wk-omeprazole-treated groups. $^{a}P < 0.05$, $^{b}P < 0.01$, *vs* the control group ($n = 6$).

omeprazole injection had no effect on intraluminal acidic environment in the colon. Our results could explain why the stimulation of colonic Mg^{2+} absorption could not normalize plasma Mg^{2+} level in the previous PPIH mouse model[13].

The overexpression of TRPM6 and CNNM4 proteins in the entire intestinal tract suggested the compensatory response in rats with PPIH. However, the rate of transcellular Mg^{2+} absorption was significantly suppressed in the duodenum, jejunum, ileum, and colon of the rats with PPIH. Hess *et al*[26], reported two common single-nucleotide polymorphisms (SNPs) in the TRPM6 gene that increase the risk for PPIH. These SNPs may explain why the overexpression of TRPM6 and CNNM4 could not increase transcellular Mg^{2+} absorption.

PPIH rats revealed normal plasma but reduced urinary Ca^{2+} concentration. Increment of plasma $1\alpha,25(OH)_2D_3$ in the rats with PPIH should stimulate intestinal Ca^{2+} absorption, renal tubular Ca^{2+} reabsorption, and bone resorption to regulate plasma Ca^{2+} concentration. Bone resorption not only increases plasma Ca^{2+} but also PO_4^{3-} levels, which trigger FGF-23 release. Plasma $1\alpha,25(OH)_2D_3$ also stimulates FGF-23 release. FGF-23 further suppresses renal tubular PO_4^{3-} reabsorption, which increases urinary PO_4^{3-} excretion[27].

Plasma $1\alpha,25(OH)_2D_3$, FGF-23, and EGF levels are altered in rats with PPIH. However, the hormonal regulation of plasma Mg^{2+} level is largely unknown. In addition, the data from the study of hormonal control of intestinal Mg^{2+} absorption are often confusing and conflicting. Previous research proposed that $1\alpha,25(OH)_2D_3$ stimulates intestinal Mg^{2+} uptake[28]. In addition, $1\alpha,25(OH)_2D_3$ treatment for 7 d exerts no effect on intestinal Mg^{2+} absorption in male C57BL/6J mice[3]. $1\alpha,25(OH)_2D_3$ increases plasma and urinary Mg^{2+} levels[3] possibly through increasing bone resorption. In consideration that $1\alpha,25(OH)_2D_3$ increases urinary Mg^{2+} excretion[3], renal Mg^{2+} wasting is probably involved in the development of hypomagnesemia in prolonged PPI administration[11]. Hypomagnesemia increases plasma FGF-23 level[19].

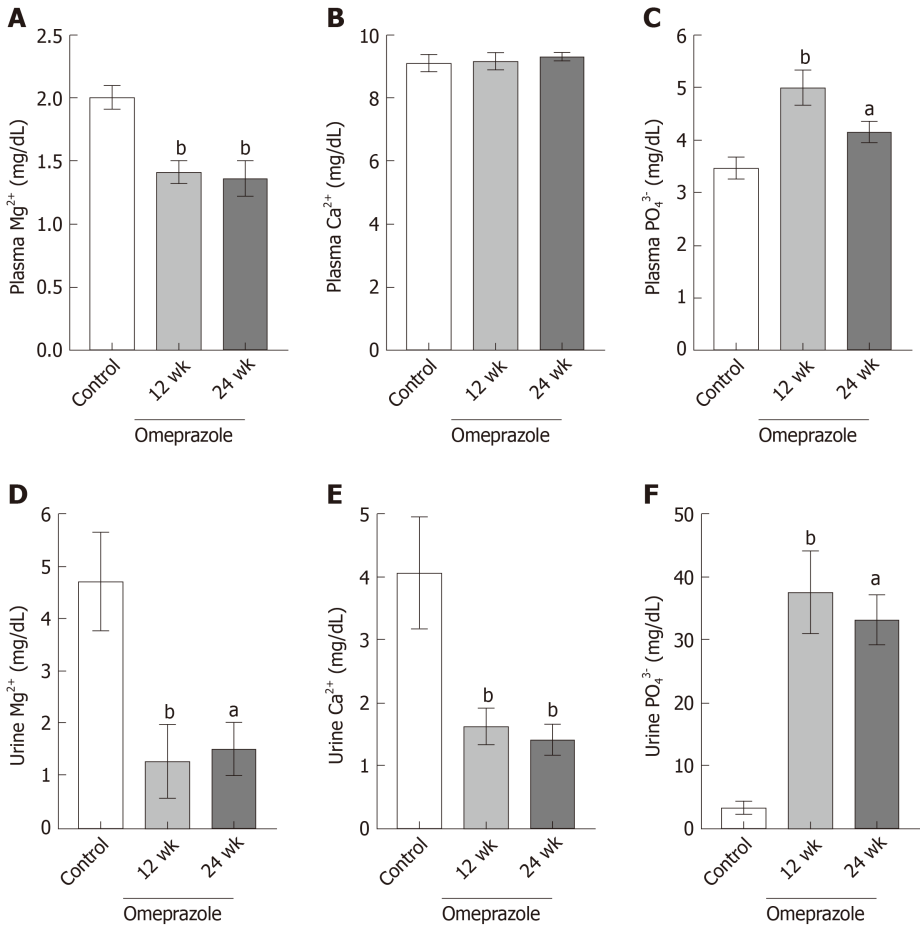

Figure 3 Effect of omeprazole on plasma and urinary Mg^{2+}, Ca^{2+}, and PO_4^{3-} levels. A: Plasma Mg^{2+}; B: Plasma Ca^{2+}; C: Plasma PO_4^{3-}; D: Urinary Mg^{2+}; E: Urinary Ca^{2+}; F: Urinary PO_4^{3-} levels of control, 12 wk-omeprazole-treated, and 24 wk-omeprazole-treated groups. $^aP < 0.05$, $^bP < 0.01$, *vs* the control group ($n = 6$).

Khuituan *et al*[29], demonstrated that FGF-23 markedly suppresses intestinal Ca^{2+} absorption. Magnesiotropic hormone EGF stimulates renal Mg^{2+} reabsorption to increase plasma Mg^{2+} level[20]. However, the direct effect of $1\alpha,25(OH)_2D_3$, FGF-23, and EGF on segmental intestinal Mg^{2+} absorption requires further study.

In conclusion, our recent study confirmed the adverse effect of prolonged PPI injection on plasma Mg^{2+} levels. In specific, PPIs can inhibit intestinal Mg^{2+} absorption. A higher level of suppression was shown in the small intestine than in the other organs. Therefore, the stimulation of small intestinal Mg^{2+} probably normalizes plasma Mg^{2+} in PPIH.

Table 1 Rate of total Mg^{2+} absorption, segmental length, and diameter of the duodenum, jejunum, ileum, and colon of the rats

	Rate of total Mg^{2+} transport		Level of suppression	Length (mm)[25]	Diameter (mm)[25]
	Control	24-wk omeprazole			
Duodenum	27.68 ± 1.36	5.02 ± 0.51	81.86%	95-100	2.5-3
Jejunum	31.01 ± 1.19	9.12 ± 0.75	70.59%	900-1350	4-5
Ileum	30.77 ± 0.94	9.40 ± 0.40	69.45%	25-35	3-5
Colon	19.76 ± 0.98	12.01 ± 0.56	39.25%	90-110	3-10

Level of suppression was a percentage decrement of total Mg^{2+} absorption in 24-wk omeprazole-treated rats compared with the corresponding control rats.

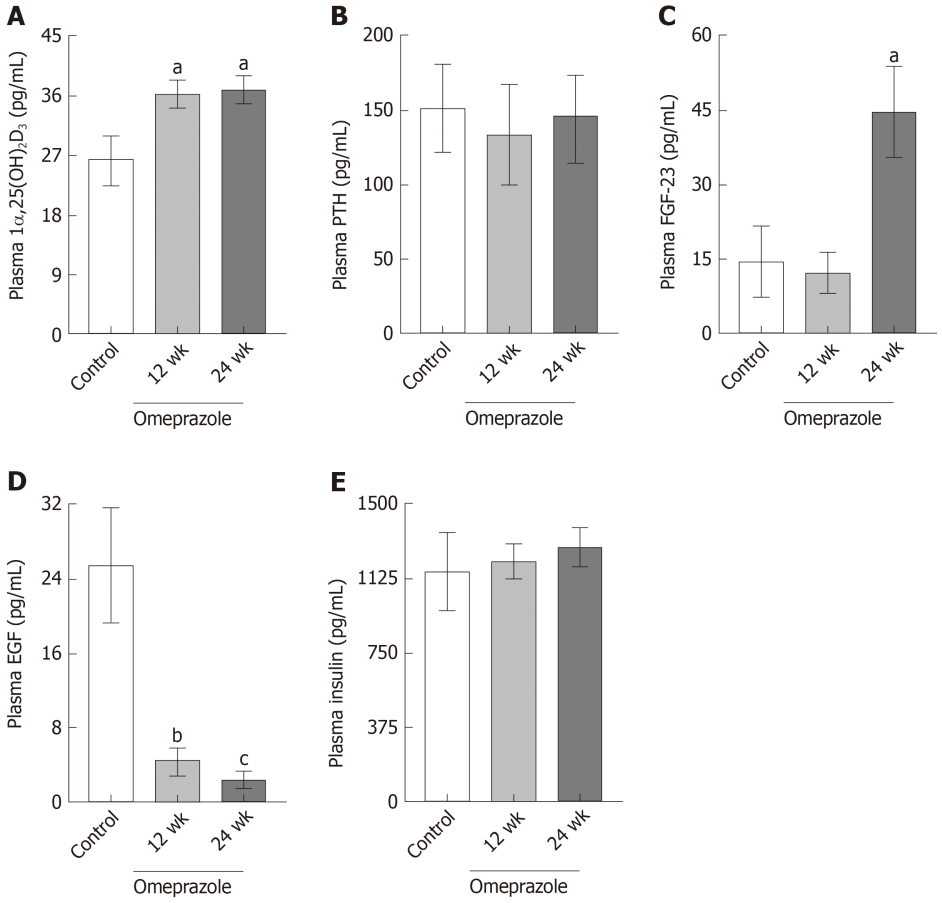

Figure 4 Effect of omeprazole on plasma 1α,25-dihydroxyvitamin D3, parathyroid hormone, fibroblast growth factor 23, epidermal growth factor, and insulin concentrations. A: Plasma 1α,25-dihydroxyvitamin D_3; B: Plasma parathyroid hormone; C: Plasma fibroblast growth factor 23; D: Plasma epidermal growth factor; E: Plasma insulin of control, 12 wk-omeprazole-treated, and 24 wk-omeprazole-treated groups. $^aP < 0.05$, $^bP < 0.01$, $^cP < 0.001$, *vs* the control group ($n = 6$). $1\alpha,25(OH)_2D_3$: 1α,25-dihydroxyvitamin D_3; PTH: Parathyroid hormone; FGF-23: Fibroblast growth factor 23; EGF: Epidermal growth factor.

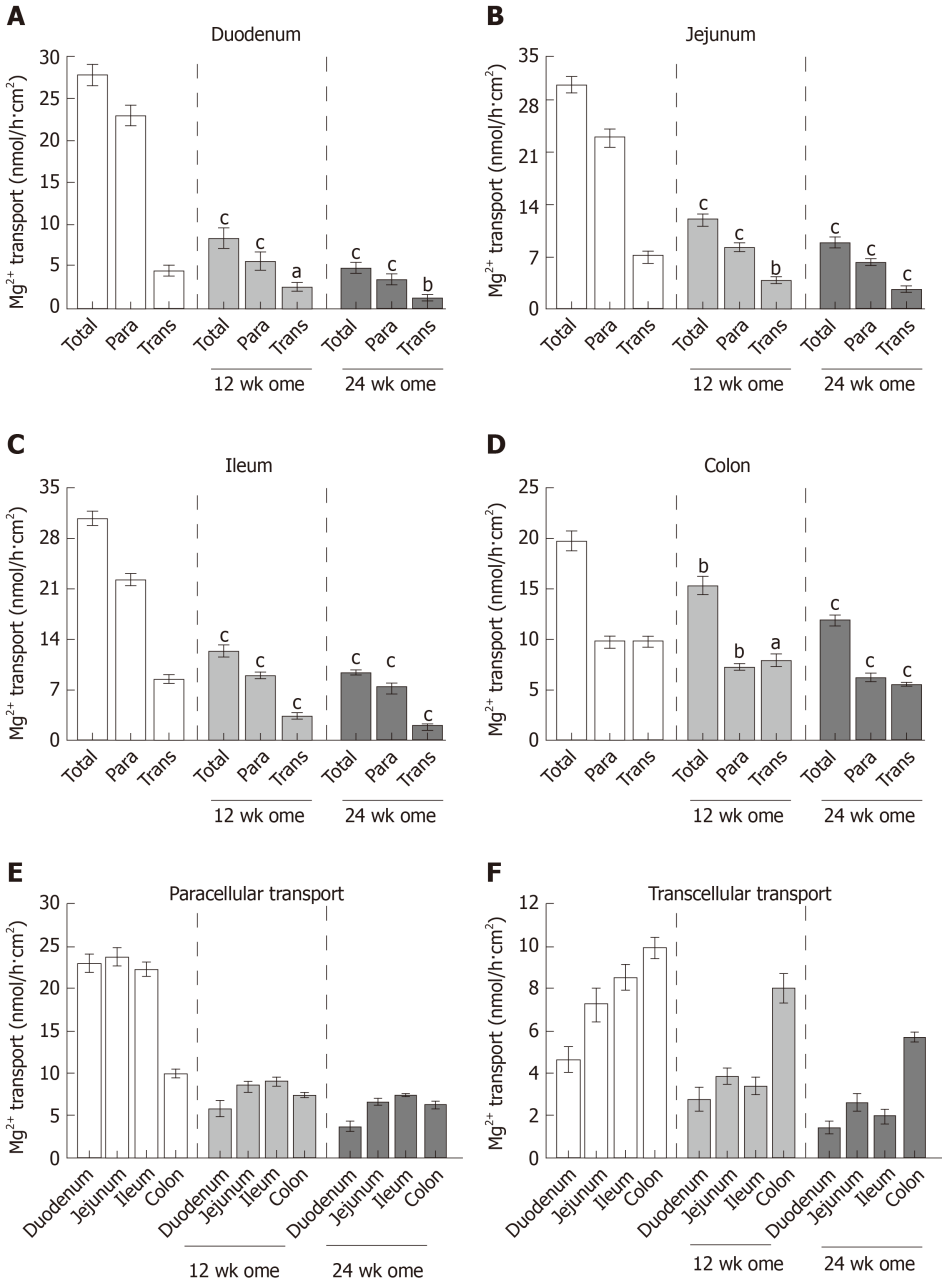

Figure 5 Effect of omeprazole on segmental intestinal Mg^{2+} absorption. A-D: Rate of total, paracellular, and transcellular Mg^{2+} transport of control, 12 wk-omeprazole-treated, and 24 wk-omeprazole-treated groups (A: Duodenum; B: Jejunum; C: Ileum; D: Colon); E: the rate paracellular; F: transcellular Mg^{2+} transport of control, 12 wk-omeprazole-treated, and 24 wk-omeprazole-treated groups. $^{a}P < 0.05$, $^{b}P < 0.01$, $^{c}P < 0.001$, *vs* the corresponding control group ($n = 6$). Para: Paracellular; Trans: transcellular.

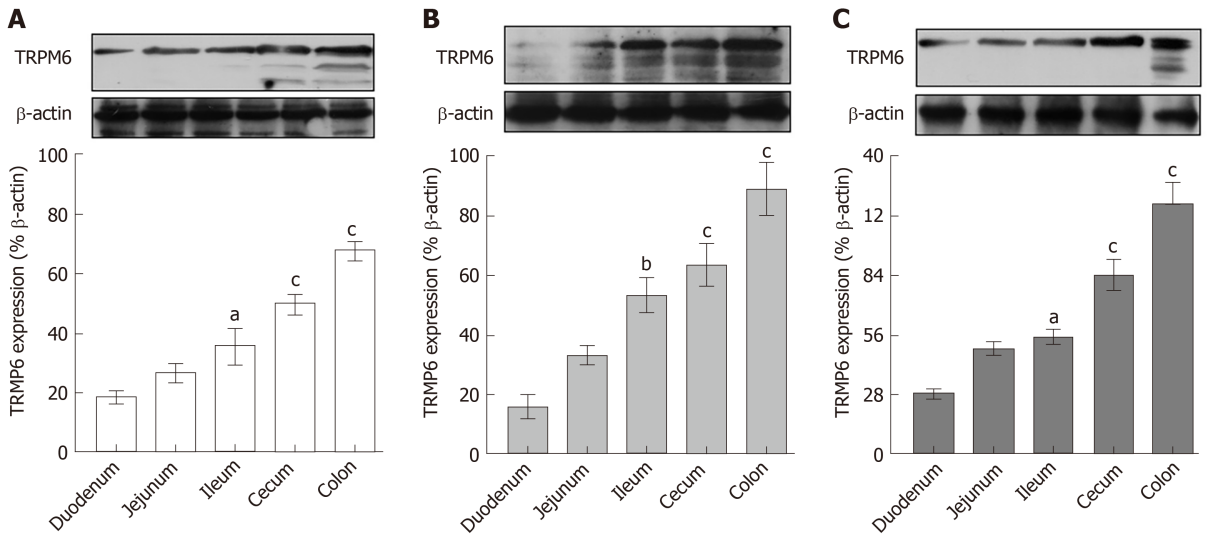

Figure 6 Transient receptor potential melastatin 6 expression in entire intestinal tract. A: Control; B: 12 wk-omeprazole-treated; C: 24 wk-omeprazole-treated groups. The quantitative immunobloting analysis and representative densitometric analysis of transient receptor potential melastatin 6 expression in duodenum, jejunum, ileum, and colon. $^{a}P < 0.05$, $^{b}P < 0.01$, $^{c}P < 0.001$, *vs* the corresponding duodenal segment ($n = 6$). TRPM6: Transient receptor potential melastatin 6.

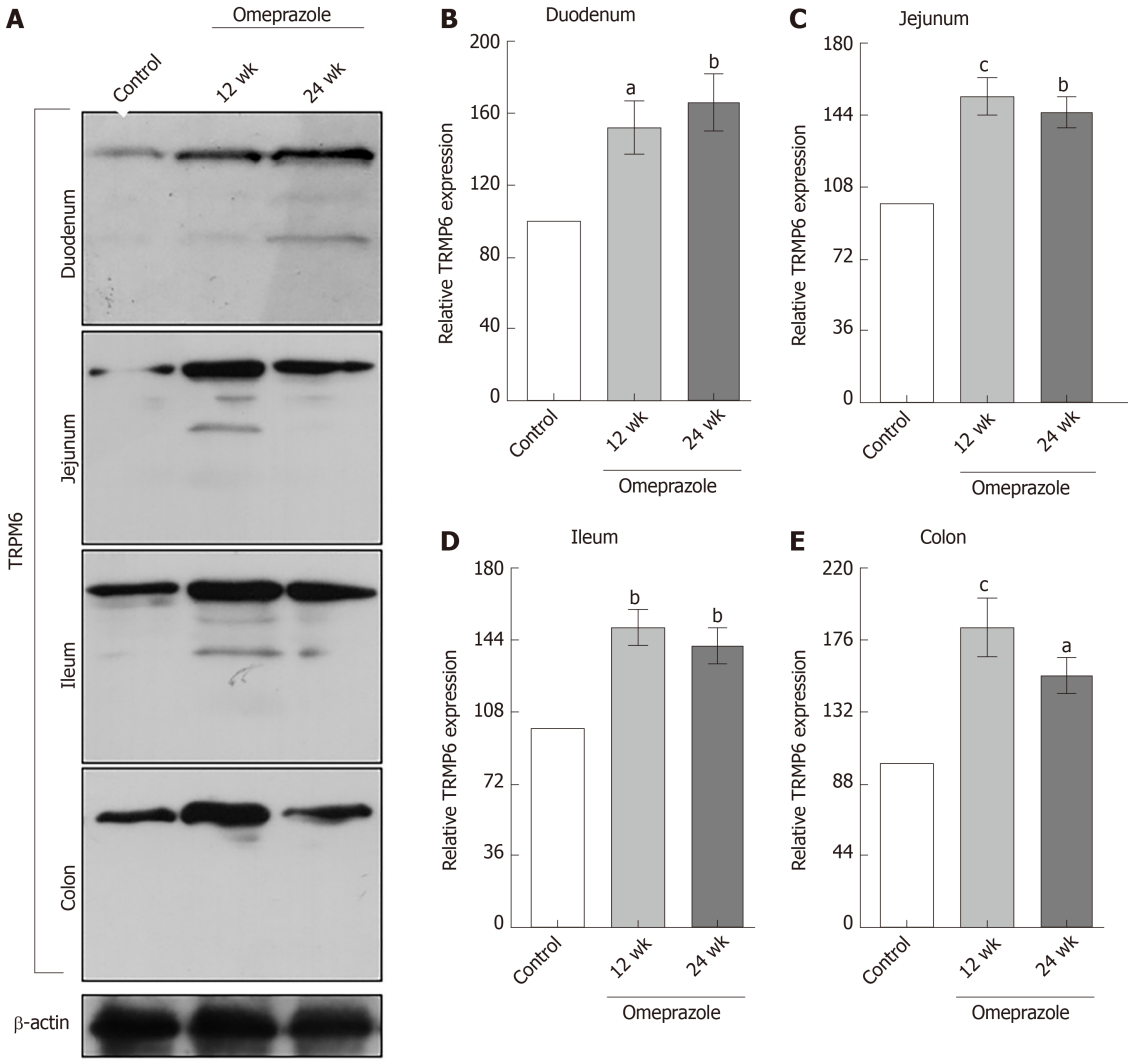

Figure 7 The effect of omeprazole on transient receptor potential melastatin 6 expression in entire intestinal tract. A: Quantitative immunobloting analysis of transient receptor potential melastatin 6 expression in duodenum, jejunum, ileum, and colon. B: Duodenum; C: Jejunum; D: Ileum; E: Colon. Representative densitometric analysis of transient receptor potential melastatin 6 expression in duodenum, jejunum, ileum, and colon of control, 12 wk-omeprazole-treated, and 24 wk-omeprazole-treated groups. $^{a}P < 0.05$, $^{b}P < 0.01$, $^{c}P < 0.001$, *vs* its corresponding vehicle-treated group ($n = 5$). TRPM6: Transient receptor potential melastatin 6.

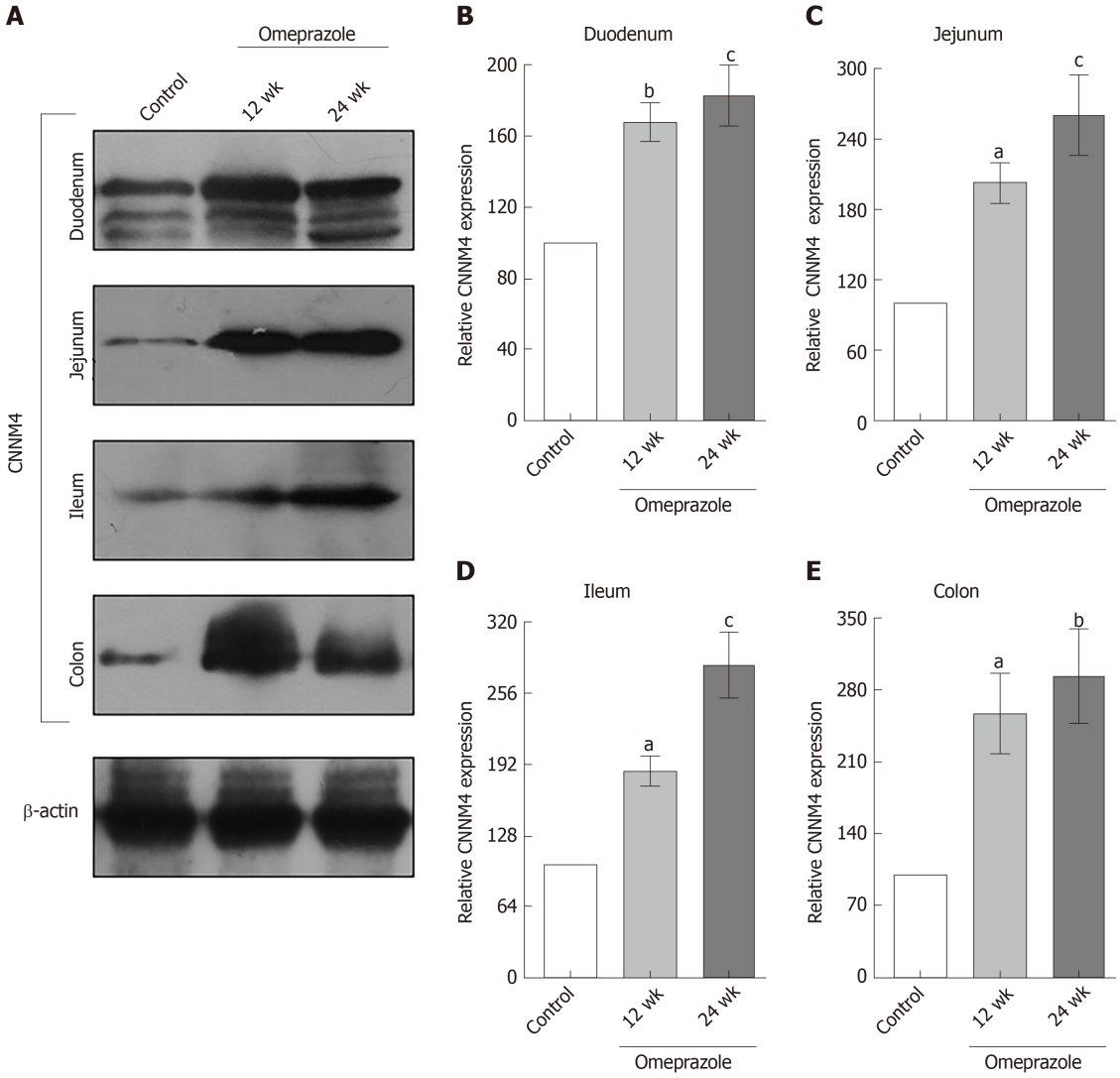

Figure 8 The effect of omeprazole on cyclin M4 expression in entire intestinal tract. A: Quantitative immunobloting analysis of cyclin M4 expression in duodenum, jejunum, ileum, and colon; B: Duodenum; C: Jejunum; D: Ileum; E: Colon. Representative densitometric analysis of cyclin M4 expression in duodenum, jejunum, ileum, and colon of control, 12 wk-omeprazole-treated, and 24 wk-omeprazole-treated groups. $^{a}P < 0.05$, $^{b}P < 0.01$, $^{c}P < 0.001$, *vs* its corresponding vehicle-treated group ($n = 5$). CNNM4: Cyclin M4.

ARTICLE HIGHLIGHTS

Research background

Dietary intake is the sole source of Mg^{2+} in humans, and intestinal absorption plays a vital role in the regulation of normal Mg^{2+} balance. Previous case reports suggested that intestinal Mg^{2+} malabsorption is a major pathophysiological mechanism in proton pump inhibitor (PPI)-induced hypomagnesemia (PPIH).

Research motivation

The exact mechanism of PPI-inhibited intestinal Mg^{2+} absorption is still controversial. In addition, a simultaneous study on transcellular and paracellular Mg^{2+} absorption in the duodenum, jejunum, ileum, and colon of normal and PPIH had not been performed.

Research objectives

The present study aimed to observe the rate of paracellular and transcellular Mg^{2+} transport across the duodenum, jejunum, ileum, and colon in control and prolonged omeprazole-treated male Sprague-Dawley rats. Magnesiotropic hormones and proteins were measured.

Research methods

The rats received subcutaneous omeprazole injection for 12 or 24 wk. The duodenum, jejunum, ileum, and colon of each rat were mounted onto individual modified Ussing chamber setups to study the rates of total, transcellular, and paracellular Mg^{2+} absorption simultaneously. Magnesiotropic hormones and proteins were observed.

Research results

Hypomagnesemia and hypomagnesuria were demonstrated in the PPIs-treated rats. Plasma 1α,25-dihydroxyvitamin D_3 and fibroblast growth factor 23 increased, whereas plasma epidermal growth factor level decreased in the omeprazole-treated rats. We clearly showed paracellular and transcellular Mg^{2+} absorption in the duodenum, jejunum, ileum, and colon of the control rats. Prolonged PPI treatment significantly inhibited transcellular and paracellular Mg^{2+} absorption in the duodenum, jejunum, ileum, and colon. High transient receptor potential melastatin 6 and cyclin M4 expression in the entire intestinal tract of the PPI-treated rats were demonstrated.

Research conclusions

Prolonged PPI administration markedly inhibits Mg^{2+} absorption throughout the entire length of intestinal tract and lead to systemic Mg^{2+} deficiency.

Research perspectives

PPIs mainly suppressed Mg^{2+} absorption in the small intestine. The stimulation of small intestinal Mg^{2+} absorption is probably nullifying the adverse effect of PPIs in chronic users.

ACKNOWLEDGEMENTS

We also thank Ms. Aroonphan Loturit, Ms. Kunlayanat Ruengwong, Ms. Narisara Tintawee, and Ms. Lamai Chaichandee of the Faculty of Allied Health Sciences, Burapha University for their excellent technical assistance.

REFERENCES

1 **de Baaij JH**, Hoenderop JG, Bindels RJ. Magnesium in man: implications for health and disease. *Physiol Rev* 2015; **95**: 1-46 [PMID: 25540137 DOI: 10.1152/physrev.00012.2014]
2 **Schuchardt JP**, Hahn A. Intestinal Absorption and Factors Influencing Bioavailability of Magnesium-An Update. *Curr Nutr Food Sci* 2017; **13**: 260-278 [PMID: 29123461 DOI: 10.2174/1573401313666170427162740]
3 **Lameris AL**, Nevalainen PI, Reijnen D, Simons E, Eygensteyn J, Monnens L, Bindels RJ, Hoenderop JG. Segmental transport of Ca² and Mg² along the gastrointestinal tract. *Am J Physiol Gastrointest Liver Physiol* 2015; **308**: G206-G216 [PMID: 25477372 DOI: 10.1152/ajpgi.00093.2014]
4 **Lameris AL**, Hess MW, van Kruijsbergen I, Hoenderop JG, Bindels RJ. Omeprazole enhances the colonic expression of the Mg(2+) transporter TRPM6. *Pflugers Arch* 2013; **465**: 1613-1620 [PMID: 23756852 DOI: 10.1007/s00424-013-1306-0]
5 **Thongon N**, Penguy J, Kulwong S, Khongmueang K, Thongma M. Omeprazole suppressed plasma magnesium level and duodenal magnesium absorption in male Sprague-Dawley rats. *Pflugers Arch* 2016; **468**: 1809-1821 [PMID: 27866273 DOI: 10.1007/s00424-016-1905-7]
6 **Voets T**, Nilius B, Hoefs S, van der Kemp AW, Droogmans G, Bindels RJ, Hoenderop JG. TRPM6 forms the Mg2+ influx channel involved in intestinal and renal Mg2+ absorption. *J Biol Chem* 2004; **279**: 19-25 [PMID: 14576148 DOI: 10.1074/jbc.M311201200]
7 **Yamazaki D**, Funato Y, Miura J, Sato S, Toyosawa S, Furutani K, Kurachi Y, Omori Y, Furukawa T, Tsuda T, Kuwabata S, Mizukami S, Kikuchi K, Miki H. Basolateral Mg2+ extrusion via CNNM4 mediates transcellular Mg2+ transport across epithelia: a mouse model. *PLoS Genet* 2013; **9**: e1003983 [PMID: 24339795 DOI: 10.1371/journal.pgen.1003983]
8 **Broeren MA**, Geerdink EA, Vader HL, van den Wall Bake AW. Hypomagnesemia induced by several proton-pump inhibitors. *Ann Intern Med* 2009; **151**: 755-756 [PMID: 19920278 DOI: 10.7326/0003-4819-151-10-200911170-00016]
9 **Cundy T**, Dissanayake A. Severe hypomagnesaemia in long-term users of proton-pump inhibitors. *Clin Endocrinol (Oxf)* 2008; **69**: 338-341 [PMID: 18221401 DOI: 10.1111/j.1365-2265.2008.03194.x]
10 **Cundy T**, Mackay J. Proton pump inhibitors and severe hypomagnesaemia. *Curr Opin Gastroenterol* 2011; **27**: 180-185 [PMID: 20856115 DOI: 10.1097/MOG.0b013e32833ff5d6]
11 **Danziger J**, William JH, Scott DJ, Lee J, Lehman LW, Mark RG, Howell MD, Celi LA, Mukamal KJ. Proton-pump inhibitor use is associated with low serum magnesium concentrations. *Kidney Int* 2013; **83**: 692-699 [PMID: 23325090 DOI: 10.1038/ki.2012.452]
12 **Epstein M**, McGrath S, Law F. Proton-pump inhibitors and hypomagnesemic hypoparathyroidism. *N Engl J Med* 2006; **355**: 1834-1836 [PMID: 17065651 DOI: 10.1056/NEJMc066308]
13 **Hess MW**, de Baaij JH, Gommers LM, Hoenderop JG, Bindels RJ. Dietary Inulin Fibers Prevent Proton-Pump Inhibitor (PPI)-Induced Hypocalcemia in Mice. *PLoS One* 2015; **10**: e0138881 [PMID: 26397986 DOI: 10.1371/journal.pone.0138881]
14 **Quasdorff M**, Mertens J, Dinter J, Steffen HM. Recurrent hypomagnesemia with proton-pump inhibitor rechallenge. *Ann Intern Med* 2011; **155**: 405-407 [PMID: 21930865 DOI: 10.7326/0003-4819-155-6-201109200-00022]
15 **Shabajee N**, Lamb EJ, Sturgess I, Sumathipala RW. Omeprazole and refractory hypomagnesaemia. *BMJ* 2008; **337**: a425 [PMID: 18617497 DOI: 10.1136/bmj.39505.738981.BE]
16 **Regolisti G**, Cabassi A, Parenti E, Maggiore U, Fiaccadori E. Severe hypomagnesemia during long-term treatment with a proton pump inhibitor. *Am J Kidney Dis* 2010; **56**: 168-174 [PMID: 20493607 DOI: 10.1053/j.ajkd.2010.03.013]
17 **Metz DC**, Sostek MB, Ruszniewski P, Forsmark CE, Monyak J, Pisegna JR. Effects of esomeprazole on acid output in patients with Zollinger-Ellison syndrome or idiopathic gastric acid hypersecretion. *Am J Gastroenterol* 2007; **102**: 2648-2654 [PMID: 17764495 DOI: 10.1111/j.1572-0241.2007.01509.x]
18 **Vetter T**, Lohse MJ. Magnesium and the parathyroid. *Curr Opin Nephrol Hypertens* 2002; **11**: 403-410

[PMID: 12105390 DOI: 10.1097/00041552-200207000-00006]
19 **Matsuzaki H**, Kajita Y, Miwa M. Magnesium deficiency increases serum fibroblast growth factor-23 levels in rats. *Magnes Res* 2013; **26**: 18-23 [PMID: 23608165 DOI: 10.1684/mrh.2013.0331]
20 **Muallem S**, Moe OW. When EGF is offside, magnesium is wasted. *J Clin Invest* 2007; **117**: 2086-2089 [PMID: 17671646 DOI: 10.1172/JCI33004]
21 **Alzaid AA**, Dinneen SF, Moyer TP, Rizza RA. Effects of insulin on plasma magnesium in noninsulin-dependent diabetes mellitus: evidence for insulin resistance. *J Clin Endocrinol Metab* 1995; **80**: 1376-1381 [PMID: 7714113 DOI: 10.1210/jcem.80.4.7714113]
22 **Quinn R**. Comparing rat's to human's age: how old is my rat in people years? *Nutrition* 2005; **21**: 775-777 [PMID: 15925305 DOI: 10.1016/j.nut.2005.04.002]
23 **Wolf FI**, Trapani V, Simonacci M, Mastrototaro L, Cittadini A, Schweigel M. Modulation of TRPM6 and Na(+)/Mg(2+) exchange in mammary epithelial cells in response to variations of magnesium availability. *J Cell Physiol* 2010; **222**: 374-381 [PMID: 19890837 DOI: 10.1002/jcp.21961]
24 **Thongon N**, Krishnamra N. Omeprazole decreases magnesium transport across Caco-2 monolayers. *World J Gastroenterol* 2011; **17**: 1574-1583 [PMID: 21472124 DOI: 10.3748/wjg.v17.i12.1574]
25 **Hebel R**, Stromberg MW, Hebel R, Stromberg MW. Digestive system. In: Hebel R, Stromberg MW. Anatomy of the Laboratory Rat. Baltimore: Wiliams and Wilkins, 1976: 43-52. Hebel R, Stromberg MW.
26 **Hess MW**, de Baaij JH, Broekman MM, Bisseling TM, Haarhuis BJ, Tan AC, Te Morsche RH, Hoenderop JG, Bindels RJ, Drenth JP. Common single nucleotide polymorphisms in transient receptor potential melastatin type 6 increase the risk for proton pump inhibitor-induced hypomagnesemia: a case-control study. *Pharmacogenet Genomics* 2017; **27**: 83-88 [PMID: 27926584 DOI: 10.1097/FPC.0000000000000259]
27 **Jacquillet G**, Unwin RJ. Physiological regulation of phosphate by vitamin D, parathyroid hormone (PTH) and phosphate (Pi). *Pflugers Arch* 2019; **471**: 83-98 [PMID: 30393837 DOI: 10.1007/s00424-018-2231-z]
28 **Hardwick LL**, Jones MR, Brautbar N, Lee DB. Magnesium absorption: mechanisms and the influence of vitamin D, calcium and phosphate. *J Nutr* 1991; **121**: 13-23 [PMID: 1992050 DOI: 10.1093/jn/121.1.13]
29 **Khuituan P**, Teerapornpuntakit J, Wongdee K, Suntornsaratoon P, Konthapakdee N, Sangsaksri J, Sripong C, Krishnamra N, Charoenphandhu N. Fibroblast growth factor-23 abolishes 1,25-dihydroxyvitamin D-enhanced duodenal calcium transport in male mice. *Am J Physiol Endocrinol Metab* 2012; **302**: E903-E913 [PMID: 22275752 DOI: 10.1152/ajpendo.00620.2011]

World Journal of Gastroenterology

Submit a Manuscript: https://www.f6publishing.com

World J Gastroenterol 2020 March 21; 26(11): 1156-1171

DOI: 10.3748/wjg.v26.i11.1156

ISSN 1007-9327 (print) ISSN 2219-2840 (online)

ORIGINAL ARTICLE

Basic Study

Protective effects of panax notoginseng saponin on dextran sulfate sodium-induced colitis in rats through phosphoinositide-3-kinase protein kinase B signaling pathway inhibition

Qing-Ge Lu, Li Zeng, Xiao-Hai Li, Yu Liu, Xue-Feng Du, Guo-Min Bai, Xin Yan

ORCID number: Qing-Ge Lu (0000-0002-7088-3190); Li Zeng (0000-0002-0985-9562); Xiao-Hai Li (0000-0002-7719-1613); Yu Liu (0000-0002-6488-252X); Xue-Feng Du (0000-0002-7318-1936); Guo-Min Bai (0000-0003-1231-4296); Xin Yan (0000-0001-7555-0670).

Author contributions: Lu QG and Zeng L designed the research; Li XH and Liu Y performed the research; Du XF and Bai GM analyzed the data; Yan X wrote the paper.

Supported by National Natural Science Foundation of China, No. 81704059; Scientific Research Project of Hebei Province Traditional Chinese Medicine Administration, No. 2017130.

Institutional review board statement: This study was reviewed and approved by the North China University of Science and Technology Ethics Committee (Approval No. NCST2018196).

Institutional animal care and use committee statement: This study was reviewed and approved by the Animal Care Welfare Committee of North China University of Science and Technology (No. 20180809).

Conflict-of-interest statement: The authors declare no conflict of interest.

Data sharing statement: No additional data are available.

ARRIVE guidelines statement: The

Qing-Ge Lu, Li Zeng, Xiao-Hai Li, Yu Liu, Xue-Feng Du, Guo-Min Bai, Department of Anorectal, Tangshan Traditional Chinese Medicine Hospital, Tangshan 063000, Hebei Province, China

Xin Yan, College of Traditional Chinese Medicine, North China University of Science and Technology, Tangshan 063210, Hebei Province, China

Corresponding author: Xin Yan, PhD, Professor, College of Traditional Chinese Medicine, North China University of Science and Technology, No. 21 Bohai Avenue, Caofeidian New Town, Tangshan 063210, Hebei Province, China. y18301212703@163.com

Abstract

BACKGROUND

Intestinal inflammation is a common digestive tract disease, which is usually treated with hormone medicines. Hormone medicines are effective to some extent, but long-term use of them may bring about many complications.

AIM

To explore the protective effects of panax notoginseng saponin (PNS) against dextran sulfate sodium (DSS)-induced intestinal inflammatory injury through phosphoinositide-3-kinase protein kinase B (PI3K/AKT) signaling pathway inhibition in rats.

METHODS

Colitis rat models were generated *via* DSS induction, and rats were divided into control (no modeling), DSS, DSS + PNS 50 mg/k, and DSS + PNS 100 mg/kg groups. Then, the intestinal injury, oxidative stress parameters, inflammatory indices, tight junction proteins, apoptosis, macrophage polarization, and TLR4/AKT signaling pathway in colon tissues from rats in each of the groups were detected. The PI3K/AKT signaling pathway in the colon tissue of rats was blocked using the PI3K/AKT signaling pathway inhibitor, LY294002.

RESULTS

Compared with rats in the control group, rats in the DSS group showed significantly shortened colon lengths, and significantly increased disease activity indices, oxidative stress reactions and inflammatory indices, as well as significantly decreased expression of tight junction-associated proteins. In addition, the DSS group showed significantly increased apoptotic cell numbers, and showed significantly increased M1 macrophages in spleen and colon tissues.

authors have read the ARRIVE guidelines, and the manuscript was prepared and revised according to the ARRIVE guidelines.

Manuscript source: Unsolicited manuscript

Received: November 12, 2019
Peer-review started: November 12, 2019
First decision: December 23, 2019
Revised: December 27, 2019
Accepted: February 21, 2020
Article in press: February 21, 2020
Published online: March 21, 2020

P-Reviewer: Maric I, M'Koma A
S-Editor: Wang JL
L-Editor: Filipodia
E-Editor: Zhang YL

They also showed significantly decreased M2 macrophages in colon tissues, as well as activation of the PI3K/AKT signaling pathway (all $P < 0.05$). Compared with rats in the DSS group, rats in the DSS + PNS group showed significantly lengthened colon lengths, decreased disease activity indices, and significantly alleviated oxidative stress reactions and inflammatory responses. In addition, this group showed significantly increased expression of tight junction-associated proteins, significantly decreased apoptotic cell numbers, and significantly decreased M1 macrophages in spleen and colon tissues. This group further showed significantly increased M2 macrophages in colon tissues, and significantly suppressed activation of the PI3K/AKT signaling pathway, as well as a dose dependency (all $P < 0.05$). When the PI3K/AKT signaling pathway was inhibited, the apoptosis rate of colon tissue cells in the DSS + LY294002 group was significantly lower than that of the DSS group ($P < 0.05$).

CONCLUSION
PNS can protect rats against DSS-induced intestinal inflammatory injury by inhibiting the PI3K/AKT signaling pathway, and therefore may be potentially used in the future as a drug for colitis.

Key words: Panax notoginseng saponin; Phosphoinositide-3-kinase protein kinase B signaling pathway; Dextran sulfate sodium; Colitis; Rat intestine; Protective effect

Core tip: Panax notoginseng saponin is a drug widely used for cardiovascular diseases and diabetes, with good proven inhibitory effects on inflammation. Our study also found that panax notoginseng saponin exerted good inhibitory effects on inflammation in dextran sulfate sodium-induced colitis.

Citation: Lu QG, Zeng L, Li XH, Liu Y, Du XF, Bai GM, Yan X. Protective effects of panax notoginseng saponin on dextran sulfate sodium-induced colitis in rats through phosphoinositide-3-kinase protein kinase B signaling pathway inhibition. *World J Gastroenterol* 2020; 26(11): 1156-1171
URL: https://www.wjgnet.com/1007-9327/full/v26/i11/1156.htm
DOI: https://dx.doi.org/10.3748/wjg.v26.i11.1156

INTRODUCTION

The gastrointestinal tract is an organ with many complex functions in terms of endocrine, immunity, nutrition, and others. These play an important role in the normal operation of the human body[1,2]. Intestinal inflammation is primarily caused by immune dysfunction due to intestinal barrier damage by invading pathogens or microbial toxins in the body[3]. Once intestinal injury occurs in the body, intestinal mucosa will release oxygen free radicals, leading to lipid peroxidation and complete loss of the intestinal barrier. This will cause the also release of inflammatory factors, which may have a more severe consequence - death or systemic inflammatory response syndromes[4,5]. At present, intestinal inflammatory injury is mainly treated with corticoid drugs for intestinal inflammation. Although these drugs are effective to some extent, long-term use of them may cause various hormone medicine-related adverse reactions, including other gastrointestinal complications and neurogenic obesity[6]. Therefore, finding a new drug that is effective for intestinal inflammatory injury is a current clinical challenge. Panax notoginseng, a traditional Chinese medicine, has been widely used for cardiovascular diseases[7], and panax notoginseng saponin (PNS) is one of the most effective ingredients of panax notoginseng. A previous study pointed out that PNS had a variety of pharmacological functions, including anti-inflammatory and anti-apoptosis effects[8]. Another study found that PNS could alleviate oxidative stress reactions and eliminate free radicals[9]. Both oxidative stress reactions and free radicals are pathological features of intestinal inflammation[10]. Although there have been discussions on the role of notoginsenoside R1, an effective component in PNS, in intestinal ischemia-reperfusion[11], there was no elaboration on PNS in enteritis. The dextran sulfate sodium (DSS)-induced colitis

model has been widely used, because it can mimics human inflammatory bowel diseases[11]. Therefore, we constructed colitis rat models based on DSS induction, and explored the role of PNS in intestinal inflammatory injury and its mechanism in rats.

MATERIALS AND METHODS

Animals and materials

A total of 80 Sprague-Dawley rats aged 6-7 wk with a body mass of about 235-290 g were raised at a temperature of 20-25 °C and a relative humidity of 45%-65%, and allowed to eat and drink freely under normal circadian rhythm alternation after being purchased from the Laboratory Animal Centre of Sun Yat-Sen University. In addition to the rats, there were other materials as follows: *Escherichia coli* DSS (Sigma, United States, L2880); PNS (Chengdu Must Biotechnology Co., Ltd., A0760); fluorescein isothiocyanate (FITC)-labeled anti-mouse CD11b antibody, phycoerythrin (PE)-labeled anti-mouse F4/80 antibody, PerCp/Cy5.5-labeled anti-mouse CD16/32 antibody, APC-labeled anti-mouse CD206 antibody (BioLegend Company, United States); interleukin-6 (IL-6), IL-1β, tumor necrosis factor-α (TNF-α), IL-10, and enzyme-linked immunosorbent assay kit (Shanghai Mlbio Co., Ltd.); p-PI3K, p-AKT, claudin-1, occludin, ZO-1, Bax, Bcl-2, and caspase-3 monoclonal antibodies (Cell Signaling Company, United States); rabbit anti-human β-actin monoclonal antibody (Proteintech Group, Inc); multiple factor flow cytometry kit (BioLegend Company, United States); in situ cell apoptosis determination kit (Roche Diagnostics, Basel, Switzerland), and fetal bovine serum (Hyclone company), and red blood cell lysate (Miltenyi Company, Germany).

Animal modeling

The rats were randomly assigned to a control group (no treatment), a DSS group, a DSS + PNS 50 mg/kg group and a DSS + PNS 100 mg/kg group, 20 rats in each group. The rats were raised normally for 3 d. After 3 d, rats in the DSS group, DSS + PNS 50 mg/kg group and DSS + PNS 100 mg/kg group were made to drink water containing 50 g/LDSS instead of their previous drinking water for 7 consecutive days. During the 7 d, rats in the DSS+PNS 50 mg/kg group were given 50 mg/kg PNS at 7 mg/mL by gavage, and rats in the DSS + PNS 100 mg/kg group were given 100 mg/kg PNS at 7 mg/mL by gavage from the 2nd day. Rats in the two groups were weighted each day, and the disease of those rats was evaluated using the disease activity index[12]. After the 7 d, the rats were killed by cervical dislocation, and their spleen and colons were collected for subsequent analysis.

Histological analysis

Colon tissues were fixed with 4% paraformaldehyde for one night, and then paraffin embedding and serial sections (3.5 μm) were performed. Subsequently, tissues were stained with hematoxylin & eosin, and images of the tissues were obtained using the Image-Pro Plus 5.0 system. Villar heights and crypt depths were measured and analyzed, and the intestinal injury of the tissues was scored[13]. The score spanned between 0 and 4, and indicated no epithelium injury and inflammatory infiltration with 0 points, slight goblet cell reduction and inflammatory infiltration into crypts with 1 point, relatively extensive goblet cell reduction and inflammatory infiltration into the mucosal muscularis with 2 points, extensive goblet cell reduction, slight crypt decrease, and extensive inflammatory infiltration into the mucosal muscularis with 3 points, and extensive decrease in crypts and inflammatory infiltration into the submucosa with 4 points.

Index detection

Inflammation-related factors and oxidative stress parameters: Enzyme-linked immunosorbent assay was employed to determine serum pro-inflammatory factors (IL-6, IL-1β, and TNF-α), and an anti-inflammatory factor (IL-10) in strict accordance with kit instructions. The electrochemiluminescence immunoassay was used to determine serum oxidative stress parameters including malondialdehyde (MDA), myeloperoxidase (MPO), catalase (CAT), and superoxide dismutase (SOD) in strict accordance with kit instructions.

Western blot assay: The total protein of the sampled colon tissues was extracted using the radio immunoprecipitation assay lysis method, and the concentration of the total protein was determined using the bicinchoninic acid method, and adjusted to 4 μg/μL. The total protein was separated using 12% sodium dodecyl sulfate-polyacrylamide gel electrophoresis, and then transferred to a polyvinylidene fluoride membrane, stained with Ponceau's stain liquid, and soaked in phosphate buffer saline

with Tween for 5 min for washing. Then, the total protein was blocked with 5% skim milk powder for 2 h, and added with p-PI3K (1:500), p-AKT (1:500), claudin-1 (1:500), occludin (1:500), ZO-1 (1:500), Bax (1:500), Bcl-2 (1:500), Caspase-3 (1:500) and β-Actin primary antibody (1:500), and blocked at 4 °C for one night. The membrane was washed to remove the primary antibody, added with horseradish peroxidase-labeled goat anti-rabbit secondary antibody (1:1000), incubated at 37 °C for 1 h, and rinsed with phosphate buffer saline (PBS) three times, 5 min each time. Filter paper was used for the membrane to remove excess liquid, and the membrane was then made to be luminescent with ECL and developed. The protein band was scanned, and the gray value was analyzed using Quantity One software. The relative expression of protein = gray value of the target protein band/gray value of the β-Actin protein band.

TUNEL assay for cell apoptosis determination: The mesenteric lymph node tissues were fixed with 4% formaldehyde at room temperature, and then washed, dehydrated, paraffin embedded, and cut into 4 μm sections. Cell apoptosis in the sections were determined in strict accordance with instructions of the in situ cell apoptosis determination kit. Cells with brown nuclei after staining were apoptotic cells, and these cells in five microscopic fields were counted under a fluorescence microscope. Cells staining positive for TUNEL were also counted.

Flow cytometry for macrophage and M1/M2 macrophage determination: Colon and spleen of rats were sampled to prepare a single-cell suspension. The spleens were placed in 0.9% sodium chloride solution, and then ground, filtered and lysed using red blood cell lysate. Subsequently, the tissues were centrifuged at 300 *g* for 5 min. After centrifugation, the tissues were washed with PBS, and resuspended. A total of 1 × 10^5 cells were taken from the tissues for determination. After being sheared, colon tissues were added into PBS containing 5% fetal bovine serum, and placed into a 37 °C water bath for 20 min. Then, epithelial cells were removed from the tissues, and the tissues were fully sheared again and placed into a solution containing 1mg/ml collagenase IV, and then placed in a 37 °C water bath for 30 min for digestion. Subsequently, the tissue suspension was filtered, centrifuged at 300 *g* for 10 min, and resuspended. A total of 1 × 10^5 cells in the middle layer were taken for detection. Then, the cells were added to human surface antibodies (FITC-CD11b, PE-F4/80, and Per Cp/Cy5.5-CD16/32), incubated at a normal temperature in the dark for 20 min, and then washed with PBS to remove excess antibodies. Subsequently, the cells were added with 2 mL of stationary liquid/membrane permeabilization buffer solution, and washed two times. Then, the cells were added to APC-CD206 antibody, incubated in the dark at 4 °C for 30 min, and added to 1 mL of stationary liquid/membrane permeabilization buffer solution, and then washed one time. Finally, the cells were isolated using flow cytometry after being resuspended in 200 μL PBS. The surface markers of macrophages, M1 and M2 macrophages were CD11b and F4/80, CD16/32 and CD206, respectively.

Statistical analysis

In this study, the collected data were statistically analyzed using the SPSS20.0 software package, and organized into figures using GraphPad 7 software. Comparison between groups was analyzed using independent *t*-tests, and comparison among multiple groups was analyzed using one-way ANOVA. Post hoc pairwise comparisons were subject to LSD-*t* tests. $P < 0.05$ indicated a significant difference.

RESULTS

Alleviation of DSS-induced intestinal injury by PNS

Compared with rats in the control group, after being injected with DSS, rats in the DSS group showed significantly shortened colon lengths, significantly increased crypt depths, and significant weight loss since the first 3rd day (all $P < 0.05$). Compared with rats in the DSS group, rats in the DSS + PNS group showed significantly lengthened colons, significantly decreased crypt depths, and significantly improved disease activity indices (all $P < 0.05$; Figure 1).

Alleviation of DSS-induced histopathological lesions in rats by PNS

Compared with rats in the control group, rats in the DSS group showed obvious intestinal pneumatosis in the small intestine, mucosa edema in the intestinal wall, and severe mesenteric venous congestion. In addition, rates in the DSS + PNS group showed mild mucosa edema in the intestinal wall, and partial mesenteric venous congestion without obvious congestion points. In addition, compared with rats in the

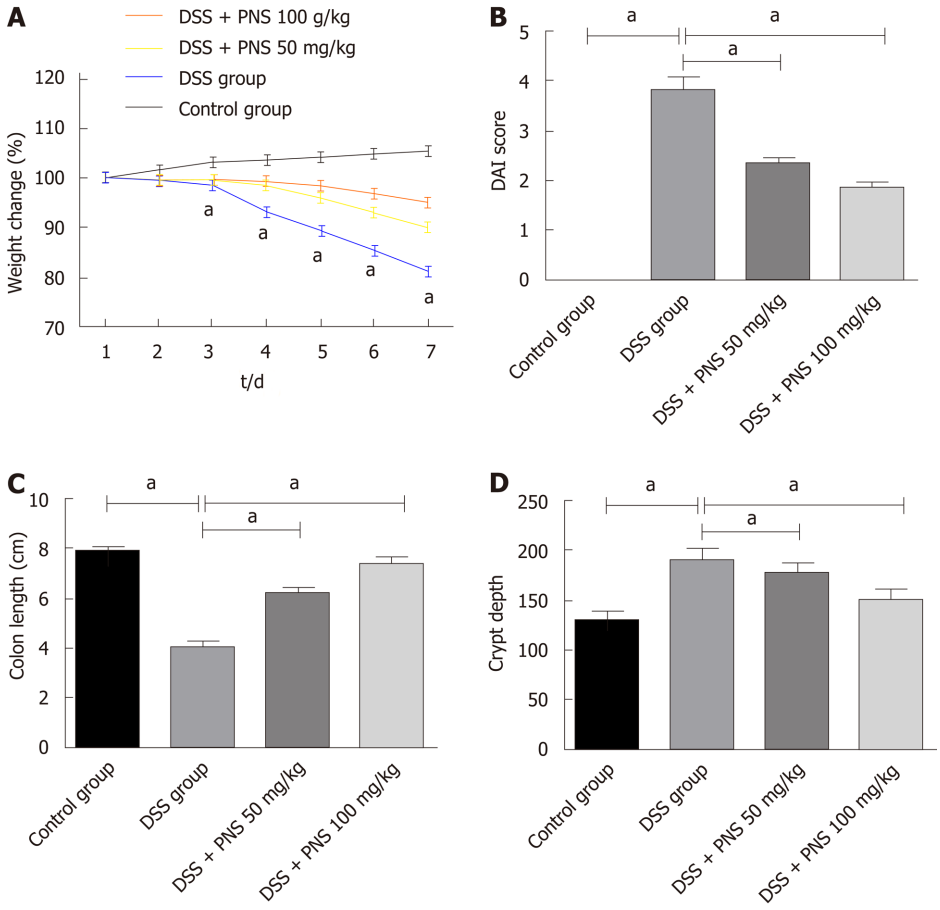

Figure 1 Panax notoginseng saponin alleviates dextran sulfate sodium-induced intestinal injury. A: Weight changes of rats in the four groups; B: Comparison among the four groups in disease activity index; C: Comparison among the four groups in colon length; D: Comparison among the four groups in crypt depth. $^{a}P < 0.05$. PNS: Panax notoginseng saponin; DSS: Dextran sulfate sodium.

control group, rats in the DSS group had significantly higher histopathological scores, but rats undergoing PNS intervention had significantly improved histopathological scores, and showed a dose-dependency (Figure 2).

Alleviation of intestinal oxidative damage in rats by PNS

Compared with rats in the control group, rats in the DSS group showed significantly increased MDA and MPO activities and significantly decreased CAT and SOD activities in intestinal tissues (all $P < 0.05$). Compared with rats in the DSS group, rats in the DSS + PNS group showed significantly decreased MDA and MPO activities, and significantly improved SOD and CAT activities in intestinal tissues (all $P < 0.05$; Figure 3).

Alleviation of intestinal inflammatory response in rats by PNS

Compared with rats in the control group, rats in the DSS groups showed significantly increased expression of IL-6, IL-1β and TNF-α, and significantly decreased expression of IL-10 in intestinal tissues (all $P < 0.05$). Compared with rats in the DSS group, rats in the DSS + PNS group showed significantly decreased expression of IL-6 and TNF-α, and significantly increased expression of IL-10 ($P < 0.05$; Figure 4).

Effects of PNS on intestinal tight junction proteins in rats

Compared with rats in the control group, rats in the DSS group showed significantly decreased expression of tight junction proteins including claudin-1, occludin, and ZO-1 in intestinal tissues (all $P < 0.05$). Compared with rats in the DSS group, rats in the DSS + PNS group showed significantly increased expression of claudin-1, occludin, and ZO-1, and showed a dose-dependency (all $P < 0.05$; Figure 5).

Effects of PNS on PI3K / AKT signaling pathway in rats

Compared with rats in the control group, rats in the DSS group showed significantly increased expression of p-PI3K and p-AKT (both $P < 0.05$). Compared with rats in the DSS group, rats in the DSS+PNS group showed significantly decreased expression of

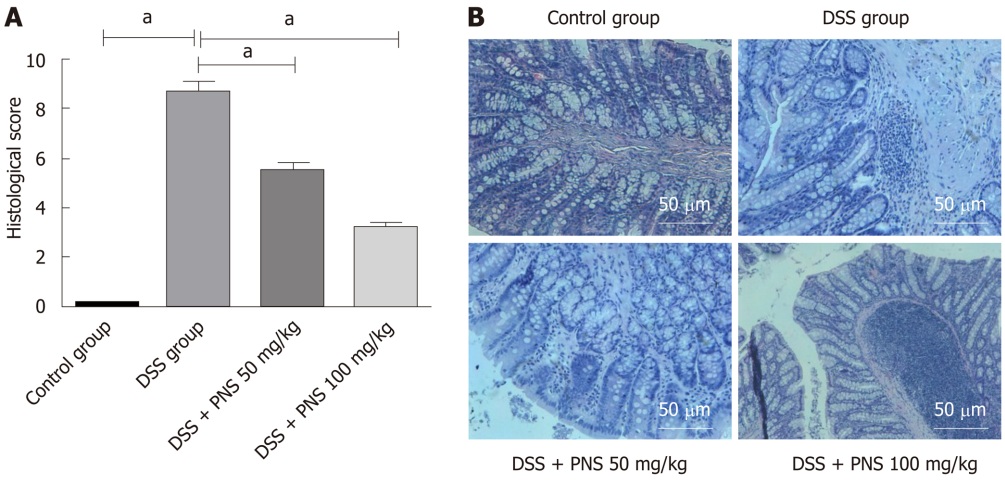

Figure 2 Panax notoginseng saponin improves histopathological scores of dextran sulfate sodium-induced rats. A: Histopathological scores; B: Hematoxylin & eosin staining. $^{a}P < 0.05$. PNS: Panax notoginseng saponin; DSS: Dextran sulfate sodium.

p-PI3K and p-AKT and showed a dose-dependency (all $P < 0.05$; Figure 6).

Effects of PNS on apoptosis of colon tissues in rats

TUNEL assay revealed that compared with the situation in the control group, DSS significantly increased the number of apoptotic TUNEL-positive cells; while compared with the use of DSS alone, PNS intervention decreased the number of apoptotic TUNEL-positive cells, and showed a dose-dependency ($P < 0.05$). Western blotting analysis consistently revealed that PNS treatment significantly up-regulated the expression of anti-apoptotic factor Bcl-2 and down-regulated the expression of pro-apoptotic factors Bax and caspase-3 (all $P < 0.05$; Figure 7).

Effects of inhibiting the PI3K/AKT signaling pathway on apoptosis of intestinal tissue cells in colitis rats

In order to further confirm that PNS has protective effects in rats against intestinal injury through PI3K/AKT signaling, we additionally selected 30 rats, and divided them into a control group, a DSS group, and a DSS+LY294002 group. We intraperitoneally injected 20 mg/kg PI3K/AKT signal pathway inhibitor, LY294002, into each rat in the DSS + LY294002 group. We found that, compared with the DSS group, the DSS + LY294002 group showed significantly decreased phosphorylation levels of PI3K and AKT in colon tissues, significantly reduced apoptosis of colon tissue cells, dramatically down-regulated expression of Bax and Caspase-3, and dramatically up-regulated expression of Bcl-3 (Figure 8).

Changes of macrophages in spleen and colon tissues

Compared with rats in the control group, rats in the DSS group showed significantly decreased percentages of $CD11b^{+}F4/80$-labeled macrophages and significantly increased percentages of M1 macrophages in the spleen (both $P < 0.05$). Compared with rats in the DSS group, rats in the DSS + PNS group showed significantly increased percentages of $CD11b^{+}F4/80$-labeled macrophages and significantly decreased percentages of M1 macrophages in the spleen, and they also showed a dose-dependency (all $P < 0.05$). There were no significant differences among the three groups in the percentage of M2 macrophages. Compared with rats in the control group, rats in the DSS group showed significantly increased percentages of $CD11b^{+}F4/80$-labeled macrophages and M1 macrophages, and significantly decreased percentages of M2 macrophages in colon tissues. Compared with rats in the DSS group, rats in the DSS + PNS group showed significantly decreased percentages of $CD11b^{+}F4/80$-labeled macrophages and M1 macrophages, and significantly increased percentages of M2 macrophages, and they also showed a dose-dependency (all $P < 0.05$; Figure 9).

DISCUSSION

Inflammatory bowel disease is a chronic inflammatory disease caused by dysfunction of the gastrointestinal mucosal immune system, which shows an increasing incidence

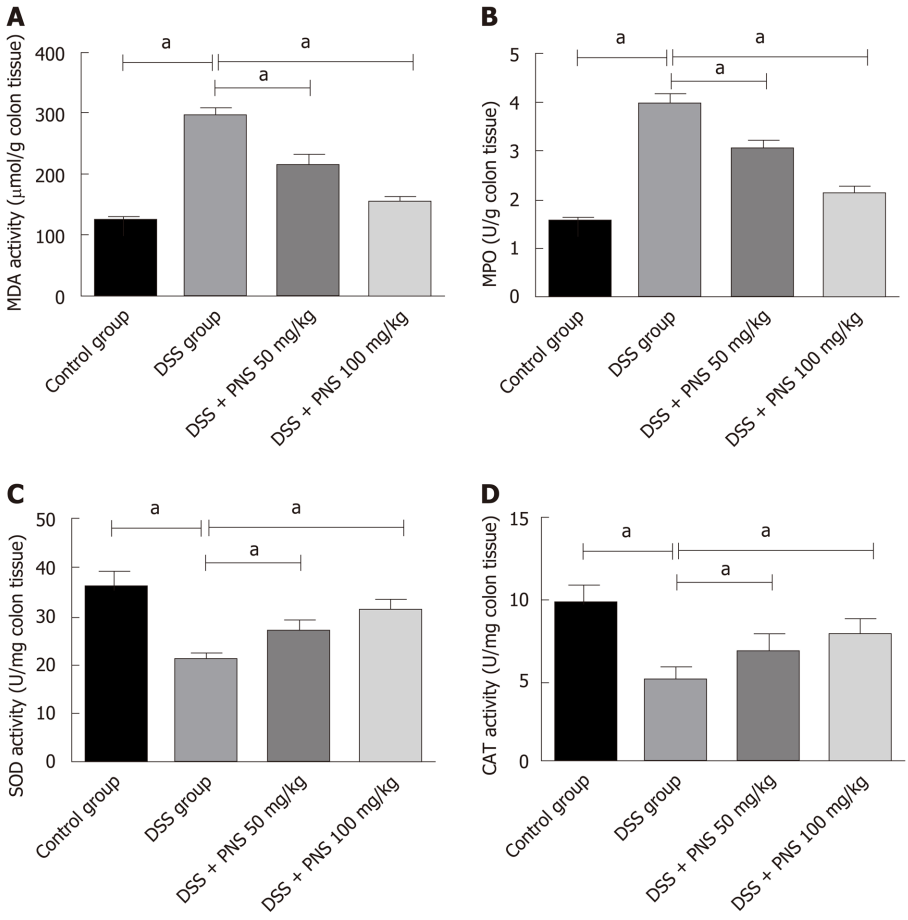

Figure 3 Panax notoginseng saponin alleviates intestinal oxidative damage in rats. A: Comparison among the four groups in malondialdehyde; B: Comparison among the four groups in myeloperoxidase; C: Comparison among the four groups in superoxide dismutase; D: Comparison among the four groups in catalase. $^{a}P < 0.05$. PNS: Panax notoginseng saponin; DSS: Dextran sulfate sodium; MDA: Malondialdehyde; MPO: Myeloperoxidase; CAT: Catalase; SOD: Superoxide dismutase.

with a change in living habits[14]. DSS, a water-soluble sulfated polysaccharide, can destroy the integrity of the intestinal mucosal barrier and lead to enteritis. This is mainly characterized by ulcers, diarrhea, or inflammatory cell infiltration, so it is an ideal choice to induce enteritis in an animal model[15].

In our study, PNS has been proven for the first time to alleviate DSS-induced colitis injury in rats. PNS, an active ingredient in panax notoginseng, is typically been used in the past to treat cardiovascular diseases or diabetes, and it has been proven to alleviate organ inflammatory damage induced by oxidative stress[16]. However, there are few studies and discussions on its role in enteritis. In this study, we found that PNS could alleviate intestinal inflammatory injury in DSS-induced colitis rats. For example, colitis rats undergoing PNS intervention showed significantly increased colon lengths, significantly improved disease activity indices and alleviated pathological damage, which all indicated that PNS could relieve intestinal injury in DSS-induced colitis rats. Enteritis is caused by a very complicated pathological process. A study pointed out that the large number of inflammatory mediators due to enteritis was an important reason for further aggravation of enteritis[17]. To verify this, we determined the inflammatory factors in intestinal tissues of DSS-induced enteritis rats, revealing that rats in the DSS group showed significantly increased expression of IL-6, IL-1β and TNF-α, significantly decreased expression of IL-10, significantly increased MDA and MPO activities, and significantly decreased CAT and SOD activities. This suggested that inflammatory and oxidative stress reactions in rats in the DSS group intensified, which was consistent with previous research results[18]. However, after PNS intervention, the rats showed significantly decreased expression of IL-6, IL-1β, TNF-α, and MDA and MPO activities, and significantly increased expression of IL-10 and CAT and SOD activities, and they also showed a dose-dependency. This suggested that PNS could alleviate intestinal inflammatory and oxidative stress reactions in enteritis rats. IL-6, IL-1β and TNF-α are all typical pro-

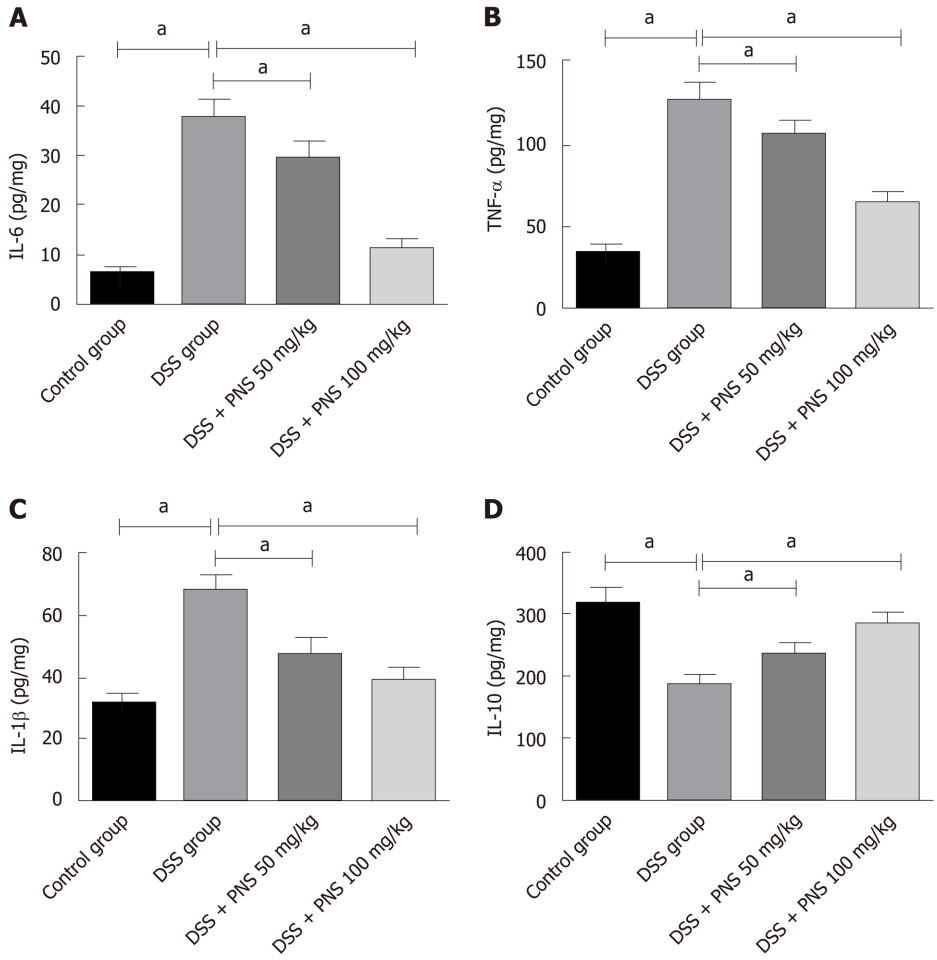

Figure 4 Panax notoginseng saponin alleviates intestinal inflammatory response in rats. A: Comparison among the four groups in interleukin-6 (IL-6); B: Comparison among the four groups in tumor necrosis factor-α; C: Comparison among the four groups in IL-1β; D: Comparison among the four groups in IL-10. $^{a}P < 0.05$. PNS: Panax notoginseng saponin; DSS: Dextran sulfate sodium; IL: Interleukin; TNF-α: Tumor necrosis factor-α.

inflammatory factors, and their up-regulated expression indicates the aggravation of the body's inflammatory reaction. IL-10 is an anti-inflammatory factor, with down-regulated expression indicating that body inflammation cannot be effectively suppressed[19,20]. MPO activity is closely related to inflammation, because MPO contains abundant neutrophils[21].

A previous study showed that the large number of inflammatory mediators, due to the polarization of macrophages to M1 macrophages caused by external stimulation, is one of the reasons for the acute inflammatory response of enteritis[22]. Macrophages can polarize into M1 macrophages or M2 macrophages. M1 macrophages can secrete inflammatory factors including IL-6 and TNF-α, and M2 macrophages can secrete anti-inflammatory factors including IL-10[23]. In our study, we detected macrophages and their polarization in the spleen and intestinal tissues of DSS-induced colitis rats. We found that the rats showed significantly decreased percentages of $CD11b^{+}F4/80$-labeled macrophages in the spleen, but significantly increased percentages of these macrophages in colon tissues, which may be due to the rapid migration of macrophages in the spleen to the intestinal inflammatory site during inflammatory reactions. In addition, we also found that the percentages of M1 macrophages in the spleen and colon significantly increased, and the percentages of M2 macrophages in the colon significantly decreased, but the spleen showed no difference. Furthermore, after PNS intervention, the colitis rats showed significantly increased percentages of $CD11b^{+}F4/80$-labeled macrophages in the spleen, significantly decreased percentages of $CD11b^{+}F4/80$-labeled macrophages and M1 macrophages in colon tissues, and significantly increased percentages of M2 macrophages in the intestine, and they also showed dose-dependency. It suggested that PNS could suppress the polarization of macrophages into M1 macrophages and induce the polarization of macrophages into M2 macrophages, thus suppressing the intestinal inflammatory response. This is also consistent with previous results for inflammatory factors. In order to explore the mechanism of PNS in relieving intestinal inflammatory injury, we determined

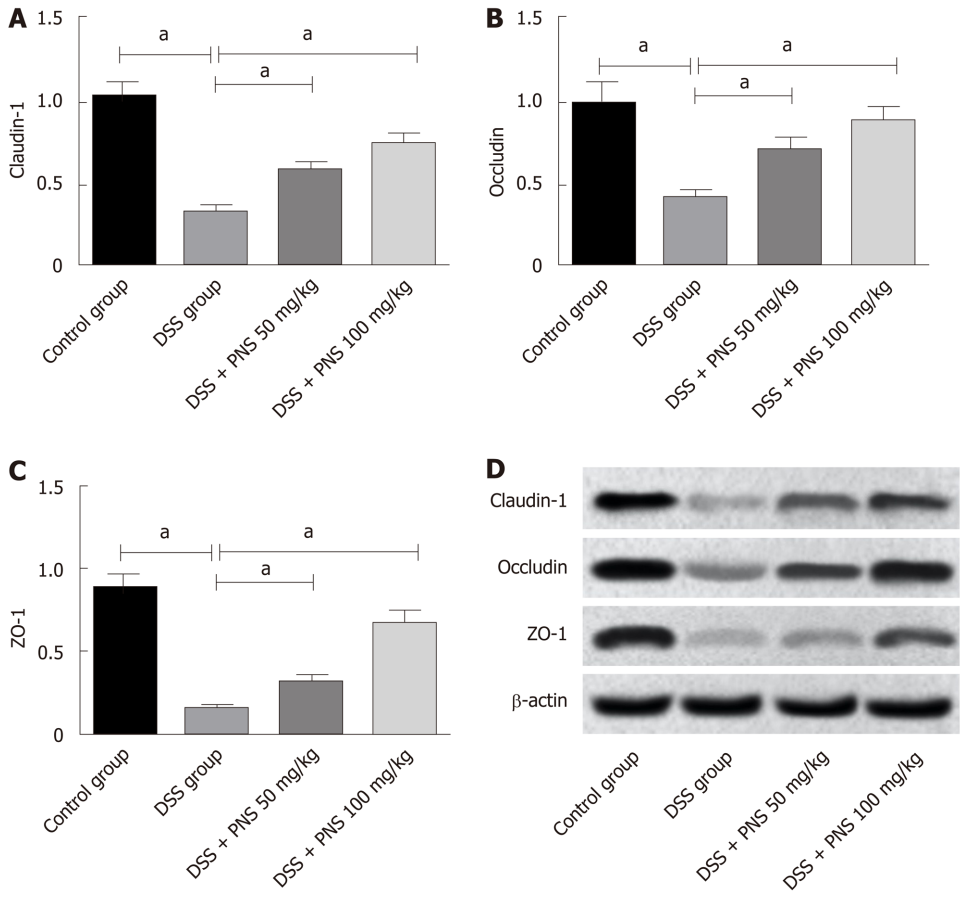

Figure 5 Effects of panax notoginseng saponin on tight junction proteins in the intestinal mechanical barrier of rats. A: Comparison of claudin-1 among the four groups; B: Comparison of occluding among the four groups; C: Comparison in ZO-1 among the four groups; D: Western blot protein map. $^{a}P < 0.05$. PNS: Panax notoginseng saponin; DSS: Dextran sulfate sodium.

PI3K/AKT signaling, revealing that after PNS intervention, colitis rats have significantly decreased phosphorylation levels of PI3K and AKT in intestinal tissues and showed a dose-dependency. This indicated that PNS could inhibit the activation of PI3K and AKT in colitis rats. In order to further confirm that PNS protects colitis rats against intestinal injury through PI3K/AKT signaling, we also intervened with the PI3K/AKT signaling pathway through its inhibitor, LY294002. It turned out that when PI3K/AKT signaling in the colon of colitis rats was inhibited, the apoptosis rate of colon cells significantly decreased, which proved that PNS protected colitis rats against intestinal injury through the PI3K/AKT signaling pathway. PI3K/AKT has long been considered as the primary way of promoting cell proliferation and preventing cell apoptosis, because AKT phosphorylation can initiate the expression of proteins involved in cell proliferation and apoptosis regulation[24,25]. The results of our study suggest that the protective effects of PNS against intestinal inflammatory injury in rats may be achieved by inhibiting the activation of the TLR4/NFκB signaling pathway. Previous studies found that PNS contributes to hepatocyte proliferation after liver regeneration by regulating the PI3K/AKT signaling pathway, which is similar to our results[26].

Tight junction proteins play a very important role in enteritis. When the tight junction is damaged, intestinal barrier function declines, which further causes migration of intestinal antigen substances to the lamina propria of the intestinal mucosa. This stimulates immune cells to produce a large number of inflammatory factors and further aggravates intestinal injury[27,28]. Based on detection, we found that the intestinal tissues of DSS-induced colitis rats showed significantly decreased expression of claudin-1, occludin, and ZO-1, but showed significantly increased expression of them after PNS intervention, which indicated that PNS could also alleviate intestinal mucosal barrier damage in colitis rats. Based on TUNEL experiments, we also found that DSS-induced colitis rats showed increased apoptotic intestinal epithelial cells, significantly increased expression of Bax and Caspase-3, and significantly decreased expression of Bcl-2, which was consistent with the TUNEL results. In addition, compared with rats in the DSS group, colitis rats undergoing PNS

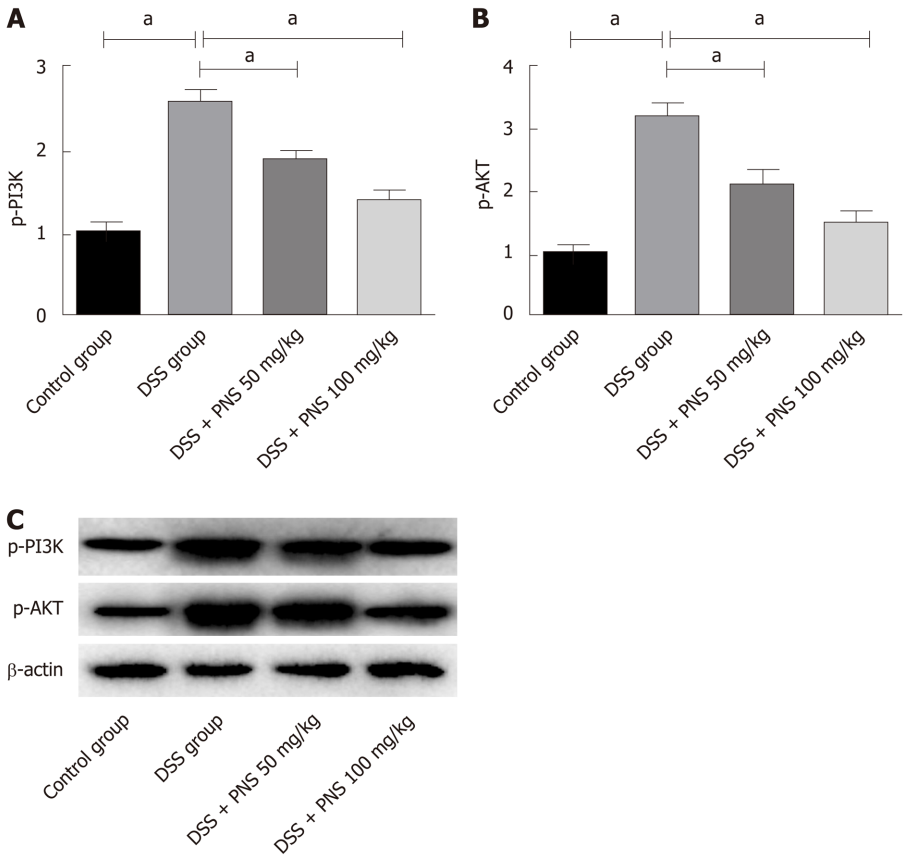

Figure 6 Effects of panax notoginseng saponin on phosphoinositide-3-kinase protein kinase B signaling pathway. A: Comparison of p-PI3 among the four groups; B: Comparison of p-AKT among the four groups; C: Western blot protein map. $^{a}P < 0.05$. PNS: Panax notoginseng saponin; DSS: Dextran sulfate sodium.

intervention showed significantly decreased apoptotic intestinal epithelial cells, significantly down-regulated expressions of Bax and Caspase-3, and significantly up-regulated expression of Bcl-2, which suggested that PNS could also inhibit the apoptosis of intestinal epithelial cells in colitis rats, thus playing a role in intestinal protection.

However, there are still some deficiencies in this study. For example, we did not carry out other *in vitro* cell experiments to explore the effects of PNS on intestinal epithelial cells, and we also did not explore other possible regulatory pathways through which PNS plays a role in colitis. In the future, we will carry out subsequent basic experiments to address these problems. Secondly, there are some differences in the pathogenesis of the DSS-induced rat enteritis model and human enteritis, which requires subsequent human experiments to prove the role of PNS in human enteritis. In summary, PNS can suppress the activation of the PI3K/AKT signaling pathway to protect DSS-induced rats against intestinal inflammatory injury, and thus it may be effective as a potential future drug for colitis.

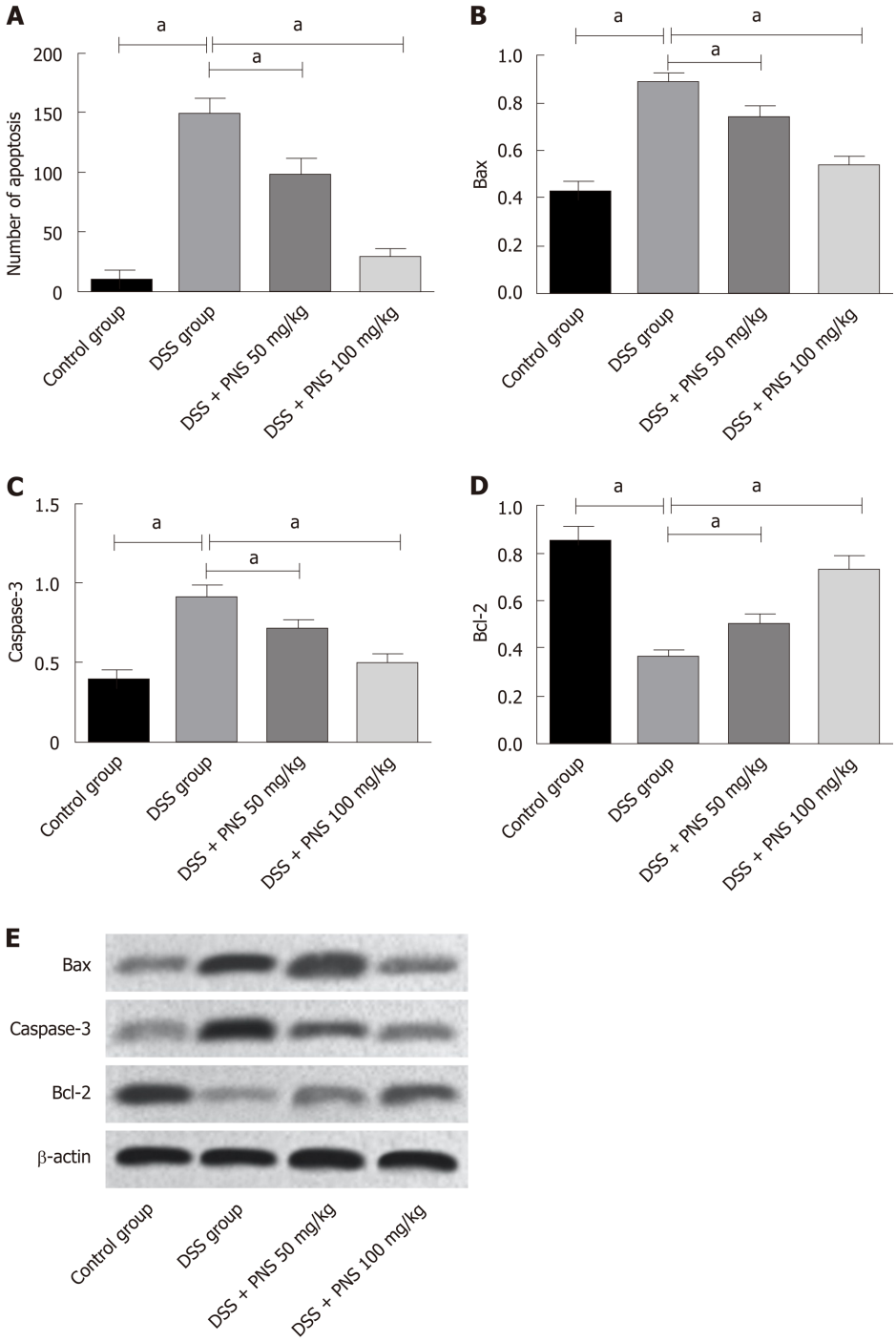

Figure 7 Effects of panax notoginseng saponin on apoptosis in the colon tissues of rats. A: The number of apoptotic TUNEL-positive cells in rats from the four groups; B: Comparison among the four groups in Bax; C: Comparison among the four groups in Caspase-3; D: Comparison among the four groups in Bcl-2; E: Western blot protein map. $^{a}P < 0.05$. PNS: Panax notoginseng saponin; DSS: Dextran sulfate sodium.

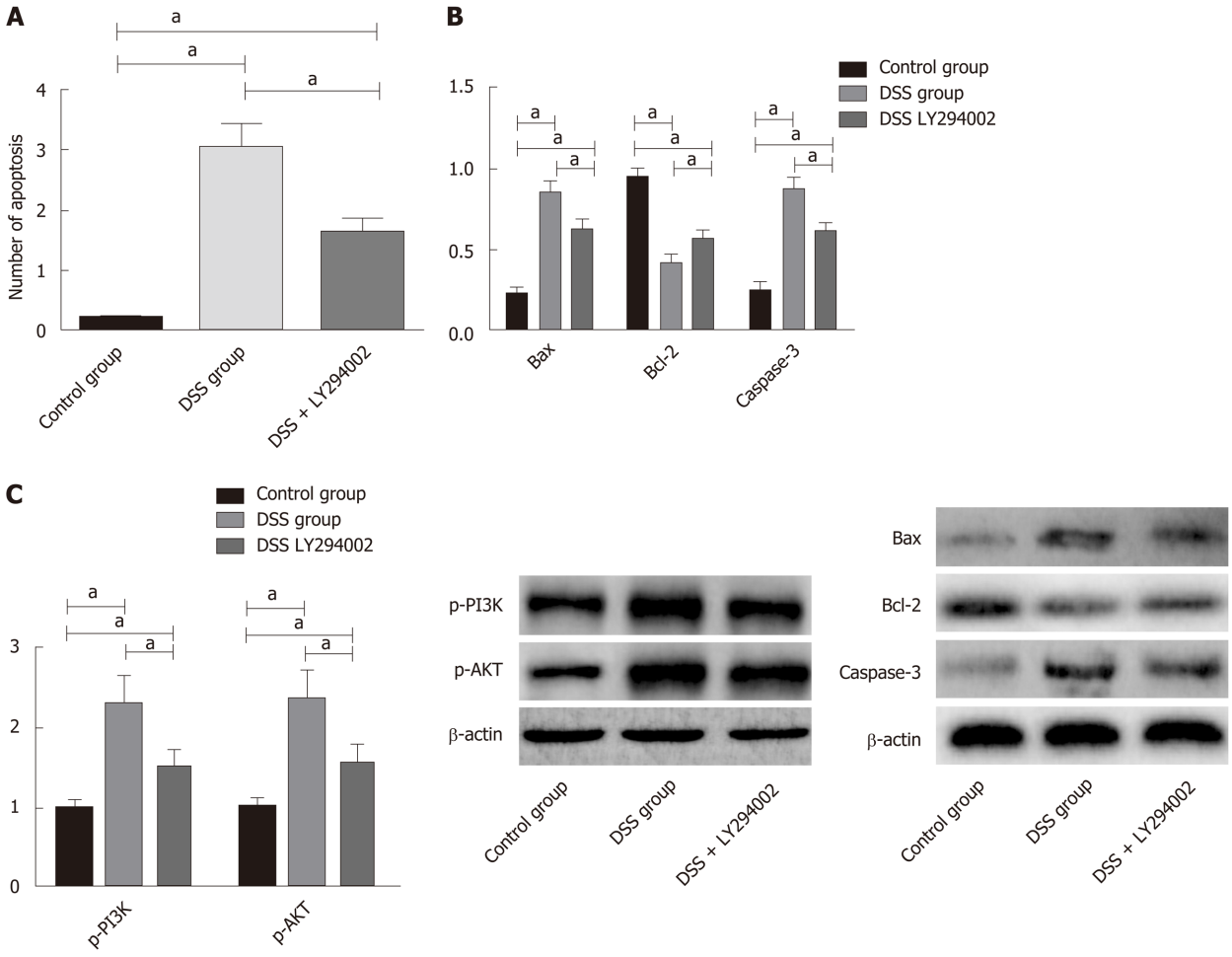

Figure 8 Effects of inhibiting the phosphoinositide-3-kinase protein kinase B signaling pathway on apoptosis of colon tissue cells in colitis rats. A: Effects of inhibiting the phosphoinositide-3-kinase protein kinase B (PI3K/AKT) signaling pathway on apoptosis rates of colon tissue cells; B: Effects of inhibiting the PI3K/AKT signaling pathway on the phosphorylation of PI3K and AKT in the colon tissues of rats; C: Effects of inhibiting the PI3K/AKT signaling pathway on apoptosis-related proteins in colon tissues. $^{a}P < 0.05$. PNS: Panax notoginseng saponin; DSS: Dextran sulfate sodium.

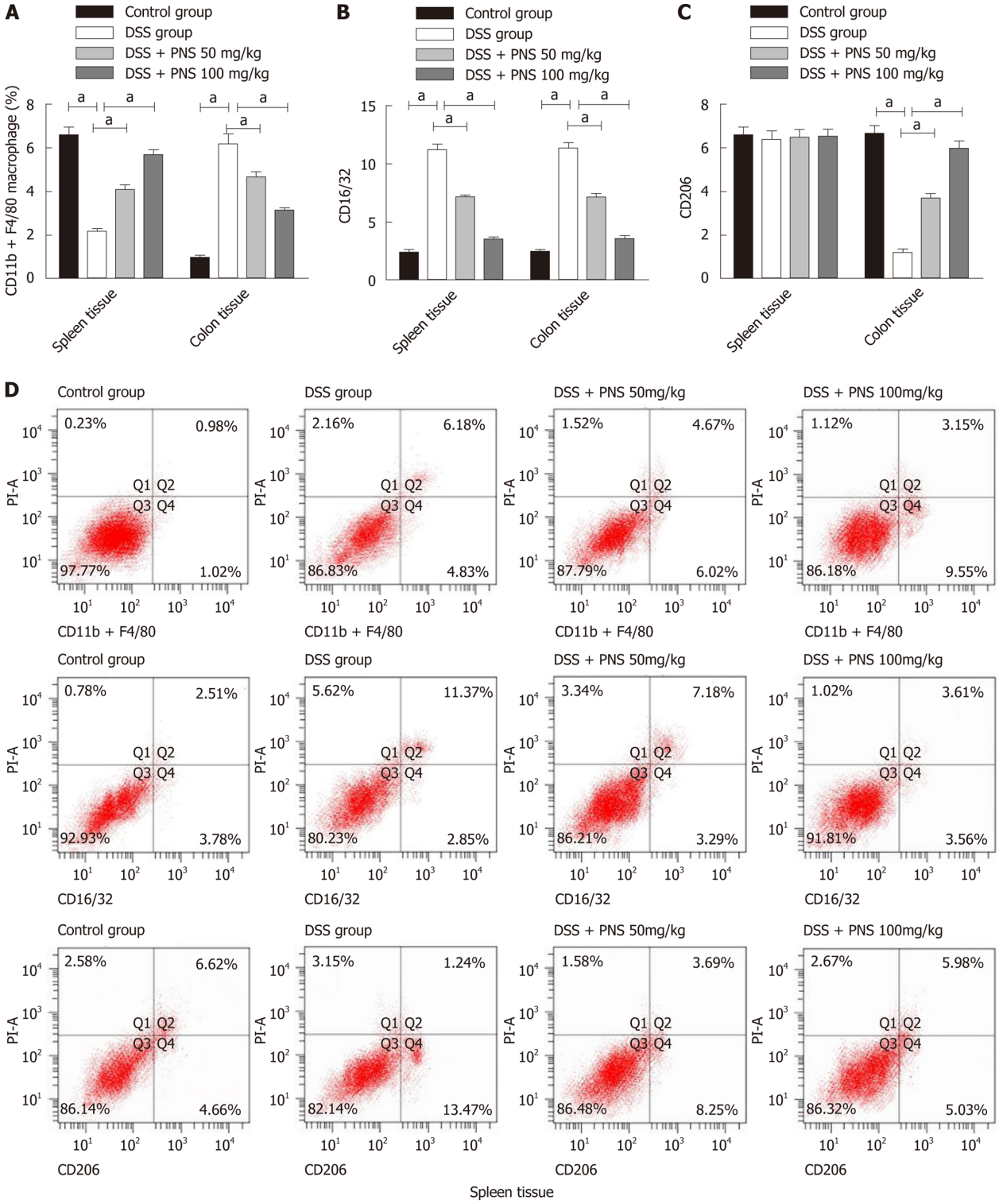
A
Control group
DSS group
DSS + PNS 50 mg/kg
DSS + PNS 100 mg/kg
CD11b + F4/80 macrophage (%)
Spleen tissue
Colon tissue
B
CD16/32
C
CD206
D
Control group
DSS group
DSS + PNS 50mg/kg
DSS + PNS 100mg/kg
CD11b + F4/80
CD16/32
CD206
PI-A
Q1 Q2
Q3 Q4
0.23% 0.98% 97.77% 1.02%
2.16% 6.18% 86.83% 4.83%
1.52% 4.67% 87.79% 6.02%
1.12% 3.15% 86.18% 9.55%
0.78% 2.51% 92.93% 3.78%
5.62% 11.37% 80.23% 2.85%
3.34% 7.18% 86.21% 3.29%
1.02% 3.61% 91.81% 3.56%
2.58% 6.62% 86.14% 4.66%
3.15% 1.24% 82.14% 13.47%
1.58% 3.69% 86.48% 8.25%
2.67% 5.98% 86.32% 5.03%
Spleen tissue

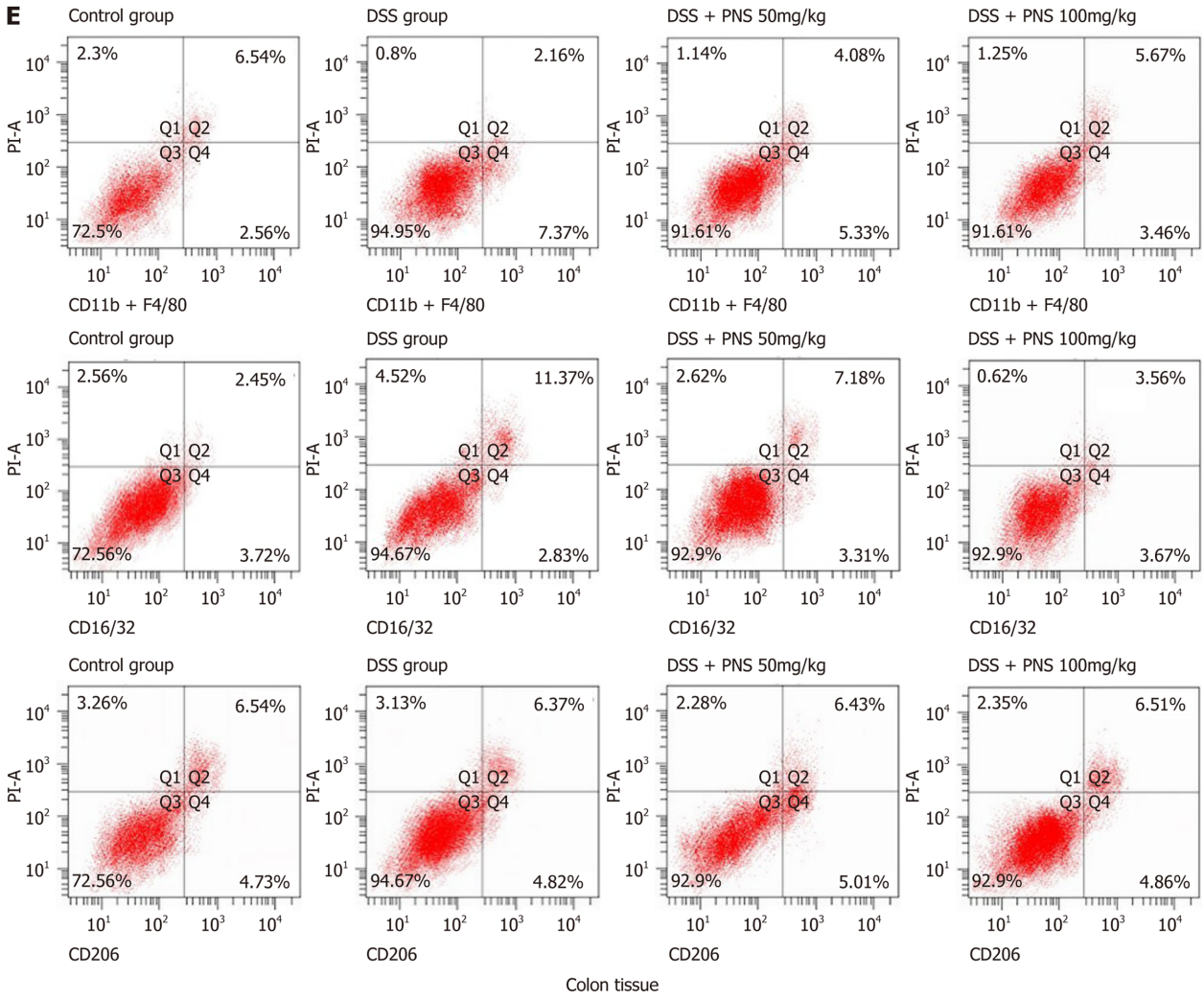

Figure 9 Macrophage changes in spleen and colon tissues. A: Percentage of CD11b$^+$F4/80-labeled macrophages in spleen and colon tissues; B: CD16/32-labeled MI macrophages in spleen and colon tissues; C: CD206-labeled M2 macrophages in spleen and colon tissues; D, E: Flow cytometry. $^aP < 0.05$. PNS: Panax notoginseng saponin; DSS: Dextran sulfate sodium.

ARTICLE HIGHLIGHTS

Research background

Intestinal inflammation is a common digestive tract disease at present, which is usually treated with hormone medications. Hormone medications are effective to some extent, but long-term use of them may bring about many complications. Therefore, it is very important to find new drugs to treat intestinal inflammation.

Research motivation

Panax notoginseng saponins (PNS) are a class of drugs widely used in cardiovascular diseases and diabetes, which have been proven to have good inflammatory inhibition effects. However, there are few studies on the role and mechanism of PNS in rat models of intestinal inflammation. PNS may be an effective drug for intestinal inflammation.

Research objectives

This study aimed to explore the effects of PNS on dextran sulfate sodium (DSS)-induced intestinal inflammatory injury in rats, and its possible mechanism.

Research methods

The colitis rat models were constructed by inducing DSS, and treating with different concentrations of PNS to inhibit the phosphoinositide-3-kinase protein kinase B (PI3K/AKT) signaling pathway in colon tissues. Then the intestinal injury, oxidative stress parameters, inflammatory indices, tight junction proteins, apoptosis, macrophage polarization, and PI3K/AKT signaling were detected in the tissues.

Research results

Compared with colitis rats, rats intervened with PNS showed significantly lengthened colons, decreased disease activity index, as well as significantly alleviated oxidative stress reactions and inflammatory responses. Furthermore, they showed significantly increased expression of tight junction-associated proteins, significantly decreased apoptotic cells, significantly decreased M1 macrophages in spleen and colon tissues, and significantly increased M2 macrophages in colon tissues. They also showed significantly suppressed activation of the PI3K /AKT signaling pathway, and dose-dependency. When the PI3K/AKT signaling pathway was inhibited, compared with colitis rats, the apoptosis rate of colon tissue treated with LY294002 decreased significantly.

Research conclusion

This study confirmed that PNS can protect rats against DSS-induced intestinal inflammatory injury by inhibiting the PI3K/AKT signaling pathway, and revealed that it may have potential to be used in the future as a drug for colitis.

Research perspective

It has been proven that PNS can play a protective role against intestinal injury in colitis rats by inhibiting the PI3K/AKT signaling pathway, and PNS may be a potential effective drug for treating colitis.

REFERENCES

1 **Blevins LK**, Crawford RB, Bach A, Rizzo MD, Zhou J, Henriquez JE, Khan DMIO, Sermet S, Arnold LL, Pennington KL, Souza NP, Cohen SM, Kaminski NE. Evaluation of immunologic and intestinal effects in rats administered an E 171-containing diet, a food grade titanium dioxide (TiO_2). *Food Chem Toxicol* 2019; **133**: 110793 [PMID: 31473338 DOI: 10.1016/j.fct.2019.110793]

2 **Wang S**, Martins R, Sullivan MC, Friedman ES, Misic AM, El-Fahmawi A, De Martinis ECP, O'Brien K, Chen Y, Bradley C, Zhang G, Berry ASF, Hunter CA, Baldassano RN, Rondeau MP, Beiting DP. Diet-induced remission in chronic enteropathy is associated with altered microbial community structure and synthesis of secondary bile acids. *Microbiome* 2019; **7**: 126 [PMID: 31472697 DOI: 10.1186/s40168-019-0740-4]

3 **Ito H**, Sadatomo A, Inoue Y, Yamada N, Aizawa E, Hishida E, Kamata R, Karasawa T, Kimura H, Watanabe S, Komada T, Horie H, Kitayama J, Sata N, Takahashi M. Role of TLR5 in inflammation and tissue damage after intestinal ischemia-reperfusion injury. *Biochem Biophys Res Commun* 2019; **519**: 15-22 [PMID: 31472954 DOI: 10.1016/j.bbrc.2019.08.083]

4 **Noval Rivas M**, Wakita D, Franklin MK, Carvalho TT, Abolhesn A, Gomez AC, Fishbein MC, Chen S, Lehman TJ, Sato K, Shibuya A, Fasano A, Kiyono H, Abe M, Tatsumoto N, Yamashita M, Crother TR, Shimada K, Arditi M. Intestinal Permeability and IgA Provoke Immune Vasculitis Linked to Cardiovascular Inflammation. *Immunity* 2019; **51**: 508-521.e6 [PMID: 31471109 DOI: 10.1016/j.immuni.2019.05.021]

5 **Silva MC**, Sales-Campos H, Oliveira CJF, Silva TL, França FBF, Oliveira F, Mineo TWP, Mineo JR. Treatment with a Zinc Metalloprotease Purified from *Bothrops moojeni* Snake Venom (BmooMP-Alpha-I) Reduces the Inflammation in an Experimental Model of Dextran Sulfate Sodium-Induced Colitis. *Mediators Inflamm* 2019; **2019**: 5195134 [PMID: 31467484 DOI: 10.1155/2019/5195134]

6 **Yao B**, He J, Yin X, Shi Y, Wan J, Tian Z. The protective effect of lithocholic acid on the intestinal epithelial barrier is mediated by the vitamin D receptor via a SIRT1/Nrf2 and NF-κB dependent mechanism in Caco-2 cells. *Toxicol Lett* 2019; **316**: 109-118 [PMID: 31472180 DOI: 10.1016/j.toxlet.2019.08.024]

7 **Yang X**, Xiong X, Wang H, Wang J. Protective effects of panax notoginseng saponins on cardiovascular diseases: a comprehensive overview of experimental studies. *Evid Based Complement Alternat Med* 2014; **2014**: 204840 [PMID: 25152758 DOI: 10.1155/2014/204840]

8 **Xu D**, Huang P, Yu Z, Xing DH, Ouyang S, Xing G. Efficacy and Safety of Panax notoginseng Saponin Therapy for Acute Intracerebral Hemorrhage, Meta-Analysis, and Mini Review of Potential Mechanisms of Action. *Front Neurol* 2014; **5**: 274 [PMID: 25620952 DOI: 10.3389/fneur.2014.00274]

9 **Hu S**, Liu T, Wu Y, Yang W, Hu S, Sun Z, Li P, Du S. Panax notoginseng saponins suppress lipopolysaccharide-induced barrier disruption and monocyte adhesion on bEnd.3 cells via the opposite modulation of Nrf2 antioxidant and NF-κB inflammatory pathways. *Phytother Res* 2019; **33**: 3163-3176 [PMID: 31468630 DOI: 10.1002/ptr.6488]

10 **Schiapaccassa A**, Maranhão PA, de Souza MDGC, Panazzolo DG, Nogueira Neto JF, Bouskela E, Kraemer-Aguiar LG. 30-days effects of vildagliptin on vascular function, plasma viscosity, inflammation, oxidative stress, and intestinal peptides on drug-naïve women with diabetes and obesity: a randomized head-to-head metformin-controlled study. *Diabetol Metab Syndr* 2019; **11**: 70 [PMID: 31462933 DOI: 10.1186/s13098-019-0466-2]

11 **Li C**, Li Q, Liu YY, Wang MX, Pan CS, Yan L, Chen YY, Fan JY, Han JY. Protective effects of Notoginsenoside R1 on intestinal ischemia-reperfusion injury in rats. *Am J Physiol Gastrointest Liver Physiol* 2014; **306**: G111-G122 [PMID: 24232000 DOI: 10.1152/ajpgi.00123.2013]

12 **Zhai Z**, Zhang F, Cao R, Ni X, Xin Z, Deng J, Wu G, Ren W, Yin Y, Deng B. Cecropin A Alleviates Inflammation Through Modulating the Gut Microbiota of C57BL/6 Mice With DSS-Induced IBD. *Front Microbiol* 2019; **10**: 1595 [PMID: 31354682 DOI: 10.3389/fmicb.2019.01595]

13 **Li HM**, Wang YY, Wang HD, Cao WJ, Yu XH, Lu DX, Qi RB, Hu CF, Yan YX. Berberine protects against lipopolysaccharide-induced intestinal injury in mice via alpha 2 adrenoceptor-independent mechanisms. *Acta Pharmacol Sin* 2011; **32**: 1364-1372 [PMID: 21963898 DOI: 10.1038/aps.2011.102]

14 **Choi YI**, Kim TJ, Park DK, Chung JW, Kim KO, Kwon KA, Kim YJ. Comparison of outcomes of continuation/discontinuation of 5-aminosalicylic acid after initiation of anti-tumor necrosis factor-alpha therapy in patients with inflammatory bowel disease. *Int J Colorectal Dis* 2019; **34**: 1713-1721 [PMID: 31471699 DOI: 10.1007/s00384-019-03368-1]

15 **Wang J**, Tian M, Li W, Hao F. Preventative delivery of IL-35 by Lactococcus lactis ameliorates DSS-

induced colitis in mice. *Appl Microbiol Biotechnol* 2019; **103**: 7931-7941 [PMID: 31456001 DOI: 10.1007/s00253-019-10094-9]

16 **Dong Y**, Duan L, Chen HW, Liu YM, Zhang Y, Wang J. Network Pharmacology-Based Prediction and Verification of the Targets and Mechanism for Panax Notoginseng Saponins against Coronary Heart Disease. *Evid Based Complement Alternat Med* 2019; **2019**: 6503752 [PMID: 31354855 DOI: 10.1155/2019/6503752]

17 **Pham TT**, Ban J, Lee K, Hong Y, Lee J, Truong AD, Lillehoj HS, Hong YH. MicroRNA gga-miR-10a-mediated transcriptional regulation of the immune genes in necrotic enteritis afflicted chickens. *Dev Comp Immunol* 2020; **102**: 103472 [PMID: 31437523 DOI: 10.1016/j.dci.2019.103472]

18 **Wang R**, Wu G, Du L, Shao J, Liu F, Yang Z, Liu D, Wei Y. Semi-bionic extraction of compound turmeric protects against dextran sulfate sodium-induced acute enteritis in rats. *J Ethnopharmacol* 2016; **190**: 288-300 [PMID: 27286916 DOI: 10.1016/j.jep.2016.05.054]

19 **Roomruangwong C**, Noto C, Kanchanatawan B, Anderson G, Kubera M, Carvalho AF, Maes M. The Role of Aberrations in the Immune-Inflammatory Response System (IRS) and the Compensatory Immune-Regulatory Reflex System (CIRS) in Different Phenotypes of Schizophrenia: the IRS-CIRS Theory of Schizophrenia. *Mol Neurobiol* 2019 [PMID: 31473906 DOI: 10.1007/s12035-019-01737-z]

20 **Zhang T**, Hu C, Wu Y, Wang S, Liu X, Zhang D, Huang F, Gao H, Wang Z. Carbon Disulfide Induces Embryo Implantation Disorder by Disturbing the Polarization of Macrophages in Mice Uteri. *Chem Res Toxicol* 2019; **32**: 1989-1996 [PMID: 31468960 DOI: 10.1021/acs.chemrestox.9b00119]

21 **Pêgo B**, Martinusso CA, Bernardazzi C, Ribeiro BE, de Araujo Cunha AF, de Souza Mesquita J, Nanini HF, Machado MP, Castelo-Branco MTL, Cavalcanti MG, de Souza HSP. *Schistosoma mansoni* Coinfection Attenuates Murine *Toxoplasma gondii*-Induced Crohn's-Like Ileitis by Preserving the Epithelial Barrier and Downregulating the Inflammatory Response. *Front Immunol* 2019; **10**: 442 [PMID: 30936867 DOI: 10.3389/fimmu.2019.00442]

22 **Kang J**, Zhang Z, Wang J, Wang G, Yan Y, Qian H, Zhang X, Xu W, Mao F. hucMSCs Attenuate IBD through Releasing miR148b-5p to Inhibit the Expression of 15-lox-1 in Macrophages. *Mediators Inflamm* 2019; **2019**: 6953963 [PMID: 31275059 DOI: 10.1155/2019/6953963]

23 **Shahbazi MA**, Sedighi M, Bauleth-Ramos T, Kant K, Correia A, Poursina N, Sarmento B, Hirvonen J, Santos HA. Targeted Reinforcement of Macrophage Reprogramming Toward M2 Polarization by IL-4-Loaded Hyaluronic Acid Particles. *ACS Omega* 2018; **3**: 18444-18455 [PMID: 31458417 DOI: 10.1021/acsomega.8b03182]

24 **Ming M**, Feng L, Shea CR, Soltani K, Zhao B, Han W, Smart RC, Trempus CS, He YY. PTEN positively regulates UVB-induced DNA damage repair. *Cancer Res* 2011; **71**: 5287-5295 [PMID: 21771908 DOI: 10.1158/0008-5472.CAN-10-4614]

25 **Brunet A**, Datta SR, Greenberg ME. Transcription-dependent and -independent control of neuronal survival by the PI3K-Akt signaling pathway. *Curr Opin Neurobiol* 2001; **11**: 297-305 [PMID: 11399427 DOI: 10.1016/s0959-4388(00)00211-7]

26 **Zhong H**, Wu H, Bai H, Wang M, Wen J, Gong J, Miao M, Yuan F. Panax notoginseng saponins promote liver regeneration through activation of the PI3K/AKT/mTOR cell proliferation pathway and upregulation of the AKT/Bad cell survival pathway in mice. *BMC Complement Altern Med* 2019; **19**: 122 [PMID: 31182089 DOI: 10.1186/s12906-019-2536-2]

27 **Shimizu Y**, Suzuki T. Brazilian propolis extract reduces intestinal barrier defects and inflammation in a colitic mouse model. *Nutr Res* 2019; **69**: 30-41 [PMID: 31470289 DOI: 10.1016/j.nutres.2019.07.003]

28 **Lopetuso LR**, Jia R, Wang XM, Jia LG, Petito V, Goodman WA, Meddings JB, Cominelli F, Reuter BK, Pizarro TT. Epithelial-specific Toll-like Receptor (TLR)5 Activation Mediates Barrier Dysfunction in Experimental Ileitis. *Inflamm Bowel Dis* 2017; **23**: 392-403 [PMID: 28146004 DOI: 10.1097/MIB.0000000000001035]

World Journal of Gastroenterology

Submit a Manuscript: https://www.f6publishing.com

World J Gastroenterol 2020 March 21; 26(11): 1172-1184

DOI: 10.3748/wjg.v26.i11.1172

ISSN 1007-9327 (print) ISSN 2219-2840 (online)

ORIGINAL ARTICLE

Retrospective Cohort Study

Non-robotic minimally invasive gastrectomy as an independent risk factor for postoperative intra-abdominal infectious complications: A single-center, retrospective and propensity score-matched analysis

Susumu Shibasaki, Koichi Suda, Masaya Nakauchi, Kenichi Nakamura, Kenji Kikuchi, Kazuki Inaba, Ichiro Uyama

ORCID number: Susumu Shibasaki (0000-0003-2454-5083); Koichi Suda (0000-0002-0423-1565); Masaya Nakauchi (0000-0002-1338-8556); Kenichi Nakamura (0000-0002-9665-3940); Kenji Kikuchi (0000-0002-6091-9292); Kazuki Inaba (0000-0003-0666-4687); Ichiro Uyama (0000-0003-1044-2948).

Author contributions: Shibasaki S, Suda K, and Uyama I made substantial contributions to conception and design of the study; Shibasaki S, Nakauchi M, Nakamura K, Kikuchi K, and Inaba K contributed to acquisition, analysis, or interpretation of the data; Shibasaki S and Nakauchi M performed the statistical analysis; Shibasaki S, Suda K, and Uyama I drafted the article and made critical revisions related to important intellectual content of the manuscript; all the authors have read and approved the final version to be published.

Institutional review board statement: This study was approved by the institutional review board of Fujita Health University.

Informed consent statement: Informed consent was obtained from all patients.

Conflict-of-interest statement: All the authors except for I. U. have no commercial association with or financial involvement that might pose a conflict of interest in connection with the submitted

Susumu Shibasaki, Koichi Suda, Masaya Nakauchi, Kenichi Nakamura, Kazuki Inaba, Ichiro Uyama, Department of Surgery, Fujita Health University, Toyoake 470-1192, Aichi, Japan

Koichi Suda, Kenji Kikuchi, Collaborative Laboratory for Research and Development in Advanced Surgical Technology, Fujita Health University School of Medicine, Toyoake 470-1192, Aichi, Japan

Corresponding author: Koichi Suda, FACS, MD, PhD, Professor, Department of Surgery, Fujita Health University, 1-98 Dengakugakubo, Kutsukake, Toyoake 470-1192, Aichi, Japan. ko-suda@nifty.com

Abstract

BACKGROUND

Minimally invasive surgery for gastric cancer (GC) has gained widespread use as a safe curative procedure especially for early GC.

AIM

To determine risk factors for postoperative complications after minimally invasive gastrectomy for GC.

METHODS

Between January 2009 and June 2019, 1716 consecutive patients were referred to our division for primary GC. Among them, 1401 patients who were diagnosed with both clinical and pathological Stage III or lower GC and underwent robotic gastrectomy (RG) or laparoscopic gastrectomy (LG) were enrolled. Retrospective chart review and multivariate analysis were performed for identifying risk factors for postoperative morbidity.

RESULTS

Morbidity following minimally invasive gastrectomy was observed in 7.5% of the patients. Multivariate analyses demonstrated that non-robotic minimally invasive surgery, male gender, and an operative time of ≥ 360 min were significant independent risk factors for morbidity. Therefore, morbidity was compared between RG and LG. Accordingly, propensity-matched cohort analysis revealed that the RG group had significantly fewer intra-abdominal infectious complications than the LG group (2.5% *vs* 5.9%, respectively; $P = 0.038$), while no significant differences were noted for other local or systemic complications.

article. I. U. has received lecture fees from Intuitive Surgical, Inc.. K. S. and K. K. have been funded by Medicaroid, Inc. in relation to Collaborative Laboratory for Research and Development in Advanced Surgical Technology. K.S. has also received advisory fees from Medicaroid, Inc. outside of the submitted work.

STROBE statement: Authors have read the STROBE Statement checklist of items and the manuscript was prepared and revised accordingly.

Manuscript source: Invited manuscript

Received: November 15, 2019
Peer-review started: November 15, 2019
First decision: February 14, 2019
Revised: March 5, 2020
Accepted: March 9, 2020
Article in press: March 9, 2020
Published online: March 21, 2020

P-Reviewer: Fusaroli P, Li Y, Petrucciani N, Wang DR, Guerra F
S-Editor: Wang YQ
L-Editor: A
E-Editor: Ma YJ

Multivariate analyses of the propensity-matched cohort revealed that non-robotic minimally invasive surgery [odds ratio = 2.463 (1.070–5.682); $P = 0.034$] was a significant independent risk factor for intra-abdominal infectious complications.

CONCLUSION
The findings showed that robotic surgery might improve short-term outcomes following minimally invasive radical gastrectomy by reducing intra-abdominal infectious complications.

Key words: Stomach neoplasms; Gastrectomy; Robotic surgical procedure; Minimally invasive procedures; Morbidity; Pancreatic fistula

Core tip: This study aimed to determine risk factors for postoperative complications after minimally invasive gastrectomy for gastric cancer. Accordingly, multivariate analysis identified non-robotic minimally invasive surgery as an independent risk factor for postoperative complications. Propensity score matching analysis showed that the robotic gastrectomy group had a significantly lower incidence of intra-abdominal infectious complications compared to the laparoscopic gastrectomy group. Additionally, multivariate analyses in the propensity score-matched cohort showed that non-robotic minimally invasive surgery was a significant independent risk factor for intra-abdominal infectious complications.

Citation: Shibasaki S, Suda K, Nakauchi M, Nakamura K, Kikuchi K, Inaba K, Uyama I. Non-robotic minimally invasive gastrectomy as an independent risk factor for postoperative intra-abdominal infectious complications: A single-center, retrospective and propensity score-matched analysis. *World J Gastroenterol* 2020; 26(11): 1172-1184
URL: https://www.wjgnet.com/1007-9327/full/v26/i11/1172.htm
DOI: https://dx.doi.org/10.3748/wjg.v26.i11.1172

INTRODUCTION

Gastric cancer (GC) is the fifth most common malignancy and the third leading cause of cancer-related death worldwide[1]. Surgical resection with or without perioperative chemotherapy has remained the only curative treatment option, with regional lymphadenectomy being recommended as part of radical gastrectomy[2-4]. Recently, laparoscopic gastrectomy (LG) has gained widespread use as it is a minimally invasive and safe curative procedure for GC especially for early GC[5-7]. Since we demonstrated the comparability of the laparoscopic D2 gastrectomy over the open D2 gastrectomy in the short- and long-term outcomes[8,9], minimally invasive surgery (MIS) has been the first choice as the standard radical procedure for GC in our institute[10].

However, several recent studies using the nationwide web-based database of Japan have revealed that LG promoted higher postoperative local complications compared with open gastrectomy (OG)[11-13]. Two main reasons may explain such findings. First, LG requires more experience, at least 40–60 surgical procedures, to achieve optimal proficiency compared with OG[14-17]. Second, LG has several technical limitations, including limited range of motion with straight forceps and hand tremors, which need to be addressed to further improve surgical outcomes following minimally invasive gastrectomy. Accordingly, two possible measures may help overcome such limitations. First is the Endoscopic Surgical Skill Qualification System (ESSQS), which was launched in 2004 by the Japanese Society for Endoscopic Surgery to develop a tool for the reliable and reproducible evaluation of trainees' surgical techniques[18]. In this system, two judges assess non-edited videotapes in a double-blinded fashion using strict criteria. Accordingly, surgeons determined to be qualified by this system experienced less frequent complications following laparoscopic distal gastrectomy (DG) compared with those who failed[18]. The second measure involves robotic surgery, which facilitates precise dissection in a confined surgical field with impressive dexterity[19-21]. In fact, a number of previous studies have shown that robotic gastrectomy (RG) resulted in significantly lower postoperative complication

rates compared to LG[20,22,23].

Considering the aforementioned discussion, the present study aimed to determine risk factors for postoperative complications after MIS for GC, focusing on the impact of robotics and surgeon qualification by the ESSQS.

MATERIALS AND METHODS

Patients

Between January 2009 and June 2019, 1716 consecutive patients were referred to our division for primary GC eligible for surgical treatment. The present study ultimately enrolled 1401 patients (robotic, n = 359 and laparoscopic, n = 1042) with both clinical and pathological Stage III or lower GC after excluding 315 patients who had clinical or pathological stage IV GC (n = 166), remnant GC (n = 53), OG (n = 25), double cancer (n = 20), and palliative or limited lymphadenectomy (n = 51) due to insufficient physical function. The patient selection process is summarized in Figure 1. This study included not only symptomatic patients but also those who were diagnosed as a result of the mass cancer screening programs, which have been executed nationwide and have contributed to earlier detection of GC. In the present study, the stage of the cancer was described according to the 15th edition of the Japanese Classification of Gastric Carcinoma[24]. Cancer staging was performed based on the findings of contrast-enhanced computed tomography, gastrography, endoscopic study, and endosonography before the beginning of any treatment and, when applicable, after the completion of chemotherapy, as we previously described[20]. Tumor invasion depth was measured ultrasonographically[25,26]. The gastric wall was assessed based on the standard five-layer sonographic structure. On the endosonographic image, the mucosal layer is visualized as a combination of the first and second hypoechoic layers, and the submucosal layer corresponds to the third hyperechoic layer. The layer of the muscularis propria is visualized as the fourth hypoechoic layer, and the fifth hyperechoic layer is the serosa, including the subserosa. Initial endoscopic diagnosis regarding invasion depth was confirmed based on the agreement by expert endoscopists at the medical conference prior to therapy. The indication of endoscopic treatment and radical gastrectomy including the extent of systematic lymph node dissection was determined based on the 2014 Japanese Gastric Cancer Treatment Guidelines[3]. The microscopic tumor-negative status in the cut end was routinely confirmed by intraoperative frozen section diagnosis as previously reported[27,28], and margins of resection (R0 or R1 resection) was pathologically diagnosed by permanent section diagnosis. In a considerable number of the enrolled patients, Helicobacter pylori was examined and systemically eradicated before surgery at each hospital or clinic at which GC of those patients was diagnosed. Details regarding indications for physical function assessment, surgical procedures, perioperative radical gastrectomy management, extent of gastric resection and lymph node dissection, type of anastomosis, and postoperative chemotherapy in addition to oncologic follow-up have been reported previously[8-10,20,21,29,30]. This study was approved by the Institutional Review Board of Fujita Health University.

Decision on procedure selection

Patients were completely involved in the decision-making process, and informed consent was obtained from all patients. However, during the study period, decision making on patient procedures was dependent on circumstances surrounding the national medical insurance coverage. Accordingly, RG had not been included in the national medical insurance coverage in Japan between January 2009 and March 2018, during which patients needed to be charged 2200000 JPY upon perioperative admission to undergo RG[20]. All patients were equally offered robotic surgery without considering their backgrounds, including physical and oncological status. Hence, 211 patients who agreed to uninsured da Vinci Surgical System (DVSS) application underwent RG, whereas the remaining 946 patients who refused uninsured DVSS application underwent LG with health insurance coverage. Meanwhile, between October 2014 and January 2017, we organized a multi-institutional, single-arm prospective clinical study approved for Advanced Medical Technology ("Senshiniryo") B[23]. Accordingly, 94 patients with cStage I/II GC who were enrolled in our institution's Senshiniryo B trial were also included in the present analysis. Since its approval for national medical insurance coverage based on the outcomes of the Senshiniryo B trial in April 2018, RG has been more favorably indicated for patients diagnosed with advanced GC who required total gastrectomy (TG) or proximal gastrectomy (PG) and desired to undergo RG at our institution. After April 2018, 52 patients underwent RG, whereas 96 underwent LG.

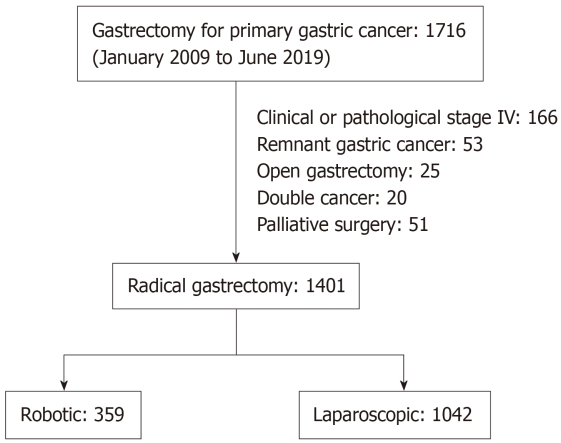

Figure 1 Flow diagram of the study selection process.

Operating surgeon selection

All LG procedures were performed or guided by the ESSQS-qualified surgeons. Meanwhile, RG was performed by surgeons certified to operate a DVSS console, qualified by the ESSQS, and certified by the Japanese Society of Gastroenterological Surgery. All procedures related to LG and RG were supervised by an expert gastric surgeon (I.U.) who had performed more than 1500 LG and 400 RG procedures.

Measurements

All patients were observed for 30 d following surgery. The primary endpoint of this single-center retrospective analysis was morbidity. Secondary endpoints comprised clinicopathological characteristics and short-term surgical outcomes, including operative time, surgeon console time, estimated blood loss, number of dissected lymph nodes, complication rates, rates for intra-abdominal infectious complications (including postoperative pancreatic fistulas, leakage, and intra-abdominal abscesses), mortality rate, and length of postoperative hospitalization. All postoperative complications Grade IIIa or above based on the Clavien–Dindo (CD) classification were recorded[31] and classified according to the Japan Clinical Oncology Group Postoperative Complications Criteria based on the CD classification ver. 2.0[32]. Total operative time was defined as the duration from the start of abdominal incision until complete wound closure, while surgeon console time was defined as the duration of DVSS operation during surgery. Blood loss was estimated by weighing suctioned blood and gauze pieces that had absorbed blood.

Perioperative management of postoperative pancreatic fistula

Diagnosis and grading of pancreatic fistula were determined according to CD classification[31] as mentioned above. Our perioperative management for postoperative pancreatic fistula was conducted as follows[20,33]: Although pancreatic fistula is defined as output *via* an operatively placed drain (or a subsequently placed percutaneous drain) of any measurable volume of drain fluid on or after postoperative day 3, with an amylase level at least over 3 times as high as the upper normal range of the serum level, it was comprehensively diagnosed according to not only drain amylase levels, but also changes in the properties of the drain and the clinical, laboratory, and imaging findings including computed tomographic scans. Patients with high drain amylase level and no abnormal physical and laboratory findings were observed without any treatment (CD Grade I). The abdominal drainage tube was removed basically after the drain amylase level was sufficiently recovered. Patients with high drain amylase level accompanied by abnormal findings such as fever, abdominal pain, and high inflammatory markers, were intensively treated with antibiotics, octreotide acetate, and parenteral nutrition while the drainage tube position was urgently confirmed using computed tomographic scans and radiographic contrast study (CD Grade II). When the drainage tube position was not appropriate, an additional or alternative drainage tube was placed into the fluid cavity using percutaneous computed tomography or ultrasonography-guided technique (CD Grade IIIa), and irrigation and drainage with saline was performed. Parenteral nutrition was gradually switched to enteral nutrition without delay, once pancreatic fistula had been confined to a certain space and inflammatory response had settled.

Propensity score-matched analysis

Propensity score-matched (PSM) analysis was used to limit confounders and overcome possible patient selection bias. Propensity scores for all patients were calculated using a logistic regression model based on the following variables: Age, gender, body mass index (BMI), American Society of Anesthesiologist (ASA) classification, presence of neoadjuvant chemotherapy, history of laparotomy, cT, cN, cStage, pT, pN, pStage, type of gastrectomy, extent of lymph node dissection, and splenectomy. Consequently, rigorous adjustment for significant differences in the baseline characteristics of PSM patients was performed using nearest neighbor matching without replacement and a caliper width of 0.2 logit of the standard deviation. An absolute standardized difference (SD) was used to measure covariate balance, in which an absolute standardized mean difference above 0.1 indicated a meaningful imbalance[11,12].

Statistical analysis

All analyses were conducted using IBM SPSS Statistics 23 (IBM Corporation, Armonk, NY, United States). Between-group comparisons were performed using the χ^2 test or Mann–Whitney *U* test. Univariate χ^2 test and multivariate logistic regression analysis were used to determine risk factors for the occurrence of postoperative complications. Data were expressed as median (range) or odds ratio (OR) (95% confidence interval) unless otherwise specified. $P < 0.05$ (two-tailed) was considered statistically significant.

RESULTS

Clinicopathological features and surgical outcomes after minimally invasive gastrectomy

Patient characteristics and surgical outcomes of MIS for GC are summarized in Table 1. Accordingly, 939 (67%) and 856 (61%) patients had cStage I and pStage I disease, respectively, while 120 (8.6%) received preoperative chemotherapy. A total of 359 and 1042 patients underwent RG and LG, while 993 (70.9%), 89 (6.4%), and 319 (22.8%) underwent DG, PG, and TG, respectively. Moreover, 767 and 634 patients underwent D1+ and D2 dissection, respectively. The rates for conversion to open procedure, reoperation within 30 d, in-hospital mortality within 30 d, and morbidity within 30 d after operation were 0.1%, 1.1%, 0.3% and 7.5%, respectively (Table 1). All patients completed successfully R0 resection.

Risk factors for morbidity after minimally invasive gastrectomy

Univariate analysis identified seven significant factors for postoperative CD grade IIIa or more complications, including non-robotic MIS, male gender, cStage II or higher, type of gastrectomy (PG and TG), splenectomy, operative time ≥ 360 min, and estimated blood loss ≥ 50 mL. Multivariate analysis determined that non-robotic MIS [OR = 2.591 (1.418–4.717); $P = 0.002$], male gender [OR = 1.969 (1.142–3.390); $P = 0.015$], and operative time ≥ 360 min [OR = 1.800 (1.098–2.952); $P = 0.020$] were significant independent risk factors for morbidity (Table 2).

Patient background factors stratified according to type of procedure

Our analysis subsequently focused on the comparison between RG and LG. Patient characteristics according to type of procedure are summarized in Table 3. Although no differences in BMI, history of laparotomy, tumor size, cT, cN, cStage, pT, pN, pStage, and number of metastatic lymph nodes were observed between the RG and LG group, significant differences were found in age [RG 67 (30–89) *vs* LG 70 (24–93); $P < 0.001$], gender (M:F, RG 233:126 *vs* LG 740:302; $P = 0.033$), ASA classification (1:2:3, RG 160:168:31 *vs* LG 340:565:137; $P < 0.001$), preoperative chemotherapy (RG 5.3% *vs* LG 9.7%; $P = 0.010$), type of resection (DG:PG:TG, RG 250:42:67 *vs* LG 743/47/252; $P < 0.001$), and extent of lymphadenectomy (D1+:D2, RG 178:181 *vs* LG 589:453; $P = 0.023$). Factors having an SD over 0.1 included age, gender, BMI, ASA classification, tumor size, use of preoperative chemotherapy, type of resection, extent of lymphadenectomy, and splenectomy (Table 3). To compensate for such differences, PSM analysis was used. The average and standard deviation of the propensity score was 0.256 and 0.111, respectively, thus yielding a caliper width of 0.02 for this study. After propensity score matching, 354 patients were included in each group (Figure 2). Propensity score distributions for each case before and after matching are presented in Figure 2. After matching, the SD for age, gender, BMI, ASA classification, presence of neoadjuvant chemotherapy, history of laparotomy, tumor size, cT, cN, cStage, pT, pN, pStage, type of resection, extent of lymph node dissection, and splenectomy decreased

Table 1 Patient backgrounds and surgical outcomes following minimally invasive gastrectomy at our institution, *n* = 1401

Clinicopathological characteristics		Surgical outcomes	
Age (yr)	69 (24–93)	No. of operators (certified surgeon)	33 (19)
Gender (M:F)	973:428	Qualified:non-qualified surgeons	925:476
Body mass index (kg/m^2)	22.3 (1 4.3–37.3)	Procedure (RG:LG)	359:1042
ASA grade (1:2:3)	500:733:168	Type of resection (DG:PG:TG)	993:89:319
History of laparotomy, *n* (%)	263 (18.8)	Extent of lymphadenectomy (D1+:D2)	767:634
Tumor size (mm)	30 (0–180)	Splenectomy, *n* (%)	40 (2.9)
cT[1] (1:2:3:4a)	751:264:224:162	Total operative time (min)	348 (147–942)
cN[1] (−:+)	1093:308	Estimated blood loss (mL)	30 (0–2150)
cStage[1] (I:IIA:IIB:III)	939:76:154:232	No. of dissected LNs	35 (6–114)
pT[1] (1:2:3:4a)	797:164:178:262	Conversion to open procedure, *n* (%)	1 (0.1)
pN[1] (0:1:2:3)	949:174:137:141	Reoperation rate, *n* (%)	15 (1.1)
pStage[1] (I:II:III)	856:280:265	In-hospital mortality, *n* (%)	4 (0.3)
No. of metastatic LNs	0 (0–63)	Morbidity, *n* (%)	105 (7.5)
Use of preoperative chemotherapy, *n* (%)	120 (8.6)	Hospital stay following surgery (d)	13 (2–195)

[1]Japanese Classification of Gastric Carcinoma, 15th edition. Data are presented as median with range unless otherwise specified. ASA: American Society of Anesthesiologist; LNs: Lymph nodes; RG: Robotic gastrectomy; LG: Laparoscopic gastrectomy; DG: Distal gastrectomy; PG: Proximal gastrectomy; TG: Total gastrectomy.

to < 0.10, indicating that a sufficient balance was achieved (Table 3).

Surgical and short-term outcomes stratified according to type of procedure

Surgical outcomes and short-term postoperative courses of the entire cohort and the PSM cohort are summarized in Table 4. Accordingly, 8 and 33 operating surgeons performed RG and LG, respectively. Moreover, 100% of the RG cases and only 56.5% (572/1042) of the LG cases ($P < 0.001$) were handled by qualified surgeons. The RG group had a significantly shorter duration of hospitalization following surgery compared to the LG group [RG 12 (2–195) d *vs* LG 13 (3–177) d; $P < 0.001$], despite having a slightly greater total operative time [RG 360 (174–942) min *vs* LG 342 (147–937) min; $P < 0.001$) and estimated blood loss [RG 36 (0–935) mL *vs* LG 29 (0–2150) mL; $P < 0.001$]. No significant differences were observed in the number of dissected lymph nodes, conversion to open procedure, and reoperation rate. In-hospital mortality was sufficiently low (RG 0.6% *vs* LG 0.3%; $P = 0.578$) throughout this series. After propensity score matching, results similar to those for the entire cohort were obtained (Table 4).

Postoperative complications

Postoperative complications are summarized in Table 5. Briefly, the RG group had a significantly better morbidity rate than the LG group (RG 3.6% *vs* LG 8.8%; $P = 0.002$). Robotic surgery promoted better attenuation of intra-abdominal infectious complications compared to non-robotic surgery (RG 2.5% *vs* LG 6.3%; $P = 0.005$), while no significant differences in other local (RG 0.8% *vs* LG 1.3%; $P = 0.632$) or systemic (RG 0.3% *vs* LG 1.6%; $P = 0.091$) complication rates were observed. After PSM analysis, results remained almost same (Table 5), with the RG group showing a significantly better morbidity rate than the LG group (RG 3.7% *vs* LG 7.6%; $P = 0.033$). Robotic surgery promoted better attenuation of intra-abdominal infectious complications compared to non-robotic surgery (RG 2.5% *vs* LG 5.9%; $P = 0.038$), while no significant differences in other local (RG 0.6% *vs* LG 1.1%; $P = 0.682$) or systemic (RG 0.3% *vs* LG 1.1%; $P = 0.369$) complication rates were observed.

Risk factors for intra-abdominal infectious complications among the propensity score-matched cohort

Univariate analysis identified several significant risk factors for intra-abdominal infectious complications, including non-robotic MIS, male gender, PG or TG, operative time ≥ 360 min, estimated blood loss ≥ 50 mL, and non-qualified surgeons (Table 6). Multivariate analysis clearly demonstrated that non-robotic MIS [OR 2.463 (1.070–5.682); $P = 0.034$], male gender [OR 3.937 (1.157–13.333); $P = 0.028$], and operative time ≥ 360 min [OR 2.779 (1.003–7.701); $P = 0.049$] were significant independent risk factors for intra-abdominal infectious complications.

Table 2 Risk factors for morbidity after minimally invasive gastrectomy, *n* = 1401

Factors	Univariate analysis, OR (95%CI)	*P* value	Multivariate analysis, OR (95%CI)	*P* value
Non-robotic minimally invasive surgery	2.438 (1.381–4.304)	0.002	2.591 (1.418–4.717)	0.002
Age ≥ 70 yr	1.020 (0.706–1.474)	0.920		
Male	2.277 (1.372–3.779)	0.001	1.969 (1.142–3.390)	0.015
Body mass index ≥ 23 kg/m^2	1.138 (0.763–1.698)	0.538		
ASA score 2 or higher	1.069 (0.703–1.625)	0.832		
cT2[1] or higher	1.296 (0.870–1.930)	0.222		
cN[1] positive	1.183 (0.745–1.879)	0.540		
cStage II[1] or higher	1.649 (1.102–2.467)	0.017	1.247 (0.809–1.922)	0.318
Proximal or total gastrectomy	1.847 (1.230–2.772)	0.004	1.208 (0.753–1.937)	0.433
D2 lymph node dissection	1.204 (0.809–1.792)	0.415		
Splenectomy	2.734 (1.179–6.339)	0.026	1.360 (0.542–3.408)	0.512
History of laparotomy	1.083 (0.658–1.783)	0.795		
Operative time ≥ 360 min	2.449 (1.613–3.718)	< 0.001	1.800 (1.098–2.952)	0.020
Estimated blood loss ≥ 50 mL	2.039 (1.367–3.042)	< 0.001	1.368 (0.873–2.143)	0.209
Tumor size ≥ 30 mm	1.119 (0.703–1.782)	0.721		
pT2[1] or higher	1.378 (0.926–2.052)	0.125		
pN[1] positive	1.155 (0.761–1.753)	0.516		
pStage II [1] or higher	1.471 (0.987–2.192)	0.061		
Use of neoadjuvant chemotherapy	1.274 (0.662–2.452)	0.467		
Non-qualified surgeons	1.148 (0.785–1.679)	0.521		

[1]Japanese Classification of Gastric Carcinoma, 15th edition. The χ^2 test was used for univariate analysis. Multivariate logistic regression was used for multivariate analyses of factors having a *P* value of < 0.05 during univariate analysis. ASA: American Society of Anesthesiologist; OR: Odds ratio; CI: Confidence interval.

DISCUSSION

The present study sought to identify risk factors for complications after MIS for GC. Accordingly, multivariate analysis revealed that non-robotic MIS was among the independent risk factors for complications. To determine whether a cause–effect relationship existed between non-RG and morbidity, short-term outcomes between RG and LG were compared using PSM analysis. Subsequent results showed that the RG group had a significantly lower incidence of intra-abdominal infectious complications compared to LG group and was more likely to be handled by an ESSQS-qualified surgeon. However, multivariate analysis of the PSM cohort showed that non-robotic MIS, but not the lack of ESSQS surgeon qualification, was a significant independent risk factor for intra-abdominal infectious complications. These findings clearly suggest that robotic surgery is at least more effective in reducing morbidity after MIS for GC than ESSQS qualification. The results presented herein support our previous evidence suggesting that the use of a robotic system significantly reduced postoperative complications[18]. In addition, the present study yielded three major findings.

First, the current study observed a 3.6% and 2.5% incidence rate for CD grade IIIa or higher morbidity and intra-abdominal infectious complications following RG, respectively. This finding was comparable to results from other prospective trials in Japan (2.5%–5.0% and 0.6%–3.3%, respectively)[23,34,35] or in other countries (reported as a range from 1.0% to 8.9%)[36]. In particular, RG seemed to have greater beneficial effects against pancreatic fistulas and intraperitoneal abscesses rather than anastomotic leakage compared to LG, although no significant difference was observed. This may be partly attributed to the meticulosity and high-definition magnified three-dimensional image of the robotic systems, which could be more effective in pancreas-protective radical lymph node dissection rather than intracorporeal alimentary tract reconstruction[30,37]. Actually, according to Table 5, there is a trend towards decrease in intraperitoneal abscess as well as pancreatic fistula in the RG group. Since intraperitoneal abscess could be induced by subclinical pancreatic fistula, the following speculation has taken place considering the results of our previous study in which RG significantly reduced pancreatic fistula: Robotic articulating forceps in combination with the magnified vivid three dimensional image enable operating surgeons to conduct radical lymph node dissection with little touch

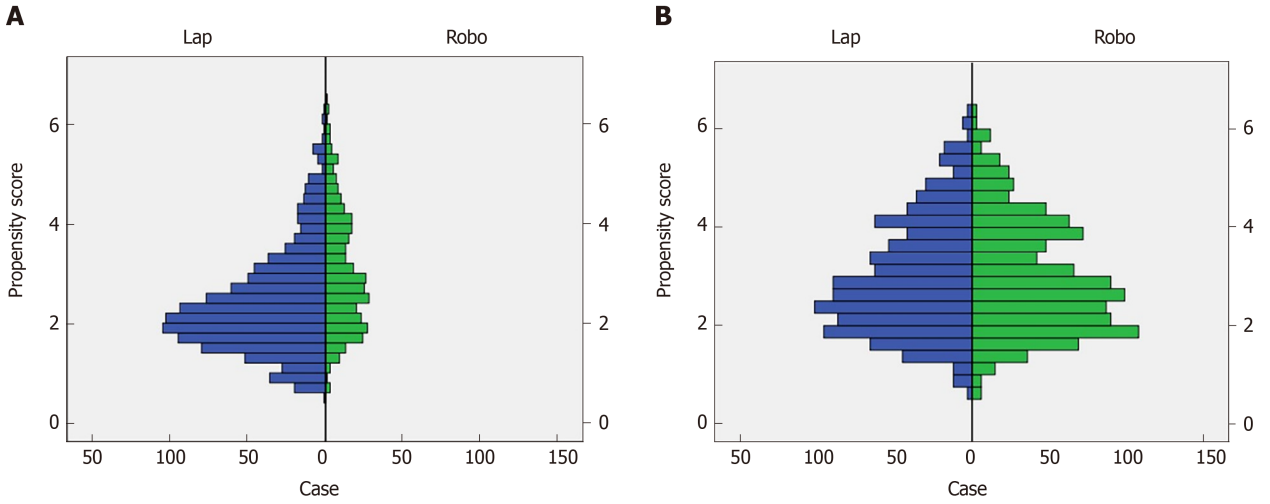

Figure 2 Mirrored histogram of propensity scores. A: Before matching; B: After matching, showing the distributions of laparoscopic gastrectomy (lap, blue-bar) and robotic gastrectomy (robo, green-bar).

on the pancreas, leading to reduction in postoperative intra-abdominal infectious complications including clinical and subclinical pancreatic fistula. In addition, the "double bipolar" method characterized by simultaneous use of Maryland bipolar forceps (bipolar forced coagulation, 420172, Intuitive) with the right hand and Fenestrated bipolar forceps (bipolar soft coagulation, 420205, Intuitive) with the left hand might also facilitate pancreas-protective dissection in RG[20,23]. However, there has been little evidence that minimally invasive gastrectomy is contributed to the reduction in postoperative pancreatic fistula, as shown in previous meta-analyses based on retrospective studies[38,39]. Therefore, further studies including multi-center randomized controlled trial are desired to establish solid evidence on RG.

Second, multivariate analysis showed that surgeon non-qualification was not an independent risk factor for morbidity. Two possible reasons may explain such a result. First is that a qualified surgeon could have guided the non-qualified surgeon performing the surgery. Second is that the qualified surgeons are able to perform high-quality surgeries even on technically demanding cases. In fact, our results showed that qualified surgeons were more likely to be in charge of more difficult procedures, including PG, TG, and D2 dissection, and there were no significant differences in morbidity rate of LG between the qualified and non-qualified surgeons (data not shown). Therefore, we still believe that ESSQS has played an important role in securing the safety and quality of MIS for GC.

Third, our findings showed that RG increased total operative time, a result consistent with those presented in many previous reports or meta-analyses[36]. In contrast, total operative time ≥ 360 min was identified as an independent risk factor for postoperative intra-abdominal infectious complications. This reduction in complications despite prolonged operative time with RG suggest its potential efficacy for addressing or overcoming certain factors that may induce complications in association with prolonged operative time. Considering that more technically-demanding procedures, such as PG/TG or D2 dissection, as well as complicated patient backgrounds, such as more advanced diseases, higher BMI, and use of preoperative chemotherapy, would likely extended operative time, they would constitute good indications for RG.

The present study has several limitations that need consideration. First, this study employed a single-center, retrospective, and non-randomized design. Moreover, financial resources necessary for RG had been changed from each patient's own expense, Senshiniryo B, to the national insurance coverage. Therefore, considering possible data biases, overall results should be interpreted cautiously. Since October 2018, all patients who underwent RG using the national medical insurance must be prospectively registered to the web-based registry of the National Clinical Database[40]. Thus, large real-world data from this prospective registry would reveal actual outcomes of RG, including intraoperative and postoperative adverse effects and long-term oncologic outcomes. Second, this study has concerns regarding operator bias given that almost half of the LG cases were performed by non-qualified surgeons, while all RG procedures were performed by qualified surgeons. Accordingly, it remains largely unclear whether the protective effects of RG on morbidity observed herein could be extrapolated to RG conducted by a non-qualified surgeon. To address

Table 3 Patient characteristics and clinicopathological features by each type of procedure

	Entire cohort (*n* = 1401)		*P* value	SD	Propensity-score matched cohort (*n* = 708)		*P* value	SD
	RG (*n* = 359)	LG (*n* = 1042)			RG (*n* = 354)	LG (*n* = 354)		
Age (yr)	67 (30–89)	70 (24–93)	< 0.001	0.24	67 (30–89)	66 (24–90)	0.315	0.10
Gender (M:F)	233:126	740:302	0.033	0.12	230:124	230:124	1.000	0
Body mass index (kg/m^2)	22.9 (14.3–32.0)	22.2 (14.5–37.3)	0.021	0.12	22.8 (14.3–32.0)	22.4 (14.9–37.3)	0.752	0.03
ASA grade (1:2:3)	160:168:31	340:565:137	< 0.001	0.25	155:168:31	149:174:31	0.905	0.03
History of laparotomy, *n* (%)	66 (18.4)	197 (18.9)	0.876	0.01	65 (18.4)	59 (16.7)	0.621	0.04
Tumor size (mm)	30 (0–170)	30 (0–180)	0.013	0.14	30 (0–170)	30 (0–180)	0.208	0.09
cT[1] (1:2:3:4a)	198:75:56:30	553:189:168:132	0.131	0.04	195:74:55:30	204:70:48:32	0.834	0.05
cN[1] (−:+)	287:72	806:236	0.337	0.06	284:70	289:65	0.702	0.04
cStage[1] (I:II:III)	249:62:48	690:168:184	0.183	0.07	246:61:47	252:59:43	0.962	0.04
pT[1] (1:2:3:4a)	210:36:46:67	587:128:132:195	0.711	0.05	208:36:46:64	213:36:39:66	0.882	0.03
pN[1] (0:1:2:3)	249:47:24:39	700:127:113:102	0.145	0.05	246:46:24:38	244:48:18:44	0.72	0.01
pStage[1] (I:II:III)	221:80:58	635:200:207	0.200	0.01	219:78:57	224:71:59	0.823	0.03
No. of metastatic LNs	0 (0–43)	0 (0–63)	0.385	0.03	0 (0–43)	0 (0–37)	0.819	0.02
Use of preoperative chemotherapy, *n* (%)	19 (5.3)	101 (9.7)	0.011	0.17	19 (5.4)	18 (5.1)	> 0.999	0.01
Type of resection (DG:PG:TG)	250:42:67	743:47:252	< 0.001	0.13	248:39:67	252:33:69	0.778	0.01
Extent of lymphadenectomy (D1+:D2)	178:181	589:453	0.023	0.14	175:179	175:179	> 0.999	0
Splenectomy, *n* (%)	6 (1.7)	34 (3.3)	0.142	0.11	6 (1.7)	7 (2.0)	> 0.999	0.02

[1]Japanese Classification of Gastric Carcinoma, 15th edition. Data are shown as median with range unless otherwise specified. The χ^2 test was used for between-group comparison of gender, American Society of Anesthesiologist grade, history of laparotomy, cT, cN, cStage, pT, pN, pStage, use of preoperative chemotherapy, type of resection, extent of lymphadenectomy, and splenectomy. The Mann–Whitney *U* test was applied for between-group comparison of age, body mass index, tumor size, and number of metastatic lymph nodes. RG: Robotic gastrectomy; LG: Laparoscopic gastrectomy; SD: Standardized difference; ASA: American Society of Anesthesiologist; LNs: Lymph nodes.

this issue, future studies comparing RG and LG performed by experts and non-qualified surgeons would be necessary. Third, the advantages of RG on oncological outcomes remained inconclusive give that long-term surveillance is still underway. However, we had previously reported that RG had long-term oncological outcomes comparable to those for LG[41]. In addition, some reports demonstrated that intra-abdominal infectious complications after gastrectomy had a negative impact on long-term oncological outcomes[42,43]. Further investigations are nonetheless warranted to determine whether RG's effect in reducing intra-abdominal infectious complications can lead to improvement in oncological outcomes after RG in the present cohort. Fourth, robotic and technological advances may influence surgical outcomes. During this study period, three DVSS systems, *i.e.*, S, Si, and Xi, had been used for RG. Although no differences in complication rates had been observe between these three systems (data not shown), further investigation on how differences in the version of the robotic system affect surgical outcomes is imperative. In addition, multivariate analysis involving the PSM cohort identified the male gender as an independent risk factor for intra-abdominal infectious complications. However, factors primarily affected have remained unclear. Hence, further investigation regarding differences in clinical and anatomical characteristics between males and females is necessary.

In conclusion, the present study shown that robotic surgery might improve short-term outcomes following minimally invasive radical gastrectomy by reducing intra-abdominal infectious complications.

Table 4 Surgical outcomes and short-term postoperative courses

	Entire cohort (*n* = 1401)		*P* value	Propensity-score matched cohort (*n* = 708)		*P* value
	RG (*n* = 359)	LG (*n* = 1042)		RG (*n* = 354)	LG (*n* = 354)	
No. of operators (qualified surgeon)	8 (8)	33 (14)	NA	8 (8)	33 (14)	NA
Qualified:non-qualified surgeons	359:0	572:475	< 0.001	354:0	186:149	< 0.001
Total operative time (min)	360 (174–942)	342 (147–937)	< 0.001	360 (174–942)	347 (149–937)	0.001
Console time (min)	306 (136–860)	NA	NA	307 (136–860)	NA	NA
Estimated blood loss (mL)	36 (0–935)	29 (0–2150)	0.007	37 (0–935)	28 (0–2150)	0.005
No. of dissected LNs	37 (7–100)	35 (6–114)	0.058	37 (7–100)	36 (6–108)	0.807
Conversion to open procedure, *n* (%)	0 (0)	1 (0.1)	> 0.999	0	0	> 0.999
Reoperation rate, *n* (%)	4 (1.1)	11 (1.1)	> 0.999	4 (1.1)	6 (1.7)	0.750
Hospital stay following surgery (d)	12 (2–195)	13 (3–177)	< 0.001	12 (2–195)	13 (3–131)	0.001
In-hospital mortality, *n* (%)	2 (0.6)	2 (0.3)	0.578	2 (0.6)	1 (0.3)	> 0.999

Data are presented as median with range unless otherwise stated. The χ^2 test was used for between group comparison of comparison of proportion of qualified and non-qualified surgeons, splenectomy, conversion to open procedure, reoperation rate, and in-hospital mortality. The Mann–Whitney *U* test was applied for between-group comparison of total operative time, estimated blood loss, number of dissected lymph nodes, and hospital stay following surgery. RG: Robotic gastrectomy; LG: Laparoscopic gastrectomy; LNs: Lymph nodes.

Table 5 Postoperative complications with a Clavien–Dindo grade of IIIa or higher, *n* (%)

	Entire cohort (*n* = 1401)		*P* value	Propensity-score matched cohort (*n* = 708)		*P* value
	RG (*n* = 359)	LG (*n* = 1042)		RG (*n* = 354)	LG (*n* = 354)	
Morbidity	13 (3.6)	92 (8.8)	0.002	13 (3.7)	27 (7.6)	0.033
Intra-abdominal infection	9 (2.5)	66 (6.3)	0.005	9 (2.5)	21 (5.9)	0.038
Anastomotic leakage	6 (1.7)	22 (2.1)	0.670	6 (1.7)	7 (2.0)	> 0.999
Pancreatic fistula	3 (0.8)	28 (2.7)	0.058	3 (0.8)	9 (2.5)	0.143
Intraperitoneal abscess	0 (0)	16 (1.5)	0.017	0 (0)	5 (1.4)	0.062
Other local complications	3 (0.8)	14 (1.3)	0.632	2 (0.6)	4 (1.1)	0.682
Intra-abdominal bleeding	2 (0.6)	4 (0.4)	> 0.999	1 (0.3)	2 (0.6)	> 0.999
Bowel obstruction	0 (0)	7 (0.6)	0.150	0 (0)	0 (0)	> 0.999
Anastomotic stenosis	1 (0.3)	3 (0.3)	> 0.999	1 (0.3)	2 (0.6)	> 0.999
Systemic complications	1 (0.3)	17 (1.6)	0.091	1 (0.3)	4 (1.1)	0.369
Pneumonia	0 (0)	9 (0.9)	0.256	0 (0)	2 (0.6)	0.499
Pulmonary embolism	1 (0.3)	2 (0.2)	0.726	1 (0.3)	0 (0)	> 0.999
Renal dysfunction	0 (0)	1 (0.1)	0.573	0 (0)	0 (0)	> 0.999
Cardiovascular disease	0 (0)	5 (0.5)	0.337	0 (0)	2 (0.6)	0.499

The χ^2 test was used for between-group comparison. RG: Robotic gastrectomy; LG: Laparoscopic gastrectomy.

Table 6 Risk factors for intra-abdominal infectious complications (propensity score-matched cohort, *n* = 708)

Factors	Univariate analysis, OR (95%CI)	*P* value	Multivariate analysis, OR (95%CI)	*P* value
Non-robotic minimally invasive surgery	2.333 (1.084–5.024)	0.038	2.463 (1.070–5.682)	0.034
Age ≥ 70 yr	1.141 (0.546–2.388)	0.849		
Male	4.852 (1.487–15.834)	0.003	3.937 (1.157–13.333)	0.028
Body mass index ≥ 23 kg/m^2	1.064 (0.511–2.214)	> 0.999		
ASA score 2 or higher	1.135 (0.538–2.393)	0.851		
cStage II[1] or more	1.394 (0.651–2.982)	0.416		
Proximal or total gastrectomy	2.513 (1.205–5.240)	0.014	1.694 (0.722–3.974)	0.226
D2 dissection	1.023 (0.508–2.061)	> 0.999		
Splenectomy	1.579 (0.467–5.339)	0.668		
Operative time ≥ 360 min	4.863 (1.963–12.048)	< 0.001	2.779 (1.003–7.701)	0.049
Estimated blood loss ≥ 50 mL	3.596 (1.682–7.687)	0.001	2.204 (0.967–5.023)	0.060
Tumor size ≥ 30 mm	1.057 (0.508–2.201)	> 0.999		
pStage II[1] or more	1.120 (0.531–2.363)	0.848		
Use of neoadjuvant chemotherapy	1.599 (0.224–11.419)	0.729		
Non-qualified surgeons	2.047 (1.018–4.118)	0.045	1.852 (0.810–4.237)	0.145

[1]Japanese Classification of Gastric Carcinoma, 15th edition. The χ^2 test was used for univariate analysis. Multivariate logistic regression was used for multivariate analyses of factors having a *P* value of < 0.05 during univariate analysis. ASA: American Society of Anesthesiologist; OR: Odds ratio; CI: Confidence interval.

ARTICLE HIGHLIGHTS

Research background

Minimally invasive surgery for gastric cancer (GC) has gained widespread use as a safe curative procedure especially for early GC. However, several recent studies using the nationwide web-based database of Japan have revealed that laparoscopic gastrectomy (LG) promoted higher postoperative local complications compared with open gastrectomy.

Research motivation

We launched robotic gastrectomy (RG) for GC in 2009. Our previous studies have consistently suggested that use of the surgical robot in LG might reduce postoperative complications, although use of the surgical robot was determined in a non-randomized manner. Actually, only experienced surgeons have performed RG, and RG was used for patients who hoped for uninsured use of the robot between 2009 and 2017.

Research objectives

This study aimed to determine risk factors for postoperative complications after minimally invasive gastrectomy for GC using our prospectively maintained database between January 2009 and June 2019.

Research methods

This study enrolled 1401 patients who underwent radical robotic gastrectomy (RG) or LG for clinical and pathological Stage III or lower GC. Retrospective chart review and multivariate analysis were performed for identifying risk factors for postoperative morbidity.

Research results

Multivariate analyses demonstrated that non-robotic minimally invasive surgery, male gender, and an operative time of ≥ 360 min were significant independent risk factors for morbidity. Therefore, morbidity was compared between RG and LG using propensity score matched analysis. As a result, RG induced significantly fewer intra-abdominal infectious complications than the LG (2.5% *vs* 5.9%, respectively; *P* = 0.038). Multivariate analyses of the propensity-matched cohort revealed that non-robotic minimally invasive surgery [OR = 2.463 (1.070–5.682); *P* = 0.034] was a significant independent risk factor for intra-abdominal infectious complications.

Research conclusions

RG might improve short-term outcomes following minimally invasive radical gastrectomy by reducing intra-abdominal infectious complications.

Research perspectives

We will conduct an RCT on this topic in the near future. Impact of RG on long-term outcomes should also be examined at least in this cohort.

REFERENCES

1 **Bray F**, Ferlay J, Soerjomataram I, Siegel RL, Torre LA, Jemal A. Global cancer statistics 2018: GLOBOCAN estimates of incidence and mortality worldwide for 36 cancers in 185 countries. *CA Cancer J Clin* 2018; **68**: 394-424 [PMID: 30207593 DOI: 10.3322/caac.21492]

2 **Sano T**, Sasako M, Yamamoto S, Nashimoto A, Kurita A, Hiratsuka M, Tsujinaka T, Kinoshita T, Arai K, Yamamura Y, Okajima K. Gastric cancer surgery: morbidity and mortality results from a prospective randomized controlled trial comparing D2 and extended para-aortic lymphadenectomy--Japan Clinical Oncology Group study 9501. *J Clin Oncol* 2004; **22**: 2767-2773 [PMID: 15199090 DOI: 10.1200/JCO.2004.10.184]

3 **Japanese Gastric Cancer Association**. Japanese gastric cancer treatment guidelines 2014 (ver. 4). *Gastric Cancer* 2017; **20**: 1-19 [PMID: 27342689 DOI: 10.1007/s10120-016-0622-4]

4 **Sasako M**. Progress in the treatment of gastric cancer in Japan over the last 50 years. *Ann Gastroenterol Surg* 2020; **4**: 21-29 [PMID: 32021955 DOI: 10.1002/ags3.12306]

5 **Kim HH**, Hyung WJ, Cho GS, Kim MC, Han SU, Kim W, Ryu SW, Lee HJ, Song KY. Morbidity and mortality of laparoscopic gastrectomy versus open gastrectomy for gastric cancer: an interim report--a phase III multicenter, prospective, randomized Trial (KLASS Trial). *Ann Surg* 2010; **251**: 417-420 [PMID: 20160637 DOI: 10.1097/SLA.0b013e3181cc8f6b]

6 **Katai H**, Sasako M, Fukuda H, Nakamura K, Hiki N, Saka M, Yamaue H, Yoshikawa T, Kojima K; JCOG Gastric Cancer Surgical Study Group. Safety and feasibility of laparoscopy-assisted distal gastrectomy with suprapancreatic nodal dissection for clinical stage I gastric cancer: a multicenter phase II trial (JCOG 0703). *Gastric Cancer* 2010; **13**: 238-244 [PMID: 21128059 DOI: 10.1007/s10120-010-0565-0]

7 **Katai H**, Mizusawa J, Katayama H, Takagi M, Yoshikawa T, Fukagawa T, Terashima M, Misawa K, Teshima S, Koeda K, Nunobe S, Fukushima N, Yasuda T, Asao Y, Fujiwara Y, Sasako M. Short-term surgical outcomes from a phase III study of laparoscopy-assisted versus open distal gastrectomy with nodal dissection for clinical stage IA/IB gastric cancer: Japan Clinical Oncology Group Study JCOG0912. *Gastric Cancer* 2017; **20**: 699-708 [PMID: 27718137 DOI: 10.1007/s10120-016-0646-9]

8 **Shinohara T**, Satoh S, Kanaya S, Ishida Y, Taniguchi K, Isogaki J, Inaba K, Yanaga K, Uyama I. Laparoscopic versus open D2 gastrectomy for advanced gastric cancer: a retrospective cohort study. *Surg Endosc* 2013; **27**: 286-294 [PMID: 22733201 DOI: 10.1007/s00464-012-2442-x]

9 **Nakauchi M**, Suda K, Kadoya S, Inaba K, Ishida Y, Uyama I. Technical aspects and short- and long-term outcomes of totally laparoscopic total gastrectomy for advanced gastric cancer: a single-institution retrospective study. *Surg Endosc* 2016; **30**: 4632-4639 [PMID: 26703126 DOI: 10.1007/s00464-015-4726-4]

10 **Uyama I**, Suda K, Satoh S. Laparoscopic surgery for advanced gastric cancer: current status and future perspectives. *J Gastric Cancer* 2013; **13**: 19-25 [PMID: 23610715 DOI: 10.5230/jgc.2013.13.1.19]

11 **Yoshida K**, Honda M, Kumamaru H, Kodera Y, Kakeji Y, Hiki N, Etoh T, Miyata H, Yamashita Y, Seto Y, Kitano S, Konno H. Surgical outcomes of laparoscopic distal gastrectomy compared to open distal gastrectomy: A retrospective cohort study based on a nationwide registry database in Japan. *Ann Gastroenterol Surg* 2018; **2**: 55-64 [PMID: 29863131 DOI: 10.1002/ags3.12054]

12 **Hiki N**, Honda M, Etoh T, Yoshida K, Kodera Y, Kakeji Y, Kumamaru H, Miyata H, Yamashita Y, Inomata M, Konno H, Seto Y, Kitano S. Higher incidence of pancreatic fistula in laparoscopic gastrectomy. Real-world evidence from a nationwide prospective cohort study. *Gastric Cancer* 2018; **21**: 162-170 [PMID: 28887712 DOI: 10.1007/s10120-017-0764-z]

13 **Kodera Y**, Yoshida K, Kumamaru H, Kakeji Y, Hiki N, Etoh T, Honda M, Miyata H, Yamashita Y, Seto Y, Kitano S, Konno H. Introducing laparoscopic total gastrectomy for gastric cancer in general practice: a retrospective cohort study based on a nationwide registry database in Japan. *Gastric Cancer* 2019; **22**: 202-213 [PMID: 29427039 DOI: 10.1007/s10120-018-0795-0]

14 **Kim MC**, Jung GJ, Kim HH. Learning curve of laparoscopy-assisted distal gastrectomy with systemic lymphadenectomy for early gastric cancer. *World J Gastroenterol* 2005; **11**: 7508-7511 [PMID: 16437724 DOI: 10.3748/wjg.v11.i47.7508]

15 **Jin SH**, Kim DY, Kim H, Jeong IH, Kim MW, Cho YK, Han SU. Multidimensional learning curve in laparoscopy-assisted gastrectomy for early gastric cancer. *Surg Endosc* 2007; **21**: 28-33 [PMID: 16960676 DOI: 10.1007/s00464-005-0634-3]

16 **Kunisaki C**, Makino H, Yamamoto N, Sato T, Oshima T, Nagano Y, Fujii S, Akiyama H, Otsuka Y, Ono HA, Kosaka T, Takagawa R, Shimada H. Learning curve for laparoscopy-assisted distal gastrectomy with regional lymph node dissection for early gastric cancer. *Surg Laparosc Endosc Percutan Tech* 2008; **18**: 236-241 [PMID: 18574408 DOI: 10.1097/SLE.0b013e31816aa13f]

17 **Hu WG**, Ma JJ, Zang L, Xue P, Xu H, Wang ML, Lu AG, Li JW, Feng B, Zheng MH. Learning curve and long-term outcomes of laparoscopy-assisted distal gastrectomy for gastric cancer. *J Laparoendosc Adv Surg Tech A* 2014; **24**: 487-492 [PMID: 24933012 DOI: 10.1089/lap.2013.0570]

18 **Mori T**, Kimura T, Kitajima M. Skill accreditation system for laparoscopic gastroenterologic surgeons in Japan. *Minim Invasive Ther Allied Technol* 2010; **19**: 18-23 [PMID: 20095893 DOI: 10.3109/13645700903492969]

19 **Suda K**, Ishida Y, Kawamura Y, Inaba K, Kanaya S, Teramukai S, Satoh S, Uyama I. Robot-assisted thoracoscopic lymphadenectomy along the left recurrent laryngeal nerve for esophageal squamous cell carcinoma in the prone position: technical report and short-term outcomes. *World J Surg* 2012; **36**: 1608-1616 [PMID: 22392356 DOI: 10.1007/s00268-012-1538-8]

20 **Suda K**, Man-I M, Ishida Y, Kawamura Y, Satoh S, Uyama I. Potential advantages of robotic radical gastrectomy for gastric adenocarcinoma in comparison with conventional laparoscopic approach: a single institutional retrospective comparative cohort study. *Surg Endosc* 2015; **29**: 673-685 [PMID: 25030478 DOI: 10.1007/s00464-014-3718-0]

21 **Uyama I**, Kanaya S, Ishida Y, Inaba K, Suda K, Satoh S. Novel integrated robotic approach for suprapancreatic D2 nodal dissection for treating gastric cancer: technique and initial experience. *World J Surg* 2012; **36**: 331-337 [PMID: 22131088 DOI: 10.1007/s00268-011-1352-8]

22 **Wang WJ**, Li HT, Yu JP, Su L, Guo CA, Chen P, Yan L, Li K, Ma YW, Wang L, Hu W, Li YM, Liu HB. Severity and incidence of complications assessed by the Clavien-Dindo classification following robotic and laparoscopic gastrectomy for advanced gastric cancer: a retrospective and propensity score-matched study. *Surg Endosc* 2019; **33**: 3341-3354 [PMID: 30560498 DOI: 10.1007/s00464-018-06624-7]

23 **Uyama I**, Suda K, Nakauchi M, Kinoshita T, Noshiro H, Takiguchi S, Ehara K, Obama K, Kuwabara S,

Okabe H, Terashima M. Clinical advantages of robotic gastrectomy for clinical stage I/II gastric cancer: a multi-institutional prospective single-arm study. *Gastric Cancer* 2019; **22**: 377-385 [PMID: 30506394 DOI: 10.1007/s10120-018-00906-8]

24 **Japanese Gastric Cancer Association**. Japanese classification of gastric carcinoma: 3rd English edition. *Gastric Cancer* 2011; **14**: 101-112 [PMID: 21573743 DOI: 10.1007/s10120-011-0041-5]

25 **Yanai H**, Matsumoto Y, Harada T, Nishiaki M, Tokiyama H, Shigemitsu T, Tada M, Okita K. Endoscopic ultrasonography and endoscopy for staging depth of invasion in early gastric cancer: a pilot study. *Gastrointest Endosc* 1997; **46**: 212-216 [PMID: 9378206 DOI: 10.1016/s0016-5107(97)70088-9]

26 **Fusaroli P**, Kypraios D, Eloubeidi MA, Caletti G. Levels of evidence in endoscopic ultrasonography: a systematic review. *Dig Dis Sci* 2012; **57**: 602-609 [PMID: 22057240 DOI: 10.1007/s10620-011-1961-y]

27 **Nakauchi M**, Suda K, Nakamura K, Shibasaki S, Kikuchi K, Nakamura T, Kadoya S, Ishida Y, Inaba K, Taniguchi K, Uyama I. Laparoscopic subtotal gastrectomy for advanced gastric cancer: technical aspects and surgical, nutritional and oncological outcomes. *Surg Endosc* 2017; **31**: 4631-4640 [PMID: 28389797 DOI: 10.1007/s00464-017-5526-9]

28 **Catena F**, Di Battista M, Ansaloni L, Pantaleo M, Fusaroli P, Di Scioscio V, Santini D, Nannini M, Saponara M, Ponti G, Persiani R, Delrio P, Coccolini F, Di Saverio S, Biasco G, Lazzareschi D, Pinna A; GISTologist Study Group. Microscopic margins of resection influence primary gastrointestinal stromal tumor survival. *Onkologie* 2012; **35**: 645-648 [PMID: 23147540 DOI: 10.1159/000343585]

29 **Shibasaki S**, Suda K, Nakauchi M, Nakamura T, Kadoya S, Kikuchi K, Inaba K, Uyama I. Outermost layer-oriented medial approach for infrapyloric nodal dissection in laparoscopic distal gastrectomy. *Surg Endosc* 2018; **32**: 2137-2148 [PMID: 29450630 DOI: 10.1007/s00464-018-6111-6]

30 **Nakamura K**, Suda K, Suzuki A, Nakauchi M, Shibasaki S, Kikuchi K, Nakamura T, Kadoya S, Inaba K, Uyama I. Intracorporeal Isosceles Right Triangle-shaped Anastomosis in Totally Laparoscopic Distal Gastrectomy. *Surg Laparosc Endosc Percutan Tech* 2018; **28**: 193-201 [PMID: 29738380 DOI: 10.1097/SLE.0000000000000535]

31 **Dindo D**, Demartines N, Clavien PA. Classification of surgical complications: a new proposal with evaluation in a cohort of 6336 patients and results of a survey. *Ann Surg* 2004; **240**: 205-213 [PMID: 15273542 DOI: 10.1097/01.sla.0000133083.54934.ae]

32 **Katayama H**, Kurokawa Y, Nakamura K, Ito H, Kanemitsu Y, Masuda N, Tsubosa Y, Satoh T, Yokomizo A, Fukuda H, Sasako M. Extended Clavien-Dindo classification of surgical complications: Japan Clinical Oncology Group postoperative complications criteria. *Surg Today* 2016; **46**: 668-685 [PMID: 26289837 DOI: 10.1007/s00595-015-1236-x]

33 **Suda K**, Nakauchi M, Inaba K, Ishida Y, Uyama I. Revising robotic surgery for stomach, potential benefits revised II: prevention of pancreatic fistula. *Transl Gastrointest Cancer* 2015; **4**: 461-467 [DOI: 10.3978/j.issn.2224-4778.2015.10.05]

34 **Okabe H**, Obama K, Tsunoda S, Matsuo K, Tanaka E, Hisamori S, Sakai Y. Feasibility of robotic radical gastrectomy using a monopolar device for gastric cancer. *Surg Today* 2019; **49**: 820-827 [PMID: 30929081 DOI: 10.1007/s00595-019-01802-z]

35 **Tokunaga M**, Makuuchi R, Miki Y, Tanizawa Y, Bando E, Kawamura T, Terashima M. Late phase II study of robot-assisted gastrectomy with nodal dissection for clinical stage I gastric cancer. *Surg Endosc* 2016; **30**: 3362-3367 [PMID: 26511119 DOI: 10.1007/s00464-015-4613-z]

36 **Shibasaki S**, Suda K, Obama K, Yoshida M, Uyama I. Should robotic gastrectomy become a standard surgical treatment option for gastric cancer? *Surg Today* 2019 [PMID: 31512060 DOI: 10.1007/s00595-019-01875-w]

37 **Inaba K**, Satoh S, Ishida Y, Taniguchi K, Isogaki J, Kanaya S, Uyama I. Overlap method: novel intracorporeal esophagojejunostomy after laparoscopic total gastrectomy. *J Am Coll Surg* 2010; **211**: e25-e29 [PMID: 21036074 DOI: 10.1016/j.jamcollsurg.2010.09.005]

38 **Guerra F**, Giuliani G, Iacobone M, Bianchi PP, Coratti A. Pancreas-related complications following gastrectomy: systematic review and meta-analysis of open versus minimally invasive surgery. *Surg Endosc* 2017; **31**: 4346-4356 [PMID: 28378074 DOI: 10.1007/s00464-017-5507-z]

39 **Guerra F**, Giuliani G, Formisano G, Bianchi PP, Patriti A, Coratti A. Pancreatic Complications After Conventional Laparoscopic Radical Gastrectomy Versus Robotic Radical Gastrectomy: Systematic Review and Meta-Analysis. *J Laparoendosc Adv Surg Tech A* 2018; **28**: 1207-1215 [PMID: 29733241 DOI: 10.1089/lap.2018.0159]

40 **Gotoh M**, Miyata H, Hashimoto H, Wakabayashi G, Konno H, Miyakawa S, Sugihara K, Mori M, Satomi S, Kokudo N, Iwanaka T. National Clinical Database feedback implementation for quality improvement of cancer treatment in Japan: from good to great through transparency. *Surg Today* 2016; **46**: 38-47 [PMID: 25797948 DOI: 10.1007/s00595-015-1146-y]

41 **Nakauchi M**, Suda K, Susumu S, Kadoya S, Inaba K, Ishida Y, Uyama I. Comparison of the long-term outcomes of robotic radical gastrectomy for gastric cancer and conventional laparoscopic approach: a single institutional retrospective cohort study. *Surg Endosc* 2016; **30**: 5444-5452 [PMID: 27129542 DOI: 10.1007/s00464-016-4904-z]

42 **Tokunaga M**, Tanizawa Y, Bando E, Kawamura T, Terashima M. Poor survival rate in patients with postoperative intra-abdominal infectious complications following curative gastrectomy for gastric cancer. *Ann Surg Oncol* 2013; **20**: 1575-1583 [PMID: 23076557 DOI: 10.1245/s10434-012-2720-9]

43 **Aurello P**, Cinquepalmi M, Petrucciani N, Moschetta G, Antolino L, Felli F, Giulitti D, Nigri G, D'Angelo F, Valabrega S, Ramacciato G. Impact of Anastomotic Leakage on Overall and Disease-free Survival After Surgery for Gastric Carcinoma: A Systematic Review. *Anticancer Res* 2020; **40**: 619-624 [PMID: 32014902 DOI: 10.21873/anticanres.13991]

World Journal of Gastroenterology

Submit a Manuscript: https://www.f6publishing.com

World J Gastroenterol 2020 March 21; 26(11): 1185-1196

DOI: 10.3748/wjg.v26.i11.1185

ISSN 1007-9327 (print) ISSN 2219-2840 (online)

ORIGINAL ARTICLE

Retrospective Cohort Study

Preoperative albumin levels predict prolonged postoperative ileus in gastrointestinal surgery

Wen-Quan Liang, Ke-Cheng Zhang, Hua Li, Jian-Xin Cui, Hong-Qing Xi, Ji-Yang Li, Ai-Zhen Cai, Yu-Hua Liu, Wang Zhang, Lan Zhang, Bo Wei, Lin Chen

ORCID number: Wen-Quan Liang (0000-0001-5211-8148); Ke-Cheng Zhang (0000-0002-9257-5607); Hua Li (0000-0001-9205-9031); Jian-Xin CUI (0000-0002-6923-7255); Hong-Qing Xi (0000-0002-0472-8299); Ji-Yang LI (0000-0001-8217-6074); Ai-Zhen Cai (0000-0002-4220-2546); Yu-Hua Liu (0000-0001-6771-6925); Wang Zhang (0000-0002-8250-4215); Lan Zhang (0000-0001-5047-5977); Bo Wei (0000-0002-6966-2219); Lin Chen (0000-0002-3507-673X).

Author contributions: Chen L, Wei B, Liang WQ, Zhang KC and Cui JX designed the study; Liang WQ, Zhang KC and Li H wrote the manuscript; Xi HQ and Cai AZ contributed to the patient material; Liu YH and Zhang L collected the clinical data; Zhang W and Li JY contributed to data analysis and validation. Liang WQ, Zhang KC, Li H and Liu YH contributed equally to this work.

Supported by the National Nature Science Foundation of China, No. 81672319 and No. 81972790; and Beijing Nova Program, No. Z181100006218011.

Institutional review board statement: The study was approved by the Research Ethics Committee of the Chinese People's Liberation Army General Hospital.

Informed consent statement: All study participants provided written consent prior to study enrollment.

Conflict-of-interest statement: All authors have no conflict of interest.

Wen-Quan Liang, Ke-Cheng Zhang, Jian-Xin Cui, Hong-Qing Xi, Ji-Yang Li, Ai-Zhen Cai, Wang Zhang, Lan Zhang, Bo Wei, Lin Chen, Department of General Surgery & Institute of General Surgery, Chinese People's Liberation Army General Hospital, Beijing 100853, China

Hua Li, Department of Surgical Oncology, Xing Tai People's Hospital, Xingtai 054001, Hebei Province China

Yu-Hua Liu, Institute of Army Hospital Management, Chinese People's Liberation Army General Hospital, Beijing 100853, China

Corresponding author: Lin Chen, MA, MD, PhD, Chief Doctor, Professor, Department of General Surgery & Institute of General Surgery, Chinese People's Liberation Army General Hospital, 28 Fuxing Road, Beijing 100853, China. chenlin@301hospital.com.cn

Abstract

BACKGROUND

Prolonged postoperative ileus (PPOI) is a prolonged state of "pathological" gastrointestinal (GI) tract dysmotility. There are relatively few studies examining the influence of preoperative nutritional status on the development of PPOI in patients who underwent GI surgery. The association between preoperative albumin and PPOI has not been fully studied. We hypothesized that preoperative albumin may be an independent indicator of PPOI.

AIM

To analyze the role of preoperative albumin in predicting PPOI and to establish a nomogram for clinical risk evaluation.

METHODS

Patients were drawn from a prospective hospital registry database of GI surgery. A total of 311 patients diagnosed with gastric or colorectal cancer between June 2016 and March 2017 were included. Potential predictors of PPOI were analyzed by univariate and multivariable logistic regression analyses, and a nomogram for quantifying the presence of PPOI was developed and internally validated.

RESULTS

The overall PPOI rate was 21.54%. Advanced tumor stage and postoperative opioid analgesic administration were associated with PPOI. Preoperative albumin was an independent predictor of PPOI, and an optimal cutoff value of 39.15 was statistically calculated. After adjusting multiple variables, per unit or

Data sharing statement: No additional data are available.

STROBE statement: The manuscript meets the requirements of the STROBE Statement.

Manuscript source: Invited manuscript

Received: December 20, 2019
Peer-review started: December 20, 2020
First decision: February 18, 2020
Revised: February 20, 2020
Accepted: February 21, 2020
Article in press: February 21, 2020
Published online: March 21, 2020

P-Reviewer: Tandon RK
S-Editor: Wang J
L-Editor: Webster J
E-Editor: Ma YJ

per SD increase in albumin resulted in a significant decrease in the incidence of PPOI of 8% (OR = 0.92, 95%CI: 0.85-1.00, *P* = 0.046) or 27% (OR = 0.73, 95%CI: 0.54-0.99, *P* = 0.046), respectively. Patients with a high level of preoperative albumin (≥ 39.15) tended to experience PPOI compared to those with low levels (< 39.15) (OR = 0.43, 95%CI: 0.24-0.78, *P* = 0.006). A nomogram for predicting PPOI was developed [area under the curve (AUC) = 0.741] and internally validated by bootstrap resampling (AUC = 0.725, 95%CI: 0.663-0.799).

CONCLUSION
Preoperative albumin is an independent predictive factor of PPOI in patients who underwent GI surgery. The nomogram provided a model to screen for early indications in the clinical setting.

Key words: Albumin; Prolonged postoperative ileus; Gastrointestinal surgery; Nomogram; Complications

Core tip: Prolonged postoperative ileus (PPOI) is a common postoperative complication in patients who undergo gastrointestinal surgery. There are relatively few studies examining the influence of a patient's preoperative nutritional status on the development of PPOI. This study found and further confirmed that preoperative albumin was an independent predictor of PPOI. We further established a nomogram to accurately quantitate the probability of PPOI occurrence. This nomogram can be used to screen for early indications in the clinical setting.

Citation: Liang WQ, Zhang KC, Li H, Cui JX, Xi HQ, Li JY, Cai AZ, Liu YH, Zhang W, Zhang L, Wei B, Chen L. Preoperative albumin levels predict prolonged postoperative ileus in gastrointestinal surgery. *World J Gastroenterol* 2020; 26(11): 1185-1196
URL: https://www.wjgnet.com/1007-9327/full/v26/i11/1185.htm
DOI: https://dx.doi.org/10.3748/wjg.v26.i11.1185

INTRODUCTION

Prolonged postoperative ileus (PPOI) is a prolonged state of "pathological" gastrointestinal (GI) tract dysmotility beyond the expected time frame[1]. Some degree of GI tract dysmotility usually occurs in all patients following intra-abdominal surgery, especially major abdominal surgery. As one of the most common postsurgical complications, PPOI occurs in 3%-30% of patients following various types of abdominal operations[2-4]. Clinically, manifestations of POI are characterized as the absence of bowel movement, nausea, vomiting, abdominal distension, and intolerance to oral intake[1,5-8]. Following abdominal surgery, PPOI causes substantial physical discomfort and increases the length of hospital stay, thereby increasing health-care costs. According to a retrospective review of studies on postoperative ileus in more than 800000 US surgical patients, the median length of hospitalization for patients with postoperative ileus was 9.3 d compared to 5.3 d for those without, which resulted in increased costs of approximately $1.5 billion annually for the health-care system[9].

PPOI is a multifactorial process and several mechanisms have been suggested, including age, previous abdominal surgery, systemic opioids, and surgical technique[10-14]. To date, there are relatively few studies examining the influence of a patient's preoperative nutritional status on the development of PPOI. Albumin is the most commonly used and reliable indicator of a patient's nutritional status[15]. Hypoalbuminemia is a proven indicator of hospital stay, clinical outcomes, death, and a series of postoperative complications[15-17]. However, the association between preoperative albumin and PPOI has not been fully studied.

The aim of the present study was to investigate the clinical risk factors for PPOI and fully determine the independent relationship between preoperative albumin and PPOI in patients who undergo GI surgery. We plan to propose a nomogram for quantifying the presence of PPOI for early-warning in the clinical setting.

MATERIALS AND METHODS

Study design and patients

We conducted a retrospective observational cohort study at the Chinese PLA General Hospital. All data were collected from a prospective registry database of PPOI in our institution. Patients diagnosed with gastric or colorectal cancer between June 2016 and March 2017 were included if they met the following eligibility criteria: (1) Age ≥ 18 years; (2) Pathologic diagnosis of adenocarcinoma of the colorectum or stomach; (3) Totally resectable tumor; (4) Primary anastomoses; and (5) Informed consent obtained. Exclusion criteria included (1) emergency surgery, (2) conversion to laparotomy in laparoscopic plan and (3) multi-visceral resection. All of the enrolled patients were scheduled to receive standard surgical tumor excision performed by the same experienced surgical team. Individual written informed consent was obtained before surgery. This study was conducted in accordance with the Declaration of Helsinki. Ethics approval was obtained from the Institutional Review Boards of the Chinese PLA General Hospital (registration number: S2016-092-01).

Definition of PPOI

A number of studies have focused on PPOI. However, controversy existed regarding the diagnostic criteria. One systematic review and global survey clarified the terminology of PPOI and proposed a concise, clinically quantifiable definition[18]. PPOI was defined as two or more of the following criteria which were assessed on or after the fourth day of the postoperative period: nausea or vomiting for 12 h or more without relief, intolerance to a solid or semi-solid oral diet, persistent abdominal distension, absence of passage of both stool and flatus for 24 hours or more, and ileus noted on plain abdominal films or CT scans. We adopted this definition and two investigators independently assessed the diagnosis of PPOI.

Data collection

Demographic and clinical data of the enrolled patients were determined from the electronic medical records of the prospective registry database before the assessment of PPOI. Baseline demographic data including sex, age, body mass index, and evidence of previous abdominal surgery were summarized during histories, physical examinations, and safety assessments. Serum chemistry, electrolytes, liver, and kidney function tests were monitored before surgery. This study drew attention to two indicators in the biochemistry tests. One was preoperative serum albumin, which is used as a measure of nutritional status[19], and the other was preoperative potassium, which is reported to play an essential role in autoregulation of intestinal smooth muscle[20]. The surgeons were blind to the enrollment of study participants, and the choice of surgical approach (laparoscopic or open surgery). Classification of the primary tumor, regional lymph nodes, and distant metastases was based on the 7th edition of the International Union Against Cancer TNM classification of malignant tumors system. Opioid medication was reported to induce opioid-related bowel dysfunction and was considered a risk factor for PPOI[8,21,22]. In this study, whether opioid analgesics were used after surgery in the enrolled group of patients was evaluated and determined by anesthesiologists who were blind to the study design.

Statistical analysis

Primary categorical variables were shown as number and percentage. Primary continuous variables were identified both as a continuous variable and as a categorical variable and expressed in two ways: mean ± SD and number and percentage, which were classified according to clinical cutoff values or statistical median. The optimal cutoff value of preoperative albumin was derived from receiver operating characteristic (ROC) curve analysis. Statistical heterogeneity was evaluated by the χ^2 test (categorical variables) and one-way ANOVA test (continuous variables). Correlations between variables and PPOI were detected by univariate logistic regression models. Multiple regression analysis was performed to examine the independent association between preoperative albumin and PPOI in three models: for the crude model, no covariates were adjusted; model I, only sociodemographic data were adjusted; and model II, covariates in model I and other elected covariates were adjusted. The variables were considered in model II if the matched odds ratio changed at least 10% as a result of adding these covariates, which was described in previous studies[23]. A multivariable binary logistic regression model following a backward step-down selection process was applied to develop the nomogram. ROC curve analysis was performed to evaluate the discriminatory ability of the nomogram. Due to the limited number of patients, 500 bootstrap computer resamples were used to reduce overfit bias. Statistical analyses were performed using R software and Empower Stats software (X&Y Solutions, Inc.). Odds ratios (ORs) are presented with

95% confidence intervals (CIs) and $P < 0.05$ was considered significant.

RESULTS

Patient demographic data and the optimal cutoff value for preoperative albumin

A total of 311 patients in this study, consisting of 218 (10.10%) male patients and 93 (29.90%) female patients, were enrolled based on the inclusion and exclusion criteria. The average age at diagnosis was 58.98 years for the whole enrolled population. There was a similar proportion of gastric (n = 162, 52.09%) and colorectal (n = 149, 47.91%) patients. The overall PPOI rate was 21.54%. Mean preoperative albumin for the entire group was 39.77 ± 3.67 g/L. Other patient demographic data are shown in Table 1. An optimal cutoff value of 39.15 for preoperative albumin was revealed by the ROC curve analysis for PPOI prediction. The area under the ROC curve for the optimal cutoff value was 0.557 with a 95%CI of 0.479-0.635, which offered the optimum mix of sensitivity (0.552) and specificity (0.598) (Figure 1). Therefore, the cutoff value of 39.15 for preoperative albumin was used as an optimal margin in this study. Patient baseline characteristics between the lower preoperative albumin group (n = 135) and the higher preoperative albumin group (n = 176) are compared in Table 1. Mean values of preoperative albumin for the lower and higher group were 36.46 ± 2.33 and 42.30 ± 2.19 g/L, respectively. The low level of preoperative albumin was significantly associated with the older age group no matter if continuous or categorical variables (all $P < 0.05$). Although not statistically significant, patients in the lower preoperative albumin group tended to have more advanced neoplasia (III-IV stage). The level of preoperative albumin was significantly associated with PPOI, which was observed to be highly prevalent in the lower preoperative albumin group (27.41%) compared to the higher preoperative albumin group (17.05%).

Association between clinical variables and PPOI

Univariate analysis was performed to determine the clinical predictors of PPOI after the initial evaluation (Table 2). As shown, preoperative albumin was a protective factor of PPOI. The rate of PPOI in the group with lower preoperative albumin was 27.41% and the rate in the higher group was 17.05%, which indicated a significant association between the level of preoperative albumin and PPOI. Patients with a higher level of preoperative albumin (≥ 39.15) had a 46% reduced risk of PPOI (OR = 0.54, 95%CI: 0.32-0.94, P = 0.029) than those with the lower-level (< 39.15). Patients in the advanced stage (III-IV) were approximately three times more likely to experience PPOI than those in the non-advanced stage (I-II) (incidence of PPOI 30.06% *vs* 11.28%, OR = 3.33, 95%CI: 1.81-6.25, $P < 0.001$), which indicated that PPOI was significantly associated with advanced tumors. In addition, patients with clinical use of postoperative analgesia were observed to be at great risk of PPOI (OR = 3.04, 95%CI: 1.74-5.30, $P < 0.001$). Other associations are shown in Table 2, and no firm correlations were observed between other clinical features.

Preoperative albumin was an independent predictor of PPOI

Our findings suggest that PPOI may be affected by a multitude of factors. Multiple regression analysis was performed to further assess the independent effect of preoperative albumin on PPOI. Three models were constructed as follows: A crude model (no variable was adjusted), model I (baseline demographics were adjusted) and model II (variables identified by the criteria described in the method were adjusted). As shown in Table 3, when preoperative albumin was regarded as a continuous variable, per unit or per standard deviation (SD) increase in albumin reduced the incidence of PPOI, although this result was just short of being significant in the crude model and model I. In model II, per unit or per SD increase in albumin significantly reduced the incidence of PPOI by 8% (OR = 0.92, 95%CI: 0.85-1.00, P = 0.046) and 27% (OR = 0.73, 95%CI: 0.54-0.99, P = 0.046) respectively. However, when preoperative albumin was regarded as a categorical variable, an independent and significant association between different levels of preoperative albumin and PPOI was firmly found in the three models. Patients with a high level of preoperative albumin (≥ 39.15) were less likely to experience PPOI with the crude model (OR = 0.54, 95%CI: 0.32-0.94, P = 0.029), model I (OR = 0.53, 95%CI: 0.31-0.92, P = 0.025) and model II (OR = 0.43, 95%CI: 0.24-0.78, P = 0.006).

Development and validation of a nomogram predicting the PPOI

To further accurately quantitate the probability of PPOI occurrence, we established a nomogram to predict PPOI by a backward step-down selection. Five variables, including cancer type, tumor stage, postoperative analgesia, sex, and preoperative albumin, were selected to form the nomogram (Figure 2). A ROC curve was drawn to

Table 1 Correlation between preoperative albumin and clinicopathologic variables in patients undergoing gastrointestinal surgery

Characteristics	Total cohort	Subgroups of preoperative albumin		*P* value
	n = 311	< 39.15, *n* = 135	≥ 39.15, *n* = 176	
Sex				0.364
Female	93 (29.90%)	44 (32.59%)	49 (27.84%)	
Male	218 (70.10%)	91 (67.41%)	127 (72.16%)	
Age (yr)	58.98 ± 10.98	60.52 ± 10.77	57.80 ± 11.03	0.030
Categorical variable				0.007
< 60	156 (50.16%)	56 (41.48%)	100 (56.82%)	
≥ 60	155 (49.84%)	79 (58.52%)	76 (43.18%)	
Body mass index (kg/m^2)	24.43 ± 3.23	24.14 ± 3.11	24.65 ± 3.31	0.173
Categorical variable				0.136
< 25	174 (55.95%)	82 (60.74%)	92 (52.27%)	
≥ 25	137 (44.05%)	53 (39.26%)	84 (47.73%)	
Previous abdominal surgery				0.178
No	252 (81.03%)	114 (84.44%)	138 (78.41%)	
Yes	59 (18.97%)	21 (15.56%)	38 (21.59%)	
Preoperative albumin (g/L)	39.77 ± 3.67	36.46 ± 2.33	42.30 ± 2.19	< 0.001
Preoperative K^+ (mmol/L)	3.96 ± 0.32	3.94 ± 0.34	3.98 ± 0.31	0.306
Categorical variable				0.948
< 3.96	155 (49.84%)	67 (49.63%)	88 (50.00%)	
≥ 3.96	156 (50.16%)	68 (50.37%)	88 (50.00%)	
Type of cancer				0.701
Gastric cancer	162 (52.09%)	72 (53.33%)	90 (51.14%)	
Colorectal cancer	149 (47.91%)	63 (46.67%)	86 (48.86%)	
Surgical technique				0.868
Endoscopic surgery	215 (69.13%)	94 (69.63%)	121 (68.75%)	
Open surgery	96 (30.87%)	41 (30.37%)	55 (31.25%)	
Tumor stage				0.094
I-II	133 (43.46%)	65 (48.87%)	68 (39.31%)	
III-IV	173 (56.54%)	68 (51.13%)	105 (60.69%)	
Postoperative opioid analgesic				0.983
No	191 (61.41%)	83 (61.48%)	108 (61.36%)	
Yes	120 (38.59%)	52 (38.52%)	68 (38.64%)	
PPOI				0.028
No	244 (78.46%)	98 (72.59%)	146 (82.95%)	
Yes	67 (21.54%)	37 (27.41%)	30 (17.05%)	

Data are presented as number of patients or mean ± standard error. PPOI: Prolonged postoperative ileus.

illustrate the diagnostic ability of the nomogram and the AUC was 0.741 (Figure 3A). Internal validity is a way to measure if the nomogram is sound, and 500 random bootstrap resamplings were performed to reduce overfit bias. Figure 3B shows that the AUC of the random bootstrap resampling was 0.725 (95%CI: 0.663-0.799), which indicated that the nomogram had satisfactory sensitivity.

DISCUSSION

In the present study, we evaluated the association between clinical features and the presence of PPOI in patients who underwent gastric or colorectal surgery. We found that patients in an advanced tumor stage and who were administered postoperative opioid analgesics were more likely to develop PPOI. This study found and further confirmed that preoperative albumin was an independent predictor of PPOI. An optimal cutoff value of 39.15 was statistically calculated and may be regarded as a

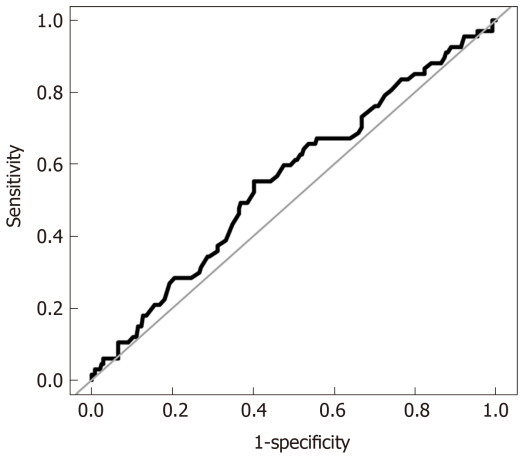

	Best threshold	Specificity	Sensitivity	AUC	95%CI low	95%CI upp
Preoperative albumin (g/L)	39.150	0.598	0.552	0.557	0.479	0.635

Figure 1 Receiver operating characteristic curves of preoperative albumin for predicting prolonged postoperative ileus in patients who underwent gastrointestinal resection. ROC: Receiver operating characteristic; AUC: Area under the curve. AUC: Null hypothesis: True area = 0.5.

warning sign before GI surgery. The level of preoperative albumin, whether a continuous or categorical variable, was significantly associated with the presence of PPOI. We further established a nomogram to accurately quantitate the probability of PPOI occurrence. This nomogram was confirmed to have good diagnostic performance and was internally validated. These findings, if further confirmed in prospective studies, would help identify individuals at high risk of PPOI before surgery.

Preoperative fasting is usually advised for patients before GI. Resections with primary anastomosis during GI surgery always result in combined stress and damage to the GI tract[24,25]. PPOI, a stage of disturbed GI motility, is one of the postoperative complications. An observation study conducted over a period of fourteen years and consisting of 2400 consecutive colorectal cancer patients showed that the incidence of PPOI was 14.0%[10]. A systematic review and meta-analysis consisting of 54 studies and comprising 18983 patients revealed a PPOI incidence of 10.3%[26]. In the present study, the incidence of PPOI was 21.54% for the whole population. The difference in the rate of PPOI can be partly attributed to the eligibility criteria and controversial definition. The duration of prolonged periods of ileus is an important factor in defining PPOI, and in previous studies varied from 3 to 7 d[6,10,14,27]. In the present study, we adopted the criteria from the results of a systematic review and global survey, and the fourth day of postoperative ileus was considered as a prolonged state[18].

Analysis of risk factors for PPOI can assist in early warning and immediate treatment. The insights of risk factors gained from this study may be of assistance to the clinical practitioner. It is now well established from a variety of studies that older age, laparoscopic approach, inflammatory response, and opioid-related dysmotility are significant risk factors for PPOI[8,12,27,28]. In the present study, we found that patients in an advanced tumor stage were more likely to develop PPOI. Tumor stage is a comprehensive factor, and the advanced stage is usually associated with increasing wound size, high operative difficulty and a long operation duration[4,29]. Opioids are very effective for the treatment of acute and chronic pain and are commonly prescribed for pain relief after surgery. One of the most common adverse effects of opioid therapy is opioid-induced bowel dysfunction[22,30]. In the present study, the incidence of PPOI was significantly lower in patients without postoperative use of opioid drugs. Similar conclusions, that reducing opioid-based analgesics shortened the duration of PPOI, were also drawn in previous studies[21,31]. In addition, opioid receptor-specific antagonist drugs, such as methylnaltrexone and alvimopan, are being investigated and hold promise for preventing or resolving the clinically relevant problem of PPOI[8,32,33].

There is a growing body of literature that recognizes serum albumin as a marker of nutritional status and that hypoalbuminemia is correlated with a higher rate of postoperative complications[17,19,34]. The present study mainly focused on the relationship between preoperative albumin and the presence of PPOI. Strong

Table 2 Univariate analysis of the potential clinicopathologic variables of Prolonged postoperative ileus

Characteristics	Without PPOI (*n* = 244)	With PPOI (*n* = 67)	Univariate OR (95%CI)	*P* value
Sex				0.362
Female	76 (81.72%)	17 (18.28%)	Ref.	
Male	168 (77.06%)	50 (22.97%)	1.33 (0.72, 2.46)	
Age (yr)				0.867
< 60	123 (78.58%)	33 (21.15%)	Ref.	
≥ 60	121 (78.06%)	34 (21.94%)	1.05 (0.61, 1.80)	
Body mass index (kg/m^2)				0.886
< 25	136 (78.16%)	38 (21.84%)	Ref.	
≥ 25	108 (78.83%)	29 (21.17%)	0.96 (0.56, 1.66)	
Previous abdominal surgery				0.803
No	197 (78.17%)	55 (21.83%)	Ref.	
Yes	47 (79.66%)	12 (20.34%)	0.91 (0.45, 1.84)	
Preoperative albumin (g/L)				0.029
< 39.15	98 (72.59%)	37 (27.41%)	Ref.	
≥ 39.15	146 (82.95%)	30 (17.05%)	0.54 (0.32, 0.94)	
Preoperative K^+ (mmol/L)				0.701
< 3.96	123 (79.35%)	32 (20.65%)	Ref.	
≥ 3.96	121 (77.56%)	35 (22.44%)	1.11 (0.65, 1.91)	
Type of cancer				0.424
Gastric cancer	130 (80.25%)	32 (19.75%)	Ref.	
Colorectal cancer	114 (76.51%)	35 (23.49%)	1.25 (0.73, 2.14)	
Surgical technique				0.839
Endoscopic surgery	168 (78.14%)	47 (21.86%)	Ref.	
Open surgery	76 (79.17%)	20 (20.83%)	0.94 (0.52, 1.70)	
Tumor stage				< 0.001
I-II	118 (88.72%)	15 (11.28%)	Ref.	
III-IV	121 (69.94%)	52 (30.06%)	3.33 (1.81, 6.25)	
Postoperative opioid analgesic				< 0.001
No	164 (85.86%)	27 (14.14%)	Ref.	
Yes	80 (66.67%)	40 (33.33%)	3.04 (1.74, 5.30)	

PPOI: Prolonged postoperative ileus; OR: Odds ratio; CI: Confidence Interval.

evidence was found of a significant positive correlation between the decrease in preoperative albumin and PPOI. This result was confirmed in different adjusted multivariate models using albumin as a continuous or categorical variable. Albumin is a protein synthesized by the liver and helps maintain plasma osmolality. It does not leak into other tissues and carries various substances throughout the body, including hormones, vitamins, and enzymes[35,36]. Hypoalbuminemia is often observed in patients with GI cancer due to diet deficiencies, weakened liver function and GI bleeding[37,38]. Low levels of preoperative albumin are always associated with more extracellular fluid filling the spaces between tissues[39], which could result in surgical site infection and anastomotic leakage[17]. Furthermore, albumin catabolism is a major source of tumor growth, and a lower level of albumin indicates the severity and duration of GI cancers[40]. Preoperative albumin was also demonstrated to be a reliable and reproducible predictor of surgical risk and postoperative complications[16,41]. Thus, the level of preoperative albumin may reflect the overall preoperative physical condition and the function of GI anastomosis after resection.

To quantitate the probability of PPOI occurrence, a nomogram was established by backward step-down selection. Preoperative albumin and the other four independent variables were filtered out. The AUC value (0.741) showed the good performance of this nomogram. We developed the prediction model using the entire data set and then used resampling techniques to evaluate the performance. Resampling techniques,

Table 3 Association between perioperative albumin and prolonged postoperative ileus by multiple regression analysis in different models

Models	Crude model	*P* value	Model I	*P* value	Model II	*P* value
Preoperative albumin (g/L)	OR (95%CI)		OR (95%CI)		OR (95%CI)	
Continuous variable						
Per unit	0.95 (0.88, 1.02)	0.174	0.95 (0.88, 1.02)	0.155	0.92 (0.85, 1.00)	0.046
Per SD (3.67)	0.83 (0.63, 1.09)	0.174	0.82 (0.62, 1.08)	0.155	0.73 (0.54, 0.99)	0.046
Categorical variable						
< 39.15	Ref.		Ref.		Ref.	
≥ 39.15	0.54 (0.32, 0.94)	0.029	0.53 (0.31, 0.92)	0.025	0.43 (0.24, 0.78)	0.006

Crude model covariants were not adjusted; Model I minimally adjusted for sex, age and body mass index (BMI); Model II fully adjusted for sex, age, BMI, type of cancer, surgical technique, tumor stage and use of a postoperative opioid analgesic. PPOI: Prolonged postoperative ileus; OR: Odds ratio; CI: Confidence Interval: SD: Standard error.

generally referred to as "internal validation", are recommended as a prerequisite for prediction model development, particularly if data are limited[42]. This nomogram could be identified as an important early warning sign of PPOI in patients who underwent GI surgery.

Our study had several strengths. First, previous studies mainly focused on investigating variables that were only determined during or after surgery when predicting PPOI. Our study firstly demonstrated preoperative albumin as a predictive indicator that would be available before surgery. Second, this study established a nomogram for quantifying the presence of PPOI, and it was further validated by internal bootstrap.

The present study also has several limitations. First, this study was retrospective in nature which may not bring out many variables in a clinical setting such as complications and blood requirement during surgery, total procedure time, bowel handling and manipulation during the procedure and the resultant release of local inflammatory mediators. Thus, further studies with a prospective and multi-centered design are warranted. Second, due to the small number of patients and the prospectively collected registry database, it was difficult to develop external validation of the nomogram. In order to make up for this limitation, we sought to validate this model using bootstrap.

In conclusion, this retrospective cohort study suggests that PPOI is a common postoperative complication in patients who undergo gastric or colorectal surgery. Advanced tumor stage, use of opioid analgesics and lower preoperative albumin level were the main risk factors for PPOI. Preoperative albumin is an independent predictive factor for PPOI in patients undergoing GI surgery. In the present study, an easy-to-use nomogram was established to quantify the presence of PPOI, which may serve as an early warning sign of PPOI in clinical practice. Due to the retrospective nature of this study, caution should be exercised in proposing the nomogram in clinical practice.

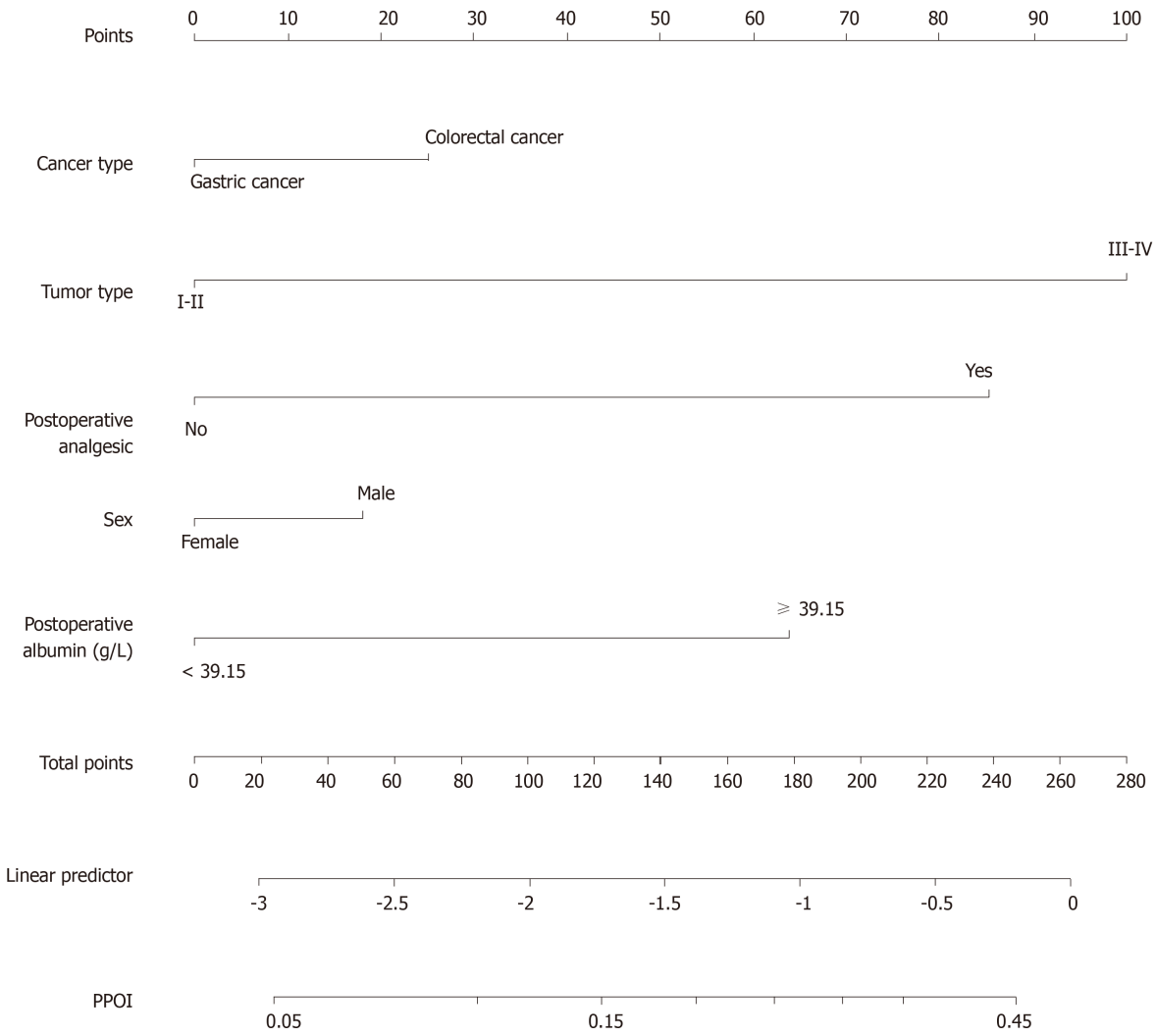

Figure 2 Nomogram prediction of prolonged postoperative ileus.

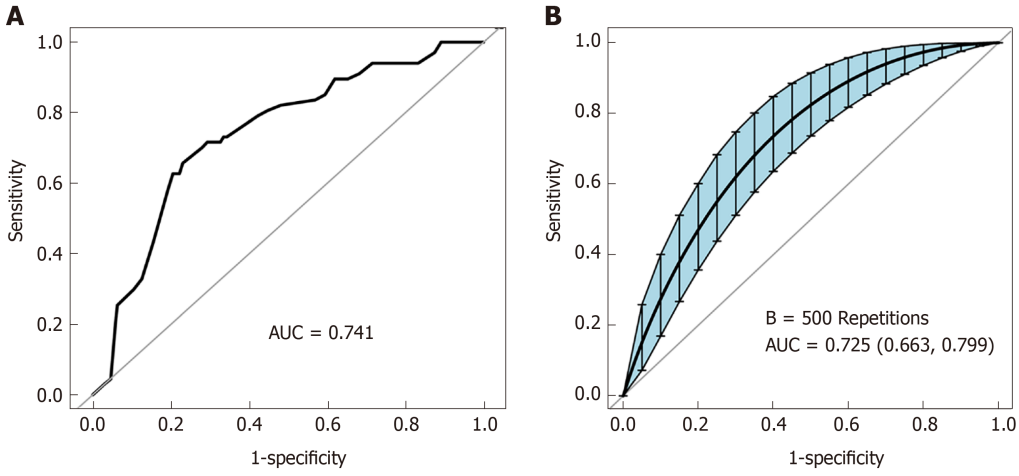

Figure 3 Receiver operating characteristic curve. A: The ROC curve of the nomogram; B: The ROC curve was measured by bootstrap for 500 repetitions. AUC: Area under the receiver operating characteristic curve.

ARTICLE HIGHLIGHTS

Research background

Prolonged postoperative ileus (PPOI) is a prolonged state of "pathological" gastrointestinal (GI)

tract dysmotility. PPOI is an essential contributor to increased hospitalization costs and prolonged hospitalization.

Research motivation
It is well known that preoperative albumin affects the outcome and mortality of patients undergoing any surgical procedure. We hypothesized that preoperative albumin may be an independent indicator of PPOI.

Research objectives
The present study aimed to investigate the association between preoperative albumin and PPOI to establish a nomogram for clinical risk evaluation.

Research methods
A total of 311 patients diagnosed with gastric or colorectal cancer were retrospectively included. We performed univariate and multivariable logistic regression analyses to determine the relationship between variables and PPOI, and a nomogram to quantify the presence of PPOI was developed and internally validated.

Research results
The overall PPOI rate was 21.54%. Patients in an advanced tumor stage and who were administered postoperative opioid analgesics were more likely to develop PPOI. This study found and further confirmed that preoperative albumin was an independent predictor of PPOI. A nomogram was established to accurately quantitate the probability of PPOI occurrence. This nomogram was confirmed to have a good diagnostic performance and was also internally validated.

Research conclusions
Preoperative albumin is an independent predictive factor of PPOI in patients who underwent GI surgery. An easy-to-use nomogram was established to quantify the presence of PPOI, which may serve as an early warning sign of PPOI in clinical practice.

Research perspectives
Due to the retrospective nature of this study, caution should be exercised in proposing the nomogram in clinical practice.

ACKNOWLEDGEMENTS

We are very grateful to Liu Jie (General Hospital of Chinese PLA), Li Haibo PhD (Peking University Hospital of Stomatology) and Li Wenjing PhD (Peking Union Medical College) for their help in statistical analysis.

REFERENCES

1 **Bragg D**, El-Sharkawy AM, Psaltis E, Maxwell-Armstrong CA, Lobo DN. Postoperative ileus: Recent developments in pathophysiology and management. *Clin Nutr* 2015; **34**: 367-376 [PMID: 25819420 DOI: 10.1016/j.clnu.2015.01.016]
2 **Pavoor R**, Milsom J. Postoperative ileus after laparoscopic colectomy: elusive and expensive. *Ann Surg* 2011; **254**: 1075; author reply 1075-1075; author reply 1076 [PMID: 22107744 DOI: 10.1097/SLA.0b013e31823ac397]
3 **Tevis SE**, Carchman EH, Foley EF, Harms BA, Heise CP, Kennedy GD. Postoperative Ileus--More than Just Prolonged Length of Stay? *J Gastrointest Surg* 2015; **19**: 1684-1690 [PMID: 26105552 DOI: 10.1007/s11605-015-2877-1]
4 **Artinyan A**, Nunoo-Mensah JW, Balasubramaniam S, Gauderman J, Essani R, Gonzalez-Ruiz C, Kaiser AM, Beart RW. Prolonged postoperative ileus-definition, risk factors, and predictors after surgery. *World J Surg* 2008; **32**: 1495-1500 [PMID: 18305994 DOI: 10.1007/s00268-008-9491-2]
5 **Chan DC**, Liu YC, Chen CJ, Yu JC, Chu HC, Chen FC, Chen TW, Hsieh HF, Chang TM, Shen KL. Preventing prolonged post-operative ileus in gastric cancer patients undergoing gastrectomy and intraperitoneal chemotherapy. *World J Gastroenterol* 2005; **11**: 4776-4781 [PMID: 16097043 DOI: 10.3748/wjg.v11.i31.4776]
6 **Kronberg U**, Kiran RP, Soliman MS, Hammel JP, Galway U, Coffey JC, Fazio VW. A characterization of factors determining postoperative ileus after laparoscopic colectomy enables the generation of a novel predictive score. *Ann Surg* 2011; **253**: 78-81 [PMID: 21233608 DOI: 10.1097/SLA.0b013e3181fcb83e]
7 **van Bree SH**, Nemethova A, Cailotto C, Gomez-Pinilla PJ, Matteoli G, Boeckxstaens GE. New therapeutic strategies for postoperative ileus. *Nat Rev Gastroenterol Hepatol* 2012; **9**: 675-683 [PMID: 22801725 DOI: 10.1038/nrgastro.2012.134]
8 **Becker G**, Blum HE. Novel opioid antagonists for opioid-induced bowel dysfunction and postoperative ileus. *The Lancet* 2009; 1198-1206 [DOI: 10.1016/s0140-6736(09)60139-2]
9 **Iyer S**, Saunders WB, Stemkowski S. Economic burden of postoperative ileus associated with colectomy in the United States. *J Manag Care Pharm* 2009; **15**: 485-494 [PMID: 19610681 DOI: 10.18553/jmcp.2009.15.6.485]
10 **Chapuis PH**, Bokey L, Keshava A, Rickard MJ, Stewart P, Young CJ, Dent OF. Risk factors for prolonged ileus after resection of colorectal cancer: an observational study of 2400 consecutive patients. *Ann Surg* 2013; **257**: 909-915 [PMID: 23579542 DOI: 10.1097/SLA.0b013e318268a693]

11 **van Bree SH**, Bemelman WA, Hollmann MW, Zwinderman AH, Matteoli G, El Temna S, The FO, Vlug MS, Bennink RJ, Boeckxstaens GE. Identification of clinical outcome measures for recovery of gastrointestinal motility in postoperative ileus. *Ann Surg* 2014; **259**: 708-714 [PMID: 23657087 DOI: 10.1097/SLA.0b013e318293ee55]

12 **Moghadamyeghaneh Z**, Hwang GS, Hanna MH, Phelan M, Carmichael JC, Mills S, Pigazzi A, Stamos MJ. Risk factors for prolonged ileus following colon surgery. *Surg Endosc* 2016; **30**: 603-609 [PMID: 26017914 DOI: 10.1007/s00464-015-4247-1]

13 **Reichert M**, Weber C, Pons-Kühnemann J, Hecker M, Padberg W, Hecker A. Protective loop ileostomy increases the risk for prolonged postoperative paralytic ileus after open oncologic rectal resection. *Int J Colorectal Dis* 2018; **33**: 1551-1557 [PMID: 30112664 DOI: 10.1007/s00384-018-3142-3]

14 **Sugawara K**, Kawaguchi Y, Nomura Y, Suka Y, Kawasaki K, Uemura Y, Koike D, Nagai M, Furuya T, Tanaka N. Perioperative Factors Predicting Prolonged Postoperative Ileus After Major Abdominal Surgery. *J Gastrointest Surg* 2018; **22**: 508-515 [PMID: 29119528 DOI: 10.1007/s11605-017-3622-8]

15 **Hennessey DB**, Burke JP, Ni-Dhonochu T, Shields C, Winter DC, Mealy K. Preoperative hypoalbuminemia is an independent risk factor for the development of surgical site infection following gastrointestinal surgery: a multi-institutional study. *Ann Surg* 2010; **252**: 325-329 [PMID: 20647925 DOI: 10.1097/SLA.0b013e3181e9819a]

16 **Blomberg J**, Lagergren P, Martin L, Mattsson F, Lagergren J. Albumin and C-reactive protein levels predict short-term mortality after percutaneous endoscopic gastrostomy in a prospective cohort study. *Gastrointest Endosc* 2011; **73**: 29-36 [PMID: 21074760 DOI: 10.1016/j.gie.2010.09.012]

17 **Shimura T**, Toiyama Y, Hiro J, Imaoka H, Fujikawa H, Kobayashi M, Ohi M, Inoue Y, Mohri Y, Kusunoki M. Monitoring perioperative serum albumin can identify anastomotic leakage in colorectal cancer patients with curative intent. *Asian J Surg* 2018; **41**: 30-38 [PMID: 27451010 DOI: 10.1016/j.asjsur.2016.07.009]

18 **Vather R**, Trivedi S, Bissett I. Defining postoperative ileus: results of a systematic review and global survey. *J Gastrointest Surg* 2013; **17**: 962-972 [PMID: 23377782 DOI: 10.1007/s11605-013-2148-y]

19 **Lehmann S**, Ferrie S, Carey S. Nutrition Management in Patients With Chronic Gastrointestinal Motility Disorders: A Systematic Literature Review. *Nutr Clin Pract* 2019 [PMID: 30989698 DOI: 10.1002/ncp.10273]

20 **Kuruba R**, Fayard N, Snyder D. Epidural analgesia and laparoscopic technique do not reduce incidence of prolonged ileus in elective colon resections. *Am J Surg* 2012; **204**: 613-618 [PMID: 22906251 DOI: 10.1016/j.amjsurg.2012.07.011]

21 **Koo KC**, Yoon YE, Chung BH, Hong SJ, Rha KH. Analgesic opioid dose is an important indicator of postoperative ileus following radical cystectomy with ileal conduit: experience in the robotic surgery era. *Yonsei Med J* 2014; **55**: 1359-1365 [PMID: 25048497 DOI: 10.3349/ymj.2014.55.5.1359]

22 **Panchal SJ**, Müller-Schwefe P, Wurzelmann JI. Opioid-induced bowel dysfunction: prevalence, pathophysiology and burden. *Int J Clin Pract* 2007; **61**: 1181-1187 [PMID: 17488292 DOI: 10.1111/j.1742-1241.2007.01415.x]

23 **Kernan WN**, Viscoli CM, Brass LM, Broderick JP, Brott T, Feldmann E, Morgenstern LB, Wilterdink JL, Horwitz RI. Phenylpropanolamine and the risk of hemorrhagic stroke. *N Engl J Med* 2000; **343**: 1826-1832 [PMID: 11117973 DOI: 10.1056/NEJM200012213432501]

24 **Anup R**, Balasubramanian KA. Surgical stress and the gastrointestinal tract. *J Surg Res* 2000; **92**: 291-300 [PMID: 10896836 DOI: 10.1006/jsre.2000.5874]

25 **Thomas S**, Balasubramanian KA. Role of intestine in postsurgical complications: involvement of free radicals. *Free Radic Biol Med* 2004; **36**: 745-756 [PMID: 14990353 DOI: 10.1016/j.freeradbiomed.2003.11.027]

26 **Wolthuis AM**, Bislenghi G, Fieuws S, de Buck van Overstraeten A, Boeckxstaens G, D'Hoore A. Incidence of prolonged postoperative ileus after colorectal surgery: a systematic review and meta-analysis. *Colorectal Dis* 2016; **18**: O1-O9 [PMID: 26558477 DOI: 10.1111/codi.13210]

27 **Huang DD**, Zhuang CL, Wang SL, Pang WY, Lou N, Zhou CJ, Chen FF, Shen X, Yu Z. Prediction of Prolonged Postoperative Ileus After Radical Gastrectomy for Gastric Cancer: A Scoring System Obtained From a Prospective Study. *Medicine (Baltimore)* 2015; **94**: e2242 [PMID: 26705206 DOI: 10.1097/MD.0000000000002242]

28 **Wehner S**, Vilz TO, Stoffels B, Kalff JC. Immune mediators of postoperative ileus. *Langenbecks Arch Surg* 2012; **397**: 591-601 [PMID: 22382699 DOI: 10.1007/s00423-012-0915-y]

29 **Vather R**, Josephson R, Jaung R, Robertson J, Bissett I. Development of a risk stratification system for the occurrence of prolonged postoperative ileus after colorectal surgery: a prospective risk factor analysis. *Surgery* 2015; **157**: 764-773 [PMID: 25724094 DOI: 10.1016/j.surg.2014.12.005]

30 **Pappagallo M**. Incidence, prevalence, and management of opioid bowel dysfunction. *Am J Surg* 2001; **182**: 11S-18S [PMID: 11755892 DOI: 10.1016/s0002-9610(01)00782-6]

31 **Delaney CP**. Clinical perspective on postoperative ileus and the effect of opiates. *Neurogastroenterol Motil* 2004; **16** Suppl 2: 61-66 [PMID: 15357853 DOI: 10.1111/j.1743-3150.2004.00559.x]

32 **Xu LL**, Zhou XQ, Yi PS, Zhang M, Li J, Xu MQ. Alvimopan combined with enhanced recovery strategy for managing postoperative ileus after open abdominal surgery: a systematic review and meta-analysis. *J Surg Res* 2016; **203**: 211-221 [PMID: 27338552 DOI: 10.1016/j.jss.2016.01.027]

33 **Nair A**. Alvimopan for post-operative ileus: What we should know? *Acta Anaesthesiol Taiwan* 2016; **54**: 97-98 [PMID: 27825721 DOI: 10.1016/j.aat.2016.10.001]

34 **Lu PH**, Wei MX, Shen W, Li C, Cai B, Tao GQ. Is preoperative serum albumin enough to ensure nutritional status in the development of surgical site infection following gastrointestinal surgery? *Ann Surg* 2011; **254**: 663-4; author reply 664 [PMID: 21892073 DOI: 10.1097/SLA.0b013e318230616c]

35 **Kmieć Z**. Cooperation of liver cells in health and disease. *Adv Anat Embryol Cell Biol* 2001; **161**: III-XIII, 1-151 [PMID: 11729749 DOI: 10.1007/978-3-642-56553-3]

36 **Lu CY**, Wu DC, Wu IC, Chu KS, Sun LC, Shih YL, Chen FM, Hsieh JS, Wang JY. Serum albumin level in the management of postoperative enteric fistula for gastrointestinal cancer patients. *J Invest Surg* 2008; **21**: 25-32 [PMID: 18197531 DOI: 10.1080/08941930701833959]

37 **Nassri A**, Zhu H, Wang DH, Ramzan Z. Serum Albumin at Diagnosis is an Independent Predictor of Early Mortality in Veteran Patients with Esophageal Cancer. *Nutr Cancer* 2018; **70**: 1246-1253 [PMID: 30235013 DOI: 10.1080/01635581.2018.1512639]

38 **SAFE Study Investigators**, Finfer S, Bellomo R, McEvoy S, Lo SK, Myburgh J, Neal B, Norton R. Effect of baseline serum albumin concentration on outcome of resuscitation with albumin or saline in patients in intensive care units: analysis of data from the saline versus albumin fluid evaluation (SAFE)

study. *BMJ* 2006; **333**: 1044 [PMID: 17040925 DOI: 10.1136/bmj.38985.398704.7C]
39 **Doweiko JP**, Nompleggi DJ. Reviews: The Role of Albumin in Human Physiology and Pathophysiology, Part III: Albumin and Disease States. *Jpen-Parenter Enter* 2016; **15**: 476-483 [PMID: 1895489 DOI: 10.1177/0148607191015004476]
40 **Kratz F**. Albumin as a drug carrier: design of prodrugs, drug conjugates and nanoparticles. *J Control Release* 2008; **132**: 171-183 [PMID: 18582981 DOI: 10.1016/j.jconrel.2008.05.010]
41 **Bendersky V**, Sun Z, Adam MA, Rushing C, Kim J, Youngwirth L, Turner M, Migaly J, Mantyh CR. Determining the Optimal Quantitative Threshold for Preoperative Albumin Level Before Elective Colorectal Surgery. *J Gastrointest Surg* 2017; **21**: 692-699 [PMID: 28138809 DOI: 10.1007/s11605-017-3370-9]
42 **Collins GS**, Reitsma JB, Altman DG, Moons KG. Transparent reporting of a multivariable prediction model for individual prognosis or diagnosis (TRIPOD): the TRIPOD statement. *BMJ* 2015; **350**: g7594 [PMID: 25569120 DOI: 10.1136/bmj.g7594]

World Journal of Gastroenterology

Submit a Manuscript: https://www.f6publishing.com

World J Gastroenterol 2020 March 21; 26(11): 1197-1207

DOI: 10.3748/wjg.v26.i11.1197

ISSN 1007-9327 (print) ISSN 2219-2840 (online)

ORIGINAL ARTICLE

Retrospective Study

Landscape of BRIP1 molecular lesions in gastrointestinal cancers from published genomic studies

Ioannis A Voutsadakis

ORCID number: Ioannis A Voutsadakis (0000-0002-9301-5951).

Author contributions: Voutsadakis IA designed research, performed research, analyzed data and wrote the paper.

Institutional review board statement: This study was a retrospective analysis of previously published data, available in the public domain, no IRB approval is required.

Informed consent statement: Given that this is a retrospective analysis of previously published, anonymized data, no patient informed consent was required or obtained.

Conflict-of-interest statement: I have no financial relationships to disclose.

Data sharing statement: No additional data are available.

Manuscript source: Invited

Ioannis A Voutsadakis, Algoma District Cancer Program, Sault Area Hospital, Sault Ste Marie, ON P6B 0A8, Canada

Ioannis A Voutsadakis, Section of Internal Medicine, Division of Clinical Sciences, Northern Ontario School of Medicine, Sudbury, ON P0M 2Z0, Canada

Corresponding author: Ioannis A Voutsadakis, MD, PhD, Assistant Professor, Doctor, Algoma District Cancer Program, Sault Area Hospital, 750 Great Northern Road, Sault Ste Marie, ON P6B 0A8, Canada. ivoutsadakis@yahoo.com

Abstract

BACKGROUND

BRIP1 is a helicase that partners with BRCA1 in the homologous recombination (HR) step in the repair of DNA inter-strand cross-link lesions. It is a rare cause of hereditary ovarian cancer in patients with no mutations of *BRCA1* or *BRCA2*. The role of the protein in other cancers such as gastrointestinal (GI) carcinomas is less well characterized but given its role in DNA repair it could be a candidate tumor suppressor similarly to the two BRCA proteins.

AIM

To analyze the role of helicase BRIP1 (FANCJ) in GI cancers pathogenesis.

METHODS

Publicly available data from genomic studies of esophageal, gastric, pancreatic, cholangiocarcinomas and colorectal cancers were interrogated to unveil the role of BRIP1 in these carcinomas and to discover associations of lesions in BRIP1 with other more common molecular defects in these cancers.

RESULTS

Molecular lesions in BRIP1 were rare (3.6% of all samples) in GI cancers and consisted almost exclusively of mutations and amplifications. Among mutations, 40% were possibly pathogenic according to the OncoKB database. A majority of *BRIP1* mutated GI cancers were hyper-mutated due to concomitant mutations in mismatch repair or polymerase ε and δ1 genes. No associations were discovered between amplifications of *BRIP1* and any mutated genes. In gastroesophageal cancers BRIP1 amplification commonly co-occurs with ERBB2 amplification.

CONCLUSION

Overall BRIP1 molecular defects do not seem to play a major role in GI cancers whereas mutations frequently occur in hypermutated carcinomas and co-occur with other HR genes mutations. Despite their rarity, BRIP1 defects may present

manuscript

Received: December 6, 2019
Peer-review started: December 6, 2019
First decision: February 16, 2020
Revised: February 21, 2020
Accepted: March 5, 2020
Article in press: March 5, 2020
Published online: March 21, 2020

P-Reviewer: Chiu KW, Cerwenka H, Hashimoto N, Slomiany BL
S-Editor: Dou Y
L-Editor: A
E-Editor: Liu JH

an opportunity for therapeutic interventions similar to other HR defects.

Key words: *BRIP1*; *FANCJ*; *BACH1*; Gastrointestinal cancers; Mutations; Copy number alterations

Core tip: *BRIP1* gene alterations are uncommon in gastrointestinal cancers. Mutations frequently occur in hypermutated carcinomas and co-occur with other homologous recombination genes mutations. Despite their rarity, BRIP1 defects may present an opportunity for therapeutic interventions similar to other homologous recombination defects.

Citation: Voutsadakis IA. Landscape of BRIP1 molecular lesions in gastrointestinal cancers from published genomic studies. *World J Gastroenterol* 2020; 26(11): 1197-1207
URL: https://www.wjgnet.com/1007-9327/full/v26/i11/1197.htm
DOI: https://dx.doi.org/10.3748/wjg.v26.i11.1197

INTRODUCTION

BRIP1 [BRCA1 interacting protein C-terminal helicase 1, alternatively called FANCJ, Fanconi Anemia (FA) complementation group J or BACH1, BRCA1 Associated C-terminal Helicase 1] is a 1249 amino-acid protein with helicase function that participates in DNA homeostasis. The gene (Gene ID: 83990) is located at human chromosome 17q23.2 and consists of 20 exons, 19 of which (exons 2 to 20) are coding. BRIP1 protein plays a role in DNA repair through homologous recombination (HR) and interacts with BRCA1[1]. BRIP1 has also BRCA1 independent effects in DNA repair that depend on the helicase activity[2]. Besides BRCA1, BRIP1 interacts with mismatch repair (MMR) protein MLH1 and promotes signaling for apoptosis at sites with O^6-methylated guanine adducts[3]. BRIP1 mutant cells that lose the ability for MLH1 interaction survive better when methyl-guanine methyltransferase MGMT is functional as MGMT has more time to process the defective site. BRIP1-MLH1 interaction may be as important as the interaction with BRCA1 in signaling from inter-strand cross-links and underlines the role of BRIP1 as a key player at the cross-roads of DNA repair though the FA pathway and the MMR as well as the HR pathway[4]. Besides inter-strand cross-links, a role of BRIP1 in repairing other abnormal DNA structures, such as G-quadruplex structures and hairpins, arising during DNA replication, under replication stress, has been recently established[5].

BRIP1 has been implicated in hereditary ovarian cancers that lack *BRCA1* or *BRCA2* mutations[6]. Up to 0.6%-0.9% of ovarian cancers may carry pathogenic variants in BRIP1, although the percentage may vary in different populations[7]. A role of *BRIP1* in hereditary breast cancer has also been proposed but is debated[8,9]. Similarly, rare cases of prostate cancer with *BRIP1* mutations reminiscent of prostate cancer in BRCA2 families have been reported[10,11]. Leukemia predisposition is part of FA and has been described with BRIP1 hereditary mutations, in common with other FA complementation group gene mutations[12]. The implication of BRIP1 as a tumor suppressor in other hereditary cancers or in sporadic cancers is even less clear.

This paper investigates the role of BRIP1 defects in gastrointestinal (GI) cancers exploring publicly available genomic data from The Cancer Genome Atlas (TCGA) available in the cBioportal of cancer genomics platform.

MATERIALS AND METHODS

Studies performed by TCGA consortium (PanCancer Atlas) that were evaluated in the current investigation included esophageal adenocarcinoma (containing 182 samples), gastric adenocarcinoma (containing 440 samples), pancreatic adenocarcinoma (containing 184 samples), colorectal cancer (containing 594 samples), cholangiocarcinoma (with 36 samples)[13-17]. Analyses were performed in the cBioCancer Genomics Portal (cBioportal, http://www.cbioportal.org) platform[18,19]. cBioportal contains 172 non-overlapping genomic studies published by TCGA and by other

investigators worldwide and empowers interrogation of each study or group of studies for genetic lesions in any gene of interest, in a user-friendly manner. The five studies selected for the current investigation cover the most updated available TCGA results of the most common GI cancers.

cBioportal currently provides assessment of the functional implications of mutations of interest using the mutation assessor and other relevant tools. The mutation assessor (mutationassessor.org) uses a multiple sequence alignment algorithm to assign a prediction score of functional significance to each mutation[20]. Data from the mutation assessor as reported in cBioportal were used for evaluation of putative functional repercussions of *BRIP1* mutations and other mutations of interest. Data from the OncoKB database, a precision oncology database annotating the biologic and oncogenic significance of somatic cancer mutations were incorporated in the functional assessment of discussed mutations[21].

Survival of gastric cancer patients with high expression of *BRIP1* mRNA *vs* those with low *BRIP1* mRNA expression was compared using the online tool Kaplan Meier Plotter (kmplot.com)[22]. This online tool currently does not include other GI cancers.

Investigation of BRIP1 promoters was performed using the EPD database (http://epd.epfl.ch) and putative transcription factor binding sites were identified using the JASPAR CORE 2018 vertebrate database[23].

For further analyses that could not be performed directly in cBioportal, the list of genes and relevant mutated or amplified samples from each study of interest was transferred to an Excel sheet (Microsoft Corp., Redmond, WA) for performance of required calculations. Categorical and continuous data were compared with the Fisher's exact test and the *t* test respectively. Correlations were explored with the Pearson correlation coefficient. All statistical comparisons were considered significant if $P < 0.05$. Correction for multiple comparisons was performed using the Benjamini-Hochberg false discovery rate correction procedure.

RESULTS

The frequency of *BRIP1* mutations was low in the GI cancers examined. Among the 1436 samples included in the 5 interrogated studies, 30 samples (2.1%) had one or more *BRIP1* mutations. There was a total of 38 *BRIP1* mutations in these 30 samples. The distribution of mutations in the exons of *BRIP1* is shown in Figure 1. Six of 38 mutations (15.8%) were listed as likely oncogenic in the OncoKB database (Table 1). These six mutations occur in different aminoacid residues in different exons besides a mutation at aminoacid I504 recurring in two samples and resulting in frame shift and protein truncation shortly thereafter. The remaining four likely oncogenic *BRIP1* mutations are nonsense mutations. The incidence of mutated *BRIP1* samples in each of the 5 studies was as follows: esophageal cancer 2.2% (4 of 182 cases), gastric cancer 1.6% (7 of 440 cases), pancreatic cancer 0.5% (1 of 184 cases), no mutations observed in the 36 samples of the cholangiocarcinoma study, colorectal cancer 3% (18 of 594 cases) (Figure 2).

The total number of mutations in *BRIP1* mutant samples varied widely ranging between 78 and 11438. The mean and median number of mutations were high (2993.2 and 1747.5 respectively) and 17 of 30 samples with *BRIP1* mutations (56.7%) had more than 1000 mutations each. Such a heavy mutation burden is usually observed in cancers with microsatellite instability (MSI) due to mutations in genes that encode for MMR proteins that include *MSH2*, *MSH6*, *MLH1* and *PMS2* or alternatively in cancers with mutations in polymerases ε and δ1 (POLE and POLD1 respectively). Indeed, 18 of the 30 *BRIP1* mutated samples (60%) contained one or more co-occurring mutations in one of these six genes. The mean number of mutations in the 18 samples with at least one co-occurring MSI/*POLE*/*POLD1* mutations was 4813 while the mean number of mutations in the 12 samples without any co-occurring MSI/*POLE*/*POLD1* mutations was 262.7. Seventeen of the 18 samples with at least one MSI/*POLE*/*POLD1* mutation had over 1000 total mutations, while none of the 12 samples with *BRIP1* mutations but no MSI/*POLE*/*POLD1* mutation had over 1000 total mutations. Two samples, including the single sample with a *BRIP1* mutation in the pancreatic cancer study that contained the higher number of total mutations, an extraordinary 11438, contained mutations in all six MSI/*POLE*/*POLD1* genes. The percentage of mutations in each of the six genes in *BRIP1*-mutated samples was significantly higher than this percentage in the samples of the 5 studies without *BRIP1* mutations (Figure 3). *POLE* mutations were observed in 14 of the 30 *BRIP1* mutant samples (46.7%). Nine of these *POLE* mutations were deemed likely oncogenic by the OncoKB database, including 4 samples with the known *POLE* hotspot mutations V411L and 2 samples with P286R/L hotspot mutations. The 5 studies contained 74

Table 1 Likely oncogenic *BRIP1* mutations in gastrointestinal cancers according to the OncoKB database

Sample ID	Cancer type	Protein change	Mutation type	Copy number	Allele frequency	Number of mutations	Exon
TCGA-A6-3807-01	Colon adenocarcinoma	S1117*	Nonsense_mutation	Diploid	0.21	90	20
TCGA-DT-5265-01	Rectal adenocarcinoma	Q227*	Nonsense_mutation	Shallow del	0.59	81	7
TCGA-AA-3496-01	Colon adenocarcinoma	I504Nfs*7	Frame_Shift_Ins	Gain	0.43	145	11
TCGA-AZ-4315-01	Colon adenocarcinoma	E357*	Nonsense_mutation	Diploid	0.32	6317	8
TCGA-L5-A4OE-01	Esophageal adenocarcinoma	Q126*	Nonsense_mutation	Gain	0.35	267	4
TCGA-CG-5721-01	Gastric adenocarcinoma	I504Sfs*22	Frame_Shift_Del	Diploid	0.22	3725	11

The column "Number of mutations" presents the total number of mutations in the respective sample. Ins: Insertion; Del: Deletion.

samples (5.1%) with mutations in *POLE* and among those 5 and 4 were the hotspot mutations V411L and P286R/L. Thus, a significant proportion of these characterized deleterious mutations co-occur with *BRIP1* mutations. Overall these data suggest that *BRIP1* mutations do not cause increased tumor burden but are commonly observed in samples with underlying MSI/*POLE*/*POLD1* mutations and thus a substantial subset of GI cancers with somatically mutated *BRIP1* have a high tumor mutation burden.

Among the six samples with likely oncogenic *BRIP1* mutations four samples had lower total mutation number (between 81 and 267, Table 1) and three of them had no concomitant MSI/*POLE*/*POLD1* mutations while the fourth, a colorectal cancer sample with a *BRIP1* frameshift mutation at I507 had a mutation in *MLH1* at L697. These data suggest that likely oncogenic *BRIP1* mutations could contribute to cancer pathogenesis without producing hypermutability. Other *BRIP1* mutations with unknown significance may be passengers in hyper-mutated cancers.

In colorectal cancer two thirds of BRIP1-mutated samples (12 of 18) contained also mutations in one or more of the commonly mutated genes of the KRAS/BRAF pathway (KRAS/NRAS/BRAF/PTEN/PIK3CA). There was a significant co-occurrence of *BRIP1* mutations with mutations in *BRAF* and *PTEN*. However, all 12 samples with *BRIP1* mutations co-occurring with the five genes of the KRAS/BRAF pathway were hypermutated and contained mutations in either *POLE* or *POLD1* or both. Thus, the presence of *BRIP1* mutations in samples with mutations in genes of the KRAS/BRAF pathway may be co-incidental due to the high mutations burden of hypermutated cancers.

Proteins directly interacting with BRIP1 during the DNA repair function include BRCA1 and MLH1. Thus, mutations of these proteins, especially in their BRIP1-interacting domains, or deletions of BRCA1 and MLH1 even in the absence of BRIP1 lesions per se may result in interference with normal function of BRIP1. BRCA1 interacts with BRIP1 through its BRCT domain (aminoacids 1662-1723 and 1757-1842). Mutations in BRCT domain of BRCA1 were observed in only one sample of the total 1436 samples in the 5 studies of GI cancers. Deletions of BRCA1 were also rare, observed in 3 samples. MLH1 interacts with BRIP1 through its carboxyterminal domain (aminoacids 478-744). Mutations in this part of MLH1 are rare, occurring in 10 samples among the 1436 total samples of the 5 GI cancers studies. Deletion of MLH1 occurred in a single sample.

Several other genes of the FA pathway were found to have low mutation frequencies in the 5 studies examined. *BRCA2* was the only gene that had a mutation percentage above 3%, specifically 6%. Despite low mutation frequencies, mutations in several of these genes such as *BRCA1*, *BRCA2, FANCI*, *FANCD2*, *PALB2*, *FANCC* and *RAD51C* were all observed to statistically significantly co-occur with *BRIP1* mutations ($P < 0.001$, $Q < 0.001$).

Comparison of *BRIP1* mutations in GI cancers with *BRIP1* mutations in breast and ovarian cancer disclosed that in breast cancers *BRIP1* mutations are uncommon (10 of 996 samples in the TCGA study of breast cancer, 1%) and contained concomitant MSI/*POLE*/*POLD1* mutations in 3 samples[24]. Similar with GI cancers, mutations of *BRIP1* in breast cancers are widely spread in different exons. In the TCGA study of ovarian cancer the 4 of 5 *BRIP1* mutated samples were observed in the absence of MSI or *POLE*/*POLD1* mutations and 3 of the 4 samples were concentrated in the DEAD-2

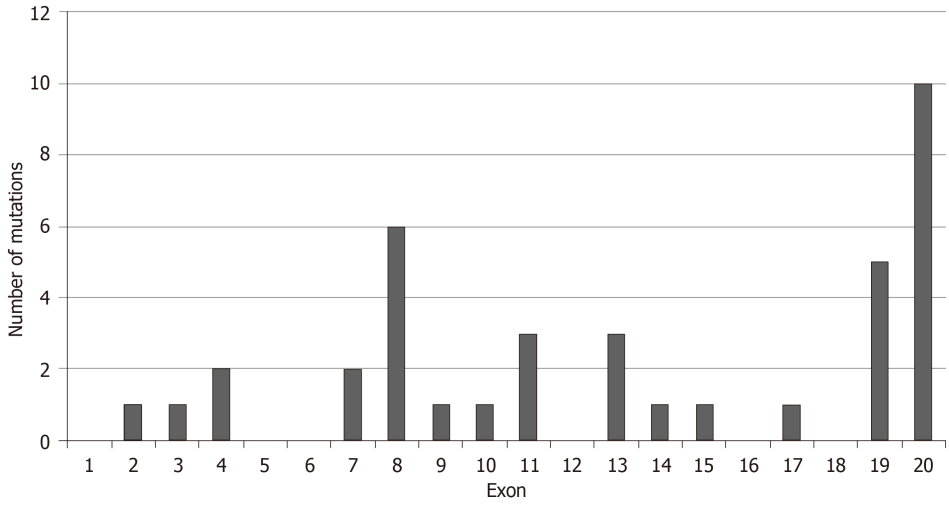

Figure 1 Number of mutations in each exon of *BRIP1*. The total number of mutations in the five gastrointestinal adenocarcinomas examined were 38 in 30 samples.

domain (aminoacids 248 to 415)[25].

Copy number alterations of *BRIP1* were also uncommon in the studies of the GI cancers examined in this analysis and included 23 *BRIP1* amplified samples (1.6%) and a single deleted sample which occurred in an esophageal cancer. Percentages of amplified samples in the various cancers are presented in Figure 4. One thousand four hundred twenty-eight genes were co-amplified significantly more often in *BRIP1* amplified samples than in *BRIP1* non-amplified. Most significant correlations, including the entire list of the top 100 most significantly co-amplified genes were neighboring genes at 17q22-17q24 loci. In gastroesophageal adenocarcinomas, *ERBB2* gene located at 17q12 is commonly amplified in about 15% of cases. Co-amplification of *ERBB2* was observed in 10 of 14 (71.4%) of *BRIP1* amplified gastroesophageal cancer cases ($P < 0.001$), suggesting that the two genes may be parts of the same amplicon in these cases. As a comparison in breast cancer, where *ERBB2* is also commonly amplified, amplification of the two genes co-occurs with statistical significance ($P < 0.001$) and 36 of the 82 cases (43.9%) with *BRIP1* amplifications contained concomitant amplification of *ERBB2*.

No significant correlations of *BRIP1* amplification with mutations in any gene were found in the GI cancers. For example, co-occurrence of *BRIP1* amplification with the most commonly mutated tumor suppressor *TP53* was observed in 45.8% of *BRIP1* amplified samples while 55.6% of *BRIP1* non-amplified samples had *TP53* mutations ($P = 0.22$). Similarly, co-occurrence of *BRIP1* amplification with the most commonly mutated oncogene *KRAS* was seen in 16.7% of *BRIP1* amplified samples, while 26.6% of *BRIP1* non-amplified samples had *KRAS* mutations ($P = 0.19$).

The promoter region of *BRIP1* gene (from -499 to 100 from Transcription Start Site) contains 5 binding motif sequences for *E2F1* transcription factor at -468, -467, -227, -72 and -71. However, despite this promoter binding potential, *E2F* and *BRIP1* overexpression does not correlate in colorectal cancer ($P = 0.13$), suggesting that E2F1 activity does not lead to over-expression of its potential target BRIP1. *E2F1* was proposed as a part of a panel of genes together with *MYBL2* and *FOXM1* that may predict tumor aneuploidy[26]. Consistent with the lack of increased *BRIP1* expression in tumors with *E2F1* over-expression, aneuploidy scores in *BRIP1* amplified GI tumors were variable, suggesting that, despite the roles of BRIP1 in DNA repair mechanisms, no direct influence of its abundance with ploidy is evident. However, despite lack of clear association with aneuploidy, increased expression of BRIP1 mRNA (above the median) was associated with improved survival in patients with gastric carcinomas compared with patients whose cancers expressed lower *BRIP1* (below the median in the series, Figure 5). Similar results were observed when only patients with localized gastric cancers were included in the survival analysis.

Another potential transcription factor of interest in the regulation of *BRIP1* is AP1 (a heterodimer of FOS and JUN) because it is often activated downstream of KRAS/BRAF/MAPK pathway, which is often dysregulated in GI cancers. However, no binding sites of AP1 were present in the *BRIP1* promoter.

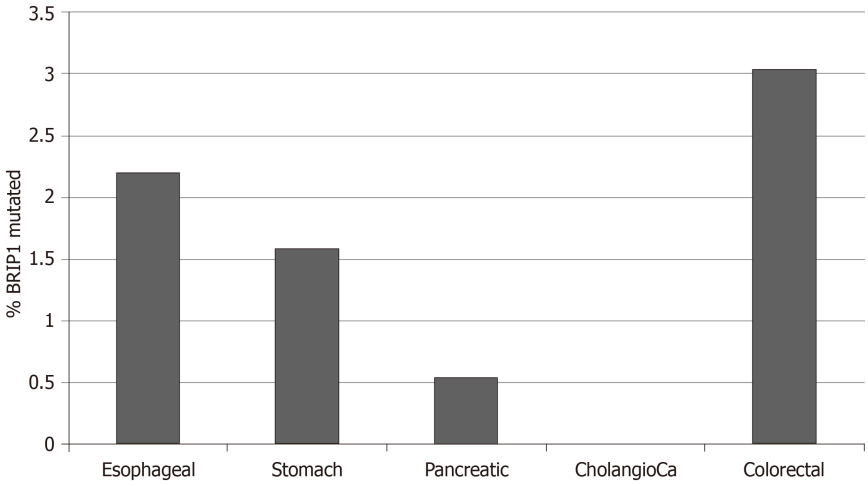

Figure 2 Percentage of *BRIP1* mutations in the five gastrointestinal adenocarcinomas.

DISCUSSION

BRIP1 (alternatively called FANCJ or BACH1) is a protein involved in DNA repair and named for both its interaction with BRCA1 and its being a FA pathway member. It belongs to a family of iron-sulfur helicases together with RTEL1, DDX11 and XPD[27]. As a BRCA1 collaborator, BRIP1 participates in DNA repair of inter-strand cross-links through HR downstream of the core FA complex and following ID2 complex (consisting of proteins FANCI and FANCD2) mono-ubiquitination[28]. Other roles of BRIP1 in DNA lesions metabolism have been revealed more recently. BRIP1 participates in protection of DNA from degradation at a stalled fork[29]. In addition, FANCJ directly interacts with MMR protein MLH1 and participates in bridging MMR complexes with the HR machinery for replication restart after inter-strand cross-links repair[30]. Moreover, a direct role of BRIP1 in resolution of G-quadruplex structures and hairpins arising during replication on single strand DNA, especially in microsatellite sites, has been revealed[31]. Consistent with this last role, cells from FANCJ FA patients show MSI, in contrast to other complementation groups[32].

The current study took advantage of published genomic data by the TCGA and the cBioportal platform as well as other online tools to investigate the role of BRIP1 in common GI cancers. Main findings include the low frequency of *BRIP1* defects in GI cancers and a significant association of *BRIP1* mutations with defects of MSI/polymerase ε and δ1 genes and the mutator phenotype. In view of the role of BRIP1 helicase in resolution of abnormal DNA structures often affecting microsatellite sites the association is intriguing and may promote MSI. Consistent with this hypothesis, samples with *BRIP1* mutations in the five studies had a mean of 4813 mutations while the mean number of mutations in the 83 samples of the colorectal TCGA study, for example, with one or more MSI/*POLE*/*POLD1* mutations was 1734. An alternative hypothesis is that samples with more functionally robust MSI/*POLE*/*POLD1* mutations, producing higher total mutation burden, would contain more commonly passenger *BRIP1* mutations.

In pancreatic cancer, where MSI and *POLE*/*POLD1* mutations are rare, *BRIP1* mutations are very rare. Specifically, only one mutation was detected in the TCGA pancreatic cancer study. Another more extensive genomic study that included 359 pancreatic adenocarcinoma samples found no *BRIP1* mutations in any of them[33].

The partner of BRIP1, BRCA1 is an important player in HR and, in this capacity, it needs to interact with chromatin. BRIP1 stabilizes this interaction. In contrast, oncogenic KRAS promotes down-regulation of BRIP1 and BRCA1 dissociation from chromatin leading to cell senescence[34]. Activating mutations in KRAS or other proteins of the pathway are common in GI cancers and thus may affect DNA repair through impairment of the BRCA1/BRIP1 function. This may imply that *KRAS* and *BRCA1*/*BRIP1* lesions would be redundant and mutually exclusive. In this study no such mutual exclusivity between *BRIP1* mutations and *KRAS* mutations was observed and in fact a co-occurrence of *BRIP1* mutations with mutations of other genes of KRAS pathways was present instead. This may be due to the common association of both *BRIP1* and *KRAS* pathway mutations with MSI/hypermutable cancers or alternatively due to lack of functional repercussions for some of these *BRIP1* mutations.

Gastric cancers with BRIP1 mRNA expression above the mean seem to have a

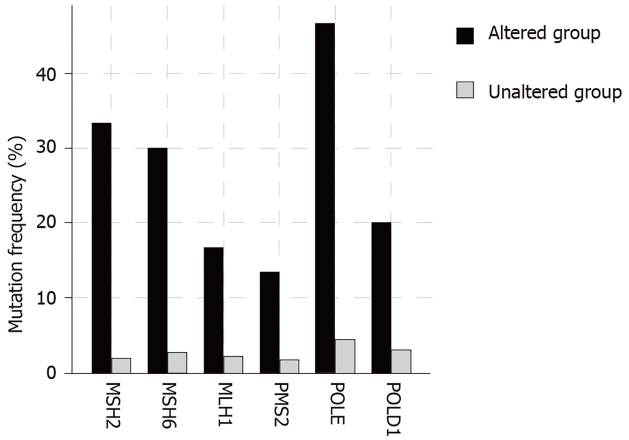

Figure 3 Mutation frequency of *MSI* and *POLE*/*POLD1* genes in gastrointestinal cancers with BRIP1 abnormalities (altered group) and without BRIP1 abnormalities (unaltered group). Comparison of the altered and unaltered group is statistically significant for all six genes.

better prognosis than counterparts with lower BRIP1 mRNA expression. This may suggest that cancers that up-regulate BRIP1 could have a less aggressive course due to a better ability to repair DNA lesions and possibly decreased genomic lesions accumulation[35].

Despite the fact that the *BRIP1* gene promoter area upstream of its transcription start site contains several putative binding motifs for transcription factor E2F1 and the fact that E2F factors have been confirmed to bind and up-regulate BRIP1 *in vitro*[36], no correlation of the expression of the two genes at the mRNA level in GI cancers was observed in the current interrogation of TCGA studies. This may imply, among other plausible explanations, that other transcription factors are involved in the regulation of BRIP1 obscuring the effect of E2F factors or that increased mRNA expression of E2F does not translate into increased expression of the proteins or increased transcription function. Another candidate transcription factor, AP1, often activated downstream of oncogenic KRAS, was ruled out as a direct regulator of *BRIP1* as it possesses no binding sites in *BRIP1* promoter.

Overall this study suggests that neutralization of BRIP1 as a tumor suppressor seems to play a minor role in GI cancers pathogenesis. However, a contribution as a defect with cumulative influence in cancers with the mutator phenotype is plausible and may be selected by promoting survival in cells with MMR or polymerase mutations, for example if it would contribute to defects in antigen presentation machinery in hypermutated cancers[37]. The association of BRIP1 with the mutator phenotype is intriguing in the current era of immunotherapy of cancer. If a contribution of BRIP1 to an expansion of instability in hypermutated cancers is confirmed, mutations in the gene may become an additional potential predictive marker of response to immunotherapies. In addition, it may suggest potential avenues for combination therapies, for example with immune checkpoint inhibitors and PARP inhibitors. Indeed, such combinations are in development[38].

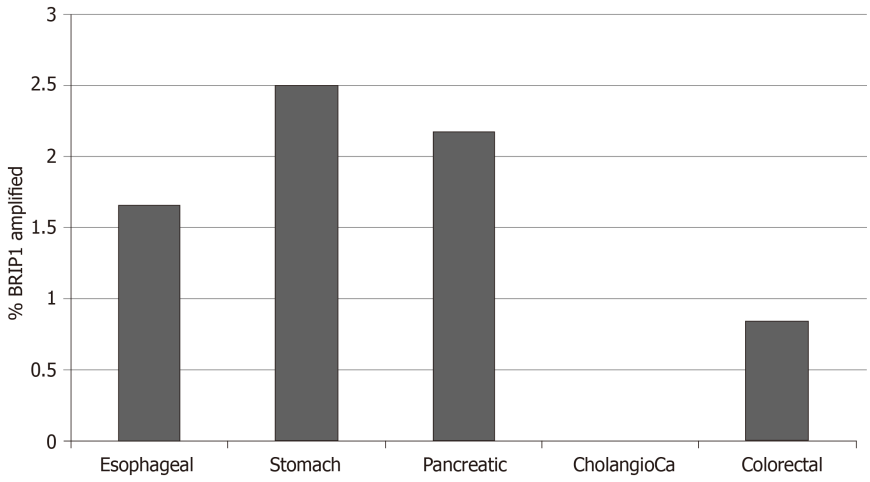

Figure 4 Percentage of BRIP1 amplifications in the five gastrointestinal adenocarcinomas.

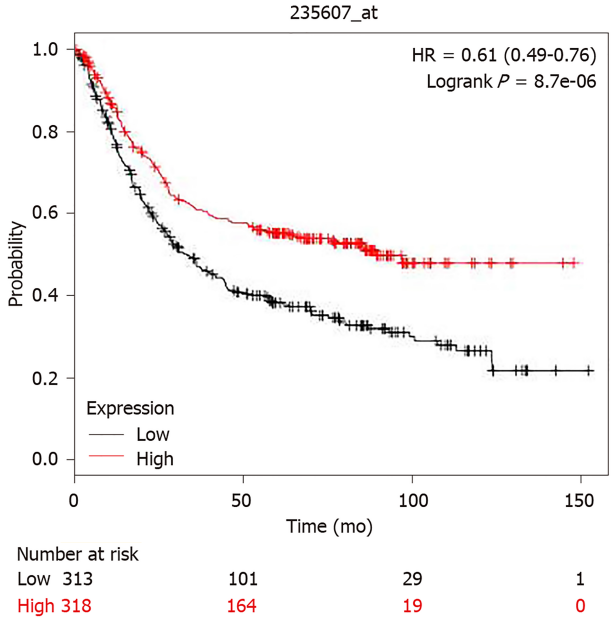

Figure 5 Comparison of overall survival in gastric cancer patients with higher (above the median) and lower (below the median) BRIP1 mRNA expression. Higher BRIP1 mRNA expression was associated with improved overall survival compared with lower BRIP1 mRNA expression in gastric cancer.

ARTICLE HIGHLIGHTS

Research background

Gastrointestinal (GI) cancers are, as a group, very common and their pathogenesis has been progressively elucidated over the last 30 years. However, the role of genetic lesions in homologous recombination (HR) DNA repair remains less well characterized in these cancers.

Research motivation

BRIP1 is a helicase with a role in HR as well as other key functions in DNA metabolism. Its specific role in GI cancers has rarely been reported. Further elucidation of molecular lesions in this gene may pave the way for targeted therapeutic interventions.

Research objectives

To analyze molecular defects of helicase BRIP1 (FANCJ) in GIcancers pathogenesis.

Research methods

GIcancer studies from The Cancer Genome Atlas (TCGA) were analyzed using the cBioportal platform and other precision medicine databases. TCGA studies were interrogated for BRIP1 mutations and copy number alterations. Associations with other key lesions in GIcancers as well as with the total tumor mutation burden in these cancers were analyzed. Additional analyses

that could not be performed directly in the cBioportal platform were performed in Excel (Microsoft Corp., Redmond, WA) after transfer of the relevant data. Appropriate statistical tests (the Fisher's exact test and the *t* test respectively) were used for analysis of categorical and continuous data.

Research results

Molecular lesions in BRIP1 are observed in 3.6% of GI cancers and consisted almost exclusively of mutations and amplifications. Two fifths of all *BRIP1* mutations are considered possibly pathogenic. Most *BRIP1* mutated GI cancers have concomitant mutations in *MMR* genes or one of the replication polymerases, polymerase ε and δ1 genes. No associations were discovered between amplifications of BRIP1 and any mutated genes. BRIP1 amplification commonly co-occurs with ERBB2 amplification, a comparatively common amplification in gastroesophageal cancers.

Research conclusions

BRIP1 gene lesions are not major pathogenic players in GI cancers. Association with microsatellite unstable cancers and ERBB2 amplifications in gastroesophageal cancers is worth noting.

Research perspectives

Molecular defects in helicase BRIP1, albeit rare, may provide opportunities for novel therapies in GI cancers. Their association with the mutator phenotype is intriguing in the current era of immunotherapy of cancer. BRIP1 defects may contribute to an expansion of instability in hypermutated cancers. Thus, *BRIP1* mutations could be an additional potential predictive marker of response to immunotherapies. A role of combination therapies, including immunotherapies with targeted therapies active in cancers with HR defects such as PARP inhibitors, in BRIP defective GI cancers is worth exploring.

REFERENCES

1 **Cantor SB**, Bell DW, Ganesan S, Kass EM, Drapkin R, Grossman S, Wahrer DC, Sgroi DC, Lane WS, Haber DA, Livingston DM. BACH1, a novel helicase-like protein, interacts directly with BRCA1 and contributes to its DNA repair function. *Cell* 2001; **105**: 149-160 [PMID: 11301010 DOI: 10.1016/S0092-8674(01)00304-X]

2 **Bridge WL**, Vandenberg CJ, Franklin RJ, Hiom K. The BRIP1 helicase functions independently of BRCA1 in the Fanconi anemia pathway for DNA crosslink repair. *Nat Genet* 2005; **37**: 953-957 [PMID: 16116421 DOI: 10.1038/ng1627]

3 **Xie J**, Guillemette S, Peng M, Gilbert C, Buermeyer A, Cantor SB. An MLH1 mutation links BACH1/FANCJ to colon cancer, signaling, and insight toward directed therapy. *Cancer Prev Res (Phila)* 2010; **3**: 1409-1416 [PMID: 20978114 DOI: 10.1158/1940-6207.CAPR-10-0118]

4 **Peng M**, Litman R, Xie J, Sharma S, Brosh RM, Cantor SB. The FANCJ/MutLalpha interaction is required for correction of the cross-link response in FA-J cells. *EMBO J* 2007; **26**: 3238-3249 [PMID: 17581638 DOI: 10.1038/sj.emboj.7601754]

5 **Bharti SK**, Awate S, Banerjee T, Brosh RM. Getting Ready for the Dance: FANCJ Irons Out DNA Wrinkles. *Genes (Basel)* 2016; **7** [PMID: 27376332 DOI: 10.3390/genes7070031]

6 **Ramus SJ**, Song H, Dicks E, Tyrer JP, Rosenthal AN, Intermaggio MP, Fraser L, Gentry-Maharaj A, Hayward J, Philpott S, Anderson C, Edlund CK, Conti D, Harrington P, Barrowdale D, Bowtell DD, Alsop K, Mitchell G; AOCS Study Group, Cicek MS, Cunningham JM, Fridley BL, Alsop J, Jimenez-Linan M, Poblete S, Lele S, Sucheston-Campbell L, Moysich KB, Sieh W, McGuire V, Lester J, Bogdanova N, Dürst M, Hillemanns P; Ovarian Cancer Association Consortium, Odunsi K, Whittemore AS, Karlan BY, Dörk T, Goode EL, Menon U, Jacobs IJ, Antoniou AC, Pharoah PD, Gayther SA. Germline Mutations in the BRIP1, BARD1, PALB2, and NBN Genes in Women With Ovarian Cancer. *J Natl Cancer Inst* 2015; **107** [PMID: 26315354 DOI: 10.1093/jnci/djv214]

7 **Weitzel JN**, Neuhausen SL, Adamson A, Tao S, Ricker C, Maoz A, Rosenblatt M, Nehoray B, Sand S, Steele L, Unzeitig G, Feldman N, Blanco AM, Hu D, Huntsman S, Castillo D, Haiman C, Slavin T, Ziv E. Pathogenic and likely pathogenic variants in PALB2, CHEK2, and other known breast cancer susceptibility genes among 1054 BRCA-negative Hispanics with breast cancer. *Cancer* 2019; **125**: 2829-2836 [PMID: 31206626 DOI: 10.1002/cncr.32083]

8 **Velázquez C**, Esteban-Cardeñosa EM, Lastra E, Abella LE, de la Cruz V, Lobatón CD, Durán M, Infante M. Unraveling the molecular effect of a rare missense mutation in BRIP1 associated with inherited breast cancer. *Mol Carcinog* 2019; **58**: 156-160 [PMID: 30230034 DOI: 10.1002/mc.22910]

9 **Venkateshwari A**, Clark DW, Nallari P, Vinod C, Kumarasamy T, Reddy G, Jyothy A, Kumar MV, Ramaiyer R, Palle K. *BRIP1/FANCJ* Mutation Analysis in a Family with History of Male and Female Breast Cancer in India. *J Breast Cancer* 2017; **20**: 104-107 [PMID: 28382101 DOI: 10.4048/jbc.2017.20.1.104]

10 **Pilié PG**, Johnson AM, Hanson KL, Dayno ME, Kapron AL, Stoffel EM, Cooney KA. Germline genetic variants in men with prostate cancer and one or more additional cancers. *Cancer* 2017; **123**: 3925-3932 [PMID: 28657667 DOI: 10.1002/cncr.30817]

11 **Kote-Jarai Z**, Jugurnauth S, Mulholland S, Leongamornlert DA, Guy M, Edwards S, Tymrakiewitcz M, O'Brien L, Hall A, Wilkinson R, Al Olama AA, Morrison J, Muir K, Neal D, Donovan J, Hamdy F, Easton DF, Eeles R; UKGPCS Collaborators; British Association of Urological Surgeons' Section of Oncology. A recurrent truncating germline mutation in the BRIP1/FANCJ gene and susceptibility to prostate cancer. *Br J Cancer* 2009; **100**: 426-430 [PMID: 19127258 DOI: 10.1038/sj.bjc.6604847]

12 **Steinberg-Shemer O**, Goldberg TA, Yacobovich J, Levin C, Koren A, Revel-Vilk S, Ben-Ami T, Kuperman AA, Shkalim Zemer V, Toren A, Kapelushnik J, Ben-Barak A, Miskin H, Krasnov T, Noy-Lotan S, Dgany O, Tamary H. Characterization and genotype-phenotype correlation of patients with Fanconi anemia in a multi-ethnic population. *Haematologica* 2019 [PMID: 31558676 DOI:

10.3324/haematol.2019.222877]
13 **Cancer Genome Atlas Research Network**; Analysis Working Group: Asan University; BC Cancer Agency; Brigham and Women's Hospital; Broad Institute; Brown University; Case Western Reserve University; Dana-Farber Cancer Institute; Duke University; Greater Poland Cancer Centre; Harvard Medical School; Institute for Systems Biology; KU Leuven; Mayo Clinic; Memorial Sloan Kettering Cancer Center; National Cancer Institute; Nationwide Children's Hospital; Stanford University; University of Alabama; University of Michigan; University of North Carolina; University of Pittsburgh; University of Rochester; University of Southern California; University of Texas MD Anderson Cancer Center; University of Washington; Van Andel Research Institute; Vanderbilt University; Washington University; Genome Sequencing Center: Broad Institute; Washington University in St. Louis; Genome Characterization Centers: BC Cancer Agency; Broad Institute; Harvard Medical School; Sidney Kimmel Comprehensive Cancer Center at Johns Hopkins University; University of North Carolina; University of Southern California Epigenome Center; University of Texas MD Anderson Cancer Center; Van Andel Research Institute; Genome Data Analysis Centers: Broad Institute; Brown University:; Harvard Medical School; Institute for Systems Biology; Memorial Sloan Kettering Cancer Center; University of California Santa Cruz; University of Texas MD Anderson Cancer Center; Biospecimen Core Resource: International Genomics Consortium; Research Institute at Nationwide Children's Hospital; Tissue Source Sites: Analytic Biologic Services; Asan Medical Center; Asterand Bioscience; Barretos Cancer Hospital; BioreclamationIVT; Botkin Municipal Clinic; Chonnam National University Medical School; Christiana Care Health System; Cureline; Duke University; Emory University; Erasmus University; Indiana University School of Medicine; Institute of Oncology of Moldova; International Genomics Consortium; Invidumed; Israelitisches Krankenhaus Hamburg; Keimyung University School of Medicine; Memorial Sloan Kettering Cancer Center; National Cancer Center Goyang; Ontario Tumour Bank; Peter MacCallum Cancer Centre; Pusan National University Medical School; Ribeirão Preto Medical School; St. Joseph's Hospital &Medical Center; St. Petersburg Academic University; Tayside Tissue Bank; University of Dundee; University of Kansas Medical Center; University of Michigan; University of North Carolina at Chapel Hill; University of Pittsburgh School of Medicine; University of Texas MD Anderson Cancer Center; Disease Working Group: Duke University; Memorial Sloan Kettering Cancer Center; National Cancer Institute; University of Texas MD Anderson Cancer Center; Yonsei University College of Medicine; Data Coordination Center: CSRA Inc; Project Team: National Institutes of Health. Integrated genomic characterization of oesophageal carcinoma. *Nature* 2017; **541**: 169-175 [PMID: 28052061 DOI: 10.1038/nature20805]
14 **Cancer Genome Atlas Research Network**. Comprehensive molecular characterization of gastric adenocarcinoma. *Nature* 2014; **513**: 202-209 [PMID: 25079317 DOI: 10.1038/nature13480]
15 **Cancer Genome Atlas Research Network**. Cancer Genome Atlas Research Network. Integrated Genomic Characterization of Pancreatic Ductal Adenocarcinoma. *Cancer Cell* 2017; **32**: 185-203.e13 [PMID: 28810144 DOI: 10.1016/j.ccell.2017.07.007]
16 **Farshidfar F**, Zheng S, Gingras MC, Newton Y, Shih J, Robertson AG, Hinoue T, Hoadley KA, Gibb EA, Roszik J, Covington KR, Wu CC, Shinbrot E, Stransky N, Hegde A, Yang JD, Reznik E, Sadeghi S, Pedamallu CS, Ojesina AI, Hess JM, Auman JT, Rhie SK, Bowlby R, Borad MJ; Cancer Genome Atlas Network, Zhu AX, Stuart JM, Sander C, Akbani R, Cherniack AD, Deshpande V, Mounajjed T, Foo WC, Torbenson MS, Kleiner DE, Laird PW, Wheeler DA, McRee AJ, Bathe OF, Andersen JB, Bardeesy N, Roberts LR, Kwong LN. Integrative Genomic Analysis of Cholangiocarcinoma Identifies Distinct IDH-Mutant Molecular Profiles. *Cell Rep* 2017; **18**: 2780-2794 [PMID: 28297679 DOI: 10.1016/j.celrep.2017.02.033]
17 **Cancer Genome Atlas Network**. Comprehensive molecular characterization of human colon and rectal cancer. *Nature* 2012; **487**: 330-337 [PMID: 22810696 DOI: 10.1038/nature11252]
18 **Cerami E**, Gao J, Dogrusoz U, Gross BE, Sumer SO, Aksoy BA, Jacobsen A, Byrne CJ, Heuer ML, Larsson E, Antipin Y, Reva B, Goldberg AP, Sander C, Schultz N. The cBio cancer genomics portal: an open platform for exploring multidimensional cancer genomics data. *Cancer Discov* 2012; **2**: 401-404 [PMID: 22588877 DOI: 10.1158/2159-8290.CD-12-0095]
19 **Gao J**, Aksoy BA, Dogrusoz U, Dresdner G, Gross B, Sumer SO, Sun Y, Jacobsen A, Sinha R, Larsson E, Cerami E, Sander C, Schultz N. Integrative analysis of complex cancer genomics and clinical profiles using the cBioPortal. *Sci Signal* 2013; **6**: pl1 [PMID: 23550210 DOI: 10.1126/scisignal.2004088]
20 **Reva B**, Antipin Y, Sander C. Predicting the functional impact of protein mutations: application to cancer genomics. *Nucleic Acids Res* 2011; **39**: e118 [PMID: 21727090 DOI: 10.1093/nar/gkr407]
21 **Chakravarty D**, Gao J, Phillips SM, Kundra R, Zhang H, Wang J, Rudolph JE, Yaeger R, Soumerai T, Nissan MH, Chang MT, Chandarlapaty S, Traina TA, Paik PK, Ho AL, Hantash FM, Grupe A, Baxi SS, Callahan MK, Snyder A, Chi P, Danila D, Gounder M, Harding JJ, Hellmann MD, Iyer G, Janjigian Y, Kaley T, Levine DA, Lowery M, Omuro A, Postow MA, Rathkopf D, Shoushtari AN, Shukla N, Voss M, Paraiso E, Zehir A, Berger MF, Taylor BS, Saltz LB, Riely GJ, Ladanyi M, Hyman DM, Baselga J, Sabbatini P, Solit DB, Schultz N. OncoKB: A Precision Oncology Knowledge Base. *JCO Precis Oncol* 2017; 2017 [PMID: 28890946 DOI: 10.1200/PO.17.00011]
22 **Szász AM**, Lánczky A, Nagy Á, Förster S, Hark K, Green JE, Boussioutas A, Busuttil R, Szabó A, Győrffy B. Cross-validation of survival associated biomarkers in gastric cancer using transcriptomic data of 1,065 patients. *Oncotarget* 2016; **7**: 49322-49333 [PMID: 27384994 DOI: 10.18632/oncotarget.10337]
23 **Khan A**, Fornes O, Stigliani A, Gheorghe M, Castro-Mondragon JA, van der Lee R, Bessy A, Chèneby J, Kulkarni SR, Tan G, Baranasic D, Arenillas DJ, Sandelin A, Vandepoele K, Lenhard B, Ballester B, Wasserman WW, Parcy F, Mathelier A. JASPAR 2018: update of the open-access database of transcription factor binding profiles and its web framework. *Nucleic Acids Res* 2018; **46**: D1284 [PMID: 29161433 DOI: 10.1093/nar/gkx1188]
24 **Cancer Genome Atlas Network**. Comprehensive molecular portraits of human breast tumours. *Nature* 2012; **490**: 61-70 [PMID: 23000897 DOI: 10.1038/nature11412]
25 **Cancer Genome Atlas Research Network**. Integrated genomic analyses of ovarian carcinoma. *Nature* 2011; **474**: 609-615 [PMID: 21720365 DOI: 10.1038/nature10166]
26 **Pfister K**, Pipka JL, Chiang C, Liu Y, Clark RA, Keller R, Skoglund P, Guertin MJ, Hall IM, Stukenberg PT. Identification of Drivers of Aneuploidy in Breast Tumors. *Cell Rep* 2018; **23**: 2758-2769 [PMID: 29847804 DOI: 10.1016/j.celrep.2018.04.102]
27 **Estep KN**, Brosh RM. RecQ and Fe-S helicases have unique roles in DNA metabolism dictated by their unwinding directionality, substrate specificity, and protein interactions. *Biochem Soc Trans* 2018; **46**: 77-95 [PMID: 29273621 DOI: 10.1042/BST20170044]

28 **Niraj J**, Färkkilä A, D'Andrea AD. The Fanconi Anemia Pathway in Cancer. *Annu Rev Cancer Biol* 2019; **3**: 457-478 [PMID: 30882047 DOI: 10.1146/annurev-cancerbio-030617-050422]

29 **Peng M**, Cong K, Panzarino NJ, Nayak S, Calvo J, Deng B, Zhu LJ, Morocz M, Hegedus L, Haracska L, Cantor SB. Opposing Roles of FANCJ and HLTF Protect Forks and Restrain Replication during Stress. *Cell Rep* 2018; **24**: 3251-3261 [PMID: 30232006 DOI: 10.1016/j.celrep.2018.08.065]

30 **Cantor SB**, Xie J. Assessing the link between BACH1/FANCJ and MLH1 in DNA crosslink repair. *Environ Mol Mutagen* 2010; **51**: 500-507 [PMID: 20658644 DOI: 10.1002/em.20568]

31 **Barthelemy J**, Hanenberg H, Leffak M. FANCJ is essential to maintain microsatellite structure genome-wide during replication stress. *Nucleic Acids Res* 2016; **44**: 6803-6816 [PMID: 27179029 DOI: 10.1093/nar/gkw433]

32 **Matsuzaki K**, Borel V, Adelman CA, Schindler D, Boulton SJ. FANCJ suppresses microsatellite instability and lymphomagenesis independent of the Fanconi anemia pathway. *Genes Dev* 2015; **29**: 2532-2546 [PMID: 26637282 DOI: 10.1101/gad.272740.115]

33 **Bailey P**, Chang DK, Nones K, Johns AL, Patch AM, Gingras MC, Miller DK, Christ AN, Bruxner TJ, Quinn MC, Nourse C, Murtaugh LC, Harliwong I, Idrisoglu S, Manning S, Nourbakhsh E, Wani S, Fink L, Holmes O, Chin V, Anderson MJ, Kazakoff S, Leonard C, Newell F, Waddell N, Wood S, Xu Q, Wilson PJ, Cloonan N, Kassahn KS, Taylor D, Quek K, Robertson A, Pantano L, Mincarelli L, Sanchez LN, Evers L, Wu J, Pinese M, Cowley MJ, Jones MD, Colvin EK, Nagrial AM, Humphrey ES, Chantrill LA, Mawson A, Humphris J, Chou A, Pajic M, Scarlett CJ, Pinho AV, Giry-Laterriere M, Rooman I, Samra JS, Kench JG, Lovell JA, Merrett ND, Toon CW, Epari K, Nguyen NQ, Barbour A, Zeps N, Moran-Jones K, Jamieson NB, Graham JS, Duthie F, Oien K, Hair J, Grützmann R, Maitra A, Iacobuzio-Donahue CA, Wolfgang CL, Morgan RA, Lawlor RT, Corbo V, Bassi C, Rusev B, Capelli P, Salvia R, Tortora G, Mukhopadhyay D, Petersen GM; Australian Pancreatic Cancer Genome Initiative, Munzy DM, Fisher WE, Karim SA, Eshleman JR, Hruban RH, Pilarsky C, Morton JP, Sansom OJ, Scarpa A, Musgrove EA, Bailey UM, Hofmann O, Sutherland RL, Wheeler DA, Gill AJ, Gibbs RA, Pearson JV, Waddell N, Biankin AV, Grimmond SMBailey P, Chang DK, Nones K, Johns AL, Patch AM, Gingras MC, Miller DK, Christ AN, Bruxner TJ, Quinn MC, Nourse C, Murtaugh LC, Harliwong I, Idrisoglu S, Manning S, Nourbakhsh E, Wani S, Fink L, Holmes O, Chin V, Anderson MJ, Kazakoff S, Leonard C, Newell F, Waddell N, Wood S, Xu Q, Wilson PJ, Cloonan N, Kassahn KS, Taylor D, Quek K, Robertson A, Pantano L, Mincarelli L, Sanchez LN, Evers L, Wu J, Pinese M, Cowley MJ, Jones MD, Colvin EK, Nagrial AM, Humphrey ES, Chantrill LA, Mawson A, Humphris J, Chou A, Pajic M, Scarlett CJ, Pinho AV, Giry-Laterriere M, Rooman I, Samra JS, Kench JG, Lovell JA, Merrett ND, Toon CW, Epari K, Nguyen NQ, Barbour A, Zeps N, Moran-Jones K, Jamieson NB, Graham JS, Duthie F, Oien K, Hair J, Grützmann R, Maitra A, Iacobuzio-Donahue CA, Wolfgang CL, Morgan RA, Lawlor RT, Corbo V, Bassi C, Rusev B, Capelli P, Salvia R, Tortora G, Mukhopadhyay D, Petersen GM; Australian Pancreatic Cancer Genome Initiative, Munzy DM, Fisher WE, Karim SA, Eshleman JR, Hruban RH, Pilarsky C, Morton JP, Sansom OJ, Scarpa A, Musgrove EA, Bailey UM, Hofmann O, Sutherland RL, Wheeler DA, Gill AJ, Gibbs RA, Pearson JV, Waddell N, Biankin AV, Grimmond SM. Genomic analyses identify molecular subtypes of pancreatic cancer. *Nature* 2016; **531**: 47-52 [PMID: 26909576 DOI: 10.1038/nature16965]

34 **Tu Z**, Aird KM, Bitler BG, Nicodemus JP, Beeharry N, Xia B, Yen TJ, Zhang R. Oncogenic RAS regulates BRIP1 expression to induce dissociation of BRCA1 from chromatin, inhibit DNA repair, and promote senescence. *Dev Cell* 2011; **21**: 1077-1091 [PMID: 22137763 DOI: 10.1016/j.devcel.2011.10.010]

35 **Nakanishi R**, Kitao H, Fujinaka Y, Yamashita N, Iimori M, Tokunaga E, Yamashita N, Morita M, Kakeji Y, Maehara Y. FANCJ expression predicts the response to 5-fluorouracil-based chemotherapy in MLH1-proficient colorectal cancer. *Ann Surg Oncol* 2012; **19**: 3627-3635 [PMID: 22526901 DOI: 10.1245/s10434-012-2349-8]

36 **Eelen G**, Vanden Bempt I, Verlinden L, Drijkoningen M, Smeets A, Neven P, Christiaens MR, Marchal K, Bouillon R, Verstuyf A. Expression of the BRCA1-interacting protein Brip1/BACH1/FANCJ is driven by E2F and correlates with human breast cancer malignancy. *Oncogene* 2008; **27**: 4233-4241 [PMID: 18345034 DOI: 10.1038/onc.2008.51]

37 **Voutsadakis IA**. Polymerase epsilon mutations and concomitant β2-microglobulin mutations in cancer. *Gene* 2018; **647**: 31-38 [PMID: 29320758 DOI: 10.1016/j.gene.2018.01.030]

38 **Zimmer AS**, Nichols E, Cimino-Mathews A, Peer C, Cao L, Lee MJ, Kohn EC, Annunziata CM, Lipkowitz S, Trepel JB, Sharma R, Mikkilineni L, Gatti-Mays M, Figg WD, Houston ND, Lee JM. A phase I study of the PD-L1 inhibitor, durvalumab, in combination with a PARP inhibitor, olaparib, and a VEGFR1-3 inhibitor, cediranib, in recurrent women's cancers with biomarker analyses. *J Immunother Cancer* 2019; **7**: 197 [PMID: 31345267 DOI: 10.1186/s40425-019-0680-3]

World Journal of Gastroenterology

Submit a Manuscript: https://www.f6publishing.com

World J Gastroenterol 2020 March 21; 26(11): 1208-1220

DOI: 10.3748/wjg.v26.i11.1208

ISSN 1007-9327 (print) ISSN 2219-2840 (online)

ORIGINAL ARTICLE

Retrospective Study

Radiomics model based on preoperative gadoxetic acid-enhanced MRI for predicting liver failure

Wang-Shu Zhu, Si-Ya Shi, Ze-Hong Yang, Chao Song, Jun Shen

ORCID number: Wang-Shu Zhu (0000-0002-9739-0767); Si-Ya Shi (0000-0002-1416-9128); Ze-Hong Yang (0000-0001-7562-3710); Chao Song (0000-0002-3538-381X); Jun Shen (0000-0001-7746-5285).

Author contributions: Zhu WS and Shi SY contributed equally to this work; Zhu W, Shi S, and Shen J designed the research; Zhu W and Shi S collected and analyzed the data, and wrote the manuscript; Yang Z and Song C analyzed and interpreted the data; Shen J wrote and revised the manuscript; All co-authors participated in writing and checking the manuscript, and approved the submitted manuscript.

Supported by the Guangdong Province Universities and Colleges Pearl River Scholar Funded Scheme (2017); and the Guangdong Natural Science Foundation, No. 2017A030313777.

Institutional review board statement: This study was reviewed and approved by the Ethics Committee of Sun Yat-Sen Memorial Hospital.

Informed consent statement: Patients were not required to give informed consent to the study because the analysis used anonymous clinical data that were obtained after each patient agreed to treatment by written consent.

Conflict-of-interest statement: The authors declare no conflict of interest.

Data sharing statement: No additional data are available.

Wang-Shu Zhu, Si-Ya Shi, Ze-Hong Yang, Chao Song, Jun Shen, Department of Radiology, Sun Yat-Sen Memorial Hospital, Sun Yat-Sen University, Guangzhou 510120, Guangdong Province, China

Wang-Shu Zhu, Si-Ya Shi, Ze-Hong Yang, Chao Song, Jun Shen, Guangdong Provincial Key Laboratory of Malignant Tumor Epigenetics and Gene Regulation, Medical Research Center, Sun Yat-Sen Memorial Hospital, Sun Yat-Sen University, Guangzhou 510120, Guangdong Province, China

Corresponding author: Jun Shen, MD, Department of Radiology, Sun Yat-Sen Memorial Hospital, Sun Yat-Sen University, No. 107 Yanjiang Road West, Guangzhou 501012, Guangdong Province, China. shenjun@mail.sysu.edu.cn

Abstract

BACKGROUND

Postoperative liver failure is the most severe complication in cirrhotic patients with hepatocellular carcinoma (HCC) after major hepatectomy. Current available clinical indexes predicting postoperative residual liver function are not sufficiently accurate.

AIM

To determine a radiomics model based on preoperative gadoxetic acid-enhanced magnetic resonance imaging for predicting liver failure in cirrhotic patients with HCC after major hepatectomy.

METHODS

For this retrospective study, a radiomics-based model was developed based on preoperative hepatobiliary phase gadoxetic acid-enhanced magnetic resonance images in 101 patients with HCC between June 2012 and June 2018. Sixty-one radiomic features were extracted from hepatobiliary phase images and selected by the least absolute shrinkage and selection operator method to construct a radiomics signature. A clinical prediction model, and radiomics-based model incorporating significant clinical indexes and radiomics signature were built using multivariable logistic regression analysis. The integrated radiomics-based model was presented as a radiomics nomogram. The performances of clinical prediction model, radiomics signature, and radiomics-based model for predicting post-operative liver failure were determined using receiver operating characteristics curve, calibration curve, and decision curve analyses.

RESULTS

Manuscript source: Unsolicited manuscript

Received: October 12, 2019
Peer-review started: October 12, 2019
First decision: January 13, 2020
Revised: February 18, 2020
Accepted: February 21, 2020
Article in press: February 21, 2020
Published online: March 21, 2020

P-Reviewer: Tsoulfas G
S-Editor: Ma YJ
L-Editor: Filipodia
E-Editor: Liu JH

Five radiomics features from hepatobiliary phase images were selected to construct the radiomics signature. The clinical prediction model, radiomics signature, and radiomics-based model incorporating indocyanine green clearance rate at 15 min and radiomics signature showed favorable performance for predicting postoperative liver failure (area under the curve: 0.809-0.894). The radiomics-based model achieved the highest performance for predicting liver failure (area under the curve: 0.894; 95%CI: 0.823-0.964). The integrated discrimination improvement analysis showed a significant improvement in the accuracy of liver failure prediction when radiomics signature was added to the clinical prediction model (integrated discrimination improvement = 0.117, P = 0.002). The calibration curve and an insignificant Hosmer-Lemeshow test statistic (P = 0.841) demonstrated good calibration of the radiomics-based model. The decision curve analysis showed that patients would benefit more from a radiomics-based prediction model than from a clinical prediction model and radiomics signature alone.

CONCLUSION
A radiomics-based model of preoperative gadoxetic acid–enhanced MRI can be used to predict liver failure in cirrhotic patients with HCC after major hepatectomy.

Key words: Liver failure; Radiomics; Gadoxetic acid; Magnetic resonance imaging; Hepatocellular carcinoma

Core tip: Serological indexes, indocyanine green clearance rate at 15 min, liver volumetry, and clinical scoring systems are commonly used to determine liver function capacity and predict postoperative residual liver function. However, these indexes are not sufficiently accurate for predicting the risk of postoperative liver failure. We constructed a radiomics signature based on preoperative hepatobiliary phase gadoxetic acid-enhanced magnetic resonance imaging. This radiomics signature achieves favorable performance in predicting liver failure in cirrhotic patients with hepatocellular carcinoma after major hepatectomy. Incorporating indocyanine green clearance rate at 15 min into the radiomics signature further improves the predictive performance for postoperative liver failure.

Citation: Zhu WS, Shi SY, Yang ZH, Song C, Shen J. Radiomics model based on preoperative gadoxetic acid-enhanced MRI for predicting liver failure. *World J Gastroenterol* 2020; 26(11): 1208-1220
URL: https://www.wjgnet.com/1007-9327/full/v26/i11/1208.htm
DOI: https://dx.doi.org/10.3748/wjg.v26.i11.1208

INTRODUCTION

Postoperative liver failure is the most serious complication for patients with hepatocellular carcinoma (HCC) after major hepatectomy, and it is caused by insufficient function of the remnant liver. Liver failure not only influences the physical state of patients and contributes to cancer recurrence, but also prolongs hospital stay, thereby increasing overall medical costs[1]. Therefore, preoperative liver function prediction is highly important for risk stratification in patients considering major hepatectomy. To date, liver function assessment primarily relies on the serological indexes, indocyanine green (ICG) retention rate at 15 min (ICG-R15)[2], liver volumetry based on computed tomography (CT)[3], and clinical scoring systems[4,5]. Unfortunately, these measures for predicting the prognosis of postoperative residual liver function after hepatectomy are not sufficiently accurate[6].

Gadoxetic acid-enhanced magnetic resonance imaging (MRI) has been widely used to distinguish benign and malignant liver lesions[7]. As gadoxetic acid can be selectively absorbed by functional hepatocytes, signal intensity of liver measured on preoperative gadoxetic acid-enhanced hepatobiliary phase (HBP) images has also

been applied to assess liver function[8,9]. However, parenchymal damage is often not homogeneously distributed in the liver[10,11] and liver abnormalities are frequently and increasingly heterogeneous during the development of cirrhosis[8]. The measurement of mean signal intensity in a predefined larger area of liver parenchyma is insensitive for identifying regional variations, thereby omitting heterogeneity that is informative for liver damage in cirrhotic patients.

Radiomics is a method utilizing high-dimensional data mined from digital medical images for quantitative measurement, and can be applied to improve predictive, diagnostic, and prognostic accuracy to support clinical decision[12,13]. Previously, radiomics approaches based on MRI or CT images have been extensively applied for differential diagnosis, monitoring of disease progression, and evaluation of the treatment response[14,15]. However, whether a radiomics-based model based on gadoxetic acid-enhanced MRI can be used for predicting liver failure in cirrhotic patients with HCC after major hepatectomy has not been determined so far.

In this study, we investigated the value of a radiomics model based on gadoxetic acid-enhanced MRI for predicting liver failure after major hepatectomy in cirrhotic patients with HCC.

MATERIALS AND METHODS

Study population

This retrospective study was approved by the Institutional Review Board of Sun Yat-Sen Memorial Hospital of Sun Yat-Sen University, and written informed consent was waived by the institutional review board. Patients with HCC who had major liver resection between June 2012 and June 2018 were identified from the institutional HCC database. Patients were enrolled in this study if they had: (1) Serologically-proven hepatitis B-related cirrhosis; (2) HCC confirmed by surgical pathology; (3) Undergone major liver resection; and (4) Undergone preoperative gadoxetic acid-enhanced MRI within 7 d before liver surgery. A total of 619 patients met this inclusion criteria. Patients were excluded if they had an unresectable tumor and previously received treatment, such as chemotherapy or transarterial chemoembolization (n = 173), had minor liver resection (< 3 Couinaud liver segments) (n = 322), or had artifacts on their HBP MRI (n = 13). Finally, 101 patients were included in this study (Figure 1). Postoperative liver failure was identified according to the method proposed by Amber *et al*[16], which defines liver failure as the presence of the following: encephalopathy with hyperbilirubinemia, total bilirubin > 4.1 mg/dL without an obstruction or bile leak, international normalized ratio of prothrombin time > 2.5, and ascites (drainage > 500 mL/d). All patients had undergone the ICG test within 7 d before surgery, as previously described[17]. The preoperative serum levels of alanine aminotransferase, aspartate aminotransferase, total bilirubin, albumin, alkaline phosphatase, platelet, prothrombin time, prealbumin, and cholinesterase, Child-Pugh classification, and the degree of liver fibrosis were retrieved from the hospital medical records. The liver fibrosis was detected by Masson staining of the resected liver specimens and graded according to a previously reported method[18].

Clinical prediction model construction

The normality of distribution of clinical variables was assessed by the Shapiro-Wilk test. Continuous variables were presented as median ± range and compared using the unpaired t-test, two-tailed t-test, or Mann-Whitney test. Categorical variables were presented as number (percentage), and compared using Mann-Whitney test. Univariable logistic regression analysis was used to determine clinical variables associated with liver failure. Those significant variables were chosen for multivariable binary logistic regression analysis using the forward likelihood ratio selection method to determine the independent risk factors for liver failure. The independent risk factors were used to construct a clinical prediction model.

MRI

MRI was performed on a 3.0 Tesla clinical scanner (Achieva TX; Philips Healthcare, Best, The Netherlands) with a 16-channel sense torso coil. The imaging sequences included axial fat-suppressed T2-weighted imaging [repetition time/echo time (TR/TE), 1650/80 ms; slice thickness/gap, 3.5/1 mm; matrix, 528 × 288; number of signals acquired (NSA), 2], axial T1-weighted imaging using mDixon fast field echo sequence (number of echoes, 2; TR, 3.4 ms; TE, 1.14 and 2.1 ms; flip angle, 10°; slice thickness/gap, 3/1 mm; matrix, 528 × 288; NSA, 1) and coronal T1 high resolution isotropic volume examination (THRIVE) sequence (TR/TE, 3.1/1.4 ms; flip angle, 10°; slice thickness/gap, 3/1 mm; matrix, 528 × 288; NSA, 2). After intravenous injection of

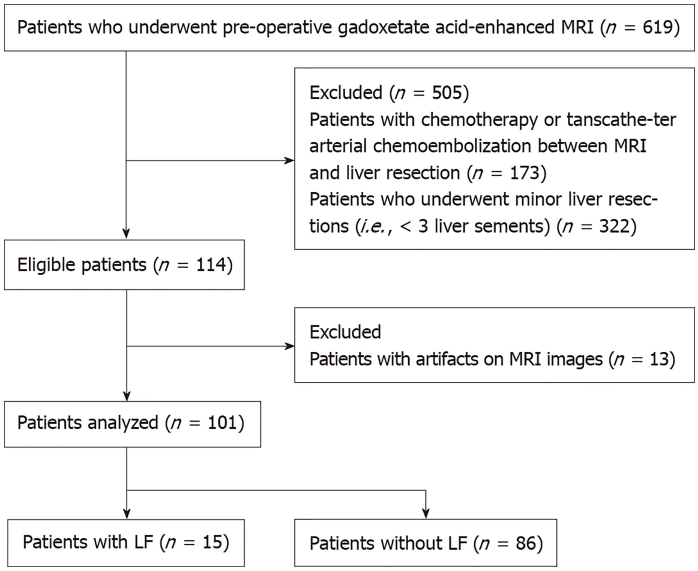

Figure 1 Flow diagram shows patient selection. LF: Liver failure; MRI: Magnetic resonance imaging.

gadoxetic acid (Gd-EOB-DTPA; Primovist, Bayer-Schering Pharma, Berlin, Germany) at a dosage of 0.025 mmol/kg of body weight *via* the antecubital vein at a rate of 2.5 mL/s, patients underwent multiphasic axial contrast-enhanced T1 high resolution isotropic volume examination (e-THRIVE) imaging, which was performed with the same parameters as their unenhanced counterparts. Early arterial phase, later arterial phase, portal phase, venous phase, and equilibrium phase images were obtained respectively at 20, 30, 40, 60 and 100 s after the injection of contrast agents. The HBP images were obtained at 20 min after the injection of gadoxetic acid.

Radiomic feature selection and radiomics signature construction

The flow diagram of radiomic feature selection and radiomics signature construction is shown in Figure 2. Region of interests (ROIs) for the liver were drawn along the margin of the entire liver parenchyma on HBP images, by excluding hepatic masses, large hepatic vessels, and bile ducts on HBP images. The ROI was further refined to exclude areas of fat, air, and bone using a thresholding procedure (Centricity PACS 4.0, GE Medical Systems). Then the processed HBP images were transferred to an off-line workstation and analyzed by a quantitative analysis software (Omni Kinetics, GE Healthcare). Radiomic features were analyzed by two radiologists (Z.W. and Y.Z. with 3 and 13 years of experience in diagnostic imaging respectively) in a blinded manner independently. For radiomic features, 61 descriptors including the first-order and distribution statistics (23 descriptors) to reflect basic characters of image uniformity, gray-level co-occurrence matrix (28 descriptors) to describe the homogeneity, and gray-level run length matrix (10 descriptors) to indicate image coarseness were obtained. The categories of the radiomic features are listed in Table 1 in detail. Intra- and inter-observer reproducibility of radiomic feature extraction was determined by the intraclass correlation coefficients (ICCs). The result from two readers were averaged for analysis. To assess intra-observer reproducibility, HBP images from 24 randomly selected patients were chosen for ROI segmentation and feature extraction analysis by reader 1 (Z.W.). After 1 wk, reader 1 repeated the same procedure. An ICC value > 0.75 represents good to excellent agreement, and the value between 0.4 and 0.75 indicates moderate agreement.

The least absolute contraction selection operator (LASSO) logistic regression was used to select radiomic features with non-zero coefficients[19]. The multivariable logistic regression with enter method was used to construct radiomics signature. The radiomics score (Rad-score) were calculated *via* a linear combination of selected features that were weighted by their respective coefficients.

Development and performance of radiomics-based prediction model

To develop an integrated radiomics-based prediction model, the independent predictors of clinical variables and radiomics signature were chosen for multivariable logistic regression analysis to determine the parameters that can best predict the risk of liver failure. A collinearity diagnosis was made on the logistic regression model to test the independence of predictors. The established radiomics-based model was presented as a radiomics nomogram. The prediction performance of this radiomics

Table 1 Categories of the quantitative radiomics features obtained for analysis

Groups	Detailed parameters
First-order and distribution statistics, n = 23	Minimum intensity, Maximum intensity, Mean intensity, Median intensity, Standard deviation, Variance, Volume count, Voxel value sum, Range mean deviation, Relative deviation, Skewness, Kurtosis, Uniformity, Energy, Entropy, Frequency size, Quantile 5, Quantile 10, Quantile 25, Quantile 50, Quantile 75, Quantile 90, Quantile 95
Gray-level co-occurrence matrix, n = 28	Glcm bin size, Glcm total frequency, Glcm matrix mean, Glcm relative Frequency, Energy, Entropy, Inertia, Correlation, Inverse difference moment, Cluster shade, Cluster prominence, Haralick correlation, Haralick entropy, Angular second moment, Contrast, Haralick variance, sum Average, sum Variance, sum Entropy, Difference variance, Difference entropy, Inverse difference moment normalized, Minimum intensity, Maximum intensity, Number of intensity bins, Minimum size, Maximum size, Number of size bins
Gray-level run length matrix, n = 10	Short run emphasis (SRE), Long run emphasis (LRE), Gray level non-uniformity (GLN), Run length non-uniformity (RLN), Low gray level run emphasis (LGLRE), High gray level run emphasis (HGLRE), Short run low gray level emphasis (SRLGLE), Short run high gray level emphasis (SRHGLE), Long run low gray level emphasis (LRLGLE), Long run high gray level emphasis (LRHGLE)

nomogram was measured by correcting 1000 bootstrap samples to reduce the overfit bias. The calibration of the nomogram was evaluated using a calibration curve. The goodness-of-fit of the nomogram was assessed by the Hosmer-Lemeshow test.

Statistical analysis

The performance of the clinical prediction model, radiomics signature and radiomics-based model for predicting liver failure was determined using the receiver operating characteristic curve analysis. The discrimination performance was quantified using the calculation of the area under the curve (AUC) and its 95% confidence intervals (CIs). The sensitivity, specificity, positive predicted value (PPV), negative predicted value and accuracy of the models were also calculated. The integrated discrimination improvement (IDI) and continuous net reclassification improvement indexes were used to assessed the additional predictive value. The net benefits for a range of threshold probabilities by the decision curve analysis was calculated to estimate the clinical utility of the clinical prediction model, radiomics signature and radiomics-based model. Statistical tests were performed using software SPSS version 21.0 (SPSS, Chicago, Ill, United States), R version 3.3.3 (R Development Core Team, Vienna, Austria) and MedCalc Statistical Software version 17.1 (MedCalc Software, Ostend, Belgium). A two sided P value < 0.05 was considered to indicate a statistically significant difference.

RESULTS

Patient characteristics and clinical prediction model

Among the 101 patients included, there were 88 men (age range, 27-78 years; median age, 55 years), and 13 women (age range, 22–66 years; median age, 53 years). Fifteen patients had liver failure after major hepatectomy, and the remaining 86 patients did not have liver failure. Among 15 patients with liver failure, 3 of them had a sustained type of liver failure and died, while 12 of them developed liver failure immediately after surgery and recovered after proper treatment. The clinicopathologic characteristics of the enrolled patients are shown in Table 2. There were no differences in the sex, age, liver fibrosis, or Child-Pugh classifications between patients with or without liver failure (P > 0.05). The aspartate aminotransferase level, alkaline phosphatase (ALP) level and ICG-R15 were significantly different between two groups (P = 0.030, 0.004, and 0.002, respectively). Univariable and multivariable logistic analysis showed that the ALP level and ICG-R15 were independent risk factors for liver failure (P < 0.05). Thus, the ALP level and ICG-R15 were selected to build the clinical prediction model and the radiomics-based model.

Radiomic feature selection and radiomics signature construction

The intra-observer ICCs (ranging from 0.780 to 0.992) and the inter-observer ICCs (ranging from 0.763 to 0.935) suggested good intra- and inter-observer reproducibility for feature extraction analysis. Among 61 radiomic features, five features were

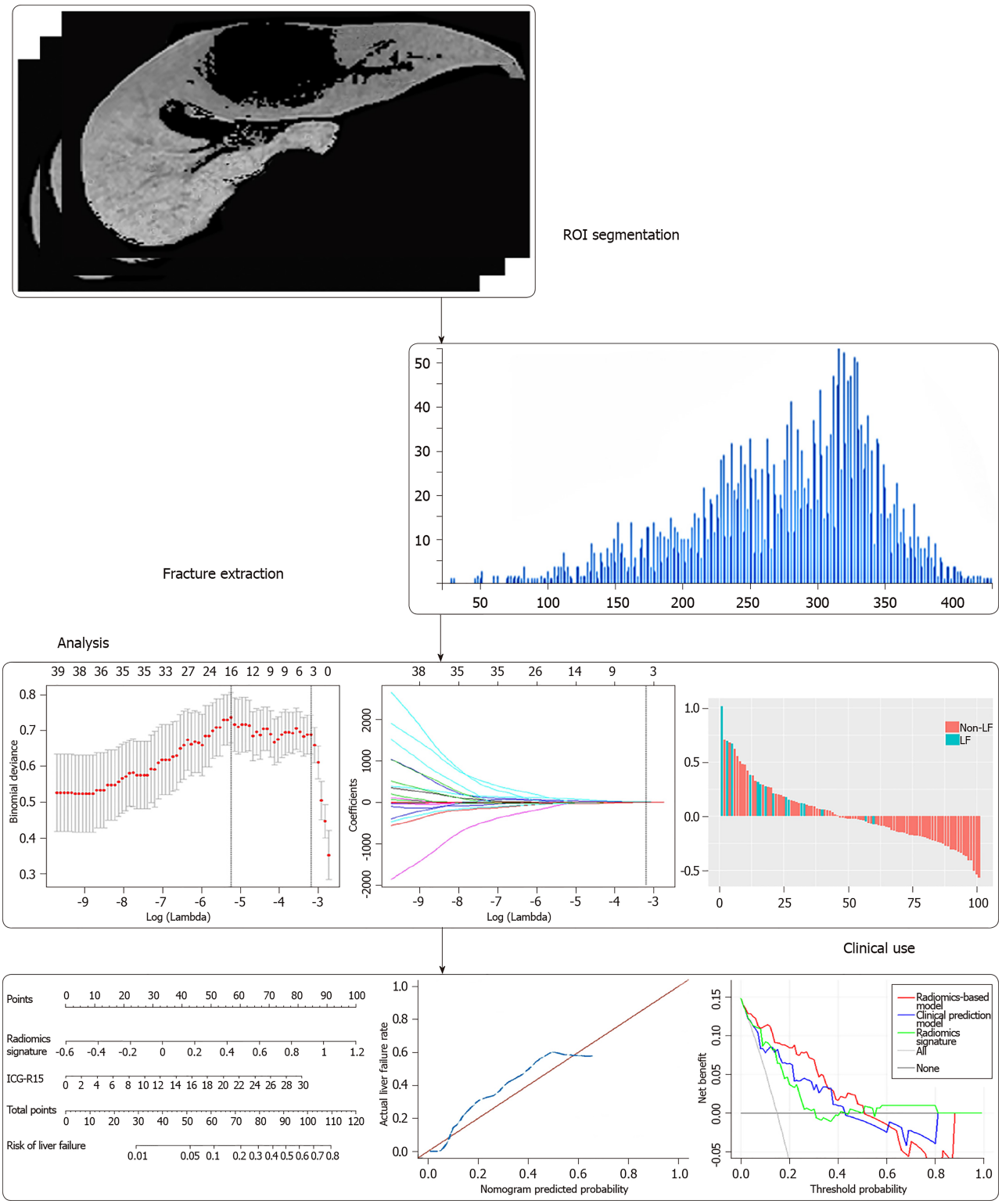

Figure 2 Workflow of necessary steps in current study. Region of interests were drawn on hepatobiliary phase gadoxetic acid-enhanced magnetic resonance images. For feature selection, the least absolute shrink-age and selection operator method was applied to select significant features. The radiomics signature was constructed by a linear combination of selected features. The performance of the prediction model was assessed by the area under a receiver operating characteristic curve and the calibration curve. To provide a more understandable outcome measure, a nomogram was built for individualized evaluation, followed by decision curve analysis. ROIs: Region of interests.

selected by LASSO regression analysis (Figure 3), including minimum intensity (first-order), uniformity(first-order), energy (first-order), cluster prominence (GLCM), and minimum intensity (GLCM). The radiomics signature was constructed by the calculation of radiomics score of these five features according to the following formula:

Radiomics scores = - 4.712031 - 1.529694×10^{-4} × minimum intensity + 5.788767 ×

Table 2 Clinicopathological characteristics of 101 hepatitis B virus-related cirrhotic patients with hepatocellular carcinoma

	Patients with	Patients without	*P* value
	Liver failure, *n* = 15	Liver failure, *n* = 86	
Sex			0.439
Male	9 (90)	50 (89)	
Female	1 (10)	6 (12)	
Age in yr	55 (22-78)	55 (40-67)	0.958
Primary tumor			
Tumor size in mm[12]	59 (15-154)	38 (10-197)	0.069
Single, *n*	4 (27)	60 (70)	
Multiple in *n*	11 (73)	26 (30)	
Baseline serological index[1]			
Aspartate aminotransferase in IU/L	59 (17-116)	33 (17-1663)	0.030
Alanine aminotransferase in IU/L	34 (17-98)	31 (11-1491)	0.248
Total bilirubin in mg/dL	18.2 (8.2-37.9)	15.7 (3.2-35.5)	0.314
Albumin in g/L	38.7 (30.9-45.8)	40.3 (23.0-50.3)	0.135
Alkaline phosphatase in U/L	131 (71-365)	91 (41-410)	0.004
Platelet as /L	200 (111-496)	188 (49-489)	0.462
Prothrombin time in s	12.8 (11.3-14.9)	12.3 (10.6-16.8)	0.138
Cholinesterase in U/L	6271 (2522-8417)	6714 (2334-12360)	0.110
ICG test[1]			
Elimination rate constant in K as min^{-1}	0.13 (0.09-0.19)	0.21 (0.12-0.29)	0.308
Retention rate at 15 min as R15 in %	8.2 (1.3-28.4)	12.8 (6.1-18.0)	0.002
The half-life as T1/2 in min	6.36 (3.73-7.88)	3.27 (2.39-5.68)	0.061
Baseline score			
Child-Pugh classification			0.786
A	15 (100)	81 (94)	
B	0 (0)	5 (6)	
C	0 (0)	0 (0)	
Fibrosis grade on specimen			0.174
F1	1 (7)	9 (11)	
F2	0 (0)	8 (9)	
F3	0 (0)	7 (8)	
F4	9 (60)	14 (16)	
N/A	5 (33)	48 (56)	

Data are numbers of patients, with percentages in parentheses, except otherwise indicated.
[1]Numbers in parentheses are ranges;
[2]If the number of lesions is greater than 2, the largest lesion was chosen to measure the maximal dimension.
N/A: Not available.

uniformity + 7.658610×energy - 3.20757210^{-9} × cluster prominence(GLCM) - 1.566187 × 10^{-6} × minimum intensity (GLCM).

Development of radiomics-based prediction model

The significant clinical variables including ALP level and ICG-R15, and radiomics signature were chosen to build the radiomics-based model. The collinearity diagnosis showed the variance inflation factors of ALP, ICG-R15 and radiomics signature ranging from 1.012 to 1.107, suggesting no multicollinearity for radiomics-based model. Multivariable logistic regression analysis showed that only ICG-R15 and radiomics signature were independent risk factors for liver failure ($P < 0.005$). Thus, the radiomics signature and ICG-R15 were incorporated to develop the radiomics-based model and presented as a nomogram (Figure 4A). The calibration curve and an insignificant Hosmer-Lemeshow test statistic ($P = 0.841$) demonstrated the good calibration of this nomogram (Figure 4C).

Comparison of predictive performance

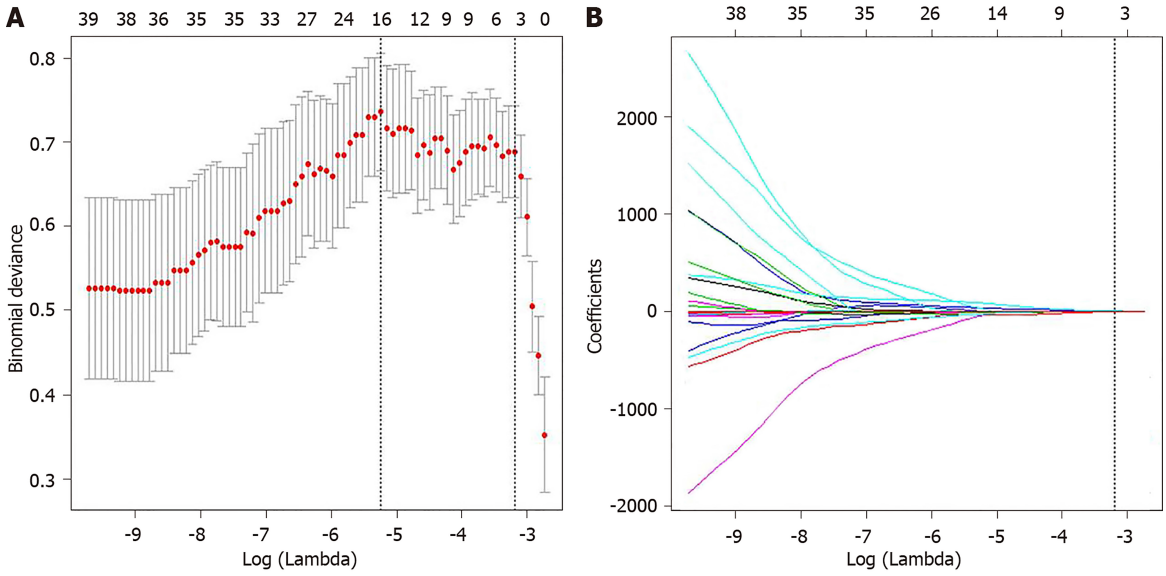

Figure 3 Radiomic feature selection using least absolute shrink-age and selection operator logistic regression. A: Selection of tuning parameters (l) in the least absolute shrink-age and selection operator model used 10-fold cross-validation *via* minimum criteria. The area under the curve was plotted *vs* log (λ). Dotted vertical lines were drawn at the optimal values using the minimum criteria and the 1 standard error of the minimum criteria (the 1 - standard error criteria); B: Least absolute shrink-age and selection operator coefficient profiles of the radiomic features. A vertical line was plotted at the optimal λ value, which resulted in five features with nonzero coefficients.

The predictive performance of clinical prediction model, radiomics signature, and radiomics-based model is shown in Table 3 and the ROCs are shown in Figure 4B. The radiomics-based model showed the highest performance for predicting liver failure, with an AUC of 0.894 (95%CI: 0.823, 0.964), which was higher than that of the clinical prediction model [AUC, 0.810 (95%CI: 0.691, 0.929)] and radiomics signature [AUC, 0.809 (95%CI: 0.713, 0.906)] (P = 0.025). The IDI showed a significant improvement in the accuracy of predicting liver failure when radiomics signature was incorporated with the clinical prediction model (IDI = 0.117, P = 0.002; continuous net reclassification improvement = 0.157, P = 0.09). The decision curve analysis for clinical prediction model, radiomics signature and radiomics-based model are presented in Figure 5.

DISCUSSION

Our study demonstrated that several radiomic features derived from HBP images of gadoxetic acid-enhanced MRI are associated with the liver failure in cirrhotic patients with HCC after major hepatectomy. Radiomics signature constructed from these radiomic features showed good performance in predicting postoperative live failure. Radiomics-based model integrating radiomics signature and ICG-R15 further improved the predictive performance.

For hepatitis B patients with active viral replication, liver disease like cirrhosis not only can progress to the stage of liver function decompensation, but also can result in the occurrence of HCC[20]. As surgery is the primary treatment for patients with HCC, it is important to assess liver functional reserve for HCC patients before surgery. At present, the main clinical factors that could help predict the risk of postoperative liver failure are serological indexes, Child-Pugh classification or IGG test. An increased ALP activity often accompanies hepatobiliary disease[21]. Previously, the ALP level was found to be useful for estimating postoperative liver failure after hepatectomy[22] . Another study showed that serum ALP and bilirubin might be an early surrogate marker for ischemic cholangiopathy and graft failure in liver transplantation[23]. In our study, the ALP level was also found to be an independent predictor of liver failure. Unlike a single serological index, Child-Pugh classification incorporates several biochemical parameters and clinical symptoms, suggesting insufficient liver function. However, the Child-Pugh classification has been proven not reliable for predicting the prognosis of hepatectomy due to its high variability[24,25]. In our study, Child-Pugh classification was not associated with the occurrence of liver failure.

The ICG clearance test is another important method to evaluate liver function, which is commonly used in clinical daily practice[26]. The results of the ICG test are

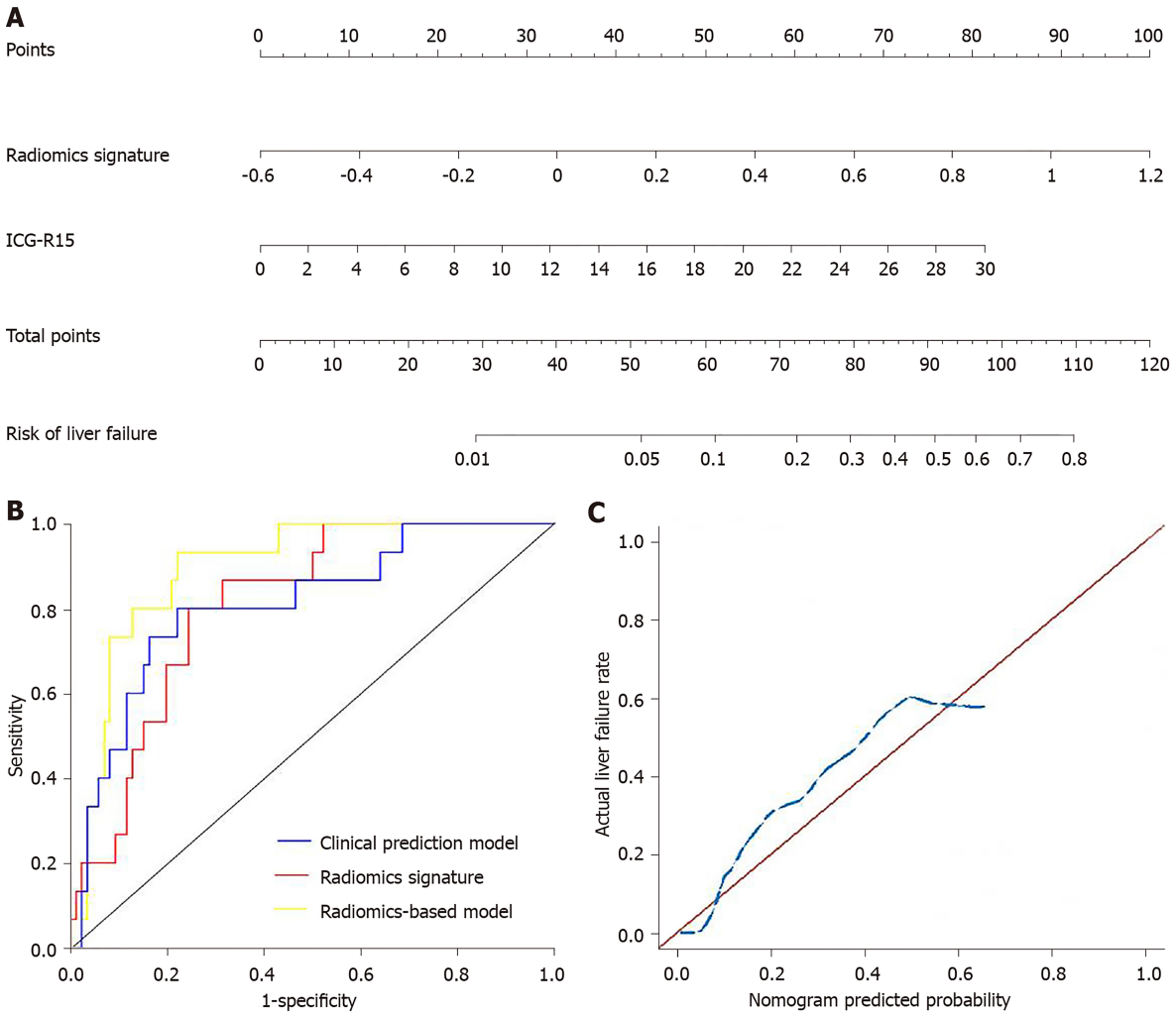

Figure 4 Radiomics nomogram and receiver operating characteristic curves and calibration curves of three predictive models. A: A nomogram was developed with incorporation of radiomics signature and indocyanine green retention rate at 15 min; B: Comparison of receiver operating characteristic curves of clinical prediction model, radiomics signature and radiomics-based model for the prediction of liver failure; C: Calibration curves of the nomogram.

considered as the most reliable risk factor, which can be used to determine the surgical indications of patients with HCC[27]. However, the ICG test has several limitations. For example, this test cannot be used in patients with jaundice. Moreover, a previous study showed that the predictive value of the ICG test for LF was nearly equal to a random guess (AUC, 0.51)[28]. In our study, 6 patients with a normal ICG-R15 value have experienced liver failure after surgery.

Several imaging biomarkers, such as liver volume measured on three-dimensional CT, receptor index (LHL_{15}) and blood clearance index (HH_{15}) on ^{99m}Tc-galactosyl serum albumin scintigraphy, have been applied to assess liver function[29]. However, the liver volume is not always relevant to the actual liver function, and the heterogeneity of the remnant liver may result in different levels of function for two patients with the same remnant liver volume on CT. The disadvantages of ^{99m}Tc-galactosyl serum albumin scintigraphy are the radiation exposure and its low spatial resolution. Gadoxetic acid-enhanced MRI has a high diagnostic efficacy for focal hepatic lesions[30] and can be used to quantify liver function[8]. The liver in patients with hepatitis B shows slow-moving changes with a common pathological process of progressive fibrosis, bridging of portal spaces and nodule regeneration of the liver parenchyma[31]. Liver damage may result in decreased number of normal hepatocytes, which impairs the uptake of gadoxetic acid, thus lowering the concentrations of gadoxetic acid in the liver parenchyma in the HBP. Moreover, such pathological process that may destroy the homogeneity of the liver parenchyma, which can be reflected by different texture features derived from MRI[32].

In our study, a radiomics signature based on HBP images was developed for predicting liver failure in patients with HCC. The AUC of radiomics signature was as high as 0.809, which suggests favorable discrimination for liver failure. The multivariable logistic regression analysis showed that ALP and ICG-R15 were

Table 3 Receiver operating characteristics analysis of the predictive value of clinical prediction model, radiomics signature and radiomics-based model

	Clinical prediction model	Radiomics signature	Radiomics-based model
AUC (95%CI)	0.810 (0.691-0.929)	0.809 (0.713-0.906)	0.894 (0.823-0.964)
Optimized Youden Index	0.579	0.556	0.712
Sensitivity (95%CI)	0.800 (0.514-0.947)	0.800 (0.514-0.947)	0.933 (0.660-0.997)
Specificity (95%CI)	0.779 (0.674-0.858)	0.756 (0.649-0.839)	0.779 (0.674-0.859)
PPV (95%CI)	0.387 (0.224-0.577)	0.364 (0.210-0.549)	0.424 (0.260-0.606)
NPV (95%CI)	0.957 (0.872-0.989)	0.956 (0.868-0.989)	0.985 (0.910-0.999)
Accuracy (95%CI)	0.782 (0.691-0.852)	0.762 (0.670-0.835)	0.802 (0.713-0.869)

AUC: Area under the curve; CI: Confidence interval; NPV: Negative predictive value; PPV: Positive predictive value.

independent clinical predictive factors for the liver failure. Then, we constructed a radiomics nomogram incorporating the clinical predictive factors and radiomics signature. Only were ICG-R15 and radiomics signature selected as independent predictive factors for the liver failure. This radiomics-based model showed good calibration and discrimination. The AUC of the nomogram increased to 0.894, and the IDI index has the significance, indicating the greater predictive efficacy of nomogram than either the radiomics signature or the clinical variables alone. Previously, several texture features derived from preoperative CT images has also been proposed to predict postoperative liver failure[16]. However, this study has a small number of patients (n = 36) and no predictive model was built[16]. In addition, the measurement of relative liver enhancement on HBP images of gadoxetic acid–enhanced magnetic resonance imaging (MRI) has been shown to be able to preoperatively assess the risk of liver failure after major liver resection with an AUC of 0.948[9]. However, only a small number of patients with liver failure (n = 3) was included in this study. The value of relative liver enhancement should be further validated by a large cohort study.

Gadoxetic acid-enhanced MRI can assist in differential diagnosis of focal liver lesion. The radiomics model built from HBP images has an advantage to be used for preoperative liver function assessment in the same examination. The proposed radiomics-based model in our study may serve as a reliable predictive tool to reduce postoperatively liver failure and mortality in cirrhotic patients with HCC after major hepatectomy. For example, it can be used in combination with ICG-R15 to improve the ability to predict postoperative liver failure when surgery is planned for a cirrhotic patient with HCC. If there is a high risk of postoperative liver failure, major hepatectomy should be avoided and some locoregional treatments such as percutaneous ethanol injection, radiofrequency ablation, trans-arterial chemoembolization and radioembolization can be applied for this patient. In addition, if a patient has uncertain results of ICG test, such as a patient with severe jaundice, the radiomics model can be used alternatively to predict the risk of postoperative live failure[33].

Our study had several limitations. First, a small number of patients with liver failure in our study, thus the validation cohort can't be allocated. After all, liver failure is a relatively rare event in our institution due to strict selection for hepatectomy. Second, we did not adopt a large quantity of radiomic features, since most of the information from feature exaction were redundant and nonreproducible[34].

In conclusion, a radiomics signature based on preoperative gadoxetic acid–enhanced MRI was developed, which showed favorable performance in predicting liver failure in cirrhotic patients with HCC after major liver resection. The radiomics model incorporating the radiomics signature and ICG-15 further improved the performance in predicting liver failure. The radiomics analysis of preoperative gadoxetic acid–enhanced MRI could be used to predict the risk of liver failure in cirrhotic patients with HCC after major hepatectomy.

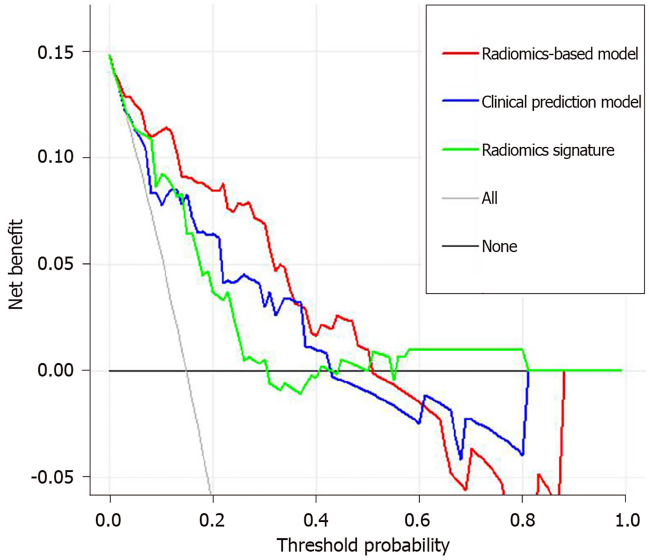

Figure 5 Decision curve analysis for each model. The y-axis measures the net benefit, which is calculated by summing the benefits (true-positive findings) and subtracting the harms (false-positive findings), weighting the latter by a factor related to the relative harm of undetected liver failure compared with the harm of unnecessary treatment. The decision curve showed the application of radiomics-based model to predict liver failure adds more benefit than treating all or none of the patients, clinical prediction model, and radiomics signature.

ARTICLE HIGHLIGHTS

Research background

Postoperative liver failure is the most serious complication for patients with hepatocellular carcinoma (HCC) after major hepatectomy. There are many methods for predicting postoperative liver failure after hepatectomy but not sufficiently accurate enough. This paper provides a radiomics model based on gadoxetic acid-enhanced magnetic resonance imaging (MRI), serve as a reliable predictive tool to reduce postoperative liver failure and mortality in cirrhotic patients with HCC after major hepatectomy.

Research motivation

In order to determine a new method to predict the postoperative liver failure after major hepatectomy and our radiomics model showed a favorable performance. However, the results obtained in this study need to be further verified in the population, and validation cohort need to be allocated.

Research objectives

The objective of this study is to determine the performance for predicting liver failure of a radiomics model based on preoperative gadoxetic acid-enhanced magnetic resonance imaging. The finding provides important information for medical decision making when surgery is required for a patient with HCC.

Research methods

The significant clinical variables were chosen and the radiomics signature was developed based on preoperative hepatobiliary phase gadoxetic acid-enhanced MRI in 101 patients with HCC from Sun Yat-Sen Memorial Hospital. The integrated radiomics-based model was presented as a radiomics nomogram. The performances for predicting post-operative liver failure were determined using receiver operating characteristics curve, calibration curve and decision curve analysis.

Research results

This study found that five radiomic features from hepatobiliary phase images were selected, and a radiomics-based model incorporating indocyanine green clearance rate at 15 min and radiomics signature showed favorable performance for predicting postoperative liver failure. The performance of radiomics model need to be further validated.

Research conclusions

The liver failure is very severe after liver resection. In this study, a radiomics signature based on preoperative gadoxetic acid–enhanced MRI was developed, which showed favorable performance in predicting liver failure in cirrhotic patients with HCC after major liver resection.

Research perspectives

This study confirmed the performance for predicting of our radiomics model. On this basis, future studies will further expand the sample size, and add the validation cohort.

REFERENCES

1 **Lock JF**, Reinhold T, Malinowski M, Pratschke J, Neuhaus P, Stockmann M. The costs of postoperative liver failure and the economic impact of liver function capacity after extended liver resection--a single-center experience. *Langenbecks Arch Surg* 2009; **394**: 1047-1056 [PMID: 19533168 DOI: 10.1007/s00423-009-0518-4]

2 **Zipprich A**, Kuss O, Rogowski S, Kleber G, Lotterer E, Seufferlein T, Fleig WE, Dollinger MM. Incorporating indocyanin green clearance into the Model for End Stage Liver Disease (MELD-ICG) improves prognostic accuracy in intermediate to advanced cirrhosis. *Gut* 2010; **59**: 963-968 [PMID: 20581243 DOI: 10.1136/gut.2010.208595]

3 **Zappa M**, Dondero F, Sibert A, Vullierme MP, Belghiti J, Vilgrain V. Liver regeneration at day 7 after right hepatectomy: global and segmental volumetric analysis by using CT. *Radiology* 2009; **252**: 426-432 [PMID: 19703882 DOI: 10.1148/radiol.2522080922]

4 **Cucchetti A**, Ercolani G, Vivarelli M, Cescon M, Ravaioli M, La Barba G, Zanello M, Grazi GL, Pinna AD. Impact of model for end-stage liver disease (MELD) score on prognosis after hepatectomy for hepatocellular carcinoma on cirrhosis. *Liver Transpl* 2006; **12**: 966-971 [PMID: 16598792 DOI: 10.1002/lt.20761]

5 **Kamath PS**, Kim WR; Advanced Liver Disease Study Group. The model for end-stage liver disease (MELD). *Hepatology* 2007; **45**: 797-805 [PMID: 17326206 DOI: 10.1002/hep.21563]

6 **Hoekstra LT**, de Graaf W, Nibourg GA, Heger M, Bennink RJ, Stieger B, van Gulik TM. Physiological and biochemical basis of clinical liver function tests: a review. *Ann Surg* 2013; **257**: 27-36 [PMID: 22836216 DOI: 10.1097/SLA.0b013e31825d5d47]

7 **Lee NK**, Kim S, Lee JW, Lee SH, Kang DH, Kim GH, Seo HI. Biliary MR imaging with Gd-EOB-DTPA and its clinical applications. *Radiographics* 2009; **29**: 1707-1724 [PMID: 19959517 DOI: 10.1148/rg.296095501]

8 **Yamada A**, Hara T, Li F, Fujinaga Y, Ueda K, Kadoya M, Doi K. Quantitative evaluation of liver function with use of gadoxetate disodium-enhanced MR imaging. *Radiology* 2011; **260**: 727-733 [PMID: 21712472 DOI: 10.1148/radiol.11100586]

9 **Wibmer A**, Prusa AM, Nolz R, Gruenberger T, Schindl M, Ba-Ssalamah A. Liver failure after major liver resection: risk assessment by using preoperative Gadoxetic acid-enhanced 3-T MR imaging. *Radiology* 2013; **269**: 777-786 [PMID: 23942606 DOI: 10.1148/radiol.13130210]

10 **Ratziu V**, Charlotte F, Heurtier A, Gombert S, Giral P, Bruckert E, Grimaldi A, Capron F, Poynard T; LIDO Study Group. Sampling variability of liver biopsy in nonalcoholic fatty liver disease. *Gastroenterology* 2005; **128**: 1898-1906 [PMID: 15940625 DOI: 10.1053/j.gastro.2005.03.084]

11 **Yoon JH**, Choi JI, Jeong YY, Schenk A, Chen L, Laue H, Kim SY, Lee JM. Pre-treatment estimation of future remnant liver function using gadoxetic acid MRI in patients with HCC. *J Hepatol* 2016; **65**: 1155-1162 [PMID: 27476767 DOI: 10.1016/j.jhep.2016.07.024]

12 **Lambin P**, Leijenaar RTH, Deist TM, Peerlings J, de Jong EEC, van Timmeren J, Sanduleanu S, Larue RTHM, Even AJG, Jochems A, van Wijk Y, Woodruff H, van Soest J, Lustberg T, Roelofs E, van Elmpt W, Dekker A, Mottaghy FM, Wildberger JE, Walsh S. Radiomics: the bridge between medical imaging and personalized medicine. *Nat Rev Clin Oncol* 2017; **14**: 749-762 [PMID: 28975929 DOI: 10.1038/nrclinonc.2017.141]

13 **Limkin EJ**, Sun R, Dercle L, Zacharaki EI, Robert C, Reuzé S, Schernberg A, Paragios N, Deutsch E, Ferté C. Promises and challenges for the implementation of computational medical imaging (radiomics) in oncology. *Ann Oncol* 2017; **28**: 1191-1206 [PMID: 28168275 DOI: 10.1093/annonc/mdx034]

14 **Ji GW**, Zhang YD, Zhang H, Zhu FP, Wang K, Xia YX, Zhang YD, Jiang WJ, Li XC, Wang XH. Biliary Tract Cancer at CT: A Radiomics-based Model to Predict Lymph Node Metastasis and Survival Outcomes. *Radiology* 2019; **290**: 90-98 [PMID: 30325283 DOI: 10.1148/radiol.2018181408]

15 **Wu S**, Zheng J, Li Y, Yu H, Shi S, Xie W, Liu H, Su Y, Huang J, Lin T. A Radiomics Nomogram for the Preoperative Prediction of Lymph Node Metastasis in Bladder Cancer. *Clin Cancer Res* 2017; **23**: 6904-6911 [PMID: 28874414 DOI: 10.1158/1078-0432.CCR-17-1510]

16 **Simpson AL**, Adams LB, Allen PJ, D'Angelica MI, DeMatteo RP, Fong Y, Kingham TP, Leung U, Miga MI, Parada EP, Jarnagin WR, Do RK. Texture analysis of preoperative CT images for prediction of postoperative hepatic insufficiency: a preliminary study. *J Am Coll Surg* 2015; **220**: 339-346 [PMID: 25537305 DOI: 10.1016/j.jamcollsurg.2014.11.027]

17 **Krieger PM**, Tamandl D, Herberger B, Faybik P, Fleischmann E, Maresch J, Gruenberger T. Evaluation of chemotherapy-associated liver injury in patients with colorectal cancer liver metastases using indocyanine green clearance testing. *Ann Surg Oncol* 2011; **18**: 1644-1650 [PMID: 21207168 DOI: 10.1245/s10434-010-1494-1]

18 **Shiha G**, Zalata K. Ishak versus METAVIR: terminology, convertibility and correlation with laboratory changes in chronic Hepatitis C. InTechOpen. 2011; 156-170 [DOI: 10.5772/20110]

19 **Tibshirani R**. Regression shrinkage and selection via the lasso. *J R Stat Soc Series B Stat Methodol* 1996; **58**: 267-88

20 **Peng CY**, Chien RN, Liaw YF. Hepatitis B virus-related decompensated liver cirrhosis: benefits of antiviral therapy. *J Hepatol* 2012; **57**: 442-450 [PMID: 22504333 DOI: 10.1016/j.jhep.2012.02.033]

21 **Moss DW**. Alkaline phosphatase isoenzymes. *Clin Chem* 1982; **28**: 2007-2016 [PMID: 6751596 DOI: 10.1093/clinchem/28.10.2007]

22 **Osada S**, Saji S. The clinical significance of monitoring alkaline phosphatase level to estimate postoperative liver failure after hepatectomy. *Hepatogastroenterology* 2004; **51**: 1434-1438 [PMID: 15362770 DOI: 10.1002/hed.20094]

23 **Halldorson JB**, Rayhill S, Bakthavatsalam R, Montenovo M, Dick A, Perkins J, Reyes J. Serum alkaline phosphatase and bilirubin are early surrogate markers for ischemic cholangiopathy and graft failure in liver transplantation from donation after circulatory death. *Transplant Proc* 2015; **47**: 465-468 [PMID: 25769592 DOI: 10.1016/j.transproceed.2014.10.055]

24 **Nagashima I**, Takada T, Okinaga K, Nagawa H. A scoring system for the assessment of the risk of mortality after partial hepatectomy in patients with chronic liver dysfunction. *J Hepatobiliary Pancreat Surg* 2005; **12**: 44-48 [PMID: 15754099 DOI: 10.1007/s00534-004-0953-0]

25 **Garcea G**, Ong SL, Maddern GJ. Predicting liver failure following major hepatectomy. *Dig Liver Dis* 2009; **41**: 798-806 [PMID: 19303376 DOI: 10.1016/j.dld.2009.01.015]

26 **Matsumata T**, Kanematsu T, Yoshida Y, Furuta T, Yanaga K, Sugimachi K. The indocyanine green test enables prediction of postoperative complications after hepatic resection. *World J Surg* 1987; **11**: 678-681

[PMID: 2823492 DOI: 10.1007/bf01655848]
27 **Ishikawa M**, Yogita S, Miyake H, Fukuda Y, Harada M, Wada D, Tashiro S. Clarification of risk factors for hepatectomy in patients with hepatocellular carcinoma. *Hepatogastroenterology* 2002; **49**: 1625-1631 [PMID: 12397750 DOI: 10.1136/gut.51.5.757]
28 **Wong JS**, Wong GL, Chan AW, Wong VW, Cheung YS, Chong CN, Wong J, Lee KF, Chan HL, Lai PB. Liver stiffness measurement by transient elastography as a predictor on posthepatectomy outcomes. *Ann Surg* 2013; **257**: 922-928 [PMID: 23001077 DOI: 10.1097/SLA.0b013e318269d2ec]
29 **Kawamura H**, Kamiyama T, Nakagawa T, Nakanishi K, Yokoo H, Tahara M, Kamachi H, Toi H, Matsushita M, Todo S. Preoperative evaluation of hepatic functional reserve by converted ICGR15 calculated from Tc-GSA scintigraphy. *J Gastroenterol Hepatol* 2008; **23**: 1235-1241 [PMID: 18522682 DOI: 10.1111/j.1440-1746.2008.05389.x]
30 **Reimer P**, Schneider G, Schima W. Hepatobiliary contrast agents for contrast-enhanced MRI of the liver: properties, clinical development and applications. *Eur Radiol* 2004; **14**: 559-578 [PMID: 14986050 DOI: 10.1007/s00330-004-2236-1]
31 **Tsochatzis EA**, Bosch J, Burroughs AK. Liver cirrhosis. *Lancet* 2014; **383**: 1749-1761 [PMID: 24480518 DOI: 10.1016/S0140-6736(14)60121-5]
32 **Wu Z**, Matsui O, Kitao A, Kozaka K, Koda W, Kobayashi S, Ryu Y, Minami T, Sanada J, Gabata T. Hepatitis C related chronic liver cirrhosis: feasibility of texture analysis of MR images for classification of fibrosis stage and necroinflammatory activity grade. *PLoS One* 2015; **10**: e0118297 [PMID: 25742285 DOI: 10.1371/journal.pone.0118297]
33 **Bruix J**, Sherman M; American Association for the Study of Liver Diseases. Management of hepatocellular carcinoma: an update. *Hepatology* 2011; **53**: 1020-1022 [PMID: 21374666 DOI: 10.1002/hep.24199]
34 **Berenguer R**, Pastor-Juan MDR, Canales-Vázquez J, Castro-García M, Villas MV, Mansilla Legorburo F, Sabater S. Radiomics of CT Features May Be Nonreproducible and Redundant: Influence of CT Acquisition Parameters. *Radiology* 2018; **288**: 407-415 [PMID: 29688159 DOI: 10.1148/radiol.2018172361]

World Journal of Gastroenterology

Submit a Manuscript: https://www.f6publishing.com

World J Gastroenterol 2020 March 21; 26(11): 1221-1230

DOI: 10.3748/wjg.v26.i11.1221

ISSN 1007-9327 (print) ISSN 2219-2840 (online)

ORIGINAL ARTICLE

Observational Study

Subtle skills: Using objective structured clinical examinations to assess gastroenterology fellow performance in system based practice milestones

Marianna Papademetriou, Gabriel Perrault, Max Pitman, Colleen Gillespie, Sondra Zabar, Elizabeth Weinshel, Renee Williams

ORCID number: Marianna Papademetriou (0000-0002-5471-3394); Gabriel Perreault (0000-0002-4530-6957); Max Pitman (0000-0002-4538-0858); Colleen Gillespie (0000-0001-9096-3430); Sondra Zabar (0000-0002-9223-1898); Elizabeth Weinshel (0000-0002-1537-8378); Renee Williams (0000-0001-5530-2207).

Author contributions: Papademetriou M, Pitman M, Williams R and Weinshel E wrote and developed content for the Objective Structured Clinical Exam; Gillespie C, Zabar S and Weinshel E served as content experts who reviewed checklists, exam content, scripts and helped coordinate and execution of the Objective Structured Clinical Examinations; Williams R collected and summarized the data. All authors contributed in the writing and editing of the final manuscript.

Institutional review board statement: This program was considered an educational performance improvement project by the New York University School of Medicine Institutional Review Board and was not considered for IRB approval. IRB submission and approval was not required.

Informed consent statement: This program was considered an educational performance improvement project by the New York University School of

Marianna Papademetriou, Division of Gastroenterology, Georgetown University Medical Center, Washington, DC 20007, United States

Marianna Papademetriou, Division of Gastroenterology, Washington DC VA Medical Center, Washington, DC 20422, United States

Gabriel Perrault, Department of Medicine, New York University Medical Center, New York, NY 10016, United States

Max Pitman, Renee Williams, Division of Gastroenterology, New York University Medical Center, New York, NY 10016, United States

Colleen Gillespie, Sondra Zabar, Department of Medicine, New York University School of Medicine, New York, NY 10016, United States

Elizabeth Weinshel, Department of Gastroenterology, VA New York Harbor Healthcare System, New York, NY 10010, United States

Corresponding author: Marianna Papademetriou, MD, Assistant Professor, Division of Gastroenterology, Washington DC VA Medical Center, 50 Irving Street NW, Washington, DC 20422, United States. marianna.papademetriou@va.gov

Abstract

BACKGROUND

System based practice (SBP) milestones require trainees to effectively navigate the larger health care system for optimal patient care. In gastroenterology training programs, the assessment of SBP is difficult due to high volume, high acuity inpatient care, as well as inconsistent direct supervision. Nevertheless, structured assessment is required for training programs. We hypothesized that objective structured clinical examination (OSCE) would be an effective tool for assessment of SBP.

AIM

To develop a novel method for SBP milestone assessment of gastroenterology fellows using the OSCE.

METHODS

For this observational study, we created 4 OSCE stations: Counseling an

Medicine Institutional Review Board. Participation in the program was voluntary. Informed consent to participate was not required.

Conflict-of-interest statement: The authors have no potential conflicts of interest to disclose.

Data sharing statement: No additional data are available.

STROBE statement: Authors have read the STROBE Statement-checklist of items and the manuscript was prepared and revised accordingly.

Manuscript source: Invited Manuscript

Received: December 5, 2019
Peer-review started: December 5, 2019
First decision: January 16, 2020
Revised: February 10, 2020
Accepted: March 5, 2020
Article in press: March 5, 2020
Published online: March 21, 2020

P-Reviewer: Caboclo JF
S-Editor: Tang JZ
L-Editor: A
E-Editor: Ma YJ

impaired colleague, handoff after overnight call, a feeding tube placement discussion, and giving feedback to a medical student on a progress note. Twenty-six first year fellows from 7 programs participated. All fellows encountered identical case presentations. Checklists were completed by trained standardized patients who interacted with each fellow participant. A report with individual and composite scores was generated and forwarded to program directors to utilize in formative assessment. Fellows also received immediate feedback from a faculty observer and completed a post-session program evaluation survey.

RESULTS

Survey response rate was 100%. The average composite score across SBP milestones for all cases were 6.22 (SBP1), 4.34 (SBP2), 3.35 (SBP3), and 6.42 (SBP4) out of 9. The lowest composite score was in SBP 3, which asks fellows to advocate for cost effective care. This highest score was in patient care 2, which asks fellows to develop comprehensive management plans. Discrepancies were identified between the fellows' perceived performance in their self-assessments and Standardized Patient checklist evaluations for each case. Eighty-seven percent of fellows agreed that OSCEs are an important component of their clinical training, and 83% stated that the cases were similar to actual clinical encounters. All participating fellows stated that the immediate feedback was "*very useful*." One hundred percent of the fellows stated they would incorporate OSCE learning into their clinical practice.

CONCLUSION

OSCEs may be used for standardized evaluation of SBP milestones. Trainees scored lower on SBP milestones than other more concrete milestones. Training programs should consider OSCEs for assessment of SBP.

Key words: Objective structured clinical exams; Medical education; Medical error; System based practice; Milestones; Gastroenterology

Core tip: In United States medical training, system based practice (SBP) milestones are often considered the most difficult to both teach and assess. While the objective standardized clinical examination is a well validated method for assessment in medical education, its use for assessment of specific SBP milestones has not been well studied. In this observational study, we created and implemented objective standardized clinical examinations geared towards assessment of SBP milestones in gastroenterology fellows in scenarios engineered to provide opportunity for medical error. We show that this method provides objective assessment of trainees for program use and may help trainees feel more prepared for real world situations.

Citation: Papademetriou M, Perrault G, Pitman M, Gillespie C, Zabar S, Weinshel E, Williams R. Subtle skills: Using objective structured clinical examinations to assess gastroenterology fellow performance in system based practice milestones. *World J Gastroenterol* 2020; 26(11): 1221-1230
URL: https://www.wjgnet.com/1007-9327/full/v26/i11/1221.htm
DOI: https://dx.doi.org/10.3748/wjg.v26.i11.1221

INTRODUCTION

Medical education assessment in the United States is currently based on six competencies as defined by the Accreditation Council for Graduate Medical Education (ACGME) in 1999: Patient care (PC), medical knowledge, practice-based learning and improvement, professionalism, interpersonal and communication skills(ICS), and system based practice (SBP)[1].

The SBP competencies require trainees to effectively recognize and navigate the larger healthcare system for optimal PC. While these are important skills to build, they are difficult to define and assess in a standardized way in daily clinical

encounters. For gastroenterology (GI) fellowships in the United States, the high acuity of inpatient consultations with little time for complete direct observation necessitates focus on tools to evaluate all milestones in addition to SBP[2-5]. Simulation based medical education such as the objective structured clinical examinations (OSCEs) are now a standard methodology for assessing clinical skill and knowledge in medical education[1]. OSCEs are the foundation of Step 2 CS of the United States Medical Licensing Examination. They have the advantage of assessing large groups of learners across a range of skills by recreating situations where there is limited opportunity for supervision and feedback with high validity and reliability[6]. While many studies have corroborated the effectiveness of OSCEs for learner assessment, there are few papers that have evaluated this setting as an effective teaching tool as well[2,7].

Furthermore, SBP milestones are particularly difficult to evaluate objectively and reproducibly in everyday clinical encounters and may be even more difficult to teach in the course of typical clinical encounters[8].

The purpose of our program was to assess first year GI fellows' skills in SBP milestones utilizing OSCEs that created opportunity for medical errors. We hypothesized that the OSCE would be an effective tool for assessment of SBP.

This is the first paper to our knowledge to focus on these milestones in GI trainees.

MATERIALS AND METHODS

OSCE station development and implementation

Four cases were developed to assess several ACGME milestones (PC, medical knowledge, ICS, SBP, professionalism). Medical education and GI content experts reviewed all 4 cases prior to implementation.

Impaired colleague: The fellows were asked to give sign out to a co-fellow demonstrating emotional and substance-related impairment. Participants were not forewarned of the impaired colleague, but were expected to screen for depression, life stressors, and substance use based on verbal and behavioral cues. This case was adapted from prior use for assessment with faculty and internal medicine residents.

Overnight handoff: The fellows were asked to give handoff to a senior fellow on an acutely ill patient and were in part evaluated on use of best practices from Illness severity, patient summary, action list, situation awareness, synthesis (I-PASS), a validated handoff tool mnemonic that stands for Illness Severity, Patient Summary, Action List, Situation Awareness, and Synthesis by the Receiver[9]. Fellows were given I-PASS resources in the days prior to the OSCE but were not required to review them. We adapted this case's checklist from a previously utilized scenario[10].

Percutaneous endoscopic gastrostomy placement: The fellows were asked to discuss percutaneous endoscopic gastrostomy (PEG) tube placement with the health care proxy of a patient in a persistent vegetative state. The proxy was aware that the patient had expressed wishes not to have a feeding tube placed prior to becoming ill. This case was newly developed for this OSCE.

Note feedback: The fellows were asked to meet with a medical student and give feedback on a consult note which contained multiple documentation errors. This case was redesigned from a previously validated case for internal medicine residents.

Actors with prior OSCE experience performed the roles of the impaired colleague and the patient's health care proxy in the PEG case. A senior GI fellow and a medical student performed the necessary roles in the overnight handoff case and in the note feedback case, respectively. Collectively these individuals were referred to as standardized persons (SPs). The SPs underwent a 2-hour training session with scripts and role-play to ensure standardization of case portrayals and assessment. The program was held in 3 sessions with different fellows participating in one of each of the three sessions over a 2-year period. The OSCEs were run during the late fall or winter period both years in order to ensure all fellows had spent similar time in fellowship training at time of participation. First year GI fellows were recruited *via* email to their program directors, and participation was voluntary. All participating fellows encountered identical case presentations with the same SPs and faculty observers and had 12 min to perform each scenario, followed by a 3-minute feedback session. The exception was the senior fellow SP, where two different fellows played this role based on availability. The SPs completed OSCE checklists scoring each fellow immediately after each encounter.

Assessment tools

We utilized validated checklists completed by the faculty observers and SPs and a post-session program evaluation tool completed by participants[11]. The checklists also included case specific questions that highlighted milestones of SBP and were reviewed by content experts prior to implementation[3,4,12,13].

The checklist items were correlated with specific ACGME milestones and were rated on a 3-point scale of "not done" (the fellow did not attempt the task), "partly done" (the fellow attempted the task, but did not perform it correctly), and "well done" (the fellow performed the task correctly). The score for each milestone was converted from this three-point scale to a composite milestone score across all the cases. For example, a participant's score for that milestone (ex. PC 1) across all the cases was divided by the total possible score which yielded a number less than 1. This number was then multiplied by 9 to get the composite score for each milestone. This allowed us to compare score between different milestones.

A report with individual and composite scores was generated and forwarded to program directors to utilize in formative assessment (Supplemental Figure 1). Following each session, fellows had a debriefing session to review the teaching points, discuss the experience and provide open-ended feedback. They also completed an exit survey assessing pre- and post-OSCE perceptions and beliefs about competencies, educational value of the experience, and case difficulty. We collected and managed the data using Research Electronic Data Capture, a secure, web-based application[14].

This program was considered an educational performance improvement project by the New York University School of Medicine Institutional Review Board and was not considered for IRB approval.

RESULTS

Twenty-six first year fellows from seven GI training programs in New York City participated. Survey response rate was 100%, however, 2 surveys contained missing data and responses for those questions were not included in the calculation.

Milestone scores

The average composite milestone scores for all 26 learners across all four OSCE cases are reported in Figure 1. A wide variation in performance was noted across the evaluated milestone metrics. The lowest composite score was in SBP 3 (identifies forces that impact the cost of health care, and advocates for, and practices cost-effective care), where the mean score was 3.64 out of 9 points. In comparison, the highest composite score was seen in PC2 (develops and achieves comprehensive management plan for each patient), with a mean score of 7.25.

Perceived performance

We evaluated how participants felt they performed in each case (Tables 1 and 2). This can be contrasted with the scores given by the SPs. SPs documented whether particular course objectives were met, which were individualized for each case. Fellows were provided each case objective during the debriefing. In the PEG case, 88% of the fellows felt they were well prepared for the case and 66% felt they did well achieving the case objectives. Conversely, only 11% of fellows were rated by the SP to have engaged in shared decision making and no fellows were noted to have assessed the SP's basic understanding of risks, two points which were identified as case objectives. No fellow fully evaluated for depression, suicidal ideation or alcohol use in the Impaired Colleague case. Only 33% screened for depression and collaborated on identifying next steps. Participants indicated they felt more prepared for these scenarios after the OSCE than before. This difference was most striking for the PEG case and Impaired Colleague case.

Program evaluation

Participants were asked about their preparedness and performance on the cases in an exit survey. These results are summarized in Tables 1, 2, 3 and 4. The fellows rated their performance highly in the Handoff and note feedback cases, with 92.3% of respondents stating their performance was either "*fine*" or "*pretty good*." Self-assessment scores were lower for the PEG discussion and Impaired Colleague case, with 34.6% of respondents stating their performance "*could have been better*," in both cases (Tables 1 and 2). The participants' overall views of the OSCE are reported in Table 4. In general, the participants responded favorably: Eighty-seven percent agreed that OSCEs are an important component of their clinical training, and 83% stated that the cases were similar to actual clinical encounters. All of the respondents stated that the immediate feedback was "*very useful*," and 100% of respondents stated they would incorporate OSCE learning into their clinical practice. For each case, a majority of

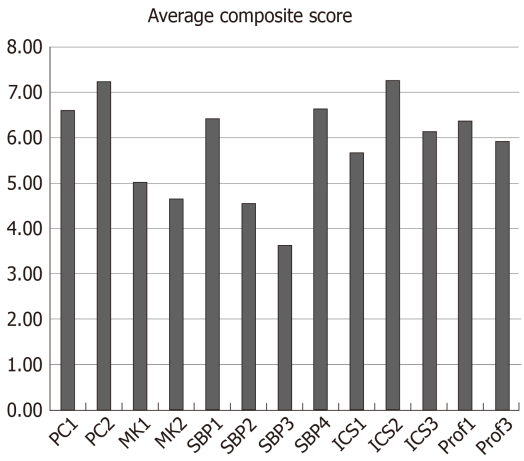

Figure 1 Average composite scores for each milestone across all cases.

respondents stated they would feel more comfortable in a similar situation after the OSCE than they did before.

DISCUSSION

Our main objective was to assess SBP milestones using novel OSCE cases. We were also interested to see if participants felt the experience was helpful as a teaching tool, although we could not assess teaching utility in this observational study.

We highlighted the following SBP milestones in our handoff and feedback cases: SBP1 "*works effectively within an inter-professional team*"; SBP3 "*Recognized system error and advocated for system improvement*"; and SBP4, "*Transitions patients effectively within and across health delivery systems.*"

A recent report calculated medical errors as the third leading cause of death within the United States[15]. Handoffs are vulnerable to communication failures that can compromise quality and safety[16-18]. A 2007 analysis of malpractice claims involving trainees found that 70% of the errors involved the lack of supervision and hand-off errors. These types of errors were disproportionately more common amongst trainees *vs* faculty[19]. Studies have demonstrated that standardizing handoffs leads to better communication between physicians and, ultimately, to safer PC[20,21]. Specifically, the mnemonic I-PASS has been shown prospectively to reduce medical errors[9]. In this OSCE, participants were given learning materials explaining the I-PASS format and were provided immediate feedback about critical communication. More fellows agreed with feeling prepared to give adequate hand off after the OSCE than did beforehand.

Graduate medical trainees also have important responsibilities to supervise and teach junior learners, yet rarely receive formal instruction on how to deliver feedback effectively. A survey of 50 graduate medical education programs found that trainees had a lower perception than staff in the "*communication and feedback about error*" domain, indicating trainees do not feel they obtain regular feedback when an error occurs[22]. After our feedback case, the number of fellows who strongly agreed they felt comfortable giving constructive criticism doubled from 35% to 70%.

We found discrepancies between how fellows felt they met case objectives *vs* how they were scored, most apparent in the PEG and the impaired colleague scenarios. These cases highlight complex situations, which we believe early trainees have not often experienced. Our PEG discussion case allowed participants to demonstrate SBP3: Competency advocating cost effective care. The case focused on sensitive issues of end of life counseling and discussing risks and benefits of a procedure - skills which fellows were least likely to demonstrate when compared to other PC skills[13]. Similarly, in this OSCE, fellows scored the lowest on the PEG case and the lowest average composite score in SBP3.

The case involving sign out to an impaired colleague is especially relevant with the current focus on physician depression, burnout and suicide. Fellows had to recognize that having an impaired colleague care for patients would directly compromise patient safety. While this situation is rare, the risks are high and the issues are complex. Singh *et al*[19] also found that 72% of medical errors involved an error in judgment and 58% a lack of competence, both of which would be present in an

Table 1 Fellow reported preparedness for each case, *n* (%)

Did you feel prepared for this case?	No	Yes
Impaired colleague[1]	6 (24)	19 (76)
Hand off with I-PASS	6 (23)	20 (77)
PEG discussion[1]	3 (13)	21 (88)
Note-writing and feedback	2 (8)	24 (92)

[1]Data missing due to incomplete survey responses. I-PASS: Illness severity, patient summary, action list, situation awareness, synthesis; PEG: Percutaneous endoscopic gastrostomy.

impaired physician. Twenty four percent of fellows felt they were not prepared for this case, the most of any of the four cases. The number of fellows who strongly agreed they could recognize signs of substance abuse and depression in a colleague more than doubled after the OSCE.

SBP milestones are difficult to assess objectively during GI training programs, as fellows may not be directly observed in situations where these competencies are required. Importantly, fellows' self-reported comfort levels increased after every OSCE case. Fellows reflected positively on the experience in the post participation survey. They universally felt that the immediate feedback was useful and would improve their clinical skills. All participants stated they would recommend this OSCE as an assessment and training tool. At the conclusion of our study, each fellow was provided a comprehensive report card documenting their performance, which could be utilized by the training program (Supplemental Figure 1). SBP milestone was shown in Supplemental Table 1.

The limitations of our OSCE study are inherent to studies involving subjective assessment, although our instructors and standardized patients were trained prior to the OSCE on scoring and the same individuals scored all 26 participants. Secondly, our study was small, as each OSCE was resource intensive. Lastly, as this was not a longitudinal study, we could not assess whether participation in and feedback from the OSCE improved performance in SBP. An interesting future direction could include the repeat assessment of the participating fellows at the end of their training to assess change in performance over time and to compare them to fellows who did not participate in the OSCE in their first year. In conclusion, OSCEs can be utilized to assess SBP milestones in high risk scenarios linked to medical errors.

Table 2 Fellow reported performance for each case, *n* (%)

How would you rate your overall performance in this case?	Could have been better	Fine	Pretty good
Impaired colleague	9 (34.6)	9 (34.6)	8 (30.8)
Hand off with I-PASS	2 (7.7)	15 (57.7)	9 (34.6)
PEG tube discussion	9 (34.6)	9 (34.6)	8 (30.8)
Note-writing and feedback	2 (7.7)	13 (50)	11 (42.3)

I-PASS: Illness severity, patient summary, action list, situation awareness, synthesis; PEG: Percutaneous endoscopic gastrostomy.

Table 3 Fellows' perceived skills and beliefs about clinical practice as reported in post-examination survey, *n* (%)

Items	Strongly disagree	Somewhat disagree	Somewhat agree	Strongly agree
Before today's OSCE, I felt comfortable discussing the utility of PEG placement in a patient with neurologic compromise	1 (4)	2 (8)	16 (67)	5 (21)
After today's OSCE, I feel more comfortable discussing the utility of PEG placement in a patient with neurologic compromise	0 (0)	0 (0)	10 (42)	14 (58)
Before today's OSCE, I felt comfortable during hand-off discussions with my co-fellows	0 (0)	1 (4)	10 (42)	13 (54)
After today's OSCE, I feel more comfortable during hand-off discussions with my co-fellows	0 (0)	1 (4)	8 (33)	15 (63)
Before today's OSCE, I felt comfortable that I would be able to recognize signs of substance abuse and depression in a colleague and referring them to the appropriate resources	2 (8)	5 (21)	12 (50)	5 (21)
After today's OSCE, I feel comfortable that I would be able to recognize signs of substance abuse and depression in a colleague and referring them to the appropriate resources	0 (0)	0 (0)	10 (42)	14 (58)
Before today's OSCE, I felt very comfortable giving constructive criticism and feedback to my learners	0 (0)	2 (9)	13 (57)	8 (35)
After today's OSCE, I feel more comfortable giving constructive criticism and feedback to my learners	0 (0)	1 (4)	6 (26)	16 (70)

OSCE: Objective structured clinical examination; PEG: Percutaneous endoscopic gastrostomy

Table 4 Fellows' views of the objective structured clinical examination based on post-examination survey, *n* (%)

Items	Strongly disagree	Somewhat disagree	Somewhat agree	Strongly agree
OSCEs are an important part of my clinical training	0 (0)	3 (13)	11 (48)	9 (39)
My performance on this OSCE accurately reflects my performance in clinical practice	1 (4)	5 (21)	13 (54)	5 (21)
These OSCE cases are similar to actual encounters	0 (0)	4 (17)	13 (54)	7 (29)
The immediate feedback that I received is very useful	0 (0)	0 (0)	4 (17)	20 (83)
I generally perform better on the OSCE than in clinical practice	8 (33)	14 (58)	0 (0)	2 (8)
I generally do better in clinical practice than I do in an OSCE	1 (4)	2 (8)	12 (50)	9 (38)
OSCEs makes me feel anxious	3 (13)	4 (17)	12 (50)	5 (21)
OSCEs are an effective means of demonstrating my interpersonal skills	0 (0)	3 (13)	16 (67)	5 (21)
OSCEs are an effective means of demonstrating my ability to demonstrate a shared decision-making approach to patient care	0 (0)	2 (8)	15 (63)	7 (29)
My clinical training fully prepared me for this OSCE	1 (4)	3 (13)	14 (58)	6 (25)
After I receive feedback on the OSCE, I will develop a plan to improve my clinical skills	0 (0)	0 (0)	12 (50)	12 (50)
I will incorporate what I have learned from this OSCE into my clinical practice	0 (0)	0 (0)	9 (38)	15 (63)
If you have participated in this OSCE before: Did your prior OSCE experience affect your participation today?	0 (0)	0 (0)	4 (31)	9 (69)

OSCE: Objective structured clinical examination.

ARTICLE HIGHLIGHTS

Research background

Medical education assessment in the United States is currently based on six competencies as defined by the Accreditation Council for Graduate Medical Education. Gastroenterology (GI) training programs must assess trainees according in all six competencies as part of formative feedback. The system based practice (SBP) competencies require trainees to effectively recognize and navigate the larger healthcare system for optimal patient care. These milestones may be considered more subtle skills to master than other concrete milestones such as patient care and medical knowledge.

Research motivation

SBP milestones are difficult to observe and assess in daily clinical encounters between patients and trainees. Therefore, alterative objective activities may be necessary to adequately assess achievement in SBP. Simulation based medical education such as the Objective Structured Clinical Examinations (OSCEs) are now a standard methodology for assessing clinical skill and knowledge in medical education. OSCEs have not been previously used to assess SBP milestones specifically.

Research objectives

The main objective of this research study was to create and then evaluate OSCEs as an effective

assessment tool for the evaluation of SBP milestones. We aimed to see if new clinical scenarios commonly encountered by GI trainees would be useful in this assessment. We also sought to evaluate how trainees felt about the experience.

Research methods

We developed four cases to help assess the Accreditation Council for Graduate Medical Education milestones with a focus on SBP. Trainees went through these four simulations with standardized patients and were evaluated by faculty experts using standardized checklists. Their performance from the checklists were aggregated and used to produce a scorecard which was sent to program directors at the conclusion of the OSCE. The trainees were then given direct feedback from the standardized patients and the faculty observer. Finally, the trainees were asked to complete a survey on the experience.

Research results

We ran three OSCE sessions involving 26 GI trainees. Scorecards indicated that, on average, trainees scored lower on SBP milestones than on other milestones categories. We identified and reported discrepancies between how well trainees believed they achieved objectives, and how they were rated by the standardized patients and faculty observers. Overall, trainees reflected positively on the experience in the post participation survey. They universally felt that the immediate feedback was useful and would improve their clinical skills. All participants stated they would recommend this OSCE as an assessment and training tool.

Research conclusions

In this study we demonstrated that OSCEs may be utilized to assess SBP milestones in an objective manner. Since SBP milestones may be difficult to assess in day-to-day activities in the hospital or clinic setting, training programs may want to utilize this type of standardized case-based simulation for assessment. Likewise, trainees reflected positively on the experience and felt they would incorporate feedback into their daily practice.

Research perspectives

Future studies are needed to assess if OSCEs may be useful teaching tools for SBP milestones. This would require repeat assessment with the same OSCE at the GI fellows' completion of training and comparison of this group to a group who did not participate in the initial OSCE in their first year.

REFERENCES

1 The Accrediting Council of Graduate Medical Education. ACGME Program Requirements for Graduate Medical Education in Internal Medicine Subspecialties. 2015 Jul [cited 20 January 2020]. Available from: URL: https://acgme.org/Portals/0/PDFs/Milestones/InternalMedicineSubspecialtyMilestones.pdf?ver=2015-11-06-120527-673

2 **Chander B**, Kule R, Baiocco P, Chokhavatia S, Kotler D, Poles M, Zabar S, Gillespie C, Ark T, Weinshel E. Teaching the competencies: using objective structured clinical encounters for gastroenterology fellows. *Clin Gastroenterol Hepatol* 2009; **7**: 509-514 [PMID: 19041733 DOI: 10.1016/j.cgh.2008.10.028]

3 **Holmboe ES**, Hawkins RE. Methods for evaluating the clinical competence of residents in internal medicine: a review. *Ann Intern Med* 1998; **129**: 42-48 [PMID: 9652999 DOI: 10.7326/0003-4819-129-1-199807010-00011]

4 **Jain SS**, DeLisa JA, Nadler S, Kirshblum S, Banerjee SN, Eyles M, Johnston M, Smith AC. One program's experience of OSCE vs. written board certification results: a pilot study. *Am J Phys Med Rehabil* 2000; **79**: 462-467 [PMID: 10994889 DOI: 10.1097/00002060-200009000-00012]

5 **Sedlack RE**. The Mayo Colonoscopy Skills Assessment Tool: validation of a unique instrument to assess colonoscopy skills in trainees. *Gastrointest Endosc* 2010; **72**: 1125-1133, 1133.e1-1133.e3 [PMID: 21111866 DOI: 10.1016/j.gie.2010.09.001]

6 **Papadakis MA**. The Step 2 clinical-skills examination. *N Engl J Med* 2004; **350**: 1703-1705 [PMID: 15102993 DOI: 10.1056/NEJMp038246]

7 **Alevi D**, Baiocco PJ, Chokhavatia S, Kotler DP, Poles M, Zabar S, Gillespie C, Ark T, Weinshel E. Teaching the competencies: using observed structured clinical examinations for faculty development. *Am J Gastroenterol* 2010; **105**: 973-977 [PMID: 20445506 DOI: 10.1038/ajg.2010.27]

8 **Johnson JK**, Miller SH, Horowitz SD. Systems-Based Practice: Improving the Safety and Quality of Patient Care by Recognizing and Improving the Systems in Which We Work. In: Henriksen K, Battles JB, Keyes MA, Grady ML, editors. Advances in Patient Safety: New Directions and Alternative. Rockville (MD): Agency for Healthcare Research and Quality (US), 2008

9 **Starmer AJ**, Spector ND, Srivastava R, West DC, Rosenbluth G, Allen AD, Noble EL, Tse LL, Dalal AK, Keohane CA, Lipsitz SR, Rothschild JM, Wien MF, Yoon CS, Zigmont KR, Wilson KM, O'Toole JK, Solan LG, Aylor M, Bismilla Z, Coffey M, Mahant S, Blankenburg RL, Destino LA, Everhart JL, Patel SJ, Bale JF, Spackman JB, Stevenson AT, Calaman S, Cole FS, Balmer DF, Hepps JH, Lopreiato JO, Yu CE, Sectish TC, Landrigan CP; I-PASS Study Group. Changes in medical errors after implementation of a handoff program. *N Engl J Med* 2014; **371**: 1803-1812 [PMID: 25372088 DOI: 10.1056/NEJMsa1405556]

10 **Williams R**, Miler R, Shah B, Chokhavatia S, Poles M, Zabar S, Gillespie C, Weinshel E. Observing handoffs and telephone management in GI fellowship training. *Am J Gastroenterol* 2011; **106**: 1410-1414 [PMID: 21811269 DOI: 10.1038/ajg.2011.107]

11 **Zabar S**. Objective structured clinical examinations: 10 steps to planning and implementing OSCEs and other standardized patient exercises. 1st ed. New York, NY: Springer-Verlag, 2013

12 **Farnan JM**, Paro JA, Rodriguez RM, Reddy ST, Horwitz LI, Johnson JK, Arora VM. Hand-off education and evaluation: piloting the observed simulated hand-off experience (OSHE). *J Gen Intern Med* 2010; **25**:

129-134 [PMID: 19924489 DOI: 10.1007/s11606-009-1170-y]
13 **Shah B**, Miler R, Poles M, Zabar S, Gillespie C, Weinshel E, Chokhavatia S. Informed consent in the older adult: OSCEs for assessing fellows' ACGME and geriatric gastroenterology competencies. *Am J Gastroenterol* 2011; **106**: 1575-1579 [PMID: 21897404 DOI: 10.1038/ajg.2011.124]
14 **Harris PA**, Taylor R, Thielke R, Payne J, Gonzalez N, Conde JG. Research electronic data capture (REDCap)--a metadata-driven methodology and workflow process for providing translational research informatics support. *J Biomed Inform* 2009; **42**: 377-381 [PMID: 18929686 DOI: 10.1016/j.jbi.2008.08.010]
15 **Makary MA**, Daniel M. Medical error-the third leading cause of death in the US. *BMJ* 2016; **353**: i2139 [PMID: 27143499 DOI: 10.1136/bmj.i2139]
16 **Arora V**, Johnson J, Lovinger D, Humphrey HJ, Meltzer DO. Communication failures in patient sign-out and suggestions for improvement: a critical incident analysis. *Qual Saf Health Care* 2005; **14**: 401-407 [PMID: 16326783 DOI: 10.1136/qshc.2005.015107]
17 **Horwitz LI**, Moin T, Krumholz HM, Wang L, Bradley EH. Consequences of inadequate sign-out for patient care. *Arch Intern Med* 2008; **168**: 1755-1760 [PMID: 18779462 DOI: 10.1001/archinte.168.16.1755]
18 **Sutcliffe KM**, Lewton E, Rosenthal MM. Communication failures: an insidious contributor to medical mishaps. *Acad Med* 2004; **79**: 186-194 [PMID: 14744724 DOI: 10.1097/00001888-200402000-00019]
19 **Singh H**, Thomas EJ, Petersen LA, Studdert DM. Medical errors involving trainees: a study of closed malpractice claims from 5 insurers. *Arch Intern Med* 2007; **167**: 2030-2036 [PMID: 17954795 DOI: 10.1001/archinte.167.19.2030]
20 **Sinha M**, Shriki J, Salness R, Blackburn PA. Need for standardized sign-out in the emergency department: a survey of emergency medicine residency and pediatric emergency medicine fellowship program directors. *Acad Emerg Med* 2007; **14**: 192-196 [PMID: 17192443 DOI: 10.1197/j.aem.2006.09.048]
21 **Riesenberg LA**, Leitzsch J, Massucci JL, Jaeger J, Rosenfeld JC, Patow C, Padmore JS, Karpovich KP. Residents' and attending physicians' handoffs: a systematic review of the literature. *Acad Med* 2009; **84**: 1775-1787 [PMID: 19940588 DOI: 10.1097/ACM.0b013e3181bf51a6]
22 **Bump GM**, Coots N, Liberi CA, Minnier TE, Phrampus PE, Gosman G, Metro DG, McCausland JB, Buchert A. Comparing Trainee and Staff Perceptions of Patient Safety Culture. *Acad Med* 2017; **92**: 116-122 [PMID: 27276009 DOI: 10.1097/ACM.0000000000001255]

Published By Baishideng Publishing Group Inc
7041 Koll Center Parkway, Suite 160, Pleasanton, CA 94566, USA
Telephone: +1-925-3991568
E-mail: bpgoffice@wjgnet.com
Help Desk:http://www.f6publishing.com/helpdesk
http://www.wjgnet.com